Alma Mater Studiorum Università di Bologna

Doctoral Thesis

The use of Ground Penetrating Radar and alternative geophysical techniques for assessing embankments and dykes safety

Guido Mori

Tutor: Prof. Monica Ghirotti

Coordinator: Prof. Ezio Todini

The use of Ground Penetrating Radar and alternative geophysical techniques for assessing embankments and dykes safety

Guido Mori

Doctoral Thesis

2009

Department Of Earth and Geoenvironmental Sciences
Alma Mater Studiorum Università di Bologna
Via Zamboni, 67 - 40126 Bologna, Italy

Ai miei migliori amici

To my best friends

ABSTRACT

The research is part of a survey for the detection of the hydraulic and geotechnical conditions of river embankments funded by the Reno River Basin Regional Technical Service of the Region Emilia-Romagna. The hydraulic safety of the Reno River, one of the main rivers in North-Eastern Italy, is indeed of primary importance to the Emilia-Romagna regional administration.

The large longitudinal extent of the banks (several hundreds of kilometres) has placed great interest in non-destructive geophysical methods, which, compared to other methods such as drilling, allow for the faster and often less expensive acquisition of high-resolution data.

The present work aims to experience the Ground Penetrating Radar (GPR) for the detection of local non-homogeneities (mainly stratigraphic contacts, cavities and conduits) inside the Reno River and its tributaries embankments, taking into account supplementary data collected with traditional destructive tests (boreholes, cone penetration tests etc.). A comparison with non-destructive methodologies likewise electric resistivity tomography (ERT), Multi-channels Analysis of Surface Waves (MASW), FDEM induction, was also carried out in order to verify the usability of GPR and to provide integration of various geophysical methods in the process of regular maintenance and check of the embankments condition.

The first part of this thesis is dedicated to the explanation of the state of art concerning the geographic, geomorphologic and geotechnical characteristics of Reno River and its tributaries embankments, as well as the description of some geophysical applications provided on embankments belonging to European and North-American Rivers, which were used as bibliographic basis for this thesis realisation.

The second part is an overview of the geophysical methods that were employed for this research, (with a particular attention to the GPR), reporting also their theoretical basis and a deepening of some techniques of the geophysical data analysis and representation, when applied to river embankments.

The successive chapters, following the main scope of this research that is to highlight advantages and drawbacks in the use of Ground Penetrating Radar applied to Reno River and its tributaries embankments, show the results obtained analyzing different cases that could yield the formation of weakness zones, which successively lead to the embankment failure. As advantages, a considerable velocity of acquisition and a spatial resolution of the obtained data, incomparable with respect to other methodologies, were recorded. With regard to the

drawbacks, some factors, related to the attenuation losses of wave propagation, due to different content in clay, silt, and sand, as well as surface effects have significantly limited the correlation between GPR profiles and geotechnical information and therefore compromised the embankment safety assessment.

Recapitulating, the Ground Penetrating Radar could represent a suitable tool for checking up river dike conditions, but its use has significantly limited by geometric and geotechnical characteristics of the Reno River and its tributaries levees. As a matter of facts, only the shallower part of the embankment was investigate, achieving also information just related to changes in electrical properties, without any numerical measurement. Furthermore, GPR application is ineffective for a preliminary assessment of embankment safety conditions, while for detailed campaigns at shallow depth, which aims to achieve immediate results with optimal precision, its usage is totally recommended.

The cases where multidisciplinary approach was tested, reveal an optimal interconnection of the various geophysical methodologies employed, producing qualitative results concerning the preliminary phase (FDEM), assuring quantitative and high confidential description of the subsoil (ERT) and finally, providing fast and highly detailed analysis (GPR). Trying to furnish some recommendations for future researches, the simultaneous exploitation of many geophysical devices to assess safety conditions of river embankments is absolutely suggested, especially to face reliable flood event, when the entire extension of the embankments themselves must be investigated.

TABLE OF CONTENTS

1. INTRODUCTION

Dams have been used to regulate rivers for centuries. Ancient civilisations built dams for drinking water supply, flood control and irrigation. Since the last century, the construction of river embankments (or levee, bank) has been increasing the population of this kind of defence works all around the world. Embankments are mostly built to protect human activities from flooding events. The benefits of such projects are obvious, and in today's society, they represent a great value. However, all the achievements reached by modern society through construction of embankments and dams, come with a price and with a responsibility. The price consists of the environment alteration and all the effects that results from that. Indeed, the responsibility that comes with levees construction is prevent catastrophes and must progress as long as the embankment itself stands. Moreover, as existing works age the importance of work safety efforts increase even more. Embankments are made of earth (essentially fine grain-size soil) and rock material and nowadays represent the most common type of dam construction in Italy as well as worldwide.

The term embankment (or levee, bank) in this thesis refers to small earth dikes (up to 12 meters high) built along the river bed that are used for the stream regulation under the flood conditions. The problem of the safety of river embankments can be easily underestimated, particularly if a relative dry period persists for a long time. The Reno River together with its tributaries covers, in the alluvial plain area, which includes the larger part of Emilia-Romagna Region (Northeast of Italy) a length extension of more than 500 km. Several hydro-meteorological events induced structural failures of the Reno River and its tributaries embankments. Concerning the last decades, the dike breakages of Reno River in 1990, Samoggia Stream in 1996, and piping phenomena of Quaderna Stream in 2005 and again Samoggia, 2008, highlight how this crucial sector of Po Plain has been exposing to a sharp hydrogeological risk and detailed research in order to prevent it are necessary.

Generally, during the survey for either hydrogeological, engineering-geological, or geotechnical purposes, it is necessary to select appropriate complex of methods and related methodology of the field works. Likewise, it is necessary to know relationship between measured physical properties of rocks, soils and parameters, which have to be finally received or indirectly determined. From the principle point of view, geophysical methods are considered indirect methods, because they substitute direct field works as e.g. drills, adits, etc. Thus, they may significantly save both, basic finance expenses, in appropriate combination

with direct methods, as well as investment of the time necessary for survey of observed environment. Last but not least, geophysical methods are successfully used also in environmental protection. Indisputable advantage is the fact that the surface geophysical methods are non-destructive. Moreover, piping and seepage problems along fractures, cavities, differently compacted and settlemented areas, cannot be easily recognised through destructive methods (largely used for the Reno River embankments description) which provide precise but punctual information. Non-invasive techniques, such as geophysical methods, result largely diffused for this topic and in constant development.

The main contribution of geophysical methods consists, therefore, in getting higher quality and backgrounds that are more trustworthy for further survey works. During their application, it is necessary to keep the principle of complexity (selection of appropriate methods), work in stages (this is related to relationship with the direct methods and further proposal of geophysical methods), and economic efficiency (getting maximal amount of information for minimal expenses). Secret of success in utilizing results of geophysical methods is in close cooperation of geophysicists with specialists in hydrogeology and engineering geology.

1.1 Geophysical methods and geologic environment

Geophysics, as a branch of science, utilizes knowledge of physics, astronomy, geology and applied mathematics. It studies naturally or artificially generated physical fields of Earth. Applied geophysics is an applied science, studying naturally or artificially generated fields to help clarify geological conditions in the Earth crust. Because the Earth crust is inhomogeneous, its particularities are reflected also in the observed geophysical fields. Its principle consists in differentiation between the contrast properties and surrounding environment. Therefore, different geophysical response is directly dependent on extent of different properties of the environment. In the same way, important is also the dependence on depth of deposition of these non-homogeneities, what closely relates to the action radius of used geophysical methods. Applied geophysics is conventionally divided into many methodical groups according to character of the field, which is monitored. These methods are gravimetric, magnetometric, geothermal, geoelectric, electromagnetic, radiometry and methods of nuclear physics, seismic and geoacoustic methods. Geophysical methods may be used in several variants, most commonly in the surface variant (measurement is performed

directly on the earth surface), in the underground variant (in the drills, cellars, etc.) and in the variant of remote monitoring from airplanes, satellites, etc. (so called remote sensing).

Geophysical parameters are dependent on surveyed environment. Response of these parameters during the measurement is given by physical properties of soils. Generally, the following soil properties are considered to belong among the basic ones: density, strength, compressibility, stability (resistivity to weathering) and permeability. These properties are crucial for evaluation of the earth or rock material from the geotechnical point of view. These properties may be determined directly for example by laboratory tests or by the field measurement. By using appropriate complex of geophysical methods, these properties may be indirectly acquired.

1.2 Geophysical measurement in function of the embankments safety evaluation

As it was already explained, river embankments are such important protective works and need as much attention is possible, in order to guarantee the safety of the human activities from flooding events. By application of appropriate complex of methods and adequate methodology of the field measurement and with help of received data, which represent current response of the rock environment to the parameters measured within the certain geophysical field, the current conditions of material of the protective embankments may be relatively depicted. Although geophysical division of environment is specific, its qualitative and quantitative aspect may serve to determination of needed specifics, dependences, and parameters, which are crucial for their reliable function. Nevertheless, mutual relationships between geophysical and hydrogeological or engineering-geological parameters are not always determinable in a simply way. The dependences considered generally valid exist, verified in practice, but it is always necessary to approach solution of each task specifically. Application of geophysical methods is based on theoretical backgrounds and practical experiences. It is, therefore, reasonable to describe basic properties of soils, serving as a construction material of embankments in mutual relation to the geophysical parameters, received from the field measurement.

Their structure and building materials primarily provide the safety of the embankments. Building materials must assure adequate stability and impermeabilization of the embankment itself. Substantial element is here also the amount of contained water, primarily in relation to the water in the surface watercourse. Besides the water contains, the

knowledge of existence and position of eventually non-homogeneity zones into the embankment are relevant problems in term of hazard and hydraulic risk, especially if river embankments themselves are old (more than one century), inserted in a densely populated area, subjected to periodic important floods and at last, detailed information on history and structure are missing. The needing to carry out a survey of hundreds of kilometres of river embankments for identifying, primarily, these weakness zones, is also a requirement of the regional government authorities. In the stability studies of river embankments, this research was carried on in order to provide a stratigraphic description and the detection all the eventual non-homogeneities inside the embankments themselves, with the employment geophysical measurement, in particular using GPR methodology.

1.3 Objectives, limitations and thesis structure

Just in this context, GPR suitability was tested in the study of river embankments. The detection of stratigraphy, animal cavities and burrows, buried pipelines, internal erosion zones, non-homogeneities areas related to different phases of construction and repaired areas of the embankment itself represent the main purpose of this research. The main questions to be answered were therefore if GPR measurements would stand a chance of detecting heterogeneous zone inside the embankment structure and if the provided results could be adequate to the realisation of models for a secure environmental protection. Measurement data were collected using several antenna frequency configurations, on various part of the embankment, in order to constitute the foundation of the thesis work. In addition, some complementary measurements were performed at other sites and comparison studies were conducted. Some limitations afflict this research; primary, a seasonal monitoring of the river embankment conditions was also scheduled; nevertheless, during the last two years no hydrogeological crisis (except the event of May 2008) have occurred, therefore constant dry conditions have characterized the river drainages. Moreover, the vegetation conditions over the embankment bodies have impeded systematically studies and many campaigns have limited by such environmental circumstances.

Must be highlighted that this thesis is focused on the application of the GPR method for detection of internal erosion, objects, cavities and anomalous areas in embankment dams; even though other geophysical methods occasionally were used, the thesis is limited to the use of the GPR. The thesis includes few theoretical descriptions in the form of mathematical formulas or equations of some geophysical basis and principal methodologies and has no

ambition of a complete coverage here, but the basic relations and references to appropriate methods are being provided.

The **chapter two** introduces the problematic strictly linked with the embankment conditions in a densely populated area as Emilia-Romagna, in particular its flatten part; this chapter also provides a description of the state of the art and historical cases of geophysical study regarding the embankment safety issue are analysed. The **chapter three** offers a detailed description of the GPR methodology, from the theoretical basis, to its application for the embankment conditions evaluation. The **chapters four** and **five** introduce the two others geophysical methodologies that were employed to realise a comparison with the GPR measurements and to implement the database of the properties related to the materials, composing the embankment. The **chapter six** presents the results obtained with the employment of GPR as unique methodology to the embankment structure definition. The GPR radargrams (electromagnetic pseudo-sections of the embankment) showed in this chapter represent the most interesting results of more than 40 km of profiles provided in these two years of research. The **chapter seven** finally presents the cases of comparison between GPR and other methodologies, which were tested in this research. Therefore, it demonstrates the utility of multidisciplinary approach, by means of the simultaneous usage of various geophysical methodologies, to evaluate, as best asl possible, the stability and safety conditions of the river embankments. Finally, the **chapter eight** is dedicated to the summary of all this thesis achievements, as well as advantages and drawbacks associated to GPR methodology.

2.   THE RIVER EMBANKMENT SAFETY EVALUATION

The term embankment (or levee, bank) in this thesis refers to small earth dikes (up to 12 meters high) built along the river bed that are used for the stream regulation under the flood conditions. An embankment is constructed with earth and rock materials. A common classification is to divide embankment into earth-fill ones and rock-fill ones. In some cases homogeneous earth-fill banks are separated into a class of its own. Homogeneous embankments are the oldest type of structure, constituted by one single type of low permeable material, sometimes with coarser material on the slopes to increase stability and protect the embankment itself from surface erosion. In the past, the embankments construction modalities commonly schedule the usage of materials taken directly from the riverbed, transported and compacted on the natural riverbanks using only wheelbarrows or other poor means of work; this is also the case of many Italian rivers, where nowadays their flood defence system does not operate, as it should, in many important nodes. Therefore, the hydraulic safety of the Reno River, one of the main rivers in North-Eastern Italy is of primary importance to the Emilia-Romagna regional administration. This concern is reasonable since in the last decades, besides the unnatural evolution of the Po Plain fluvial system, several hydro-meteorological events induced structural failures of the Reno River and its tributaries embankments.

2.1 Introduction

Embankments represent a great value in today's society and their safety is of primary importance to all the environmental administrations. Nevertheless, during the last decades many inundations due also to levee breakages have occurred in Europe causing losses of human lives and financial damages, which were aggravated, in several cases, by the intense urbanisation of flood prone areas. Two extended floods occurred in Central Europe during the last 15 years, and both events hit the territories of Germany and Czech Republic. The Odra flood produced several disasters in the eastern parts of Czech Republic (Moravia region, the Odra and Morava River basins) in July 1997, afflicting 325 municipalities and causing 20 causalities, while the western part (Bohemia region, Labe river basin) was widely stricken by the Labe-Elbe flood in August 2002 (Rezacova et alii, 2005). Concerning the flood events in Morava River basin in 1997, the monitoring of dike condition was neglected; therefore project IMPACT (financed by 5th FP EU) was carried out, in order to acquire a precise description of dike conditions, providing a selection of appropriate geophysical method through GMS

(Geophysical Monitoring System) methodology (Morris, 2005; Boukalová & Beneš, 2007). The Elbe floods (Germany) in 2002 and 2006 have brought much public attention to the present state of river embankments, their investigation, strengthening or replacement. As many embankments are more than one hundred years old and no detailed geotechnical data even from recently refurbished sites are available, the demand for fast and accurate investigation methods is increasing (Niederleithinger et alii, 2007).

Considering the Italian case and some of the most significant events only, the Po River was affected by two remarkable floods (1994 and 2000) in a few years, and catastrophic inundations have occurred in Piedmont (1994 and 2000), Valle d'Aosta (2000), Tuscany (1996), Liguria (2000) and Calabria (2000). After these disasters, the question has often been raised about the possibility that they are due, at least partially, to an increased vulnerability because of the land use change that took place in northern Italy in the last five decades. These concerns have therefore urged the hydrologic community to investigate the effect of human activities on the river flow regime (Surian & Rinaldi, 2003). During the past tens or hundreds of years, in many Italian fluvial systems, river dynamics have been significantly affected by human disturbances such as land use changes, urbanization, channelization, dams, diversions, gravel and sand mining. Since these disturbances cause substantial changes to the flow and sediment regimes, at present few rivers are in a natural or semi-natural condition. Several studies have analysed the response of rivers to human impact, showing that remarkable channel changes generally take place, such as vertical adjustment, changes in channel width and pattern.

These changes are generally much larger than those that could be expected from natural channel evolution and they represent part of the several causes that, during the last decades, following intense rainfall phenomena, triggered numerous flooding events in Italy. Surian & Rinaldi (2003) carried out a systematic review of the studies regarding morphological changes and their relative effects on structures and environment in Italian rivers (Figure 2.1). Therefore, besides the morphological changes, the hydraulic safety of the Reno River, one of the main rivers in North-Eastern Italy is indeed of primary importance to the Emilia-Romagna regional administration. Especially the structural conditions assessments of river embankments, which are mainly constitutes by carryover materials and have the purpose to safeguard the anthropized surroundings from flooding, is of importance. This concern is reasonable since, in the last decades, besides the unnatural evolution of the complete fluvial system, several hydro-meteorological events induced structural failures of the Reno River and its tributaries embankments. Some of them were particularly serious, such

as the dike breakages of Reno River in 1990, Samoggia Stream in 1996, and piping phenomena of Quaderna Stream in 2005 and again Samoggia, 2008.

Recent channel adjustments in Italian rivers and relative causes and effects

River	Morphological changes	Location and time of morphological changes	Causes	Location and time of human intervention	Effects on structures and environment
Po	Channel shifting		Neotectonics, embankments		
	Channel narrowing; reduction of sinuosity Incision (1–6 m); reduction of channel length; reduction of sinuosity; meander cutoff; channel narrowing; changes in channel pattern	1920s to 1950s, 1960s up to the present	River engineering (at least in part) Changes in flood regime; gravel and sand mining; channelization; intervention at basin level	1930s up to the present Since the Roman times, but particularly intense from 1950s up to the present	Undermining of bank-protection structures and bridges; loss of groundwater resources; loss of agricultural land; increase of flow velocity
Rivers of the Piedmont Region (High Po Plain)	Channel narrowing (in several cases more than 50%); incision (up to 5–8 m); decrease of braiding index; changes in channel pattern (from braided to wandering)	Piedmont and alluvial plain reaches; 1950s to 1980s	Gravel mining; channelization	1950s to ?	Loss of groundwater resources
Brenta	Incision (up to 7–8 m)	Alluvial plain reach; 1960s to 1970s	Gravel mining; dams	Alluvial plain reach; 1960s to 1970s	Failure of bridges; loss of groundwater resources
Piave	Channel narrowing (more than 50%); decrease of braiding index; incision (up to 2–3 m); changes in channel pattern (from braided to wandering)	Mountain and alluvial plain reaches; 1900s up to the present	Dams; diversions; gravel mining; channelization	Mountain and alluvial plain reaches; 1930s up to the present	Loss of groundwater resources
Rivers of the Emilia Romagna Region	Incision (3–4 m on average, up to 12–13 m); channel narrowing, changes in channel pattern (from braided to meandering)	Piedmont and alluvial plain reaches: 1950s to 1980s (particularly intense in 1970s)	Gravel mining, dams, construction of weirs	Piedmont reach; 1950s to 1980s	Failure and damage to bridges and protection structures; loss of groundwater resources; increase of flow velocity; reduction of sediment supply to the beaches
Arno	Incision (2–5 m on average, up to 9 m)	Alluvial and coastal plain reaches; two phases of incision: minor phase from the beginning of 1900; second phase from 1945–60 to 1990s	Interventions at basin level (construction of weirs, reforestation) Intense gravel-mining; Dams	Mountain areas, from the end of 1800 and first decades of 1900 Alluvial reaches: 1950s to 1980s 1957	Damage to bridges, bank protections and levees; upstream migration on tributaries; riverbanks instability; loss of groundwater resources; reduction of sediment supply to the beaches
Rivers of the Tuscany Region	Incision (usually 0.5–2 m; more than 2 m in some cases); channel narrowing (in several reaches more than 50%); changes in channel pattern	Alluvial plain reaches: 1950s to 1990s	Interventions at basin level (construction of weirs, reforestation) Gravel mining	Mountain areas, from the end of 1800 and first decades of 1900 Alluvial reaches: 1950s to 1980s	Damage to bridges, bank protections and levees; riverbanks instability; loss of groundwater resources; reduction of sediment supply to the beaches

Figure 2.1 - Recent channel adjustments in Central-North Italian rivers and relative causes and effects (Surian & Rinaldi, 2003).

9

In spite of the well-developed system of embankments of the Reno River and its tributaries, dating in some cases over one hundred years, there is a lack of knowledge on their structural status. Therefore, many geotechnical surveys were planned during the last decade to investigate the Reno River catchment embankments structure. The STBR (Regional Technical Service of the Reno River Basin) of the Emilia-Romagna Region has recently begun a survey programme, financed by the Authority of the Reno River Basin, focused on the study of the hydraulic and geotechnical conditions of the river dikes inside the territory under its jurisdictional authority (Mazzini & Simoni 2004). Actually, destructive methods (such as SPT-CPT tests, boreholes) represent the most largely used techniques to describe the stratigraphy as well as geotechnical parameters of the river embankments. The most utilised direct methodologies are successively shown.

2.2 Geotechnical Investigations

Site investigations and assessment require a thorough understanding of the geology of the site. The following aspects or parts thereof must be taken into account: stratigraphic sequence, thickness and lateral extent of strata and other geological units, lithology, homogeneity and heterogeneity, bedding conditions, tectonic structures, fractures, and impact of weathering. Concerning soils, the extent and thickness of the lithological units are determined using geological methods (e.g., geological mapping, geotechnical tests, direct push sounding) in combination with geophysical and remote sensing methods. The lithological unit identification is based on its mineralogical composition, colour, grain size, texture, and other physical properties. The following properties are important for an assessment of the homogeneity/heterogeneity of the ground on a small scale with with respect to:

- Texture, grain size, mineral content, density, water content.
- Strength (compressibility, shear strength).
- Porosity and degree of saturation with water.
- Permeability.

These properties can be determined among other methods directly by analysis of samples in the laboratory. Soil samples become increasingly difficult to obtain with increasing depth. Soil mechanical tests in the laboratory are expensive and time consuming. For this reason, geophysical methods are made to gain additional information. The geophysical methods results cannot be unequivocally interpreted without calibration on the

basis of samples and laboratory tests. Sampling and geophysical methods are, therefore, complementary. The methods should be selected so that optimal investigation results are obtained in the most economical way. In many countries, there are already standards and regulations for various kinds of geological investigations, their quality requests and their documentation.

With regard to the river embankment investigations, the easiest and therefore commonly used methods to provide geotechnical properties are drilling (boreholes) and direct pushing technology (Cone Penetrometric Tests), which will be following described. They provide a punctual stratigraphic description and a geotechnical parameters characterization of the subsoil with acceptable time-consuming and costs.

2.2.1 Drilling

Drilling is the process of making a circular hole with a drill or other cutting tool. Samples can be obtained from the drill cuttings or by coring during the drilling. Boreholes are used to obtain detailed information about rock-sediment types, mineral content, rock fabric and the relationships between rock or sediment layers at selected locations. Boreholes can also be used as monitoring wells, test wells and production wells in hydrogeological investigations. In some cases, boreholes are plugged back to the surface after core sampling or logging, but in most cases, they are used as monitoring wells. Monitoring wells are drilled to different depths of the aquifer to obtain information about the spatial distribution of contaminants as well as water table and changes over time. The locations for drilling are selected using information obtained by geological, geophysical and/or geochemical methods; pertaining to river embankment, generally boreholes are located on the top of the embankment itself, in order to provide its complete stratigraphic analysis.

Three principal drilling methods are widely used for shallow-depth boreholes, depending on the type of information required and/or the rock types being drilled.

- ▪ Cable tool method: cable percussion drilling is the oldest, simplest, most reliable, and economical technology available for drilling water wells (figure 2.2a). It can be used to drill any material – from soft sands and clays to hard rock like granite. It requires no mud, mud pits, auxiliary pumps or chemicals, but the drilling depth is only limited by the length of the wire cable. The equipment consists of a tripod with pulley, strong rope or cable, heavy drill stem with a drill bit or bailer, and a drum or pitman at the other end of the rope. By using the drum to alternately pull the rope taut and let it go slack, the drill bit is raised and allowed to fall; therefore, this method is a percussion drilling method,

undisturbed material is not obtained, but it is easy to determine the lithology from the mixed sample from each meter.
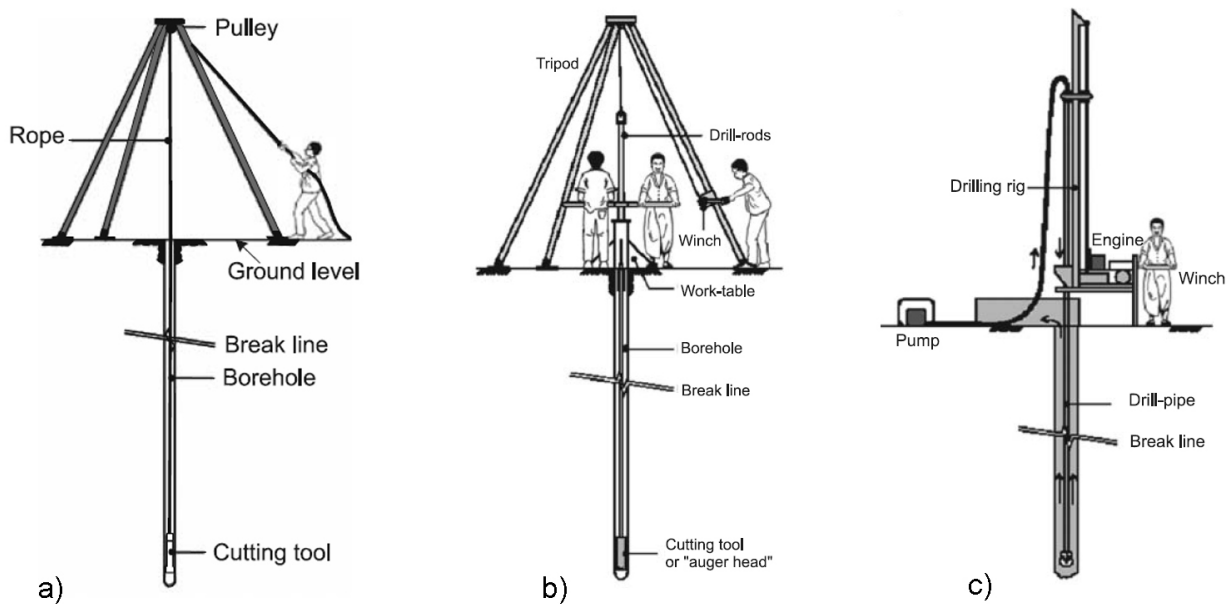
Figure 2.2 - Principle of drillings: (a) cable tool drilling manual version; b) Hand-auger drilling; c) rotary drilling with flush (Knödel et alii, 2008).

▪ Auger drilling: is a drilling tool designed so that the cuttings are continuously carried by helical grooves on the rotating drill pipe to the top of the hole during drilling. Hand-auger drilling is suitable only for unconsolidated deposits and drilling to a shallow depth. It is inexpensive but slow compared to other methods. This method allows drilling through unconsolidated or semi-consolidated materials such as sands, gravel, silt and clay (Figure 2.2b). Water is needed for dry holes. On the basis of the cuttings transported to the surface, it is possible to determine the geological profile to within 50 cm resolution. The cuttings can be used for grain-size analysis and for geochemical laboratory analyses. The auger method is the preferable method for drilling on waste or contaminated sites, but it is not recommended for water wells.

▪ Rotary drilling: is one of the most common drilling methods and it was used for the geotechnical campaigns for Reno River and its tributaries embankments. In this method, the entire drill string is rotated at the surface to turn the drill bit (Figure 2.2c), and cuttings are removed from the hole by a circulating fluid (Figure 2.3a). Water, mud or air is used as drilling fluid to cool and lubricate the drill bit, flush the drill cuttings up and out of the borehole, support and stabilize the borehole wall to prevent caving in, and to seal the borehole wall to reduce fluid loss. There are two basic types of mud or water rotary drilling: the *direct* and *reverse* methods. In the *direct rotary* method, the drilling fluid is

pumped down through the drill pipe and out of the bit. The fluid then flows upwards in the annular space between the hole and the drill stem, carrying the cuttings in suspension to the surface into the mud pit. In *reverse rotary* drilling, the fluid and its load of cuttings flow upwards inside the drill pipe and are discharged by a suction or vacuum pump into the mud pit. Three types of bits are used for rotary drilling of water wells: a drag (blade or fishtail) bit, a roller (tricone) bit and a reamer bit. Reamer bits are used to widen a borehole for well installation. The most common drilling mud is a suspension of benthonite (sodium montmorillonite clay) in water, but it can be advantageous under certain circumstances (depending on availability, geological conditions, etc.) to use other artificial or natural mixtures, such as Tixoton (calcium montmorillonite), Revert (a synthetic polymer), or mixtures of local clay.

Figure 2.3 – a) Drilling test, provided for Reno river embankments, using the direct water rotary method; b) example of silty-sand samples collected.

After the fluid is mixed, sufficient time must be allowed to elapse to insure complete hydration of the clay prior to its being circulated into the borehole. It is very important to have a strictly controlled fluid scheme during the entire drilling. The weight, viscosity, mud losses, and pumping rate must be monitored continuously and conditions adjusted

accordingly. On the one hand, the drilling mud must be thick enough to bring up the cuttings, but on the other hand, if it is too thick, it will be difficult to pump and the cuttings will not settle out in the mud pit. Moreover, if mud is too thin, excessive migration of the mud into aquiferous layers can occur, changing the geochemical conditions.

The drilling method assures the granulometric and therefore stratigraphic characterization of the subsoil. Borehole investigations for Reno River and its tributaries an embankment represent a very important tool for the realization of stratigraphic sketches of the embankment structure and is necessary to provide a correct calibration of geophysical methods (Figure 2.3b).

2.2.2 Direct push technology

Direct push methods are used for investigation of soils and sediments by driving, pushing, and/or vibrating small-diameter hollow steel rods into the ground. Their use is limited to unconsolidated sediments and semi-consolidated sediments and is generally not possible in consolidated rocks. An enormous variety of equipment is available and, depending on the survey objectives and selected methods, ranges from 15 kg manual hammers (Figure 2.4a) to hydraulic pressure systems mounted on a heavy-duty truck (figure 2.4b).

CPT (sometimes called Dutch CPT) has been continuously developed and used since the 1930s, to determine soil mechanical parameter values for engineering geology purposes. CPT can provide a highly detailed, three-dimensional picture of the subsurface in less time than needed by traditional methods (e.g., boreholes). CPT systems consist of a thrust machine capable of 20 to 200 KN thrusting force and a counterweight system (the rig and truck), a cone penetrometer (tool) as well as recording equipment. For Cone Penetration Testing (CPT), the mass of the truck (10 to 30 t) is used as a counterweight to the hydraulic pressure unit used to achieve depths larger than 20 m. In contrast to the CPT method, a percussion hammer is used for depths smaller than 20 m by hammering rods into the ground or by vibration under pressure. In this case, the mass of the truck can be considerably smaller than for CPT (usually less than four tons). Because the trucks are smaller, the percussion hammer method can be used even within buildings, as well as in difficult terrain. The rods used for the CPT method are one meter long. They have male threads on one end and female threads on the other. The rods used for the percussion method are 1.5 - 3.5 m long. There are two types of rod systems: single rod and cased. The most common type of rod systems is the single rod.
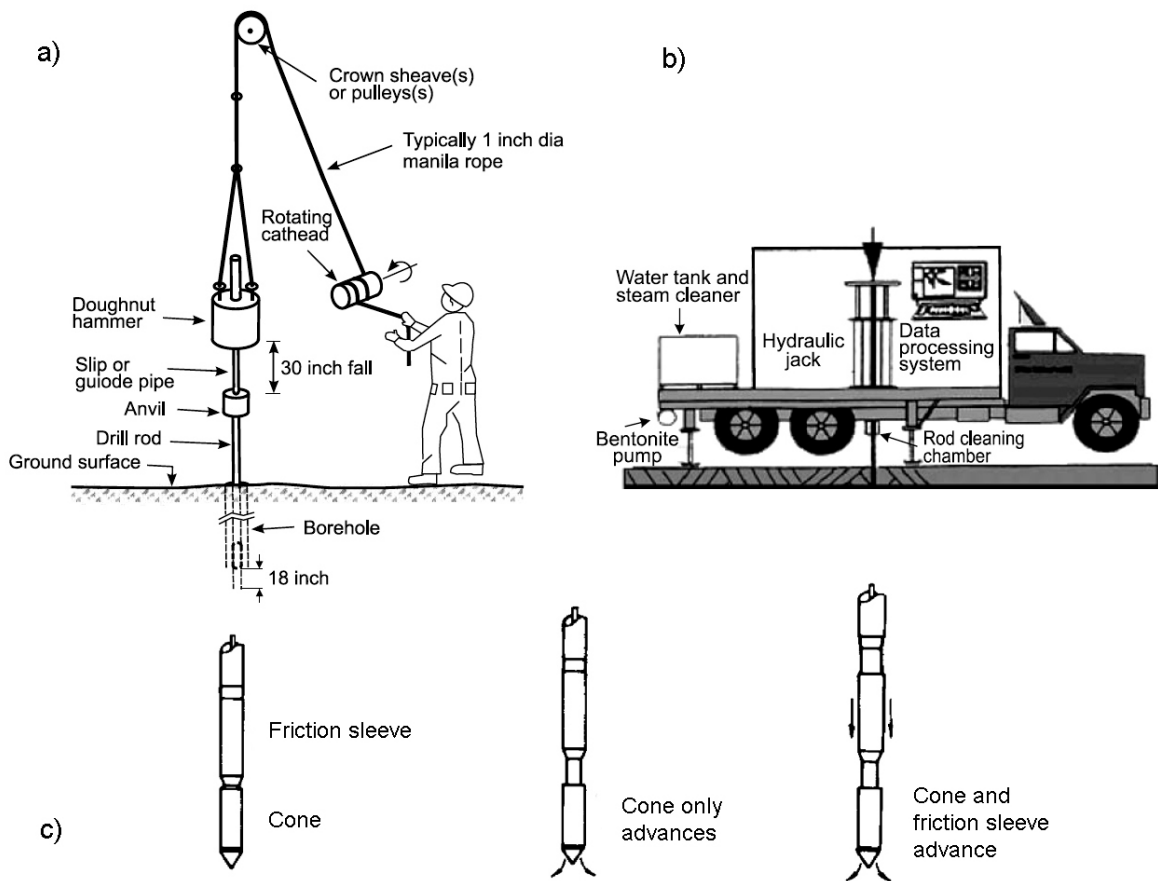
Figure 2.4 - Equipments for cone penetration testing: a) standard, b) mounted on a heavy-duty truck, c) working sequence of Dutch CPT.

The diameter of the rods is typically 1 inch (2.54 cm), but can range from 0.5 to 2.125 inches (1.27 to 5.40 cm). Cased systems, also called dual-tube systems, have an outer tube, or casing, and a separate inner sampling rod. The casing can be advanced simultaneously with the inner rod or immediately afterwards. Samples can be collected without removing the entire string of rods from the ground. The outer tube diameter is typically 2.4 inches (6.10 cm), but can range between 1.25 and 4.2 inches (3.18 to 10.67 cm). Single-rod systems are easier to use (EPA Superfund, 2005). If a hard one underlies a soft layer, it is possible that the rods will bend. For this reason, deviation from the vertical is automatically registered in the CPT method by an inclinometer in the tool (cone with sensors at the lower end of the first rod). The rods and tools must be decontaminated when they are removed from the ground. In the CPT method, this is done with hot water or steam automatically while the rods are withdrawn. The accepted reference is a cone penetrometer that has a cone with a 10 cm^2 base area and an apex angle of sixty degrees and is specified as the standard in the International Reference Test Procedure (IRTP, 2001).

The following parameters are measured with geological/geotechnical tools (cone penetrometers): cone (tip) resistance, sleeve friction, inclination, depth, and in some cases pore water pressure. The most commonly measured parameters are either cone resistance and sleeve friction, or cone resistance and total force on the penetrometer in the CPT method. Cone resistance, sleeve friction and pore water pressure are the commonly measured parameters in the CPTU method. Inclination and depth are measured with both methods. Additional measurement of the pore water pressure at one or more locations on the penetrometer surface gives a more reliable determination of stratification, soil type and mechanical soil properties with respect to standard CPT.

There are two types of cone penetrometers: subtraction cones and compression cones.

- Subtraction cones measure the total force on the penetrometer (sleeve + tip) and the cone resistance (q_c). The sleeve friction (f_s) is calculated by subtracting the cone resistance from the total force. There is no upper limit for the sleeve friction of the subtraction cone (Figure 2.4c). The only limit is on the total force on the penetrometer.

- Compression cone measures the cone resistance (q_c) and the sleeve friction (f_s) separately. This results in a lower maximum value (1 MPa) for the sleeve friction. The friction ratio Rf [%] can be used to identify the soil type.

$$R_f = 100 \frac{f_s}{q_c} ; \qquad\qquad\qquad (2.1)$$

where f_s = unit sleeve friction (MPa) and q_c = cone resistance (MPa). Figure 2.5 shows the most common soil classification methods, using cone resistance, sleeve friction and friction ratio values. CPT and CPTU usage is widespread for the Reno River and its tributaries embankments; the results of such measurements will be successively showed, whereas were important for a geophysical methods calibration as well as for the geotechnical parameters description. Besides their well-developed utilization as well as the ability to characterizes the structural conditions of the subsoil, the geotechnical surveys, planned to investigate the embankment structures, do not guarantee detailed information, because destructive tests (such as SPT-CPT tests, boreholes) achieve just punctual data.
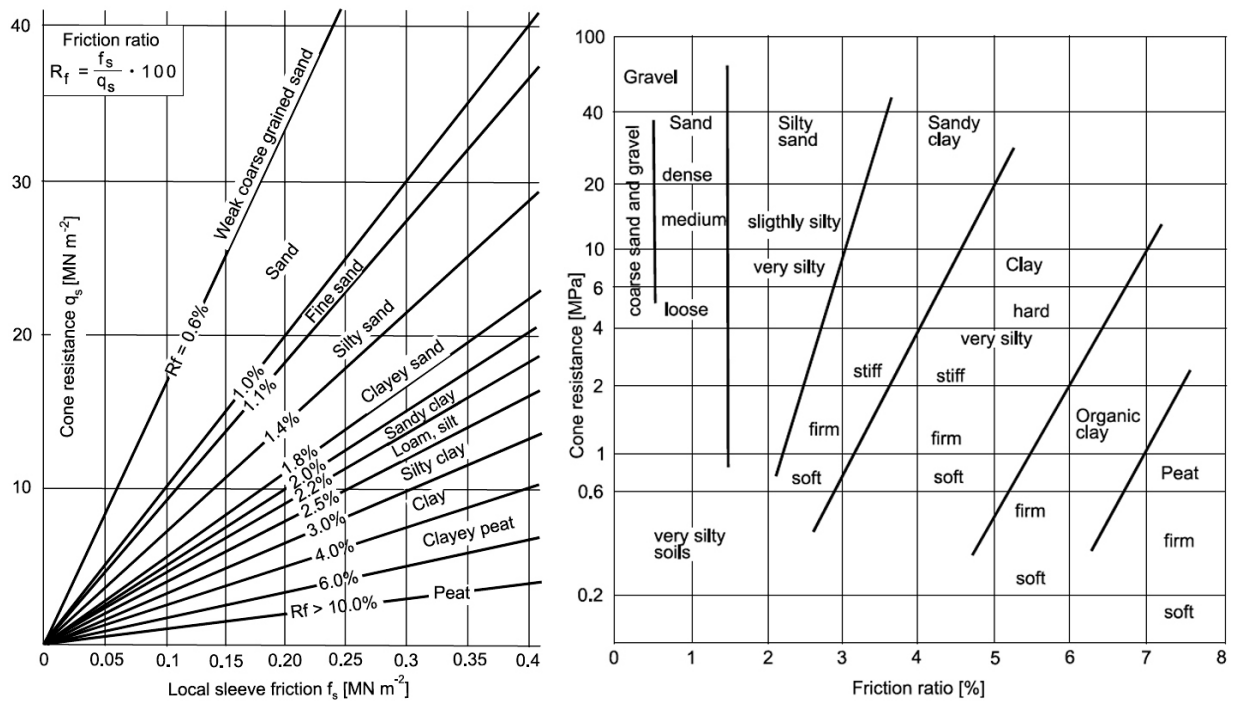
Figure 2.5 - Soil classification using cone resistance and local sleeve friction from CPT measurements (Knödel et alii, 2008) and using cone resistance and friction ratio (Brouwer, 2002).

Hence, the large longitudinal extent of the embankments (several hundreds of kilometres) has placed great interest in non-destructive geophysical methods, which, compared to other methods such as drillings, allow a faster and often less expensive acquisition of high-resolution data. The knowledge of the existence and the position of eventually non-homogeneity zones into the embankment are relevant problems in term of hazard and hydraulic risk, especially if river embankments themselves are old (more than one century), inserted in a densely populated area, subjected to periodic important floods and at last, detailed information on history and structure are missing. The need to carry out a survey of hundreds of kilometres of river embankments for identifying, primarily, these weakness zones, is also a requirement of the regional government authorities.

Just in this context, GPR and other geophysical methodologies suitability was tested in the study of river embankments; the main purposes were the detection of stratigraphy, animal cavities and burrows, buried pipelines, non-homogeneities in general and also related to different phases of construction and repaired areas of the embankment itself. The next paragraph will introduce the geological and hydrogeological background of the Reno River catchment and the principal causes of danger and instability of the river embankments will be successively described.

2.3 Geographical and geological settings of the study area

The Reno River and its tributaries area belongs to the structural domain of the Apennine belt, in particular to its front portion, covered by recent alluvial deposits and underlain by terrigenous layers of Plio-Pleistocene sediments. The geological setting can be considered as the result of a foreland basin evolution process lying on the northern end-member of the Adriatic–Apulia block. Ricci Lucchi (1984) describes the Po Basin fill as a syntectonic sedimentary wedge forming the infill of the Pliocene-Pleistocene Apenninic foredeep, showing opposite polarity of tectonic transport. It attains a total thickness in excess of 4000 m; the Quaternary deposits are about 1000-1500 m thick (Pieri & Groppi, 1981). Recently, Picotti & Pazzaglia (2008) document that the Po Plain around Bologna is a subsiding sag basin, superposed on top of the former pro-foreland basin, where shallow thrust-cored folds appear to be mostly inactive since the middle Pleistocene. The main finding of their investigation is that the Bologna mountain front is an actively growing structure, cored by a mid-crustal flat-ramp structure that accommodates ongoing shortening driven by Adria subduction.
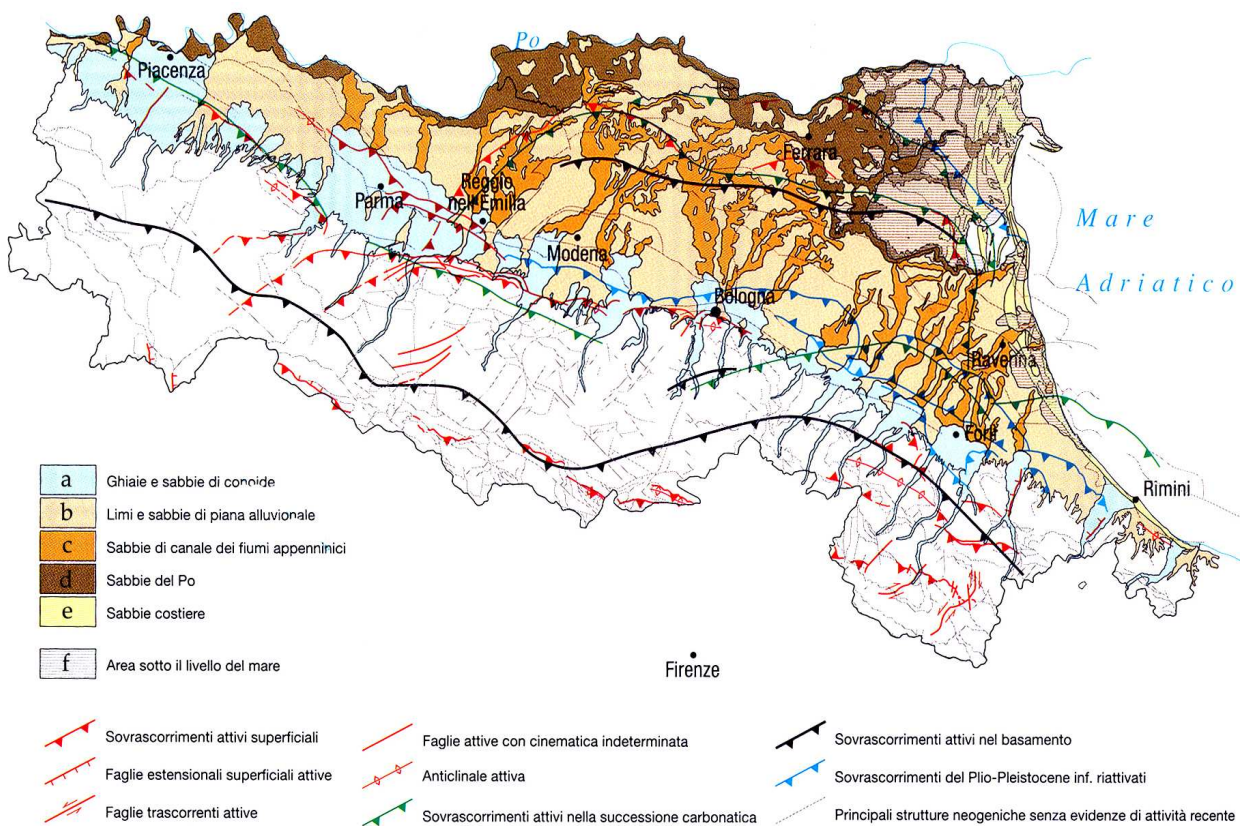
Figure 2.6 - Geological sketch of surface and subsurface main structures of the Emilia-Romagna Region flatten area. Legend: (a) gravels and sands of alluvial fan; (b) silts and sands of alluvial plan; (c) channel sands of Apenninic rivers; (d) Po sands; (e) Coastal sands; (f) Below sea level area; Boccaletti et alii (2004).

Therefore, prominent cyclic facies architecture is the dominant feature of the Quaternary alluvial to coastal infill of the Po River Basin, a rapidly subsiding foreland basin bounded by the Alps to the North and the Apennines to the South (Amorosi & Colalongo, 2005). Close to the southern basin margin, stratigraphic architecture is dominated by amalgamated alluvial-fan gravel bodies, passing in distal locations into alternating gravel (fluvial-channel) and predominantly muddy (overbank) sediment bodies. Moreover, the tectonic uplift of the Apennine mountain chain is considered the main reason for the northward migrations of the Po River, occurring during the last 3000 years (Bondesan, 2001). The Figure 2.6 shows the geological map of the Po Plain area inside Emilia-Romagna, where the river embankments issues are particularly apprehended by Regional and Local Administrations.

As widely documented, the Po Plain is affected by subsidence due to the combination of a long-term "natural" movement and the surface effects of "anthropogenic" activity (Carminati et alii, 2003). Natural movements are the surface expression of different causes. In the literature, such causes are commonly referred to both tectonics originated from the North Apennine thrust belt activity, sedimentary (loading and compaction) and postglacial rebound. These movements are not localized, but their influence is at a regional scale. According to many studies, dealing with natural subsidence, it is well noticeable that subsidence reached for the first half of the 20th century a rate of 2.5 mm/year (Carminati & Martinelli, 2002). As far as anthropogenic causes are concerned, soil subsidence of the Po Plain area is the surface effect of the overexploitation of the aquifers, as largely documented by technical reports. Since the fifties, the urban area of Bologna rapidly expanded as a consequence of the industrial and agricultural development. Therefore, from 1957 to 2001, the average subsidence increased at 40–50 mm/year, and some benchmarks detected subsidence rates up to 60 mm/year in the northern suburbs of Bologna (Figure 2.7). These subsidence rates in the Bologna city area are also confirmed by some GPS and gravimetric measurements that were monitored form 1992 to 2000 using an advanced DInSAR technique. This technique allows monitoring the temporal evolution of a deformation phenomenon, via the generation of mean deformation velocity maps and displacement time series from a data set of acquired SAR images (Stramondo et alii, 2007).
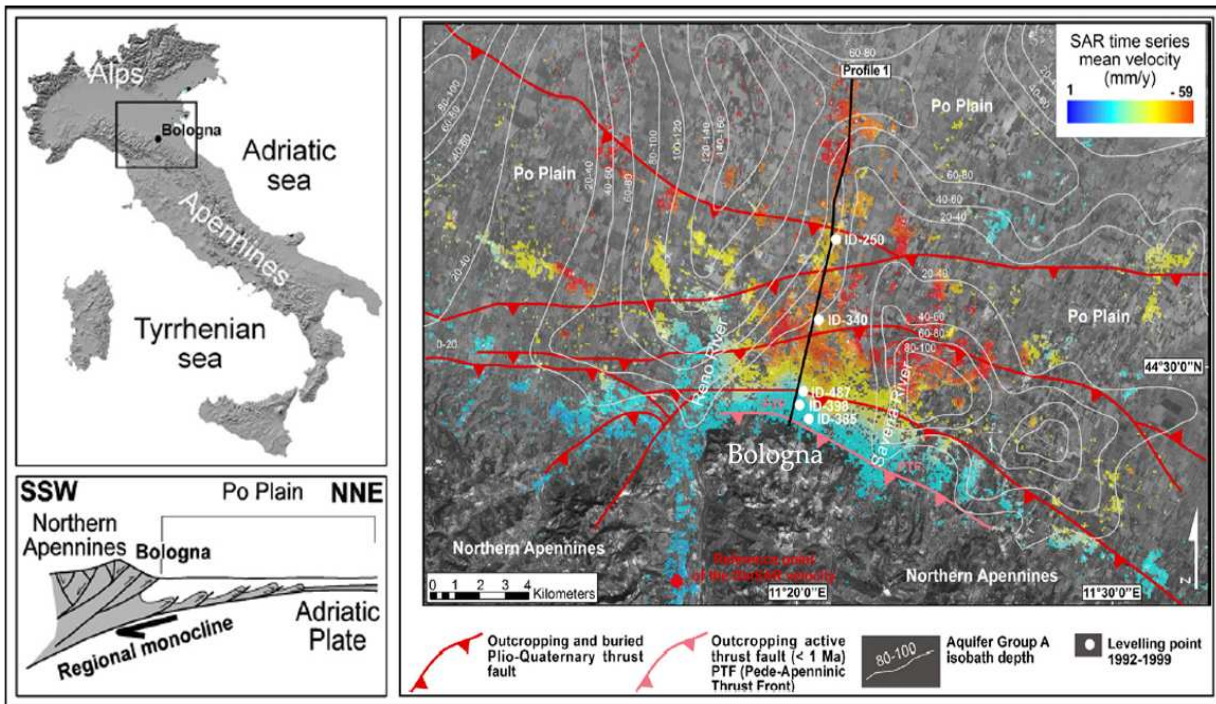
Figure 2.7 – Schematic geological section of the Bologna area and Surface DInSAR mean deformation velocity map spanning 1992–2000, (redrawn after Stramondo et alii, 2007).

The evolution of the studied area was significantly influenced by morphological changes, together with political and social events of the last centuries. As one of its right tributaries, the Reno River was keeping a transversal direction to the Po (SW-NE), swamping and over flooding in the alluvial plain until its channelization. From the Middle Age to the present, the hydraulic network completely changed with respect to the natural attitude of those areas: the Reno River was forced to flow partially along an abandoned Po River trace. Some important hydraulic structures were designed in order to protect the plain from recurrent destructive floods; among artificial structures, the Napoleonic Channel (completed in 1965) still enables to switch the exceeding part of the greatest flood of the Reno River in the winter, acting as a water reservoir for agriculture in the summer. Also these rivers are affected by subsidence phenomena; the massive vertical displacement taxes, given by the subsidence of the entire area, exceeding from 20 to 40 times the natural taxes, indicate a territory that suffer an antrophic stress, which is responsible of the river bed adaptation, forced in artificial levees. Figure 2.8 shows that the Reno River bed altimetry during the XIX century was 4-8 meters higher than the actual, while its Po Plan segment is characterized by an altitude decreasing of 4-6 meters during last century.

20
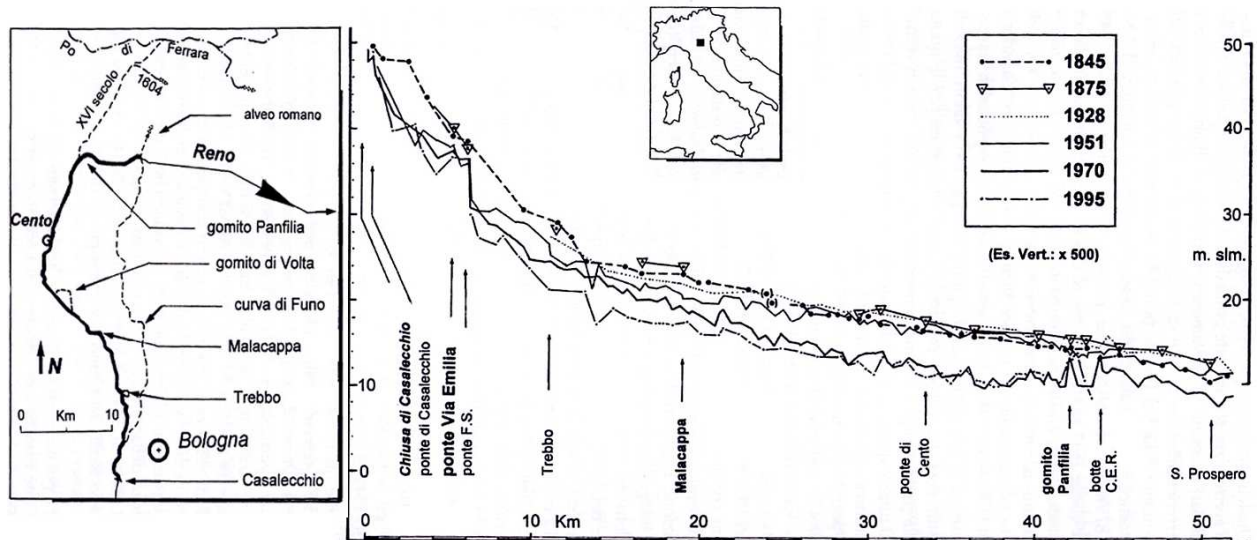
Figure 2.8 – Planimetric contest of Reno River and its longitudinal profile evolution during last century (Cremonini, 2003 redrawn).

Generally, as well as the subsidence issues, embankments are still affected by many different problems (which will be treated in the next paragraph) like erosion, animal excavations, human impacts, but over all by the inappropriate building techniques that have been used throughout their history. Earth materials were usually taken directly from the riverbed, transported and compacted on the natural riverbanks using only wheelbarrows or other poor means of work. As a result, the flood defence system of the complex Reno River network does not operate as it should in many important nodes.

2.4 Problems affecting the river embankments

Regarding the well-developed system of embankments worldwide, homogeneous embankments are the oldest type of structure, constituted in theory by one single type of low permeable material, In some cases with coarser material on the slopes to increase stability and protect the dam from surface erosion. Due to stability problems, or more specifically due to the risk of slips, the slopes must be built moderate, which extends the size of the embankment itself. Earth-fill embankments are mainly constituted by compacted earth material, whereas rock-fill embankments are to the larger extent built up from crushed rock. These types of embankments built in the past are strictly linked to the surrounding presence of construction materials or they were simply built up using the soils, which constitute the riverbed and the adjacent areas.

2.4.1 Ideal dam

Basically, an ideal embankment or dam, which corresponds to the recent constructive criteria (for example adopted for the construction of protection works in Sweden) can be hypothesized as a complex structure divided in zones; each zone then has different material properties and functionality (figure 2.9). The principal zones are composed out of various materials with different properties and functionality according to the following:

- Core: this is the low-permeable zone of the dam, and its main purpose is to control the seepage flow through the dam. The core consists typically of fine-grained soils, such as clays, clayey sands and silty sands (Fell et al. 1992). Recommended tills are of a silty or sandy character with 15-40 % fines content, calculated as amount of the soil passing 0.06 mm in relation to the total material passing the 20 mm sieve, and with low content of coarser fractions. Higher percentages of fines content may cause practical difficulties during construction and lower percentages may result in too high hydraulic conductivities. A hydraulic conductivity in the approximate range of 10^{-7} to 10^{-9} m/s is considered satisfactory.

Ideal embankment or dam

▬ Coarse free draining material, high structural stability		▬ Waterproofing core	
▬ Sand or gravelly sand filters		≡ Grouting of cement-bentonite	
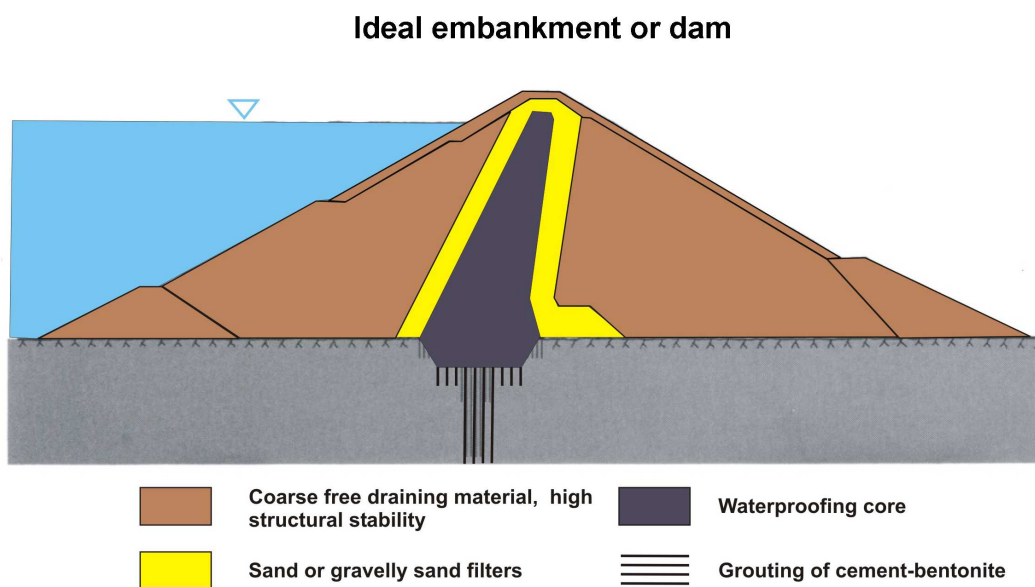
Figure 2.9 - Cross-section of a zoned embankment dam with a central, slightly inclined core; fine, medium and coarse filters and external support fill.

- Filters: the filters constitute a protection against material transport from the core. In addition, seepage water is effectively drained so that pore pressures cannot build up downstream of the core. Filter can be placed in one or more zones, with a gradual increase in grain size from the core and outwards. Between each step, appropriate filter criteria

should be fulfilled. Fine filters are typically sand or gravelly sand and coarse filters are normally gravelly sand or sandy gravel (Fell et al. 1992). The filter zone immediately downstream the core is considered the most important. The filter zone immediately upstream the core may help healing the core if internal erosion occurs, in that material from the filter is transported into the eroded part of the core.

▪ Support fill: the support fill provides stability for the dam. This zone consists of coarse free draining material, commonly crushed rock. For dams with coarse rock-fill, several filter zones are needed to fulfil the filter requirements between filter and fill. In earth-fill embankment, the stability problems, due to the risk of slips, must be taking in accounts and the slopes must be built moderate, which extends the size of the embankment itself.

▪ Grouting of cement-benthonite: the grouting of cement-benthonite represents the zone that aims to guarantee the protection of the embankment basement from the possibility of under-seepage occurrence. The under-seepage phenomenon is frequent for embankments that assure an adequate waterproofing, but are not well connected with the foundation ground; therefore the grouting of cement-benthonite, whereas it doesn't constrain completely the water infiltration, can force the water that eventually permeates from the base of the river bed, to cover a larger distance to eventually outcrops externally.

The correct embankment project section, showed in figure 2.9, is currently used for the new structures construction and, even if its realisation must be validate with constant measurements or monitoring of geotechnical parameters, it can guarantee the resolution of the problems connected with structural failures of the embankments.

2.4.2 Case Histories

In real cases, concerning the well-developed system of artificial embankments built in the past, the building criteria corresponded to the exigencies of a fast and most economical as possible construction. In Europe, almost all the embankments were simply built up using the soils that constitute the riverbed and the adjacent areas. Furthermore, a considerable part of the embankment system is more than one hundred years old and the construction criteria (earth materials were taken transported and compacted on the natural river banks using only wheelbarrows or other poor means of work) are not able to guarantee the complete structural safety as well as waterproofing.

In Hungary, for example, the majority of the flooding events were triggered by an overtopping phenomenon, but an important percentage of dramatically breakages are reported (Nagy & Tóth, 2001); during the 19th and the early 20th century, safety meant identical dike

size (identical crest width, identical slope inclination). Dikes were built and strengthened in line with standardized cross sections along river sections and were reinforced after each flooding, with an increment in dimensions and height, but without the necessary knowledge of the used materials (figure 2.10). The outflow flood hydrograph from a dam failure is dependent upon many factors. The primary factors are the physical characteristics of the dam, the volume of the reservoir and the mode of failure.
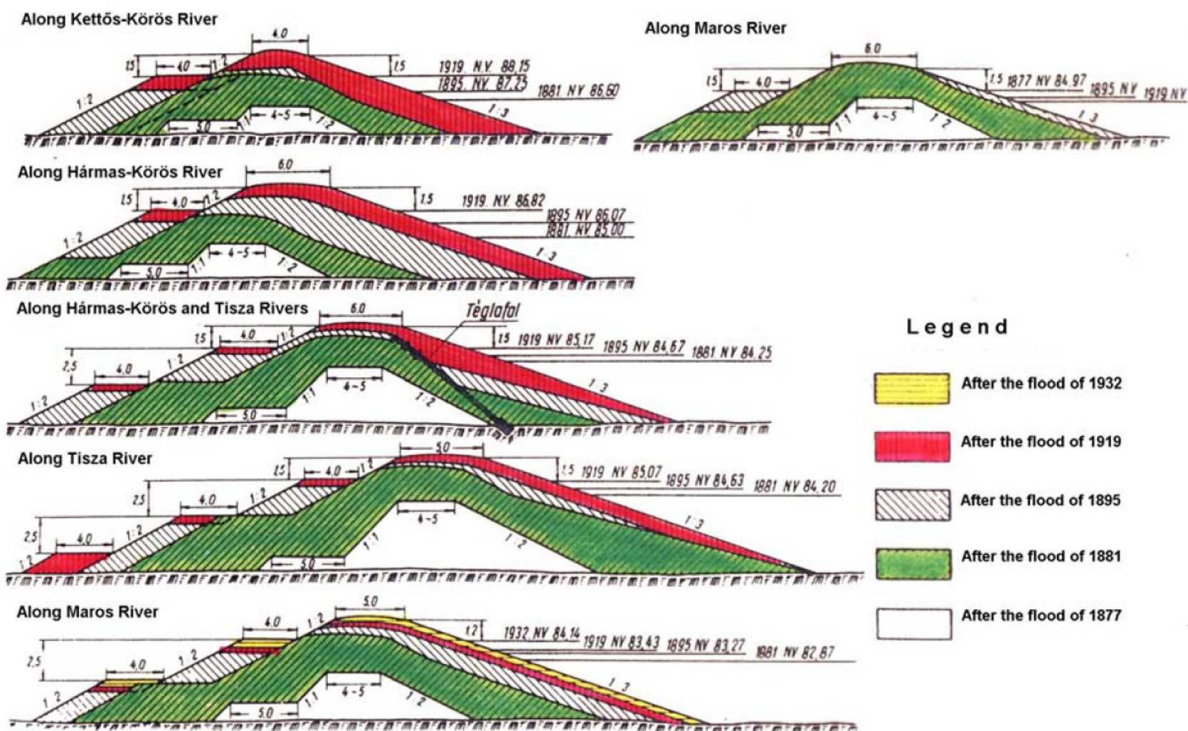
Figure 2.10 - Standard cross sections of many Hungarian rivers, which show the construction modalities trough the time (Nagy & Tóth, 2001).

The parameters, which control the magnitude of the peak discharge and the shape of the outflow hydrograph, include the breach dimensions, the manner and length of time for the breach to develop, the depth and volume of water stored in the reservoir and the inflow to the reservoir at the time of failure. The shape and size of the breach and the elapsed time of the breach development are in turn dependent upon the geometry of the dam, construction materials and the causal agent for failure.

Concerning United States dams and embankments, information on the causal agent for the failures have been collected since the 1850s; technology has obviously changed drastically since that time and improved design standards and construction practices continue to reduce the number of failures. Nonetheless, the relative proportions of dam failures attributable to a specific cause have been remained relatively constant over the years. According to the Washington State Department of Ecology, which provided the summarization of observed

24

causal agents and their frequency of occurrence for 220 dam failures during the period 1850-1950, some consideration must be done (table 2.1). It is interesting to notice that, besides the 30 % of causes that triggered dam failures, due to overtopping phenomena, the 40% of the causes are relative to seepage, piping and internal erosion phenomena, which mean that the failures occurred for inadequate geotechnical and geometrical characteristics. Moreover, the problem result relative to not only old embankments and dams, the Washington State Department of Ecology report evidences that the half of the studied failures occurred in recent dams, in particular within the first five years and the 20 % failed upon first filling. A prevision of breakage, failure events, especially for river embankments is very difficult, both because of the large extension of the embankments themselves and because there is a lack of monitoring measurements which can be capable to define areas of potential structural danger.

CAUSE	SOURCE MECHANISM	% OF TOTAL
OVERTOPPING	FLOOD	30%
PIPING/INTERNAL EROSION OF EMBANKMENT OR FOUNDATION CONDUIT LEAKAGE DAMAGE/FAILURE OF UPSTREAM MEMBRANE/SLOPE PAVING	SEEPAGE, PIPING AND INTERNAL EROSION	25% 13% 5%
EMBANKMENT INSTABILITY-SLIDES	VARIES	15%
MISCELLANEOUS	VARIES	12%

Table 2.1 – Observed causal agents of United States dams failure and their frequency of occurrence for the period 1850-1950 (WSDE, 1992).

Observations on the formation and progress of the breach processes fail in the significant majority of the cases: especially along smaller rivers, only the 'result' can be seen, not the processes. Many breaching episodes in Italy, as well as other European countries, happened without any previous sign. It is very rare that a process leading to dike breach can be observed by anyone, especially by professionals. Even in case of a phenomena threatening with failure, all efforts are concentrated on defence interventions and in case of breach all efforts are concentrated on the preparation of possibly fastest closure of the breach, on evacuation, on the confinement (localisation of inundation) etc., but not on observation,

measurements, data collection. Therefore observation concerning for example the water levels on the protected side starts always with considerable delay (placement of temporary gauges needs time and the same vehicles which are engaged in flood fighting, localisation and evacuation). Indicators of performance of the dikes can be hardly derived from breach data since the majority of breaches were caused by overtopping. Indicators of performance of a flood embankment can be derived from the resistance calculated from the geometry and geotechnical parameters of the dike and that of the foundation layers compared with the loads. Hence, stability or failure probability of dikes can be calculated, and earthen embankments to withstand certain load can be dimensioned. The reverse process, to derive performance indicators from breach parameters is rather difficult due to high scale inhomogeneity of earthen structures. However, with the utilisation of the geophysical methods, selection of dike sections deviating from those in the neighbourhood and posing problems during flood events can be done and the reinforcement of these 'weakest chains' can properly be done.

2.5 Nature of embankment failures

An introduction about the nature of embankment failures must be done, as far as it is quite complex; an inhomogeneity of material properties within the dike body or the subsoil will result in a failure only if definite limits of outside influences will be exceeded. Nevertheless, Niederleithinger et alii (2007) suggest that is possible to identify four main categories, affecting the stability of a dike system and, in regard of them, operate complexes investigations for damage prevention. Figure 2.11 shows that problems due to soil properties of dike or subsoil material can be summarized in four categories: soil properties of dike and subsoil, effects of water, anthropogenic effects, and biological effects.

2.5.1 Soil properties of dike and subsoil

Category A is composed by shear parameters of the soil and stratification of the soil layers; this category play a very important role. As higher the grains size as higher the permeability, which inside the dike body determines the percolation velocity of water through the dike and therefore its stability, too. The stratification of the soil layers is a fundamental factor in areas with presence of coarse sand to gravel horizons: Czech Republic disasters of 1997 and 2003 were triggered also by the occurrence of gravel lenses inside the embankments themselves, which dramatically collapsed during the flooding.
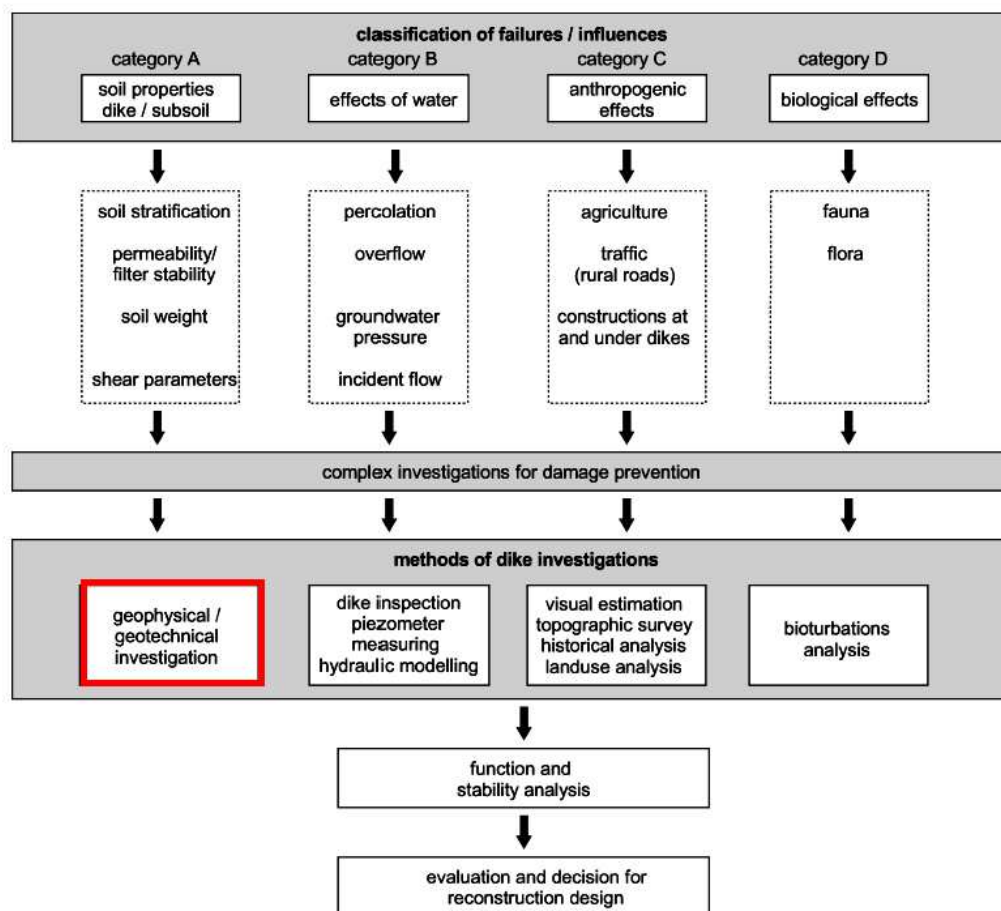
Figure 2.11 - Classification of failures/influences and methods of dike investigations (Niederleithinger et alii, 2007).

Some embankments collapsed, which were mainly composed by sand and gravel, showed also the presence of wooden bars inside the embankment itself, testifying how carefulness during the construction of such important works was neglected (Figure 2.12a).

An embankment is a structure, which has to have the inner part characterized by a waterproofing core, mainly made up of clay material, in order to prevent the water infiltration and the possible internal erosion associated with water percolation. The construction of levees without such impermeable part can trigger hazardous erosion phenomena and compromise the stability of these very important works, figure 2.12b shows the presence of gravel horizons the internal part of the embankment collapsed, which can be recognisable with geophysical methods. As a matter of facts, the figure 2.12c shows a resistivity profile, provided with a Frequency Domain Electromagnetic Method (which will be successively treated) just above the area where the borehole test was provided, nearby the failure zone. The resistivity measured by this device, over the borehole test J19, shows an abrupt increasing, reaching 500

27

Ohm·m of value, evidencing the presence of high resistivity bodies in the subsoil, associated to the presence of gravel.
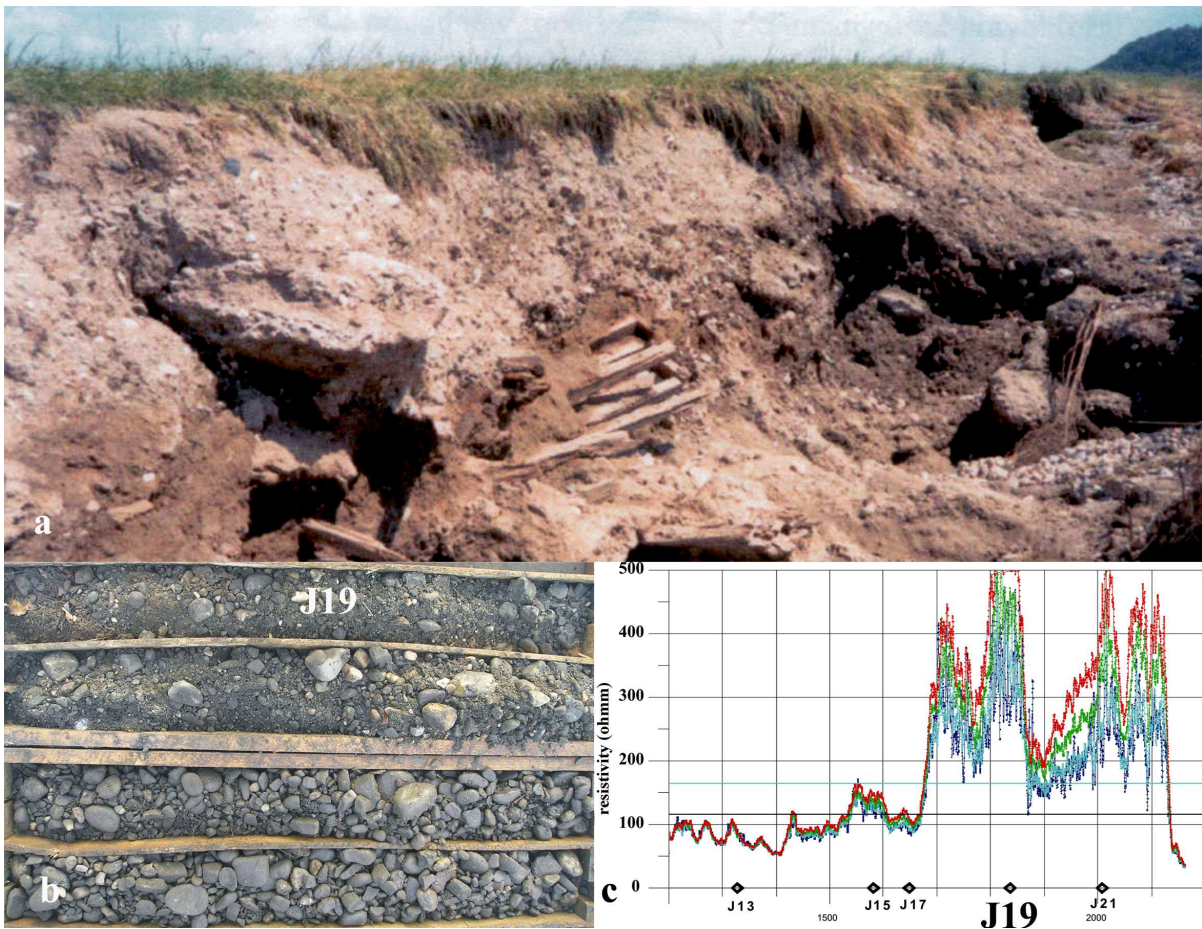
Figure 2.12 – Flooding of 2003 in Czech Republic; a) failure of an embankment composed heterogeneous materials (wooden bars and gravel layers are clearly visible). b) Borehole test, provided near the failure, which evidence gravel horizons and c) FDEM associated profile, provided on the top of the embankment.

Regarding Italian cases, into the Po Plain subsurface, which is mainly constitute of medium-fine material, the occurrence of larger grain size layers or lenses is of importance. The frequent presence of sandy soil horizons, which could be used in the past to build the embankments, is a factor that can seriously compromise the safety of well-developed areas. The Reno River course is regimed by a massive system of embankments, which are sometimes 12 m high, and were mainly made up with materials retrieved in the immediate surroundings. These materials were therefore usually also taken directly from the riverbed and compacted on the natural riverbanks using only wheelbarrows or other poor means of work; a detailed knowledge of their composition is absolutely of importance. In some cases the grain size conditions also of the subsoil can waste the action of protection works as levee or dams; the Napoleonic Channel case is an emblematic example. The Napoleonic Channel was originally designed with the purpose of diverting part of the floods of the Reno River into the

River Po, or if needed to keep a considerable volume of water inside its own bed, in order to reduce the flooding (overbank spillage) risk along the artificial course of Reno River. The historical studies and reconstructions carried out demonstrate that the excessive attention of the designers to the hydraulic efficiency of the channel has generated important geotechnical drawbacks, such as the intersection of the waterway with abandoned channels just under the channel bed, which trigger the embankments under-seepage phenomenon. Because of the very high permeability of such channel bed, the "Cavo Napoleonico" cannot be used at its maximum capacity. Indeed, in the past when the fill-in volume exceeded one-third of the maximum filling size, several seepage phenomena occurred in the surrounding areas.

2.5.2 Effects of water

The second influence (category B) is the effect of water; the water percolates through the dike body and may cause instabilities due to processes of suffusion and erosion. Actually, one of the most common failure scenarios of embankment and dams starts with internal erosion. It can be described as process where soil particles from the inner parts of the bank are being carried downstream by the seepage. The process may then accelerate with increasing seepage flow, followed by further transport of fines, and so forth. Finally, a severe leakage and high water pressure in the inner body or foundation will be obtained, which may lead to the failure of the embankment. The duration of the process from the start of an increased seepage to a complete failure of the structure may vary considerably, from a few hours to many years. Due to the large body of work that has completed on embankment erosion and piping research, and the fact that the work is the product of international and multi-discipline study, there are a number of definitions in the literature regarding piping phenomena. It was common for practicing engineers to lump all these definitions under the generic term ''piping''. For a detailed discussion about the piping definitions, the Richards & Reddy (2007) paper is recommended. According to the authors, based on accumulation of 267 dam piping failures, the piping cases were statistically analysed. The majority of piping failures may be attributed to a variety of causes, such as piping along conduits, other structures and internal erosion (49.8%) into or along foundations or abutments (15%), or piping due to biological activity (4.1%). It is interesting to note that the dams that failed by biological activity are commonly less than 9 m in height and that failure by piping into the foundation tends to occur in large dams. In some cases the seepage and consequently the internal erosion process initiates but stops as the embankment heals by itself. In any case, there is a strong urge to detect such a process at an early stage of its development or, however, before its

complete failure. Moreover, if the surface water table exceeds the top of the embankments, the surface erosion could result in an immediate breaking of the dike. The high pore pressure behind the levees is sometimes responsible for base failure and uplift problems. Last but not least, the high current velocity of the river water accompanied by a direct incident flow to the levee front (*flow stress*) is another cause of failure.

2.5.3 Anthropogenic effects

The human activities in the surrounding of the dike systems, i.e. agriculture, traffic and constructions of buildings or pipes in or beneath the dike are classified as category C. All of the previously mentioned activities mainly affect the safety of dikes. Damages on the grass cover of the dike could result in erosion problems, potentially dangerous, as well as the insufficient control by the authorities of both the vegetation state and structural conditions of the embankment. Constructions at or within the dike body are preferential ways of strong gradient of water flow. The 1990 breaking event in Reno River indeed is attributable to the presence at the embankment base level of a large conduit, properties of SNAM gas society, which compromised the stability of such embankments segment. As a matter of facts, several conduits and pipelines pass nowadays through the embankment bodies of the Po Plain, mostly of them are regularly built and in safety conditions, nevertheless this territory is afflicted by several cases of illegal excavations or prohibited land use. Niederleithinger et alii (2007) reports that topographic surveys, a constant visual estimation and both historical and land use analysis are the common methods of dike investigation for anthropogenic effects. Geophysical methods (GPR, EM induction methods, which can detect metallic objects or conduits) can be important tools also to prevent damages created by anthropogenic issues.

2.5.4 Biological effects

Dikes are part of the landscapes and influenced by biological processes (category D). Digging activities of animals and roots of plants have negative effects on the dike stability. As a result, voids may occur in levee bodies. Dikes are part of the landscapes and influenced by biological processes. Despite of the strong Po Plain anthropization, several mammals have found a comfortable habitat both in the internal and external part of river embankments, where they are proliferating. Often the embankments are not constantly surveyed and their maintenance works (cleaning, vegetation cutting) are neglected; such animals create their lairs when particular environmental characteristics occur. High vegetation coverage, quite areas and soft soils, which are easy to dig are favourable to the cavities proliferation.

The species that can be found on the river embankment habitat are some various mammal types: the European badger (*Meles Meles*)**,** the fox (*Vulpes Vulpes*)**,** the wild rabbit (**Oryctolagus cuniculus)* and the nutria (*Myocastor coypus)*. While the fox and the European badger are animals historically involved in soils and dikes erosion, recently the occurrence of others species has significantly increased the embankment safety issues. Their habitude is represented by digging of long, deep and articulate cavities to provide the children safety, sparking the possibility of collapses. The collapse process is indicate in Figure 2.13; when the cavity is dug inside internal side of the embankment, after heavy precipitations, the rising water can inundate it, activating the central part of the levee imbibition. When the water phase out of the cavity, a collapse can be triggered. While the nutria creates generally cavities in the internal flanks of the embankment because of the water necessity, foxes and European badgers, as well as wild rabbits, dig their lairs in the external part of such structure. Obviously, a cavity dug in external flank is less dangerous but foxes and European badgers can reach such large depths that in case of embankment imbibition, their hole inside the structure can create several stability problems in itself. Often the embankments are not constantly surveyed and their maintenance works (cleaning, vegetation cutting) are neglected; such animals create their lairs when particular ambient characteristics occur. High vegetation coverage, quite areas and soils, which are easy to dig are favourable to the cavities proliferation.
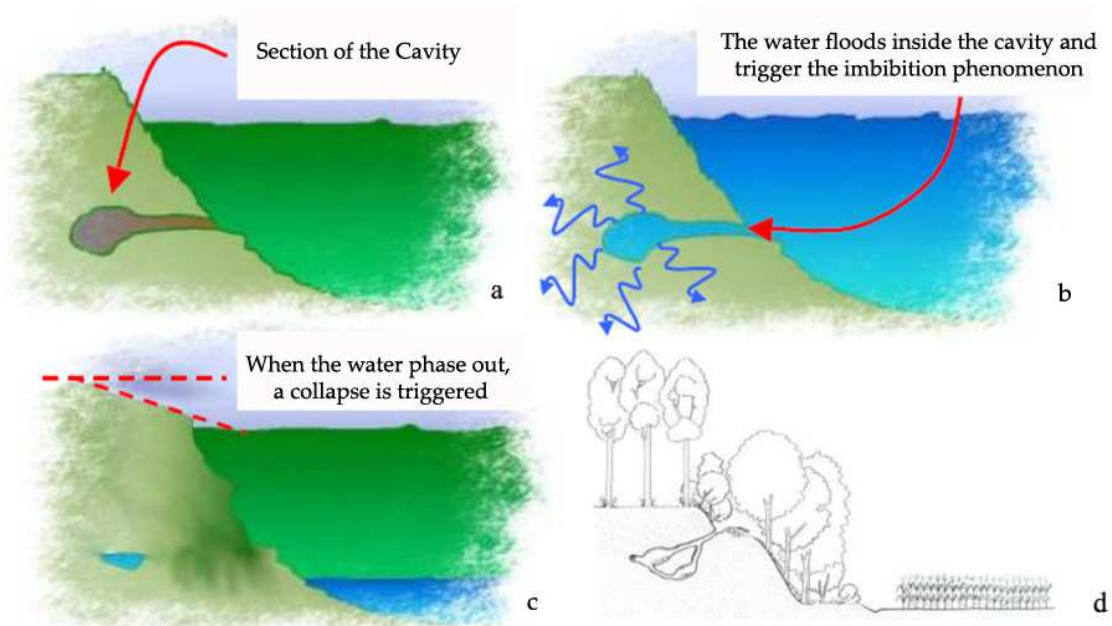
Figure 2.13 – Example of animal cavities developed on river embankments: a), b) and c) processes of embankment collapsing (Covelli, 2006, modified). d) Example of cavity on the levee external flank.

All the categories of failures / influences previously stated require complex investigations for damage prevention, apart of well-known historical studies and destructive methods, the geophysical investigations can be an important tool in function of a correct embankment safety modelling and evaluation.

2.6 The Reno River case

After the depiction of the geological and geographical setting of the study area and the description of the possible problems affecting the embankments, a summary for the Reno River situation must be formulate. The Reno River embankments system has shown in the Po Plain territory a series of geotechnical and hydraulic problems that in many cases, during exceptional flood events, resulted in catastrophic inundations. The main causes of these problems (evidenced in figure 2.14) can be related to:

- Land subsidence
- Variations in water discharge;
- Variations of river bed profiles;
- Anthropogenic interventions (expansions of urban areas, quarry exploitation of the river beds, underground excavations, presence of conduits etc.);
- Consolidation of underground terrains (below the dykes);
- Consolidation of the earth embankments (dykes);
- Piping or seepage problems;
- Animal excavations and biological alterations.

The levees, inspected with standardised field or laboratory tests were and are still affected by many different problems like subsidence, erosion, landslides, piping, animal excavation, human impacts, but over all by the inappropriate building techniques that were used throughout history. As a result, the flood defence system of the complex Reno River network does not operate as it should in many important nodes. The knowledge of the existence and the position of eventually non-homogeneity zones into the embankment are relevant problems in term of hazard and hydraulic risk, especially because Reno River embankments themselves are old (more than one century), inserted in a densely populated area, subjected to periodic important floods.

The need to carry out a survey of hundreds of kilometres of river embankments in the Reno River catchment for identifying, primarily, these weakness zones, is also a requirement of the regional government authorities. Therefore, the STBR (Regional Technical Service of the Reno River Basin) of the Emilia-Romagna Region and the Department Of Earth and Geo-environmental Sciences of Bologna University have stipulated an agreement in order to verify the GPR and other geophysical methodologies (FDEM, ERT, MASW) suitability in the study of river embankments.
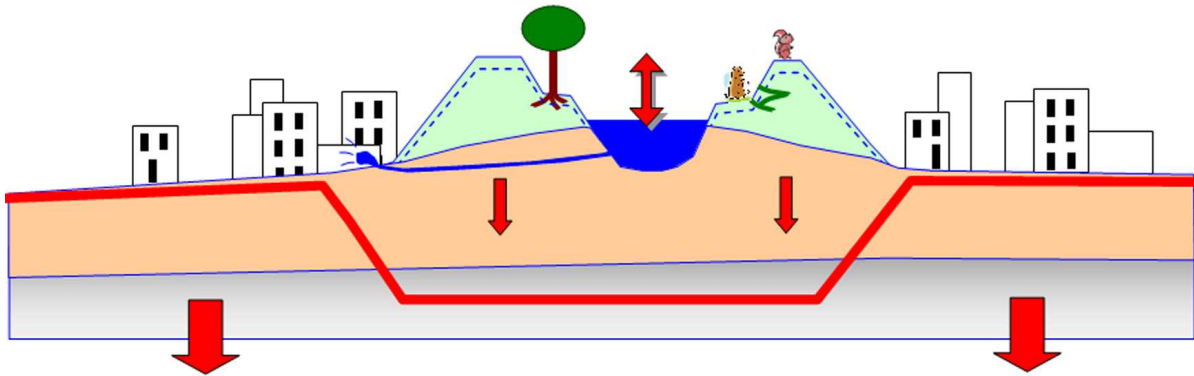
Figure 2.14 - Problems affecting a hypothetical Reno River section (not in scale).

The main purposes were the detection of stratigraphy, animal cavities and burrows, buried pipelines, non-homogeneities in general and also related to various phases of construction and repaired areas of the embankment itself.

2.7 Geophysical methods applied to river bank investigations

Applied geophysics can contribute to the solution of most geotechnical engineering and environmental problems; obviously, the geophysical technique often does not directly measure the parameter needed to solve the problem under consideration and it is based on many geologic assumptions. Geological division of environment is given by its lithological diversity. Although the geophysical division is derived from classification of environment according to its physical properties, it is not identical with its geological division. Each geophysical procedure measures a contrast (e.g. GPR utilizes the contrast of electric properties) and the correlation of measured geophysical contrasts with geologic inferences, which is most often empirical and dependent on the quality of both the results and the hypotheses, is a crucial point to achieve the knowledge of the tasks.

2.7.1 Geophysical Parameters

Geophysical parameters are dependent on surveyed environment. Response of these parameters during the measurement is given by physical properties of soils. Generally, the following soil properties are considered to belong among the basic ones: density, strength, compressibility, stability (resistivity to weathering) and permeability. These properties are crucial for evaluation of the earth or rock material from the geotechnical point of view. These properties may be determined directly i.e. by laboratory tests or by the field measurement. Water significantly influences the physics and mechanical properties of soils. Its presence changes also soils geophysical parameters. Content of water in the soils is given primarily by measure of porosity of the environment (and thus also of permeability) and other physically chemical properties. Limiting the focus to the problems of embankment bodies, serving as protective barrier against the increased water levels, presence of water in these bodies is thus totally cardinal for their reliable functioning. Therefore, definition of environment from its geophysical properties point of view, such methodologies can discriminate layers or blocks differing from their surrounding by their physical properties, as density, specific resistivity, velocity of propagation of elastic waves, etc. This hypothesis itself, as already affirmed, may require geologic assessment with borings or other field exploration, nevertheless non-destructive geophysical methods should have capabilities for fast reconnaissance, optimization of borehole locations and interpolation between them.

2.7.2 Background

Varieties of methods have been attempted for dam status investigations and leakage detection investigations on embankment dams. Johansson et al. (2003) summarises new possible methods for investigations of embankment dams in a comprehensive report. Numerous methods are considered useful for dam integrity investigations in a limited zone of the dam. For detection of anomalous seepage and internal erosion, however, it is concluded that the self-potential method (IS), the resistivity method and temperature measurements may have the best prospects. Nevertheless, all of these geophysical measurements assure a time-consuming adequate knowledge only for short segment or parts of the embankment itself. When something like hundred kilometres of embankment structures needs to be investigated, the necessity of faster measurements of the material properties is evident.

Recently, a geophysical characterization of a portion of American River levees in Sacramento, California, was conducted in May 2007. Targets of interest included the distribution and thickness of sand lenses that underlie the levees and the depth to a clay unit

that underlies the sand. The concern was that the erosion of these sand lenses could lead to levee failure in highly populated areas of Sacramento. Resistivity (OhmMapper by Geometric and SuperSting R8 systems by Advanced Geosciences Inc.) and electromagnetic surveys (GEM-2 by Geophex) were conducted over a 6-mile length of the levee on roads and bicycle and horse trails. Two-dimensional inversions were conducted on all the geophysical data. The results showed that six areas were suggested as possible trench locations to verify the interpretation presented in the report (Asch et alii, 2008). These six locations were selected because they overlie either thick sand lenses, clay deposits, or a mixture of both. Trenching in these locations should provide greater confidence in the interpretations presented for the rest of the area investigated. Despite issues with the GEM-2 inversion, this geophysical investigation successfully delineated sand lenses and clay deposits along the American River levee system and the approximate depths to underlying clay zones. The results of this geophysical investigation should help the U.S. Army Corps of Engineers (USACE) to maintain the current levee system while also assisting the designers and planners of levee enhancements with the knowledge of what is to be expected from the near-surface geology and where zones of concern may be located.

Morris (2005) realised that, concerning geophysical methods applied to river levees investigations, there is a lack of information on selection of suitable methods, measurement parameters, spacing etc., especially when both velocity of acquisition and accuracy of results are required. Only recently, some scientific articles have been released and many researches are starting all around Europe and North America, demonstrating how this field can represent an open task of primary importance for human activities safety. Although geophysical division of environment is specific, its qualitative and quantitative aspect may serve to determination of needed specifics, dependences, and parameters, which are crucial for their reliable function. The stability of embankments is primarily given by their structure and building material. Substantial element is the amount of contained water, primarily in relation to the water in the surface watercourse. The IMPACT Project, which was the base for the development of this research, utilized and compared several geophysical methodologies to assert the physical parameters and therefore describe all the embankment parameters and structural defects, evaluating the usability of each tested method (Figure 2.15), in order to assure a safety protection of river levees. The test areas were along chosen Czech Republic Rivers, which are bounded by embankments that differs in geometrical as well litotechnical characteristics from Italian Po Plain Rivers, being smaller and made up of larger grain-size materials. However, by application of appropriate complex of methods and adequate field

measurement methodology, with the help of received data, which represent current response of the rock environment to the parameters measured within the certain geophysical field, relatively reliably current conditions of material of the protective embankments may be determined. According to IMPACT project, electric resistivity methodology is the most recommended way to describe dike structure and homogeneity, seepage phenomenon and to recognise lithologic contacts until a reasonable depth. However, seismic and gravimetric measurements can provide important information also about geo-mechanical parameters, allowing a detailed description of the embankment structure.

Geophysical method	Observed physical parameters	Embankment survey usability evaluation	Parameters and Defects
Geoelectric methods	Specific electric resistance Conductivity Electric potential	Recommended	Dike Structure and Homogeneity Seepage Contact Dike - Subsoil
GPR – geological radar	Relative permitivity Specific electric resistance	Suitable	Dike Structure and Homogeneity
Seismic methods	Elastic waves diffusion velocity Elastic waves frequency	Suitable	Geomechanical Parameters Contact Dike - Subsoil
Gravimetry	Gravitation acceleration Specific volume weight	Suitable	Geomechanical Parameters
Thermometry	Temperature Temperature flow	Suitable	
Magnetometometry	Magnetic susceptibility Magnetisation	Conditional	
Radiometry	α, β, γ activity radionuclides content	Conditional	

Figure 2.15 – An overview of common dike defects and geophysical methods appropriate for the detection of such defects and physical parameters involved (Morris, 2005, redrawn).

Therefore, seismic, gravimetric, as well as self-potential and electric tomography methods, have a drawback strictly linked with their velocity of acquisition; indeed the total length of river network in the Reno plain basin is too spread (about 500 km long) for the usage of common geophysics techniques in a preliminary phase of study, searching for hazardous areas. Looking for lower time-consuming methods, providing also a reasonable resolution for the detection of non-homogeneities, the attention has turned to alternative methods such as ground-penetrating radar (GPR) and, by the way, in FDEM or also dipole electromagnetic profiling method. The innovative electromagnetic method (FDEM induction), employing the GEM-2 device, was tested and verified in European Projects (Boukalová & Beneš, 2007); it carries out basic assessment of the dikes condition and their material

composition in large areas with quick and not highly money-consuming measurement. In the following chapters, will be analyzed in more details the GPR methodology and a comparison with other geophysical methods in relationship to their application for determination of states, properties, and character of material of protective embankment bodies will be provided.

3. GROUND PENETRATING RADAR

The possibility of detecting buried objects remotely has fascinated humankind over centuries. A single technique, which could render the ground and its contents clearly visible, is potentially so attractive that considerable scientific and engineering effort has gone into devising suitable methods of exploration. Yet, no single method has been found to provide a complete answer, but seismic, electrical resistivity, induced polarization, gravity surveying, magnetic surveying, nucleonic, radiometric, thermographic and electromagnetic methods have all proved useful. Ground penetrating radar has been found to be an attractive option.

The term "Ground Penetrating Radar (GPR)", "ground probing radar", "sub-surface radar" or "Surface-Penetrating Radar (SPR)" refer to a range of electromagnetic techniques designed primarily for the location of objects or interfaces buried beneath the earth's surface or located within a visually opaque structure. Daniels (2004) prefers the term "Surface Penetrating", as it describes most accurately the application of the method to the majority of situations including buildings, bridges etc as well as probing through the ground. GPR provides a safe and non-invasive method of conducting fast searches without the need of unnecessary disruption and excavation. GPR has significantly improved the efficiency of the exploratory work that is fundamental to the construction and civil engineering industries, the police and forensic sectors, security/intelligence forces and archaeological surveys. GPR was used for surveying many different types of geological strata ranging from exploration of the Artic and Antarctic icecaps and the permafrost regions of North America, to mapping of granite, limestone, marble and other rocks as well as geophysical strata; its application to river embankments is an open task that is rapidly acquiring importance.

3.1 Basis of Electromagnetic theory

In 1873, the Scottish mathematical physicist James Clerk Maxwell unified the observations early in the 19th of electrical and magnetic phenomena century by Coulomb, Oersted, Ampère, Gauss and Faraday. Maxwell gathered existing knowledge and unified it in a way that allowed the prediction of other phenomena. He proposed the theory of the *electromagnetic field*, which classifies light as an electromagnetic phenomenon in the same sense as electricity and magnetism. This ultimately led to the recognition of the wave nature of matter. The German physicist Heinrich Hertz established the existence of electromagnetic

wave experimentally in 1887, eight years after Maxwell's premature death (e.g. Lowrie, 1997). Constitutive relationships are the means of quantifying the physical properties of materials. In EM induction and GPR methods the electric and magnetic properties are of importance. Constitutive equations provide a macroscopic description of how electrons/atoms/molecules/ions etc., respond en masse to the application of a field. Coulomb's law shows that an electric charge is surrounded by an electric field, which exerts forces on other charges, causing them to move, if they are free to do so. Ampère law shows that an electric charge (or current) moving in a conductor produces a magnetic field proportional to the speed of the charge. If the electric field increases, so that the charge is accelerated, its changing velocity produces a changing magnetic field, which in turn induces another electric field in the conductor (Faraday's law) and thereby influences the movement of the accelerated charge. The coupling of the electric and magnetic fields is called *electromagnetism*. If two straight conductors are laid end-to-end and connected in series, they act as an electrical dipole. An alternating electric field applied to the conductors causes the dipole to oscillate, acting as an antenna for the emission of EM wave. An electromagnetic wave consist of a magnetic field *H* and an electric field *E*, which vary with the frequency of the oscillator, and are oriented at right angles to each other in the plane perpendicular to the direction of propagation (Fig.3.1).
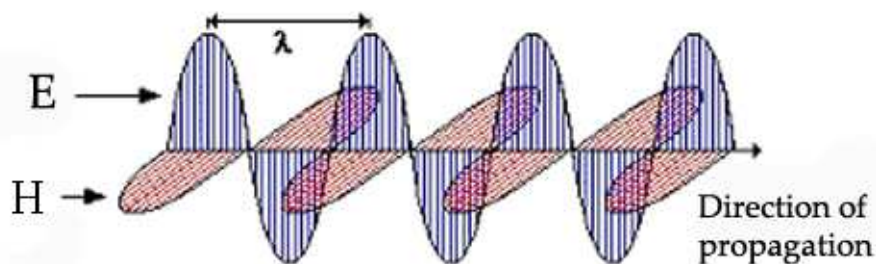
Figure 3.1 – Electromagnetic wave; electric (E) and magnetic fields (H) fluctuate normal to each other in the plane normal to the propagation direction.

In a vacuum all electromagnetic waves travel at the speed of light (c=2, 99792458*10^8 m s^{-1}, about 300000 km s^{-1}), which is one of the fundamental constants of nature. The derivation of electromagnetic field equations from Maxwell's equations is beyond the level of this thesis, but their meaning can be understood: taking in accounts that:

σ = electrical conductivity;

μ = magnetic permeability; which in most material (unless they are ferromagnetic) is close to the value for the free space ($\mu_0 = 4\pi$ x 10^{-7} NA^{-2}).

40

ε = electrical permittivity of the material, that it will be deeply treated in this chapter.

Two equations, identical in form, are obtained; they describe the propagation of *magnetic field H* and *electrical field H* vectors, respectively and they can be written as:

$$\nabla^2 H = \mu_0 \sigma \frac{\partial H}{\partial t} + \mu_0 \varepsilon \frac{\partial^2 H}{\partial t^2} \qquad (3.1)$$

$$\nabla^2 E = \mu_0 \sigma \frac{\partial E}{\partial t} + \mu_0 \varepsilon \frac{\partial^2 E}{\partial t^2} \qquad (3.2)$$

where $\nabla^2 = \dfrac{\partial^2}{\partial x^2} + \dfrac{\partial^2}{\partial y^2} + \dfrac{\partial^2}{\partial z^2}$

By the way, an important relationship can be immediately stated: the amplitude of the magnetic field can be directly related to the electric field and vice versa because of the field coupling. A common term in electrical engineering is the *electromagnetic impedance Z*, defined as:

$$Z = \frac{E}{H} = \sqrt{\frac{\mu}{\varepsilon}} \qquad (3.3)$$

In equations (3.1 and 3.2), the left side describes the variation of the respectively *H* and *E* component of the electromagnetic wave in space (conduction in a conductor); the right side identifies its variation with time and so its frequency dependence (displacement currents, introduced by Maxwell). Electromagnetic radiation encompasses a wide frequency spectrum. It extends from very high frequency (short wavelength) to low frequency (long-wavelength) radio signals. Two ranges of electromagnetic radiation are of particular importance for the geophysics methods here treated: a high-frequency range for the GPR application and a low-frequency range for EM induction (figure 3.2).
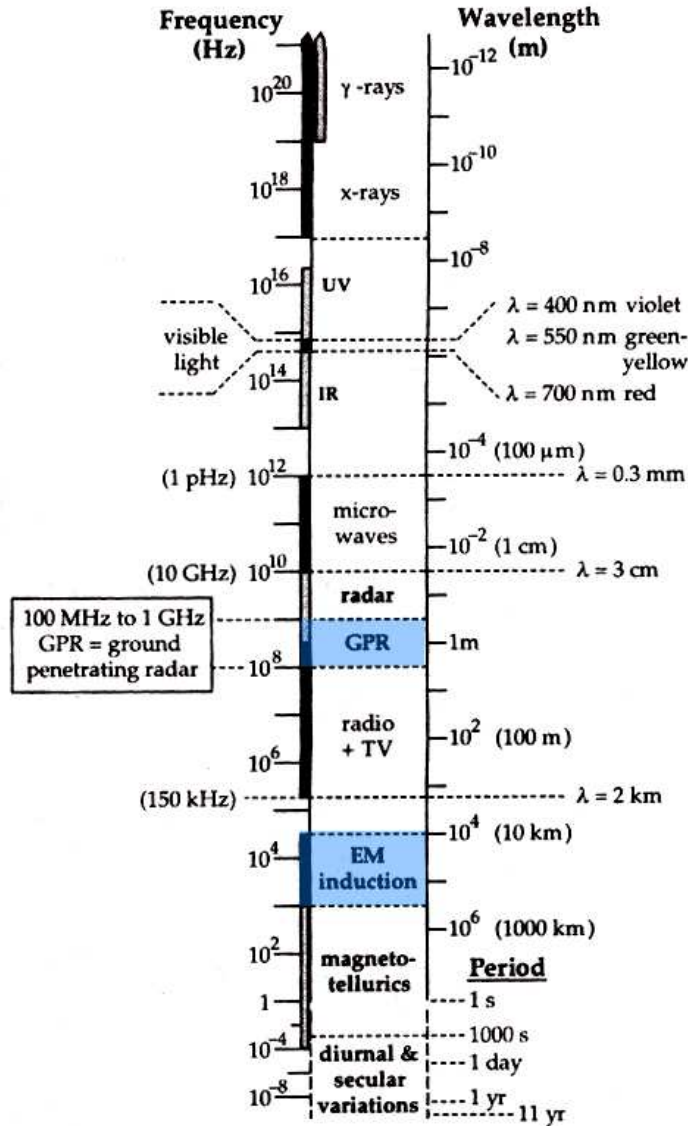
Figure 3.2 – The electromagnetic spectrum, showing the frequency and wavelength ranges for the most common electromagnetic surveys (Lowrie, 1997).

Ground penetrating radar is also an electromagnetic (EM); however, it differs significantly from the induction EM method. At the lower frequencies (kilohertz range) where EM induction instruments operate, conduction currents (currents that flow via electrons in a metallic matrix or ions in solution) dominate and energy diffuses into the ground. At the higher frequencies (megahertz range) used by GPR, displacement currents (currents associated with charges that are constrained from moving any distance) dominate and EM energy propagates into the ground as a wave (Bennett et alii, 2005).

3.2 GPR methodology

3.2.1 Historical mentions

The first use of electromagnetic signals to determine the presence of remote terrestrial metal objects is generally attributed to Hülsmeyer in 1904, but the first description of their use for location of buried objects appeared six years later in a German patent by Leimbach and Löwy. Their technique consisted of burying dipole antennas in an array of vertical boreholes and comparing the magnitude of signals received when successive pairs were used to transmit and receive. These authors described an alternative technique, which used separate, surface-mounted antennas to detect the reflection from a sub-surface interface due to ground water or to an ore deposit. The work of Hülsenbeck, in 1926 appears to be the first use of pulsed techniques to determine the structure of buried features. He noted that any dielectric variation, not necessarily involving conductivity, would also produce reflections and that technique, through the easier realisation of directional sources, had advantages over seismic methods. Pulsed techniques were developed form the 1930s onwards as a means of probing to considerable depths in ice, fresh water, salt deposit, desert sand and rock formations. In 1960, John C. Cook made the first proposal for using radar to detect subsurface reflections in his article "*Proposed monocycle-pulse, VHF radar for airborne ice and snow measurements*" (Cook, 1960). Cook and others continued to develop radar systems to detect reflections beneath the ground surface (1974, 1975). Annan and Davis (1976) did work focussed on permafrost soil applications. Probing of rock and coal was also investigate by Roe and Ellerbruch (1979), although the higher attenuation in the latter material meant that depths greater than few meters were impractical. A more extended account of the history of GPR and its growth up in the mid of 1970s is given by Nillson (1978).

Renewed interest in the subject was generated in the early 1970s when lunar investigations and landings were in progress. From the 1970s until the present day, the range of applications has been expanding steadily, and now includes building and structural non-destructive testing (Soldovieri et alii, 2006), archaeology (Goodman, 1994; Leucci, 2006), road, railways track and tunnel quality assessment (Sussmann et alii, 2003, Cardarelli et alii, 2003). Other applications consist in location of voids and containers, tunnels and mineshafts (Hendrickx et alii, 2003), pipe and cable detection (Lester & Bernold, 2006), as well as remote sensing by satellite. Purpose-built equipment for each of these applications is being developed and the user now has a better choice of equipment and techniques. After an experimental period concerning mostly archaeological and urban purposes (Al-Quadi and

Lahouar, 2005; Loizos and Plati, 2007), interest in GPR survey for geological issues increased considerably in the 1990s. As an example, the GPR has unquestionable advantages, respectful of other techniques for the estimation of detritic cone thickness of hardly accessible mountain areas (Otto and Sass, 2005). Moreover, GPR capability in the determination of buried geological structures makes this technique a powerful tool in sedimentology (Smith and Jol, 1995; Jol & Bristow, 2003); even if the extraction of meaningful information on the deposition style and on the sedimentary structures needs systematic and accurate data processing (Neal, 2004). In geological and geomorphological studies, Schrott and Sass (2008) suggest using the GPR technique integrated with other geophysical techniques, in order to prevent interpretation misunderstandings. Concerning the application of GPR to river embankments, very few applications are to date known for this issue (Morris, 2005; Niederleithinger et al., 2007).

3.2.2 Ground Penetrating Radar System

Ground penetrating radar (or GPR for short) is the general term applied to techniques which employ radio waves, typically in the 10 to 1000 MHz frequency range, to map structure and features buried in the ground (or in man-made structures). However, the GPR description has become almost universally accepted and its technology is largely applications-oriented and the overall design philosophy, as well as the hardware, is usually dependent on the target type and the material of the target and its surroundings. The range of applications for GPR methods is very wide and the sophistication of signal recovery techniques, hardware designs and operating practices is increasing as the technology matures (Daniels, 2004). As an understanding of strengths and weaknesses of the method became apparent, its application areas broadened as described by Davis and Annan (1989).

The majority of today's GPR technology is based on ultra-wideband impulse radar principles due to the depths at which most targets are located. A GPR system is conceptually very simple because it is composed by three parts (as shown in figure 2.3): a timing unit or control unit, an antenna and the processing system, represented by a laptop.

Timing unit: the heart of the system is the timing unit that controls the generation of the radar signal and then the detection of received signals as a function of time. Impulse GPR systems generate a very short duration high voltage pulse (Input power: 12V DC, operating in a range 10.5-13 Volts for GPR Zond by Radsys), achieving an adequate Scan Rate. The Scan Rate is the number of vertical traces computed inside the investigated material (ex. 220 scans/sec at 256 samples/scan, 16 bit 120 scans/sec at 512 samples/scan, 16 bit, SIR 3000 by

GSSI). Each scan can is composed by a huge number of samples (256, 512, 1024, 2048, 4096, 8192), and the reflected signal given by the amount of the samples can be amplified by a gain control, manual or automatic, from -20 to +80 dB (Radsys, GSSI).
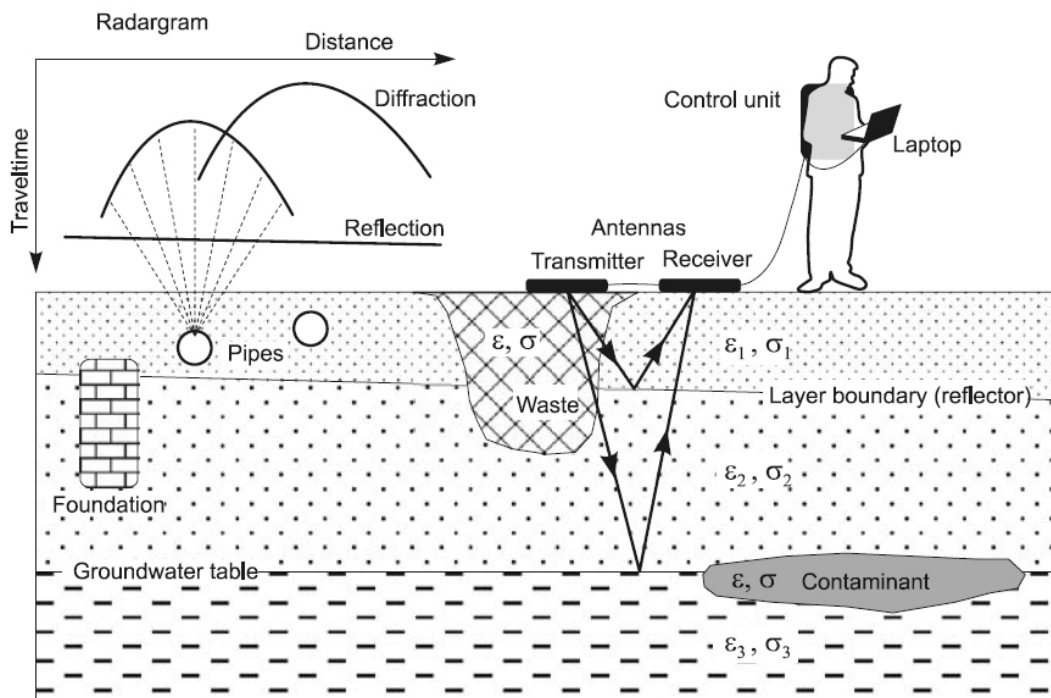
Figure 3.3 - Block diagram depicting main components and principle of a GPR system (Knödel et alii, 2008).

The **Antenna** is designed to radiate the radar signal with fidelity so that the pulse entering the ground is a reasonable facsimile of the electronically generated pulse. In general, the electronics and antenna form an interactive pair which, combined with ground conditions, govern the temporal shape (or frequency content) of the radiated pulse. Among the principal antenna types, which are dipole- folded dipole (low frequency application), horn, and centre-fed, half waves bowtie, the last one is massively used, thanks to its wide broadband. The receiver subsystem is similar to the transmitter in that it consists of an antenna plus an electronics package. The receiving antenna is usually identical to the transmitting antenna; when they are separate by a constant offset the system is called *bistatic*, which is a useful configuration in order to calculate the velocity of the ground with common mid point method (CMP, see "EM wave velocity" section). A GPR is called *monostatic* when the transmitting and receiving antennas are the same. The facts that radiated antenna signals are directionally dependent yields important effects on the received amplitude responses. However, the polarized signal detected by the receiver is dependent upon the scattering properties of the subsurface as well as the properties of the transmitter. All antennas transmit polarized signals

45

and are generally designated to generate one of the three types of polarized wave: linear, elliptical and circular. Most commercially available GPR antennas generate linearly polarized EM waves where E and H are contained in an equiphase plane as they vary in magnitude with time. Elliptical and circular polarization exhibits a rotating E that follows a path that traces an elliptical (or circular) pattern with time, instead linearly polarized waves are unique because E does not rotate with time, then the only way to change the orientation of E in an isotropic material is to reorient the transmitting and/or receiving antenna. Polarization due to antenna orientation is determined by the location of E and H relative to the vertical plane of incidence. The orientation of E and H can be controlled via the orientation of the GPR antennas. For GPR devices that use centre-fed, half wave, dipole antennas, E is oriented parallel to the long axis of the antenna and H is oriented perpendicular to the long axis. There are multiple equivalent terminologies in literature for two common types of antenna polarization used in GPR data collection. These names are based on the orientation of the field intensity components (E or H) to a reference direction, which is often the direction of propagation. Nowadays the most appropriate terminology is suggested by Baker & Jol (2007); the first type of polarization is based on E, contained within a horizontal plane that is perpendicular to the vertical plane of incidence (horizontal polarization or transverse electric polarization, EH, figure 3.4a). The second type of polarization has E oriented within a vertical plane that is generally referred to as vertical, parallel, H (vertical polarization or transverse magnetic polarization, EV, figure 3.4b). For most GPR applications, the direction and magnitude of E relative to a target orientation is more important than the direction and orientation of H; therefore, better results can be obtained knowing in advance the target orientation and how to use antenna orientation to generate E. GPR data are often exclusively collected using broadside antenna orientations, which generate EH polarized data, because EH polarized data generally have a higher signal-to-noise ratio relative to the EV polarized data.

Generating and recording EH or EV polarizations is a function of antenna orientations and the use of reciprocal transmitters and receivers (figure 3.4c); these orientations are not only based on the antenna position relative to each other, but also to their orientation relative to the survey line direction (figure 3.4d).

Besides the different kinds of polarizations as well as orientations, the GPR signal is fed from the antenna to the receiver electronics where it is detected and passed on for recording. Planar impulse radar antennas generally operate closely coupled to the ground and they are usually designed so that the polarization of the transmitted and received signals will be parallel. The exception to this is the crossed dipole antenna, which was used (see Savena

Abbandonato river surveys, Chapter 4) for detecting either linear feature such as voids, pipes and cables in the material or small targets such as buried iron or brick objects. While certain pulses are being reflected back to the receiver, others are being scattered and refracted. The echo captured by the receiver is called a trace and it represents the cumulative reflections over a short period of time (e.g., nanoseconds) in time after a pulse was launched from the transmitter.
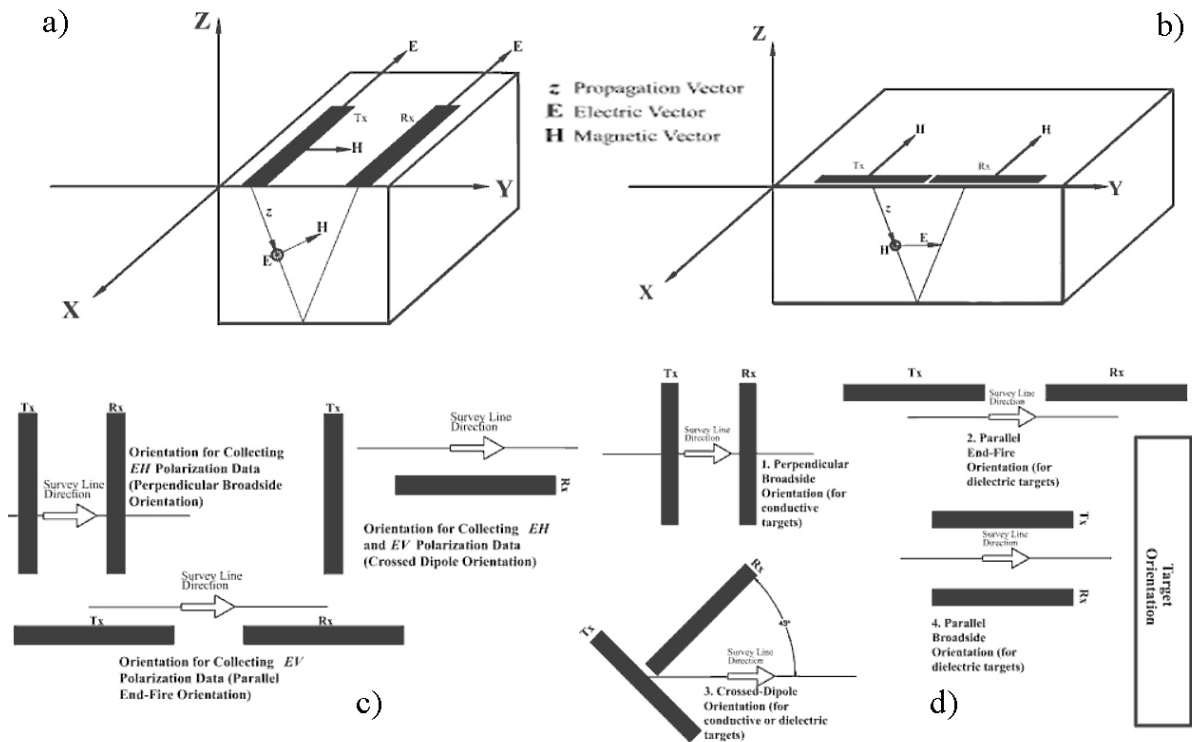
Figure 3.4 – a) EH and b) EV polarizations. c) Common antenna orientations for recording EH and EV polarized waves; d) antenna orientations for delineating buried targets (Baker & Jol, 2007).

The **Acquisition system:** The objective is to measure the magnitude of the received signal as a function of time after the transmitter has initiated. Distance ranging is determined by measuring the time of flight of the signals out to and back from the object detected. The trace produced by the reflected signal is called *Ricker wavelet*, the negative normalized second derivative of a Gaussian function, which is used in seismology due to its *zero-phase* (is symmetrical about zero time) property. The wavelet can be considered as a transient event with a definite time of arrival and finite energy content (Daniels, 2004). Dealing with GPR data, the most important aim of the processing is in the widest sense the extraction of a localised wavelet function from a time series, which displays very similar time domain characteristics to the wavelet. The range of time that can be chosen to analyze two-way travel time of the wave is called *time windows* and it depends by the antenna frequency and material condition.

47
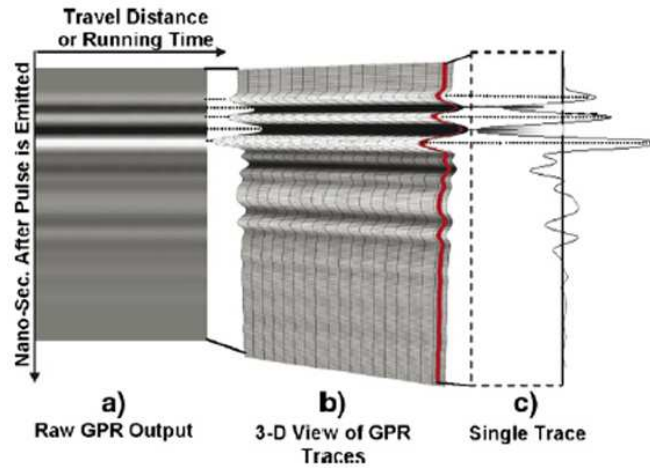
Figure 3.5 - Three views of radar trace profiles in homogenous material (Lester & Bernold, 2006).

The process aims to gather radar data that can be displayed in a *radargram*. A *radargram* consists of several single scans plotted together to form a coherent radar profile. The Figure 3.5 presents the result of moving the GPR across a homogenous half-space with a constant material property; the underground is seldom homogenous especially in embankment structures created by humans. Layers of sands, clays, gravel, are mixed with stones, tree roots, construction debris, and of course, utilities of all kinds. The union of single scans (wiggle/single trace) forms the radargram: this resulting radar images show streaks of black and white bands in various forms and shapes (real vision); some commercial software guarantee the data visualization in other formats, with coloured zones of same reflection amplitude (modular vision). The general procedure when processing data is to store the data in the appropriate dimensional format and then apply appropriate algorithms. With reference of the figure 3.5, the data can be considered of the form:

$$f(x, y, z) = A(x_i, y_j, z_k);$$ (3.4)

over the ranges k = 1 to N, j = 1 to M, and i = 1 to P, with A = data sample; is noticeable that time and depth of the z-axis can be considered to be interrelated by the velocity of propagation inside the material where the wave is circulating. A single waveform or single scan (A-scan or wiggle/single trace) is defined as:

$$f(z) = A(x_i, y_j, z_k);$$ (3.5)

over the range k = 1 to N, j = constant, i = constant, while an ensemble waveform set or (B-scan) is defined as (Daniels, 2004):

$$f(x, z) = A(x_i, y_j, z_k);$$ (3.6)

over the range k = 1 to N, i = 1 to P, j = constant; the figure 3.6 represents the coordinate system for the scan description.
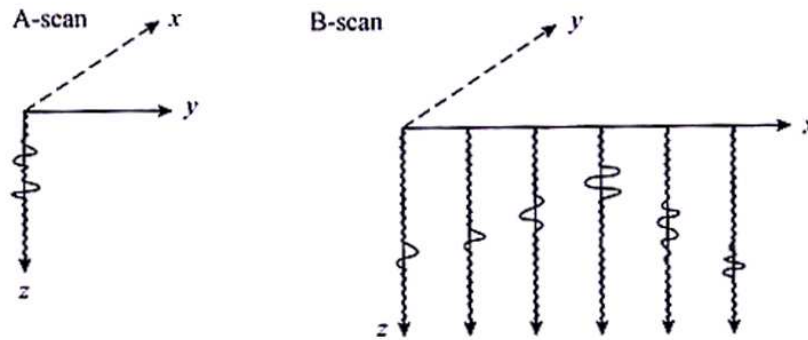
Figure 3.6 – Coordinate system for A-scan and B-scan description (Daniels, 2004).

The selection of suitable signal processing method is very important, considering the objective represented by the optimisation the wavelet output. Processing software hence enables the application of different filters and gain functions to visualize the resulting reflection values as best is possible.

3.2.3 Fundamental parameters

The GPR as well as each geophysical procedure, measures a contrast; in this research, the electrical properties of the ground are considered. Constitutive relationships are the means of quantifying the physical properties of materials. For virtually all practical GPR issues, three quantities (that were previous defined) are of importance; these quantities are treated by simplification as field independent scalar qualities.

Magnetic permeability (μ), which describes how intrinsic atomic and molecular magnetic moments respond to a magnetic field; is a parameter that in normal conditions (not magnetic soils) is considered unitary and can be neglected.

Electric conductivity (σ) is associated to an electric field (E), when it is applied; the electric field creates conduction currents (its density is defined as J). It should be noted that

electrical conductivity and resistivity (ρ) are directly related, being the one the inverse of the other.

$$J = \sigma E \text{, so } E = \rho J \text{ ;}$$ (3.7)

Conductivity represents an energy dissipating mechanism for an electromagnetic field and it influences the EM wave depth penetration and velocity (figure 3.7).
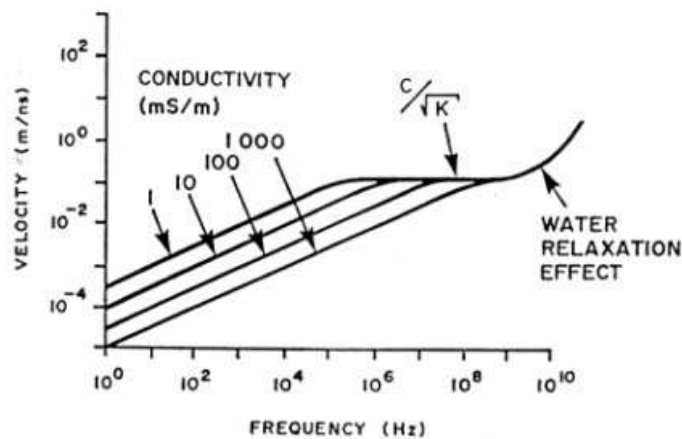
Figure 3.7 – EM wave: propagation velocity versus conductivity of the material involved (Davis & Annan, 1989).

The performance of GPR is therefore dependent upon the electrical conductivity of soils. Soils having high electrical conductivity rapidly attenuate the radar energy, restrict penetration depths and severely limit the effectiveness of GPR. Factors influencing the electrical conductivity of soils include the amount and type of salts in solution and the clay content. Electrical conductivity is a measure of the concentration of water-soluble salts in soils, and is directly related to the concentration of dissolved salts in solution, as well as the type of exchangeable cations and the degree of dissociation of these ions salts on soil particles (Doolittle, 2005).

Dielectric constant or relative permittivity (K) is the ratio of dielectric permittivity of material to that of free space; It is often more convenient to deal with this dimensionless term.

$$K = \frac{\varepsilon}{\varepsilon_0} \text{ ;}$$ (3.8)

The electric permittivity (ε) is associated to the displacement currents, developed with bound charges, which are constrained to limited distance of movement. When an electric field

50

(E) is applied, bound charge moves to another static configuration creating a dipole moment. The dipole moment density is given by:

$$D = E\varepsilon;$$ (3.9)

The electric permittivity is never zero and even in a vacuum (ε_0), it takes on a finite value of 8.85 x 10^{-12} F/m (Farads per meter). In rocks and sediments, dielectric properties are primarily a function of mineralogy, porosity, water saturation, frequency, and depend on the rock lithology, component geometries, and electrochemical interactions. In addition, researchers were able to show that the dielectric constant of soil is a function of the percent of water in the soil, increasing with increasing water percentage in the soil. Therefore, reflections of EM waves are usually generated by changes in the dielectrical properties of rocks, variations in water content, and changes in bulk density at stratigraphic interfaces. The phase polarity of the incoming wavelet will be reversed if the reflection is caused by an interface going from high to low permittivity and conversely. Therefore, by knowing the phase polarity of the direct coupling wave and preferably a reflection from a known interface (metal plate or similar) we can determine if the reflection is caused by a high over low permittivity contrast or vice versa (Brandt et alii, 2007). For example, when an antenna is loaded on snow or sediments, it has a *Ricker wavelet* consisting of three major half-cycles described by a positive–negative–positive pulse + − + (or in the grey scale imagery white/black/white, Figure 3.4). This phase polarity corresponds to the expected reflection with this antenna at interfaces from lower to higher permittivity. The opposite reflection, on the other hand, gives a 180° phase change and the three major half-cycles have a − + − (black/white/black) phase. The polarity of the reflection can hence characterize the interface passage, indicating a rough composition of the material.

$$R = \frac{\sqrt{K_2} - \sqrt{K_1}}{\sqrt{K_2} + \sqrt{K_1}};$$ (3.10)

where R is the reflection coefficient and K the relative permittivity values of the two materials at the interface.

3.2.4 EM wave pattern in embankment soils

GPR as it is known today was developed as a tool for mapping the internal structure of materials, primarily the ground but not necessarily limited to that: in this research, soil materials constitute the embankment structures. The penetration depth and resolution of the reflection data are functions of both the wavelength and the dielectric constant values. In river embankments, GPR deals with lossy dielectric materials, which quickly absorb the radio wave energy as the signals traverse through the medium: the crucial problem of the losses, strictly linked with depth penetration and consequently vertical and horizontal resolution will be treated in the following paragraph. When a localized source is above the embankment surface, for a localized target in the ground, there can be several possible paths that energy can travel from a transmitter to the receiver and the signals can spread out as direct air signal, direct ground signal and direct reflected (scattered) signal. A very important feature of placing the antenna on the ground is that the majority of the energy goes down into the ground and only a small amount leaks up into the air, as it is visible in the figure 3.8.
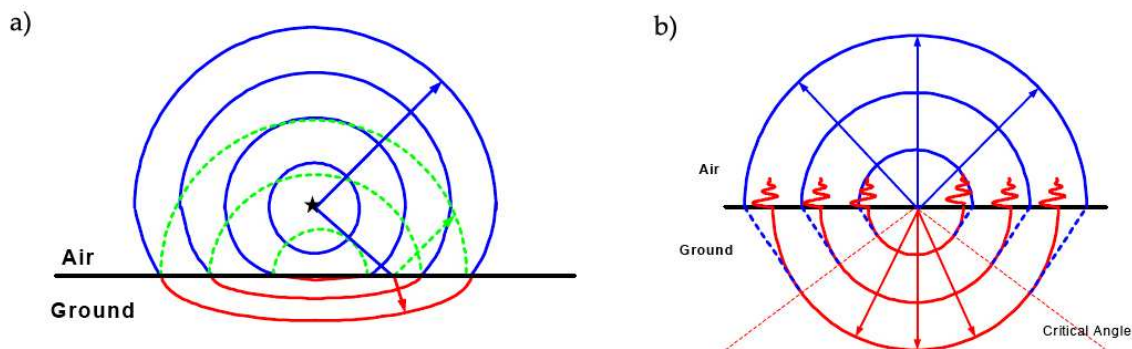
Figure 3.8 - Wavefronts spreading out from a localized source; a) located above the ground and b) located on the air-ground interface (Annan, 2001).

The spherical wave front descends on the ground. Ignoring finite source dimension and wavelengths, the field at any point along the ground interface can be visualized locally as a planar wave impinging on the boundary at a specific incidence angle defined by geometry (source height and lateral distance). Locally the signal is reflected and refracted according to Snell's law and the Fresnel reflection coefficient. If one examines the wavefront in the ground, it is no longer spherical as bending occurs with differing degrees depending on the varying incidence angle. To understand what is happening in the ground and near the interface, the limiting case of the source right at the interface is informative (Figure 3.8). The incident and reflected waves in the air coalesce into an up-going spherical wave. In the

ground, the transmitted signal divides into two parts, a spherical wave and a planar wavefront travelling at the critical angle, which links the direct spherical airwave and the spherical ground wave. Near the interface, the spherical ground wave extends into the air as an evanescent field (Annan, 2001). The antenna pattern of the radar system is what dictates how the radar system can be deployed to detect objects. Basically the antenna pattern tells in what direction the system is most sensitive and hence the area which is being "viewed" by the system. With GPR systems, the antennas are placed on or very close to the ground surface. The antennas generally interact with the ground and characteristics of the antenna are very much controlled by the electrical properties of the ground. In virtually all GPR systems, the antennas, which are used, are some form of dipole antenna. Generally the dipoles are resistively loaded so that they are not tuned and thus have a broader bandwidth. The broad bandwidth is achieved at the expense of energy loss and system sensitivity. When an electric dipole antenna is placed on or near the ground surface (within about 0.1 wavelengths or less), the antenna pattern is significantly affected by the electrical properties of the ground. Variations into the antenna pattern lobes are shown in Figure 3.9. As the relative permittivity (dielectric constant) of the ground increases, the directionality of the antenna increases and more energy goes down and less up.
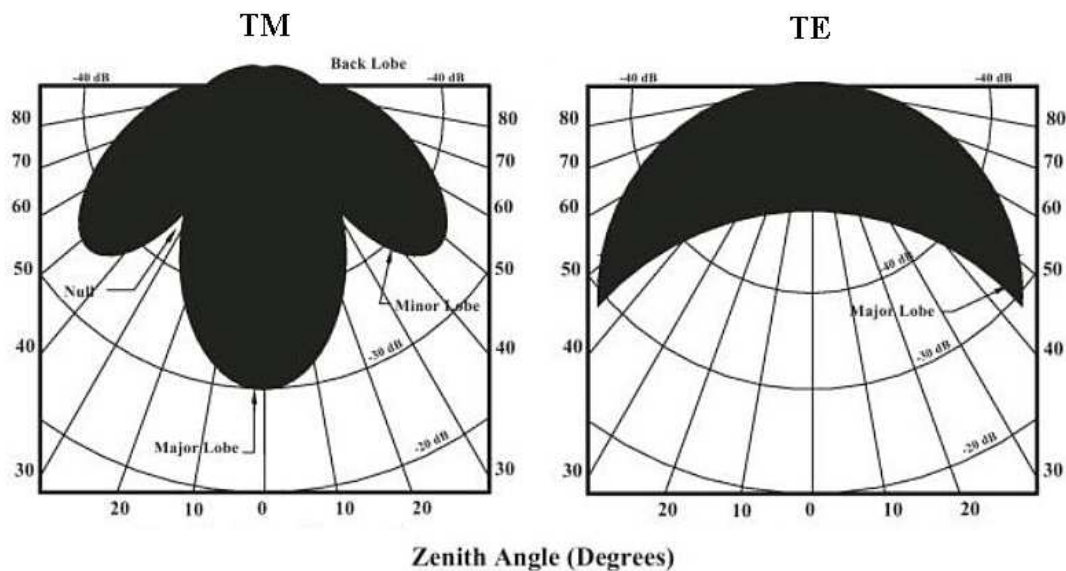
Figure 3.9 – Generalized polar diagram of TM and TE mode radiation pattern (Baker & Jol, 2007).

3.2.5 GPR System design

It might be thought that a GPR needs to have as low a frequency of operation as possible to achieve adequate penetration in wet materials. However, the ability to resolve the

53

details of a target or separately detect two targets is proportional to the size or spacing of the target in relation to the wavelength of the incident radiation. Consequently, a high frequency is desirable for resolution. A compromise between penetration and resolution could be done to capitalize the survey and it is an important consideration in either the selection of system bandwidth or the range of frequencies to be radiated. Consideration needs also to be given to the fact that, not only does attenuation decrease with frequency, but so does target scattering cross-section; this leads to the situation where it is possible that, for certain targets, material properties and depths, the received signal decreases with frequency (Daniels, 2004).

This paragraph handles with the principal factors affecting the design of a GPR in order to illustrate those factors, which need to be considered. The propagation path of the EM wave produced by GPR consists in general of a lossy, inhomogeneous dielectric, which, in addiction to being occasionally anisotropic, exhibits a frequency dependent attenuation and hence acts as a low-pass filter. The upper frequency of operation of the system and hence the antenna, is therefore limited by the properties of the material. The need to obtain a high value of range resolution requires the antenna to exhibit a wide-band bandwidth. The range of GPR is primarily governed by the total path loss, and the three main contributions to this are the material loss, the spreading loss and the target reflection loss or scattering loss. Hendrickx et alii (2003) have shown the attenuation, reflection and total losses variation path for increasing of water content (figure 3.10).
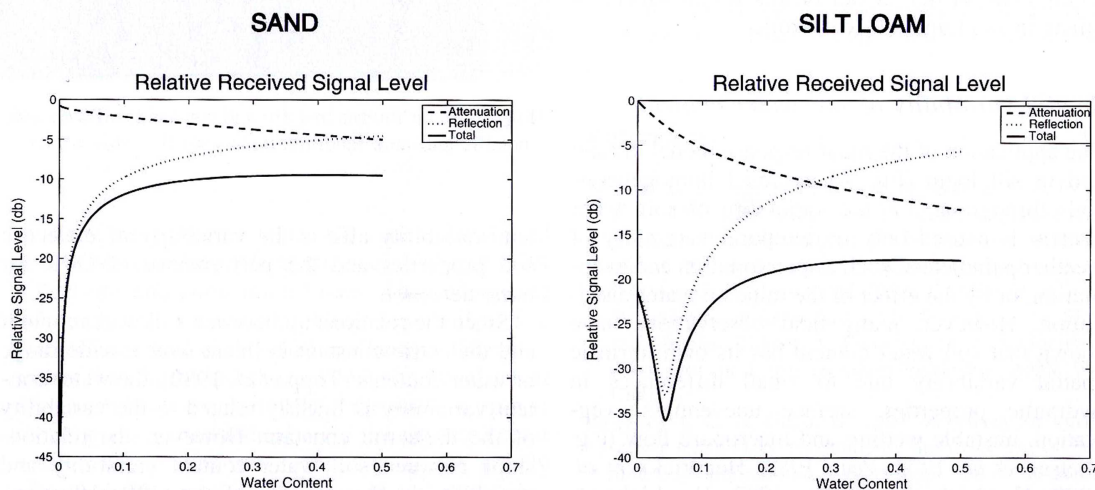
Figure 3.10 – Attenuation, reflection and total losses predicted with the radar response model in a sand and a silt loam at water content from 0 V% to 50 V% (Hendrickx et alii, 2003).

An example of a basic general method is given in this section. The signal that is detected by the receiver undergoes various losses in its propagation path from the transmitter to the receiver. Loss and absorption of EM waves for non-magnetic materials is frequency and

wetness dependent, and are caused by both conduction and dielectric effects. Regardless, it is important to estimate the loss, determine how frequency dependent the ground materials are to the signals and relate this to the noise floor. Given the loss we can give an indication of the maximum depth at which an ice body could potentially be detected. Daniels (2004) gives the total path loss for a particular distance, remembering that an accurate prediction of total losses the computation needs to be made over a wide band of frequencies.

$$L_T = L_e + L_m + L_{t1} + L_{t2} + L_s + L_a + L_{sc} \tag{3.11}$$

Where:

L_e = antenna efficiency loss in dB: this is a measure of the power available for radiation as a proportion of the power applied to the antenna terminals. It can be an important losses factor, especially in the case of resistively loaded antenna. For a pair of loaded dipole antennas the losses are obviously the twice.

L_m = antenna mismatch loss in dB: is a measure of how well the antenna is matched to the transmitter, usually only a small amount of power is lost

$L_{t1} + L_{t2}$ = transmission-coupling loss (from air to material) retransmission loss (from material to air), expressed in dB: in the case of antennas operated on the surface of the material, the transmission-retransmission losses from the antenna to the material are given by:

$$L_{t1} = L_{t2} = -20\log_{10}\left(\frac{4Z_m Z_a}{\left|Z_m + Z_a\right|^2}\right); \tag{3.12}$$

where Z_a and Z_m represent the characteristic impedances (i.e. equation 3.3) of air (377Ω) and material (many earth materials have 125Ω).

L_s = antenna spreading losses in dB: in conventional free-space radar the target is in the far field of the antenna and spreading loss is proportional to the inverse fourth power of distance provided that the target is a point source. In many situations, relating to ground penetrating radar the target is in the near field so that Fresnel zone and the relationship is no longer valid. However, for this example an R^{-4} spreading loss will be assumed, even though for a planar interface this is not valid and a correction is included. The spreading loss is proportional to the ratio of the received power to the transmitted power:

$$L_s = -10\log_{10}\frac{G_t A_r \sigma}{\left(4\pi R^2\right)^2} \; ; \tag{3.13}$$

where:

G_t = gain of transmitting antenna (loaded dipole);

A_r = receiving aperture (loaded dipole)

R = range to the target; the spreading losses are directly proportional to this factor and, moreover, considerably backscattered energy will be returned if the target is a planar reflector at a given depth This factor in Equation 3.10 is of importance.

σ = radar cross-section.

L_a = attenuation loss of material in dB, is given by the Equation:

$$L_a = 8{,}686 \times 2 \times R \times 2\pi f \sqrt{\left(\frac{\mu_o \mu_r \varepsilon_0 \varepsilon_r}{2}\left(\sqrt{\left(1+\tan^2\delta\right)}\right)-1\right)} \; ; \tag{3.14}$$

where:

f = frequency in Hz;

tan δ = loss tangent of material;

ε_r and ε_0 = relative permittivity of material and absolute permittivity of free space;

μ_r and μ_0 = relative magnetic susceptibility of material and absolute susceptibility of free space.

The principal loss mechanism in rocks and soils at frequencies over 500 MHz is the absorption of energy by water present in the pores. The dielectric properties of naturally occurring water (or ice) can be adequately described when there is the knowledge of its temperature and low frequency conductivity, but generally, we can assert that the velocity of wave propagation is slowed substantially with increasing ionic concentrations. This has the most pronounced influence at frequencies below 200 MH and, above this frequency; the wave velocity closely approaches that of pure water. If the water content is large enough the permittivity of the material may be determined firstly by the dielectric properties of water and to a second order by those of the dry material (figure 3.11).

L_{sc} = target scattering loss in dB, considered in the case of an interface between the material and a plane, where both the lateral dimensions of interface and the overburden are large. When the physical dimensions of the interface or anomaly are small, the L_{sc} increases and the returned signal becomes smaller. Under some condition the physical dimensions of

the anomaly are such as to create a resonant structure, it is possible to distinguish air-filled voids, and water filled voids by examination of their resonant characteristics and the relative phase of the reflected wavelet.

Material	Attenuation, $dB\,m^{-1}$	Relative permittivity range	Conductivity, Sm^{-1}
Air	0	1	0
Asphalt dry	2–15	2–4	$10^{-2}:10^{-1}$
Asphalt wet	2–20	6–12	$10^{-3}:10^{-1}$
Clay dry	10–50	2–6	$10^{-1}:10^{-0}$
Clay wet	20–100	5–40	$10^{-1}:10^{-0}$
Coal dry	1–10	3.5	$10^{-3}:10^{-2}$
Coal wet	2–20	8	$10^{-3}:10^{-1}$
Concrete dry	2–12	4–10	$10^{-3}:10^{-2}$
Concrete wet	10–25	10–20	$10^{-2}:10^{-1}$
Freshwater	0.01	81	$10^{-6}:10^{-2}$
Freshwater ice	0.1–2	4	$10^{-4}:10^{-3}$
Granite dry	0.5–3	5	$10^{-8}:10^{-6}$
Granite wet	2–5	7	$10^{-3}:10^{-2}$
Limestone dry	0.5–10	7	$10^{-8}:10^{-6}$
Limestone wet	1–20	8	$10^{-2}:10^{-1}$
Permafrost	0.1–5	4–8	$10^{-5}:10^{-2}$
Rock salt dry	0.01–1	4–7	$10^{-4}:10^{-2}$
Sand dry	0.01–1	2–6	$10^{-7}:10^{-3}$
Sand wet	0.5–5	10–30	$10^{-3}:10^{-2}$
Sandstone dry	2–10	2–5	$10^{-6}:10^{-5}$
Sandstone wet	4–20	5–10	$10^{-4}:10^{-2}$
Sea water	100	81	10^{2}
Sea-water ice	1–30	4–8	$10^{-2}:10^{-1}$
Shale dry	1–10	4–9	$10^{-3}:10^{-2}$
Shale saturated	5–30	9–16	$10^{-3}:10^{-1}$
Snow firm	0.1–2	6–12	$10^{-6}:10^{-5}$
Soil clay dry	0.3–3	4–10	$10^{-2}:10^{-1}$
Soil clay wet	5–50	10–30	$10^{-3}:10^{-0}$
Soil loamy dry	0.5–3	4–10	$10^{-4}:10^{-3}$
Soil loamy wet	1–6	10–30	$10^{-2}:10^{-1}$
Soil sandy dry	0.1–2	4–10	$10^{-4}:10^{-2}$
Soil sandy wet	1–5	10–30	$10^{-2}:10^{-1}$

Figure 3.11 – Attenuation and typical range of dielectric characteristics of various materials measured at 100 MHz, (Daniels, 2004, redrawn).

3.2.6 Velocity of Propagation

A transmitting antenna on the ground surface emits EM waves in distinct pulses into the ground that propagate, reflect and/or diffract at interfaces where the dielectric permittivity of the subsurface changes. It can easily be recognised that if the propagation velocity can be measured, or derived, an absolute measurement of depth or thickness can be made. For homogeneous and isotropic materials, the relative propagation velocity can be calculated from:

$$V_r = \frac{c}{\sqrt{K}} \; ; \tag{3.15}$$

thus the depth can be derived (considering a two-way travel time of the reflected wave) from:

$$d = v_r \frac{t}{2} \; ; \tag{3.16}$$

where K is the relative permittivity and t is the transit time from the target. Nevertheless, in most trial situations the relative permittivity is unknown, because the material is never homogeneous and multi-layer dielectric mediums must be considered; EM wave velocity data allows conversion of a time record of reflections to an estimated depth. The mean velocity value may be obtained from:

- Standard field procedures (e.g. bi-static common mid-point radar sounding or CMP). The propagation velocity can be determined by WARR measurements (wide-angle reflection and refraction), where the position of one antenna is kept constant while the second one is moved along the profile line. This array is slightly easier to carry out in rough terrain. The more commonly used CMP (common mid point) measurements instead consist in reciprocal movements of both transmitting and receiving antennas. Generally, the measured CMP and WARR velocities are, strictly speaking, valid only in the uppermost few meters of sediment. Information on the velocity of the deeper subsurface can be derived from the shape of eventual refraction hyperbolae which are, however, not always present. The propagation velocity in river embankments is likely to decrease with depth due to compaction and a higher content of water and fines (Sass, 2007).

- Representative values in the literature derived from laboratory electromagnetic characterisation; this method was generally adopted, considering the typical Reno River embankment structure, which is made up of sand and silt in slightly different ratios.

- Calibration with reflectors observed both in the field and by using other geophysical techniques, it will be treated successively. This method was applied for the Savena Abbandonato Stream, where a metallic object, giving a reflected signal was put into the ground at a known depth. However, this kind of velocity test is no longer valid under the reflector depth.

3.2.7 Resolution VS depth

According to Annan & Cosway (1994), "Resolution of two events requires that the radar pulse envelope time duration be shorter than twice the separation delay time between two features to be resolved". It might be thought that a GPR needs to have as low a frequency of operation as possible to achieve adequate penetration in wet materials. However, the ability to resolve the details of a target or separately detect two targets, both in vertical and horizontal directions, is proportional to the size or spacing of the target in relation to the wavelength of the incident radiation. Consequently, a high frequency is desirable for resolution. The compromise between penetration and resolution must be made and it represent the winning factor for a successfully GPR campaign. When a GPR system is placed on the ground it looks out in quite a broad area beneath the antenna as well as off to the side: spatial resolution is determined by this broad area of the region illuminated by a GPR antenna, often referred to as the *Fresnel zone* or *antenna footprint*. GPR data are often exclusively collected using broadside antenna orientations, which generate EH polarized data, because EH polarized data generally have a higher signal-to-noise ratio relative to the EV polarized data. This can be partially attributed to the orientation of the long axis of the illumination ellipse or antenna footprint relative to the survey line direction, as shown in figure 3.12. From the illumination ellipse it can be observed that the transmitted EV polarized data are weighted toward off-survey line features, whereas the EH polarized data are weighted toward in-line features. Therefore, transmitted EV polarized data are more susceptible to noise from buried off-survey line features. In generalized form, the subsurface area illuminated is an ellipse that can be estimated from the equations in figure 3.12, by defining the length of the major (A) and minor (B) radii of the ellipse. These equations are also used to determine the spatial resolution of GPR antenna. Figure 3.12 shows the relationship between the radius A, which is oriented perpendicular to the long dimension (broadside) of the antenna, and radius B, which is oriented parallel to the broadside of the antenna. It can be observed that collecting data with the antennas oriented parallel broadside result in the elongated axis of the illuminated surface area ellipse being parallel to the survey line direction. Data collected using parallel end-fire orientations will result in the elongated axis of the illuminated surface area ellipse being perpendicular to the line survey direction. This increases the possibility of including unwanted signal from off-line features.

$$A = \frac{\lambda}{4} + \left(z_0 - z_d\right)\sqrt{k-1}$$

$$B = \frac{A}{2}$$
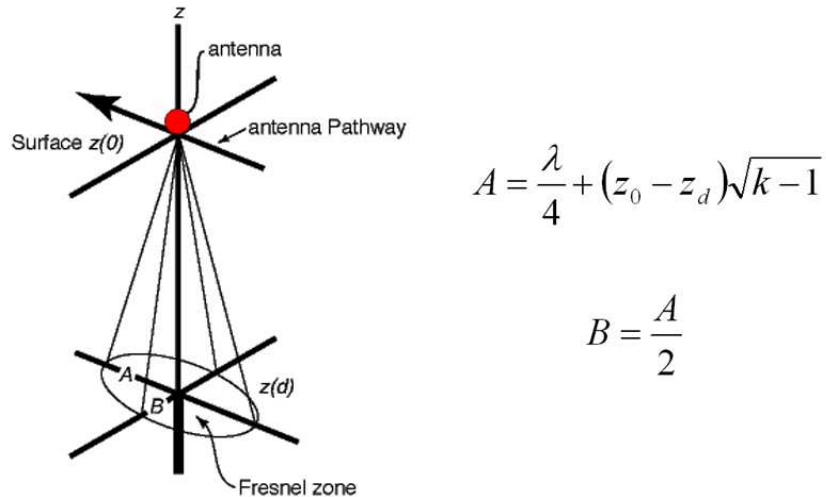
Figure 3.12 - Approximate GPR-antenna footprint (Fresnel zone) for bi-static, dipole antennas and relative equations, to define the major and minor radii of the ellipse.

In the equations of figure 3.12 z_d is the depth of the Fresnel zone in the subsurface, A is the radius of the Fresnel zone parallel to the long axis at depth z_d, B is the radius perpendicular to the long axis at depth z_d, and z_0 is the antenna elevation relative to ground level (Annan, 1996). Equations in fig. 3.11 indicate that GPR patterns become more focused with increasing dielectric constant, resulting in greater spatial resolution, at the detriment of penetrating depth. The equations can be used to determine antenna frequencies suitable for imaging subsurface targets with known spatial dimensions. Because of the footprint, one can detect responses from features, which are not directly below the system when making a measurement. The off 'bore site' responses give rise to hyperbolic features on GPR records and are the classic signature of localized features such as pipes, cables, or other limited spatial extent objects. The theoretical resolving limit of the vertical resolution is ¼ to ½ of the wavelength for Sheriff & Geldart (1982), and ¼ to Yilmaz and Doherty (1987); here in figure 3.13 are presented the frequency-related vertical resolution theoretical values for typical sedimentary environments.

Antenna frequency	Lithology		
	Saturated sand 0.06 m/ns	Damp sand 0.1 m/ns	Dry sand 0.15 m/ns
50 MHz	0.3–0.6 m	0.5–1.0 m	0.75–1.5 m
100 MHz	0.15–0.3 m	0.25–0.50 m	0.375–0.75 m
200 MHz	0.075–0.15 m	0.125–0.25 m	0.1875–0.375 m

Figure 3.13 – Theoretical values for vertical resolution of GPR in typical sedimentary environments for various antennae frequencies, considering an average wave velocity by laboratory tests (Jol & Bristow, 2003).

The horizontal or plan resolution is important when there is a need to distinguish between more than one target at the same depth; it is defined by the characteristic of the antenna and the signal processing employed. Plan resolution improves as attenuation increases, assuming that there is sufficient signal to discriminate under the prevailing clutter conditions (Daniels, 2004).

3.2.8 Clutters

Concerning the application of GPR in soils, filed measurements have produced a wide scatter of results primarily due to the inherent variability of the "natural" environment caused by the presence of stones, boulders and localised regions of higher conductivity within the ground mass (figure 3.14). Such variations cause the dielectric parameters to change in a statistically unpredictable way as the radar antenna is scanned over the "ground" surface introducing clutter in the received signal. The clutter that affects GPR measurements can be defined as those signals that are unrelated to the target scattering characteristic but occur in the same sample time window and have similar spectral characteristic to the target wavelet (Daniels, 2004). Clutter can be caused by breakthrough between transmit and receive antennas as well as multiple reflections between the antenna and the ground surface.
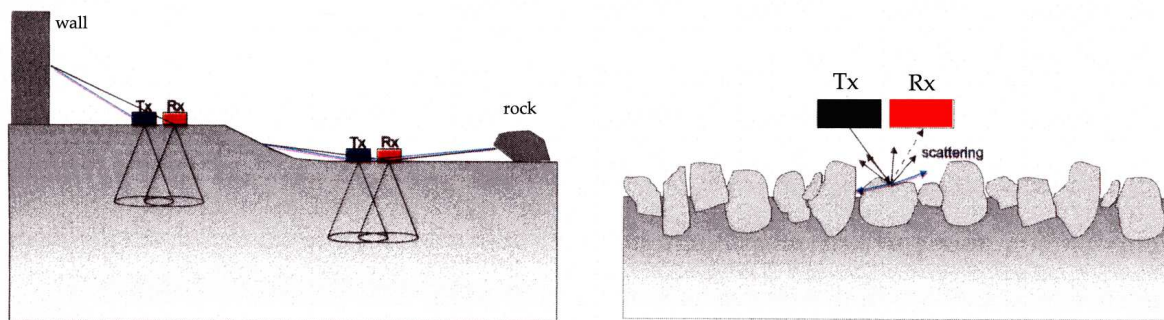
Figure 3.14 – Clutter effects, given by reflections from targets, above the ground surface or immediately below it (Vettore, 2008, modified).

Clutter will vary according to the type of antenna configuration, and the parallel planar dipole arrangement is one where the stability of the level of breakthrough is most constant. Local variations in the characteristic impedance of the ground can also cause clutter, as can inclusions of groups of small reflection sources within the material. In addiction, reflections from targets in the side lobes of the antenna, often above the ground surface, can be particularly troublesome. This problem can be overcome by careful antenna design and incorporating radar absorbing material to attenuate the side and back lobe radiation from

antenna. In general, clutter is more significant at short-range times and decreases at longer times, leading to the consequent limitation on near-range radar performance.

3.2.9 Processing GPR Data

After obtaining GPR data, this data must be processed in order to be more easily visualized and interpreted. For Daniels, 2004, the signal processing is primarily means of reducing clutter; fundamentally, the signal to clutter ratio of the radar data is the key to target detection. Most system noise in GPR systems can be reduced by averaging. GPR is heavily contaminated by clutter, and reduction of this is a key objective. Most important, the general objective of signal processing as applied to surface-penetrating radar is either to present an image that can readily be interpreted by the operator or to classify the target return with with respect to a known test procedure or template. However, since data obtained from GPR surveys is similar to data obtained from seismic reflection surveys, many of the same techniques used to process seismic data can be used to process GPR data. In many cases, it is possible to use the results from a GPR survey with very modest processing. In these cases, the only processes that need to be made are to convert the data to a usable digital format, to make gain adjustments to the data, and to determine the depth to each eventual reflector (such as the water table) in the subsurface (this involves converting time to depth). Normally, processing the data can involve the following steps (not in application order):

- Converting the data to a usable digital format. In most recently manufactured GPR units, the data is automatically recorded in digital format. There are many different file formats to work with, and there are many utility programs available for converting between different file formats. Data from GPR units purchased from Geophysical Survey Systems Incorporated can be uploaded to computers and processed with software available from the same company. GPR by Radsys produces data in a standard format (sgy) that can be processed with each software; IDS Company provides its own data format and relative elaboration software
- Time zero assessing. Time zero is a function of the system timing, cable lengths, and antenna positioning. It is necessary, in order to perform an accurate GPR survey in the ground, to calculate the two-way travel time from the precise moment when the EM wave pass between the air to ground interface.
- Background subtractions. Noise that occurs because of the geometry of the system, clutter, artefacts and static reflections can be reduced with a background removal. The

background filter subtracts reflections, which are constant over the entire radargram (Heilig et alii, 2008). The software computes the average of all the scans accumulated and it removes them, to eliminate the antenna ringing and horizontal banding across the image; generally the first interface air-ground is involved in the process and cancelled, so that reflection and hyperbolas previously hidden by horizontal traces can hence be readily visible. The background removal also removes other horizontal features such as flat lying geology and the surface of the Earth, so time zero had to be located first.

▪ Gain adjustments to the data. As the transmitted signal from a GPR unit penetrates into the ground, attenuation of the GPR trace occurs. This attenuation can be corrected by applying gain adjustments to each trace. Several models exist for computing gain adjustments, applying mathematical models for the exponential or linear amplification of the trace. In one model, each data value in the entire trace is multiplied by a factor related the depth of the signal.

▪ Enhancement stretch. Enhancement stretch can be applied to bring out some details in the radargrams. This step loses all the absolute amplitude information (that will be recovered later) and enhances not only geological details but also noise. These steps are done to improve the ability to see the tails of hyperbolas, to evidence many contrasts on the host material, as boundaries between soil horizons characterized by different electric properties.

▪ Data static adjustments. This involves removing the effects of changes in elevation and effects from levelling the GPR; this function it is generally included in commercial software for the data processing.

▪ Deconvolution. The dominant frequencies of the emitted signals typically range from about 50 to 500 MHz, depending on the length of the antennas used. This electromagnetic frequency range corresponds to wavelengths ranging from approximately 2 to 0.5 m in typical Earth materials, which makes GPR the geophysical remote sensing method with arguably the highest spatial resolution. The procedure of deconvolution does substantially enhance the spectral bandwidth and the compactness of the signal, and thus potentially the vertical resolution of the data. From a geological point of view many care has to be taken, because this result is rather unsatisfactory as the procedure introduces a large amount of noise on a significant number of traces and thus weaken, rather than improve, the interpretability of the GPR section (Belina et alii, 2008).

▪ Filtering the data. The purpose of filtering is to remove unwanted background noise. For example, if a cellular phone antenna or power transmission line is located in the area,

it may create unwanted noise along the trace at a certain frequency. To remove this unwanted noise, the time-domain trace data is converted to the frequency domain using the Fourier transform. Desired frequencies are zeroed out, and then the trace is converted back to the time domain using the inverse Fourier transform. Olhoeft (2000) discusses filtering the results from GPR surveys. Filtering strategies can include band pass (removing frequencies in a certain range), low pass (removing low-frequency signals), and high pass filtering (removing high-frequency signals). High-pass filtering is a useful means of improving the signal to clutter ratio in situations where clutter is caused by additional low frequency energy generated by antenna ground interactions; in addition, excessive high frequency noise can usefully be reduced by low-pass filtering.

▪ Velocity analysis (previously introduced). If the radargram reveals some hyperbolas, many computations can be done; the slopes of the asymptotes of the hyperbola are controlled by the velocity of propagation and thus calibrate the dielectric permittivity between the antenna and the target, and give a calibration and conversion of the two-way travel time into depth. The radius of curvature at the peak of the hyperbola and the lengths of the asymptotes (by taking into account the antenna pattern) give the size of the object causing it. The ellipse drawn within the hyperbola indicates the size of the object, assuming the object is a circular cylinder with axis perpendicular to the plane of the data image (Olhoeft, 2000). When known reflector or hyperbolas are not present in radargrams, the velocity estimation can be afforded assuming a gradual velocity change. For embankments lithology, generally characterized by fine grains, if we have a passage between, for example, 0.11 m/ns to 0.09 m/ns in the deeper subsurface, the possible error would be just fewer than 10%. Under very unfavourable conditions (coarse sand (0.14 m /ns) overlying silt (0.09 m /ns), the error could amount to an over-estimation of interface depth by ca. 20% if the surface velocity was used for the time–depth conversion of the entire radargram. However, the change of the radar facies makes it possible to assign a realistic velocity to each layer and thus, reduce the possible error (Sass, 2007).

▪ Migration. The Migration process essentially constructs the target reflector surface from the record surface; this technique has much developed and nowadays employs wave equation methods such as Kirchhoff migration, finite difference migration and frequency wave-number migration. Migration technique aims to relocate reflections to their true spatial position based on the velocity spectrum, to produce a real structure map of subsurface features. A relatively straightforward geometric approach is given by Daniels (2004) and can be used in the two-dimensional case of a material with known constant

velocity. With regard to the Equation 3.16, at any position of the x-axis the distance d is also given by:

$$d_i = \sqrt{(x_i - x_0)^2 + d_0{}^2} \; ; \tag{3.17}$$

This equation shows that the measured wavefront appears as a hyperbolic image or a curve of maximum convexity. The geometric migration technique simply moves (or migrates) a segment of an A-scan time sample to the apex of a curve of maximum convexity; obviously the hyperbolic curve needs to be well separate from other features and a good signal to noise ratio is needed. Alternative methods are known as maximum convexity migration and wavefront migration, which in this context are just mentioned, characterized by the common assumption of a constant velocity. Image processing hyperbola mask has to be applied to the data to collapse or focus the hyperbola.

After migration (14cm/ns)
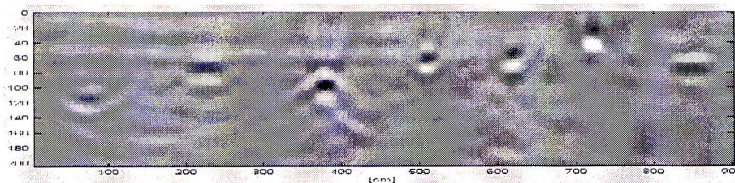
10 cm/ns
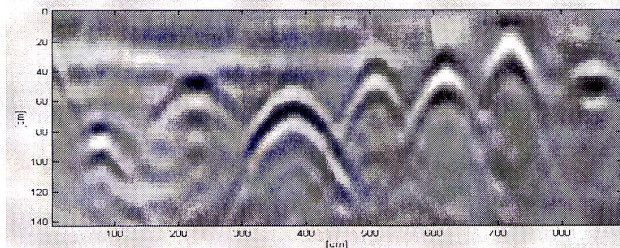
20 cm/ns
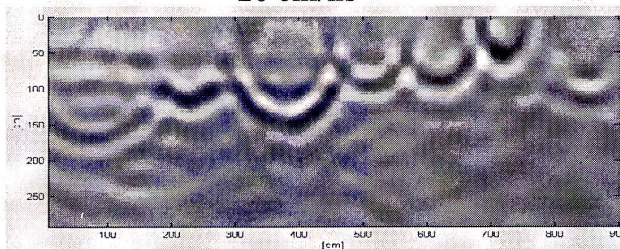
Figure 3.15 – Migration process applied to subsurface features with an average velocity of 14 m /ns; is clearly visible what can happen with not accurate velocity estimation.

The image must show only the scattering cross-section of the visible radius of curvature of the target (figure 3.14). By looking at other hyperbolas in the image (if presents), their over or under migration focusing (residual hyperbolic shapes pointed upwards or

downwards) indicates the variability of the velocity and hence dielectric permittivity throughout the section. In some cases for a correct migration, many attempts, changing velocity are needed, finally as higher the velocity accuracy, as higher the real reproduction of the detected target. A velocity overestimation or underestimation can induce the phenomena reproduced in figure 3.15.

4. EM INDUCTION

The electromagnetic surveys are based on the principle of electromagnetic induction. It differs from magnetometer, which is used in a geophysical survey to measure magnetic susceptibility variations in earth; the magnetometer is a passive sensor because it uses the ambient earth magnetic field as the source of excitation. Instead, in EM induction method an alternating magnetic field in a coil or cable induces electric currents in a conductor. The conductivity of rock and soils is too poor to enable significant induction currents, but when a good conductor is present, a system of eddy-currents is set up. In turns, the eddy-currents produce secondary magnetic field that is superposed on the primary field and can be measured at the ground surface (figure 4.1).
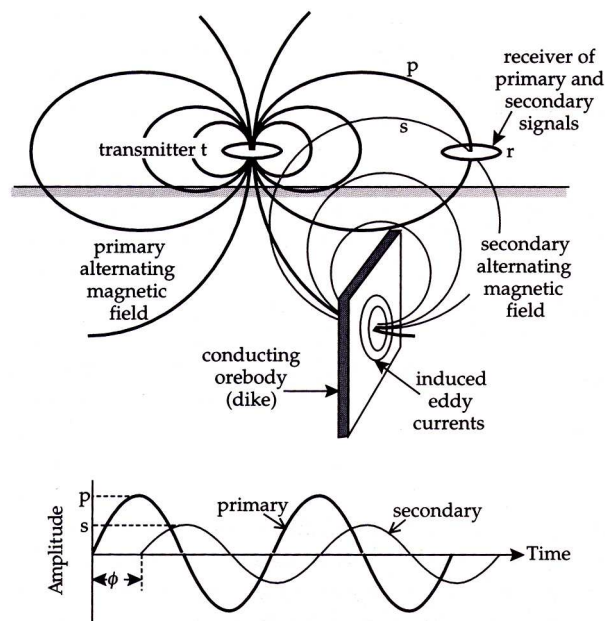
Figure 4.1 – Illustration of the EM induction method for shallow conductive bodies, with primary and secondary field amplitudes and phases (Lowrie, 1997).

The typical EM induction device is generally characterized by two dipoles at a constant distance. The transmitter dipole creates a primary electromagnetic field that provides an induction in the studied medium, producing a secondary electromagnetic field; their amount is recorded by the receiver and the relation between the primary and the secondary field can be converted to conductivity of the medium in which induction occurs. The instrument is not designed to be a metal detector but highly conductivity metals also generate a strong signal in response to the meter and their response tends to overload the circuitry (but it can be opportunely removed). Rather, it is designed to measure the much smaller signals

67

generated by the conductivity properties of soils. The electronics of the device converts the signal into the measure of conductivity (because of its small size, p.p.m. and/or millisiemens per meter; mS/m). Electromagnetic techniques can be broadly divided into two groups. In **frequency-domain** instrumentation (FDEM, Frequency Domain Electromagnetic Method), the transmitter current varies sinusoidally with time at a fixed frequency which is selected because of the desired depth of exploration of the measurement (high frequencies result in shallower depths). In most **time-domain** (TDEM) instrumentation, on the other hand, the transmitter current, while still periodic, is a modified symmetrical square wave, where after every second n-period the transmitter current is abruptly reduced to zero for one n-period, whereupon it flows in the opposite direction. FDEM method, more practical than TDEM concerning their utilization in field surveys, can operate in two different dipolar configurations: VDM and HDM; VDM (Vertical Dipole Method) has the vertical magnetic dipole referred to the transmitting coil; instead, in HDM (Horizontal Dipole Method) the magnetic dipole has horizontal direction. Generally the investigation depth of VDM is the twice of HDM. FDEM involves fixed source–receiver geometry so the sensor may be built into a single rigid body that precisely maintains its geometry. The goal of depth sounding is to determine a mono-dimensional earth structure below a survey location. The resolution decreases with depth because of either lateral averaging in geometrical sounding or with downward spreading of the source field in frequency sounding. The frequency of the signal may vary, but critical to the design of the induction meter is the feature that there is no electrical connection between the survey instrument and the ground. Conductivity contrasts can be created which a conductivimeter might record. In most cases, this will be true if there is variation in soil composition in the local soil column. In addition, the composition and texture of the soil may change by cultural activity and natural forces as well. An EM earth induction meter may record all of these events, but is quite important before doing a conductivity survey to have some idea of the local soil column, most directly but on a theoretical level, by consulting the local soil map and the description of the soil type (Clay, 2001).

4.1 Theoretical Basis

Respect to GPR, which operate with relatively high frequencies, in EM induction method (frequencies employed less than 50 KHz), the displacement currents are negligible compared to conduction currents. The equation (3.1) becomes:

$$\frac{\partial^2 B}{\partial z^2} = \mu_0 \sigma \frac{\partial B}{\partial t} ; \qquad (4.1)$$

where the magnetic fields have components B_x and B_y: the solution of equation (4.1) for the components B_x or B_y of an alternating magnetic field, with angular frequency $\omega = 2\pi r$ in a conductor with conductivity σ is:

$$B_{x,y}(z,t) = B_o e^{-zld} \cos\left(\omega t - \frac{z}{d}\right) ; \qquad (4.2)$$

where: $d = \sqrt{\dfrac{2}{\sigma\mu\omega}} ; \qquad (4.3)$

is called the *skin depth* and *zld* term is the phase shift that the magnetic field in conductor does experiences, due to the conductivity. Avoiding complexes equations, given the current systems in transmitter, receiver and conductor be represented by simple loops carrying currents, a voltage is induced in the conductor by the changing current in the transmitting circuit. The received voltage is formed by a primary voltage (induced by transmitting current), and a secondary voltage (induced by eddy-currents); their ratio (or *response* in measuring system) is composed by two parts (real and imaginary parts respectively). The real part has the same phase as the primary signal and is called *in-phase component*, while the imaginary part is 90° out of phase with the primary signal and it is called the *quadrature component*. The term *depth of investigation* has evolved and become standardized (Spies, 1989) to mean the practical depth of investigation, defined as a maximum depth at which a given target in a given host can be detected by a given sensor. The *skin depth* has been widely used as an estimate of depth of investigation of EM systems, which is rigorously defined in classical EM theory as the distance in a homogeneous medium over which the amplitude of a plane wave is attenuated by a factor of $1/e$, or to about 37% of the original amplitude.

Although in some geophysical textbooks, the term *depth of penetration* appears synonymously with skin depth, the depth of penetration is clearly empirical; it is affected by the properties of the target and host medium as well as by factors related to the investigation modality, such as sensor sensitivity, accuracy, frequency, coil configuration, ambient noise, and data processing and interpretation methods. Under ideal conditions, the depth of

investigation can be greater than the skin depth, while in real geologically complex conditions and/or environmentally noisy areas, the skin depth can be largely larger than the depth of investigation. However, the skin depth of the survey can be estimated by the usage of a simple nomogram, which is a simple graph that links the ground conductivity, the frequencies employed by the FDEM device and the skin depth itself (figure 4.2).
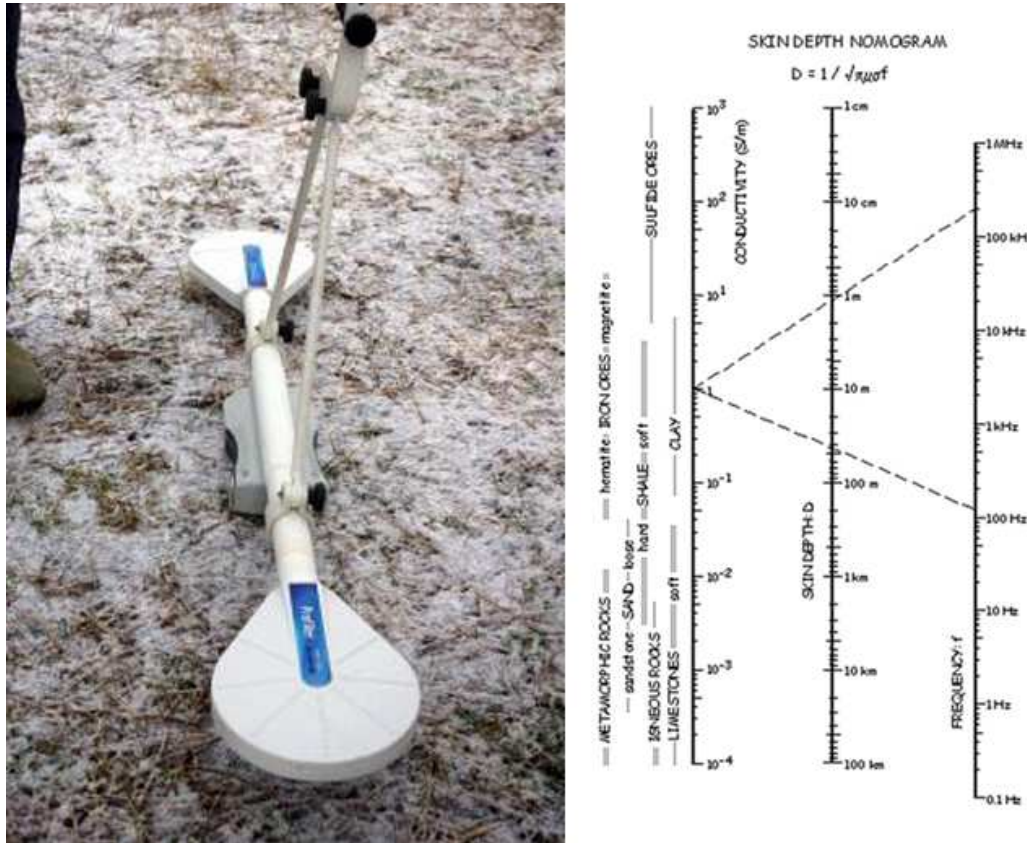
Figure 4.2 – EM induction tool on the left (EMP-400 Profiler, by GSSI), and relationship among source frequency, ground conductivity, and skin depth on the right (from Won, 1996).

McNeill (1990) gives an excellent review and tutorial of electromagnetic methods and much of his discussion on the terrain conductivity meter is excerpted here. He assert that the operating frequency is low enough at each of the intercoil spacing that the electrical skin depth in the ground is always significantly greater than the intercoil spacing. Under this condition (known as "operating at low induction numbers") virtually all response from the ground is in the quadrature phase component of the received signal. With these constraints, the secondary magnetic field can be represented as:

$$\frac{H_s}{H_P} = \frac{i\omega\mu_o\sigma s^2}{4} \tag{4.4}$$

where

H_S = secondary magnetic field at the receiver coil

H_P = primary magnetic field at the receiver coil

$\omega = 2\pi f$

f = frequency in Hz

μ_o = permeability of free space

σ = ground conductivity in S/m (mho/m)

s = intercoil spacing in m

$i = (-1)^{1/2}$, denoting that the secondary field is 90° out of phase with the primary field.

Thus, for low and moderate conductivities, the quadrature phase component is linearly proportional to ground conductivity, so the instruments read conductivity directly. For a given H_S/H_P ratio, the apparent conductivity indicated by the instrument and derived from the quadrature component is defined as:

$$\sigma_a = 4\frac{\left[\dfrac{H_s}{H_P}\right]}{\omega\mu_o s^2} \;; \tag{4.5}$$

Therefore, the mono-dimensional earth structure below a survey location can be estimate by changing in apparent conductivity.

4.2 EM surveying

The conductivity profile curve is achieved by shifting a sensor along the profile (originally constructed for military purposes, especially for the detection of ammunitions and subsurface inhomogeneities). A sensor with a small coil separation can be used for depth sounding if it has several characteristic set up, following described. The sensor has to be supplied by a method that cancels the strong transmitter field existing at the receiver coil; it must have sufficient sensitivity and accuracy to resolve small changes in earth conductivity and a large dynamic range to accommodate near-surface effects (Huang, 2005). Moreover, a wide bandwidth to cover desired ranges in skin depth, and an ability to avoid certain frequencies with high environmental noise levels caused by cultural sources such as power lines are required.
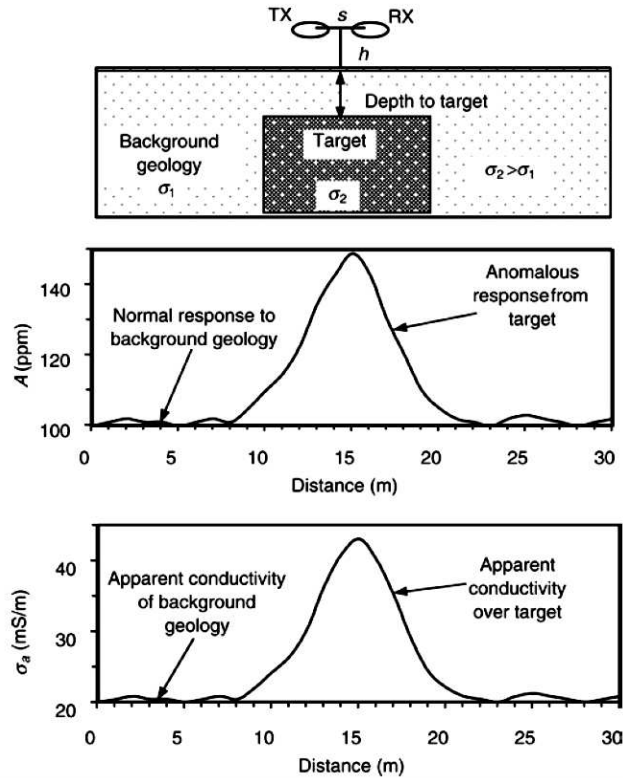
Figure 4.3 -Schematic representation of the FDEM method, where TX is the transmitter, RX is the receiver. The presence of a conductive body creates an EM amplitude anomaly over such target as well as an apparent conductivity peak (Huang, 2005).

The GEM-2 device (Geophex Inc.), which was tested during measurements campaigns of the European Project GEMSTONE for some dikes of Czech Republic, has a transmitter-receiver coil separation (s) of 1.66 m and standard survey height (h) of 1 m. A third coil is used to monitor and cancels, or bucks, the transmitter field. The sensor operates in a bandwidth from 300 Hz to 48000 Hz. Raw data are the in-phase and quadrature components of the secondary magnetic field as parts per million (p.p.m.) against the primary field at the receiver coil (figure 4.3).

Making such small, broadband EM sensor, however, some technical issues must be resolved: primary field cancellation and broadband operation. Because of the source–receiver proximity, the primary field at the receiver is strong and thus must be sufficiently reduced (or bucked) to evidence the small secondary field. This requires precise coil design and placement. The broadband requirement means that the bandwidth must be as wide as possible to cover desired ranges in skin depth. However, operating a single set of coils in a broadband requires very advanced power-switching technology and high-speed, real-time digital electronics. Because of these technical difficulties, there have few commercial broadband EM sensors until very recently. The EM response given by FDEM device is the in-phase (*I*) and

quadrature (Q) components of the secondary magnetic field at each frequency, given the conductivity and thickness of each possible layer encountered in the ground. Important for the understanding of EM effects is the response function f(Q). This complex-valued function describes the electromagnetic response from conductive ground structures to an electromagnetic excitation field:

$$f(\theta) = \frac{\theta^2 + i\theta}{1 + \theta^2};$$

(4.6)

The argument of f(θ), called the response parameter θ or induction number, depends on the operating frequency, conductivity of the ground and the target, and on the size of the target and the geometry of the transmitter and receiver loops:

$$\theta = \mu\sigma\omega l^2;$$

(4.7)

where "ω" is the angular frequency, "σ" is the conductivity, "μ" is the magnetic permeability, and "l" is the parameter for the geometry of the target and/or loop-system (e.g. coil separation in a homogeneous half-space). Although higher frequencies result in a stronger response for a given ground situation and system geometry, increasing the frequency will lead to a reduction in penetration depth. Hence, when multi-frequency instruments are used, it is important to select a frequency (or frequencies) that will give both an optimal response and desired penetration depth. The response parameters can change for different models (homogeneous half-space, horizontal plate, sphere, layered earth), if one of the variables changes, then one or more of the others must be changed to keep Q constant. The behaviour of the complex-valued response function f(θ) for layered ground in is shown in figure 4.4. For values of θ < 1 and θ > 1 the imaginary part (quadrature) and the in-phase part, prevail, respectively. When θ << 1, the contribution of the real part to the measured signal is negligible and the information about the ground conductivity is mainly depicted in the quadrature component (Spies and Frischknecht, 1991). The EM response in the range θ < 0,02 is small and of small frequency dependence, which renders frequency sounding impractical; alternatively, when θ>> 1, I reaches its highest value and Q goes to zero, which also makes the sounding impractical because no EM energy penetrates the earth. Therefore, a successful EM sounder should operate at a moderate induction number. Thanks to the geometry of the FDEM devices, many geological formations fall into a low to middle induction number where

both *I* and *Q* have high intensity and strong frequency dependence. Figure 4.4 illustrates an induction number zone for a layered earth structure covered by a 1 to 48 KHz bandwidth (GEM-2 characteristics) over a five ohm-m (conductivity = 0.2 S/m) earth, which can be common for environmental sites. As can be seen, the sensor covers a low to middle induction number zone where both *I* and *Q* are strong and frequency dependent, testifying that a small sensor can be used for soundings in such environments. In practice, the environmental noise level, which is site dependent and is always higher than the instrument noise level, governs ultimate utility of the sensor.
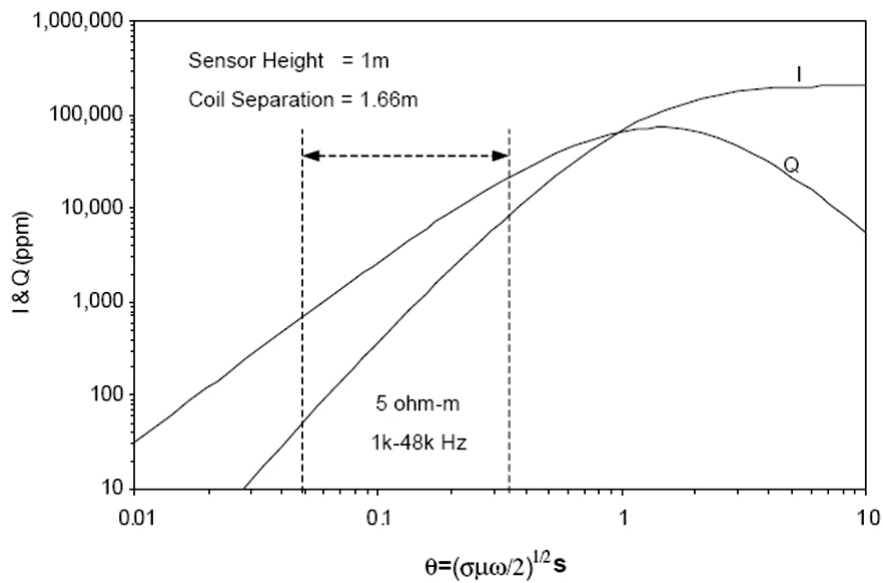
Figure 4.4 - The in-phase and quadrature responses as a function of induction number θ (Huang & Won, 2003).

The foremost incentive of a small, handheld sensor is its portability, survey speed, and easy use, which is comparable with GPR methodology and in some case even better than that. Indeed, the GPR campaigns provided in the Reno river Basin were disturbed many times by the roughness of the embankment surface as well as by the vegetation presence; this may not happen with the FDEM methodology, which is contact-less. The FDEM device works associate with GPS station, normally it can operates with several simultaneous frequencies; the lowest frequency that can be selected is around 500 to1000 Hz; under this range the cultural noise, especially in West European countries, compromise the signal to noise ratio. The depth of the survey can be estimated by means of the nomogram usage, and it is proportional to the resistivity of the material investigated, as lower the conductivity as higher the penetration of the EM wave. The calibration with direct geotechnical tests is always suitable. As already stated, FDEM methodology can measure the apparent resistivity, which

represent the average values measured of the ground between the two poles of the device. The production of impulses enables the data acquisition with normal walking velocity by the single operator, computing around 1 to 5 points each meter (sampling frequency from 1 to 5 Hz); the variations of resistivity along the profile can be associated with differences in lithology or moisture changes. Using four frequencies, 4 profiles of apparent resistivity can be visible (figure 4.5); generally the anomalies are characterized by an inversion of the profiles, because in normal condition, as lowest the frequency as higher the conductivity, because at shallow depth the surface effect increase normally the resistivity response. Anyway, some idea of the local soil column, most directly but on a theoretical level, by consulting the local soil map and the description of the soil type, is required.

Recently GSSI offered an earth induction meter called the Gem 300 that purports to discriminate depth in conductivity by varying the frequency of the transmitter (Won et. al. 1996), under the general theory that lower frequencies penetrate to a greater depth than do higher ones. By the same society, a new tool (the Profiler EMP – 400), a frequency domain system, recently released, was used for the purposes of this research (Samoggia piping phenomena, treated in Chapter 7).
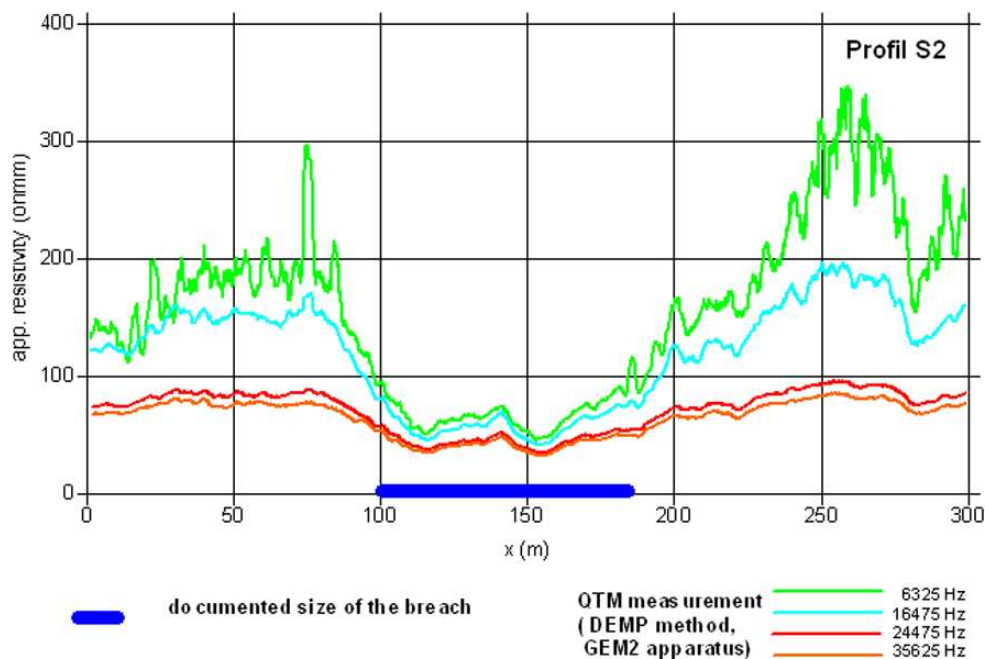
Figure 4.5 – Example of GEM-2 application in river embankment levees, with measures carried out to define the resistivity characteristic of a breach (Morris, 2005).

By acquiring multiple frequencies, the user can select the frequencies that provide the best results for a specific application. The GSSI Profiler can be configured to simultaneously measure up to 3 frequencies between 1 KHz and 16 KHz. The system can be deployed in

either the vertical or horizontal dipole mode. The output is the mutual coupling ratio (Q) in parts per million (p.p.m.) for both the in-phase and quadrature, or apparent conductivity in mS/m. All survey acquisition parameters and EM data are stored on internal memory. Files are structured in Excel spreadsheet format (ASCII text file), for simple download to a PC, for immediate presentation on commercial mapping software packages.

4.3 River Embankment application

Concerning the river embankment application, some encouraging results have achieved in recent applications (Boukalová and Beneš, 2007), and this methodology has many possibilities to be applied in many geological contexts. FDEM method is contact-less and this is its main advantage (no problems with the electrodes grounding), and is very efficient. A single operator can perform the operation and within one second, it is possible to execute up to 5 measurements of conductivity (if GEM-2 device is used, otherwise 3 employing GSSI). This enables an easy measurement of more than 10 km of the embankment per day. The work efficiency can be further increased by using GPS system synchronised with conductivity measurement for navigation. The device is very easy to use. Resistivity is an appropriate parameter for dike material description. Better coefficient of correlation generally can be almost always found in the measurement performed in dry conditions.

Tests carried out for European Projects (Boukalová and Beneš, 2007) introduce the division into quasihomogeneous blocks (Figure 4.6), in order to evaluate parts of the bank with homogenous electrical properties. Material description based on resistivities has to be adapted to soil moisture contents at the time of the measurement; however, the FDEM methodology shows higher accuracy in the measurement in dry conditions. The induction EM devices must be calibrated to define the depth reached by the operating frequencies. Sharp local resistivity anomalies (if they are not a showing of artificial conductors) can be detected; they mostly correspond to a distinct change in the dike material; however, the interpretation of sharp anomalies can be made more accurate through the analysis of other measured parameters as magnetic susceptibility. This analysis can be provided with the employment of several frequencies, however frequency 6525 Hz can be enough, because a larger space can be investigable.

The result of the measurement is output in the form of curves (graphs) of apparent conductivity or resistivity along the tested profile for the individual measured frequencies (the so-called depths layers).
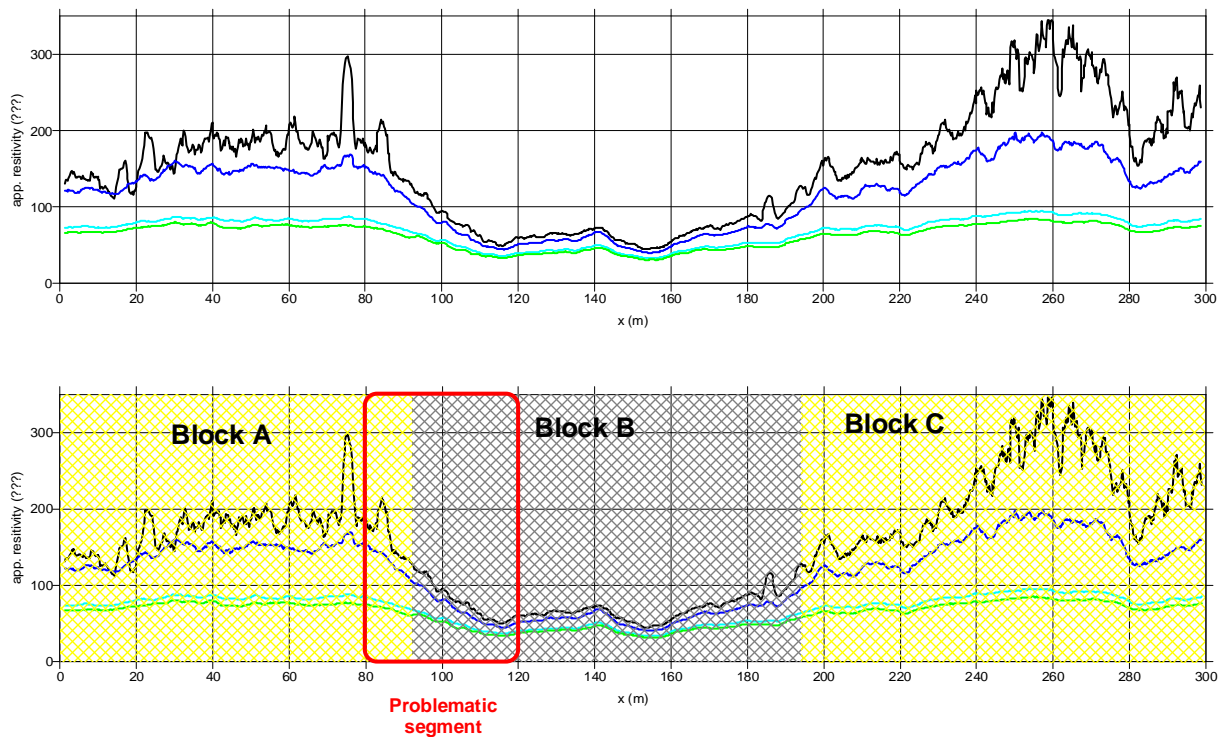
Figure 4.6 - Results of quick measure testing carried out using GEM-2 and delimitation of quasi-homogeneous blocks, in order to evaluate parts of the bank with homogenous electrical properties (Morris, 2005).

The curves can be analysed in the similar way as the resistance graphs based on self-induction electrical measurements. It allows the analysis of embankment material homogeneity, the location of sections with relatively higher permeability or with some leakage suspicion. On condition that the device will be calibrated and the stability of measured data will be certified, this method can be also used for quick repeated measurements. It allows prompt location of sections with abnormal changes of conductivity in the course of time (e.g. in time of high water level) which often correlates with the leakage section.

FDEM induction devices can achieve a huge amount of information in really short time, indeed it can be used in a variety of ground conditions (grass/brush/tree cover, ridged ground etc.) where other techniques may be more difficult to use (GPR for example is massively influenced by surface conditions). The results are characterized by a considerable repeatability, demonstrating that EM method works well in different conditions and it can used in dry periods as well as wet. GEM-2 or EMP-400 can measure magnetic susceptibility (p.p.m.) as well as earth conductivity (mS/m), achieving furthermore a certain degree of vertical separation of geophysical phenomena. Some cautions must be managed with field technique, as the sensitivity for temperature drifts eventual digital lags, and an appropriate

visual output and data processing is required. EM methods in some cases can present drawbacks associated with sensitivity to a wide range of metals and even much greater sensitivity of near-surface targets and it is subject to electrical interference of certain electromagnetic frequency (overhead power lines). As a matter of facts, Asch et alii, 2008 in American river levees encountered several problems using FDEM methodology, especially searching to achieve quantitative data with the usage of inversion programs: this is primarily because of a low induction number in a noisy environment. Indeed, when FDEM device encounters a strong resistive ground, its small separation distance between the transmitter and receiver, and a band-limited frequency range can let it operate in the "low induction number" range, previously introduced. Within the low induction number range, the sensor response is linearly dependent on frequency and not on variations in the ground resistivity. For the FDEM devices geometry, assuming non-magnetic ground, a low induction number corresponds to a not sufficient "conductivity by frequency "product; the EM response in this range is small (with the EM in-phase component being significantly smaller than the quadrature component), so that resistivity changes at a given investigation frequency may not produce large enough variations in the measured data. In addition, the observed response of the tool at multiple investigation frequencies can be almost linearly correlated and therefore depend on the measured frequency and not on the electrical resistivity of the ground. The result of this is that electrically conductive and resistive anomalies can be detected and then located, but conductivity depth images (i.e., thicknesses of anomalous zones) cannot be developed by numerical inversion; it leads to consider this methodology very useful for a preliminary investigation of the subsoil, which can delimitate anomalous zones, successively analyzed with methods that are more detailed. Furthermore, in case of very resistive grounds, the low degree of EM signal attenuation observed results in large skin depths that exceed practical depths of exploration. All the resistivity depth variations would be lumped into a single equivalent layer.

5. ELECTRICAL RESISTIVITY TOMOGRAPHY

Electrical resistivity method is a geophysical method, which utilizes direct currents or low frequency alternating currents to investigate the electrical properties (resistivity) of the subsurface. Surface electrical resistivity surveying is based on the principle that the distribution of electrical potential in the ground around a current-carrying electrode depends on the electrical resistivity and distribution of the surrounding soils and rocks. The usual practice in the field is to apply an electrical direct current (DC) between two electrodes implanted in the ground and to measure the difference of potential between two additional electrodes that do not carry current. The electrical resistivity method is one of the most widely used, a relatively quick and cheap way of getting subsurface information. The method is also known as **geoelectricity, electrical resistivity tomography (ERT)** and **direct current resistivity (DC resistivity)**. The purpose of resistivity surveys is to determine the subsurface resistivity distribution by making measurements on the ground surface.

5.1 Resistivity of rocks and minerals

The concept of electric resistivity will be right now stated; electric resistivity is a property of natural rocks and sediments and can vary greatly, depending on a number of factors. The amount and interconnectivity of various minerals plays an important role. The typical range of electrical resistivities of earth materials is visible in figure 5.1.
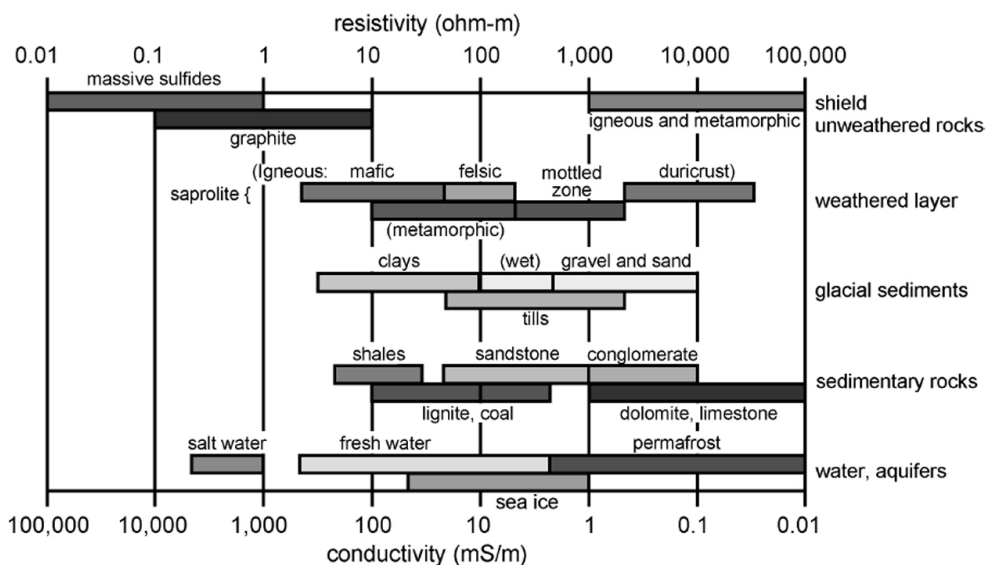
Figure 5.1 – Ranges of electrical resistivity for some common rocks, soils and ores (Sjodahl, 2006).

Mineral grains composing soils and rocks are essentially nonconductive, except metallic ores, so the resistivity of soils and rocks is governed primarily by the amount of pore water, its resistivity, and the arrangement of the pores. The resistivity of water depends significantly on the concentration of salts, which provide dissolved ions that act as charge carriers. Fresh groundwater will usually have a resistivity in the range of 10 to 100 Ωm, while saltwater is more conductive by a factor from 100 to 1000 and consequently significantly less resistive (0.1 Ωm). To the extent that differences of lithology are accompanied by differences of resistivity, resistivity surveys can be useful in detecting bodies of anomalous materials or in estimating the depths of bedrock surfaces. In coarse granular soils, the groundwater surface is generally marked by an abrupt change in water saturation and thus by a change of resistivity. In fine-grained soils, however, there may be no such resistivity change coinciding with a piezometric surface. Generally, since the resistivity of a soil or rock is controlled primarily by the pore water conditions, there are wide ranges in resistivity for any particular soil or rock type, and resistivity values cannot be directly interpreted in terms of soil type or lithology. However, zones of distinctive resistivity can be associated with specific soil or rock units on the basis of local field or drills information, and resistivity surveys can be used profitably to extend field investigations into areas with very limited or nonexistent data. In addition, resistivity surveys may be used as a reconnaissance method, to detect anomalies that can be further investigated by complementary geophysical methods and/or drill holes.

5.2 Theoretical Basis

The ability of a medium to conduct an electric current is termed electrical conductivity σ (S/m) and the inverse of it is called electrical resistivity ρ (Ωm). When a static electric field E (V/m) is applied, a current density J (A/m^2) is established. Ohm's law in the case of a linear isotropic medium state that:

$$E = \rho J = \frac{J}{\sigma} \tag{5.1}$$

Earth bulk materials are comprised of a solid phase (rocks and soils) and a space phase (pores, cracks, micro fissures, fractures, etc.) that occupy the space between the solid materials. Thus the bulk resistivity of earth materials is associated with the resistivity of the solid phase (rock matrix), and the resistivity of materials that fill the open space, which may

be air, oil or any liquid. The resistivity of an electrolyte in pore spaces dominates the formation resistivity in most cases. The degree of pore interconnectivity greatly influences a rock's bulk resistivity and the shape of the pores has some effect. The most widely used relationship between the porosity (ϕ), water saturation (S_w), resistivity of the electrolyte (ρ_w) and bulk resistivity (ρ) can be expressed by Archie's law.

$$\rho = \rho_w S_w^{-n} \phi^{-m} \tag{5.2}$$

where m is the cementation exponent of the rock (usually in the range 1.8–2.0), and n is the saturation exponent (usually close to 2). The rock matrix cannot be assumed as an insulator when clay minerals are present. Indeed clay minerals are very good conductors due to the presence of mobile ions adsorbed to the grains. At the interface between the grains of clay minerals and the electrolyte, the ions in the electrolyte will be attracted or repelled from the clay surface and produce an electric double layer. The resistivity of an electrical double layer is the surface resistivity ρ_s ($= 1/\sigma_s$), expressed in ohmmeter. The bulk resistivity when the surface resistivity is present is expressed by a modification of Archie's law:

$$\rho = \rho_w S_w^{-n} \phi^{-m} + \sigma_s \tag{5.3}$$

This property is present for all silicate minerals to a greater or lesser extent. For very well cemented or crystalline rocks with lower porosity, it might be dominating conductivity mechanism even when no clay present. The resistivity readings of the ground, which are measured by injecting current with two electrodes and measuring the resulting potential difference with two other electrodes, are usually converted to an apparent resistivity, corresponding to the resistivity of a homogeneous half-space that would give the same result. The investigated volume can be changed by moving the electrodes. Large separations give larger investigation depths. Modern data acquisition systems have made it feasible to measure resistivity along profiles with several electrode separations.

The data are usually inverted to a vertical resistivity section also called **pseudo-sections**, assuming 2D geometry perpendicular to the profile. If an electric current I (A) is flowing through a linear conductor of uniform cross-section A (m^2) and a length L (m). Ohm's law states that:

$$\Delta V = IR \tag{5.4}$$

where ΔV is the potential difference (volt, V) between the ends of the conductor and R (ohm, Ω) is the resistance of the conductor. The resistivity (ρ) that is the physical property of the conductor that can be defined by:

$$\rho = \frac{RA}{L} \tag{5.5}$$

The basis of the electrical resistivity method is to introduce a known current into the ground and measure potential differences on the surface to estimate the resistivity of the subsurface. Considering a homogeneous and isotropic half-space, electrical equipotentials are hemispherical, when the current electrodes are located at the soil surface. The current density J (A/m^2) has then to be calculated for all the radial directions with:

$$J = \frac{I}{2\pi r^2} \tag{5.6}$$

where $2\pi r^2$ is the area of a hemispherical sphere of radius r. The potential V can then be expressed as follows:

$$V = \frac{\rho I}{2\pi r} \tag{5.7}$$

5.3 Resistivity surveying

The resistivity measurements are made by introducing a DC or low frequency alternating current into the ground by means of two electrodes (A, B) connected to a portable power source. The resulting potential difference is measured on the ground with two potential electrodes (M, N). The potential field produced in the underground is dependent on the dispersion of the specific electrical resistance; hypothesizing the resistance homogenous, the electric current and potential field lines are produced as illustrated in Figure 5.2.
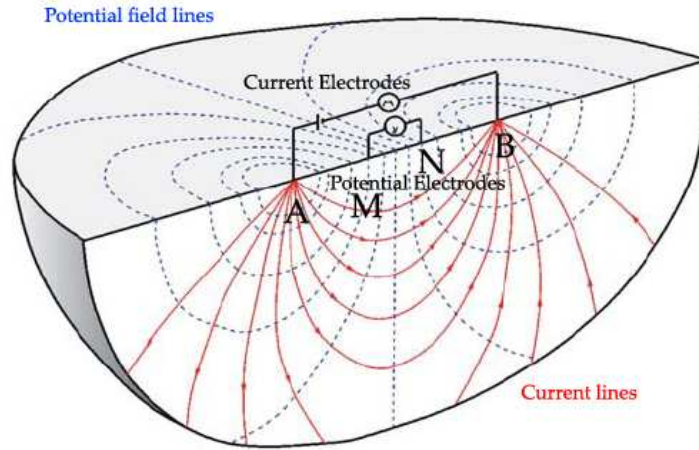
Figure 5.2 - Current and potential field showed in the situation of homogenous dispersion resistance (Mainali, 2006).

There are a number of different electrode configurations available for resistivity surveys. The arrays that are most commonly used for two dimensions (2D) resistivity imaging surveys are Wenner, Dipole-Dipole, Wenner-Schlumberger, Pole-Pole and Pole-Dipole. There are other electrode configurations, which are used experimentally or for non-geotechnical problems or are not in wide popularity today. Some of these include the Lee, half-Schlumberger, polar dipole, dipole dipole, and gradient arrays, as well as the boreholes configurations (Fig. 5.3). Choice of array generally depends on the nature of the investigation, field condition, and the sensitivity of the resistivity meter, the background noise level and work force. The sensitivity of the array is estimated from the potential difference that can be measured from a specific change in resistivity. Normally, the highest sensitivity can be obtained closest to the electrode.

The Potential difference (ΔV) measured between the electrodes M and N is given by the following equations:

$$\Delta V = V_M - V_N \text{, where}$$

$$V_M = \frac{\rho I}{2\pi}\left(\frac{1}{AM} - \frac{1}{BM}\right), \text{ and } V_N = \frac{\rho I}{2\pi}\left(\frac{1}{AN} - \frac{1}{BN}\right), \text{ thus}$$

$$\rho = \frac{2\pi}{\left(\frac{1}{AM} - \frac{1}{BM} - \frac{1}{AN} + \frac{1}{BN}\right)}\left(\frac{\Delta V}{I}\right) = \frac{K\Delta V}{I} \tag{5.8}$$

where K is the geometric coefficient that depends on the arrangement of the four electrodes A, B, M and N. The previous equation can be used to calculate the true resistivity of the underground if the medium is homogenous.

Electrode array	Electrode configuration	Configuration factor
Wenner Wenner α Lee		$K = 2\pi\, a$
Schlumberger		$K = \pi\, n\,(n+1)\,a$ $n > 3$
dipole-dipole axial dipole Wenner β		$K = \pi\, n\,(n+1)\,(n+2)\,a$
pole-dipole half Schlumberger Hummel		$K = 2\pi\, n\,(n+1)\,a$ $n > 3$
pole-pole		$K = 2\pi\, a$
gradient		$K = 2\pi \left[\dfrac{1-X}{(Y^2 + (1-X)^2)^{\frac{3}{2}}} + \dfrac{1+X}{(Y^2 + (1+X)^2)^{\frac{3}{2}}} \right]^{-1}$ $\left(X = \dfrac{x}{\Delta};\ Y = \dfrac{y}{\Delta} \right)$
surface-borehole dipole-dipole pole-dipole pole-pole		
in boreholes dipole-dipole pole-dipole pole-pole		

Figure 5.3 - Common electrode arrays that are used in resistivity surveys (Knödel et alii, 2008).

The resistivity so obtained will be constant and independent of both electrode configuration on and surface location. If the ground is inhomogeneous, the resistivity (ρ) varies on altering the geometrical arrangement of the electrodes. The resistivity that is then

calculated is termed the apparent resistivity, ρ_a and it should be considered as some sort of average resistivity encountered in the heterogeneous underground. In general, all field data are apparent resistivity. They are interpreted to obtain the true resistivity of the layers in the ground. The apparent resistivity will be close to the true resistivity close to the electrodes when the relative electrode spacing is very small.

There are various methods involved to get the apparent resistivity of the subsurface. Resistivity profiling is on, in which the spacing of electrodes is kept constant along the survey line; this provides a lateral resistivity distribution at a constant depth. **Vertical electrical sounding (VES)** method gives the apparent resistivity variation with depth for a horizontal layered earth by taking number of measurements at a common midpoint with successive larger electrode separation. The calculated resistivity is plotted as a function of electrode separation to produce a sounding curve; anyway, this method produces results that must be calibrated with boreholes or other destructive tests. A VES line of descent is represented by the two dimensional electrical profiling; also known as electrical imaging or **electrical tomography**, which provides pseudo-section of electrical resistivity distribution (both later and vertical) of subsurface and has almost completely replaced the VES method. In this method, utilized for the purposes of this research, the current and potential electrodes are expanded to obtain the information from greater depth and shifted along a profile line to determine lateral changes in electrical resistivity. The choice of the "best" array for a field survey depends on the type of structure to be mapped, the sensitivity of the resistivity meter and the background noise level. In practice, the arrays that are most commonly used for 2-D imaging surveys are the Wenner, dipole-dipole Wenner- Schlumberger, pole-pole and pole-dipole. Among the characteristics of an array that should be considered are the depth of investigation, the sensitivity of the array to vertical and horizontal changes in the subsurface resistivity, the horizontal data coverage and the signal strength. Among all the types of electrode arrays, a brief description of the configuration that are most commonly used (Schlumberger, Wenner, and dipole-dipole) is here presented and illustrated in Figure 5.3. The geometric factor for any four-electrode system can be found from Equation 5.8 and it can be developed for more complicated systems by using the rule illustrated by Equation 5.7. It can also be seen from Equation 5.8 that the current and potential electrodes can be interchanged without affecting the results; this property is called *reciprocity*.

- **Wenner array** (Figure 5.3a). This basic array consists of four electrodes in line, separated by equal intervals, denoted *a*. Applying Equation 5.8, the geometric factor K is equal to 2πa, and therefore the apparent resistivity is given by:

$$\rho_a = 2\pi a \frac{\Delta V}{I} \; ; \qquad\qquad\qquad (5.9)$$

Because of this property, the Wenner array is relatively sensitive to vertical changes in the subsurface resistivity below the centre of the array. However, it is less sensitive to horizontal changes in the subsurface resistivity. In general, the Wenner is good in resolving vertical changes (i.e. horizontal structures), but relatively poor in detecting horizontal changes (i.e. narrow vertical structures). Wenner electrodes configuration has a relative shallow penetration depth, which can be estimated as 0,5 times the electrodes spacing *a*. While the Schlumberger array has always been the favoured array in Europe, until recently, the Wenner array was used more extensively than the Schlumberger array in the United States. In the past, for a survey with varying electrode spacing, field operations with the Schlumberger array were faster, because all four electrodes of the Wenner array are moved between successive observations, but with the Schlumberger array, only the outer ones needed to be moved. Nowadays, the Schlumberger array is considered superior in distinguishing lateral from vertical variations in resistivity. On the other hand, the Wenner array demands less instrument sensitivity, has the strongest signal intensity and the consequent reduction of noise is an important factor when a survey close to zones characterized by antrophic activities is needed. This configuration was used for the measurements campaign for Reno River embankments in locality Case Reno Sabbioni.

- **Dipole-dipole array** (Figure 5.3b). This array was, and is still, widely used in resistivity and IP surveys because of the low EM coupling between the current and potential circuits. The dipole-dipole array is one member of a family of arrays using dipoles (closely spaced electrode pairs) to measure the curvature of the potential field. If the separation between both pairs of electrodes is the same *a* and the separation between the centres of the dipoles is restricted to *a(n+1)*, the apparent resistivity is given by:

$$\rho_a = \pi a n (n+1)(n+2) \frac{\Delta V}{I} \; ; \qquad\qquad\qquad (5.10)$$

Is important to remark that this electrodes configuration has the current dipole and potential dipole separation, achieving the less EM noise value, indeed this array is widely used for both resistivity and self-potential measures. This array is especially useful for measuring lateral resistivity changes and has been increasingly used in geotechnical

86

applications. The penetration depth reached is similar to the Wenner array penetration depth but dipole-dipole array offers a wider horizontal analyzed surface. For the Samoggia River application, this method was successfully chosen to check the embankment condition after filtering and piping phenomena.

- **Schlumberger array** (Figure 5.3c). For this array, given *a* as the electrode spacing, in the limit as *a* approaches zero, the quantity *V/a* approaches the value of the potential gradient at the midpoint of the array. In practice, the sensitivity of the instruments limits the ratio of *s* to *a* and usually keeps it within the limits of about 3 to 30. Therefore, it is typical practice to use a finite electrode spacing and Equation 4.12 to compute the geometric factor. The apparent resistivity is:

$$\rho_a = \pi a \left[\left(\frac{s}{a} \right)^2 - \frac{1}{4} \right] \frac{\Delta V}{I} \ ; \tag{5.11}$$

In usual field operations, the inner (potential) electrodes remain fixed, while the outer (current) electrodes are adjusted to vary the distance s. The spacing *a* is adjusted when it is needed because of decreasing sensitivity of measurement. The spacing a must never be larger than 0.4 *s* or the potential gradient assumption is no longer valid. Also, the *a* spacing may sometimes be adjusted with *s* held constant in order to detect the presence of local in-homogeneities or lateral changes in the neighbourhood of the potential electrodes. Technology has significantly improved the acquisition field works and nowadays many powerful systems, consisting of a multi-channel board for connecting two current and numerous potential electrodes to multi-channel software are available. The multi-electrode system can perform high-resolution 2D and 3D resistivity surveys. The penetration depth of this array is obviously influenced by electrodes spacing and it can be estimated as 0,6 times the *a* value. This array is moderately sensitive to both horizontal (for low "n" values) and vertical structures (for high "n" values). In areas where both types of geological structures are expected, this array might be a good compromise between the Wenner and the dipole-dipole array.

Recapitulating, there are many different types of electrode arrays (also called spreads or configurations) although in practice only a few of them are used. Just the most important were previously introduced. Each array has its advantages and disadvantages with regard to depth of investigation, resolution of horizontal and vertical structures, sensitivity to lateral changes in resistivity (lateral effects) and inhomogeneity, to depth of targets, to dip and

topography, etc. Depending on the array characteristics and the objective, the appropriate array has to be selected for each survey. A sensitivity matrix is an important part of the inversion algorithms. For a given electrode array, this matrix is used to evaluate the contribution of the spatial elements of the subsurface model to the measured apparent resistivity. Sensitivity matrices are very helpful for the understanding of measured data and, especially for the planning a survey, as they allow conclusions to be drawn about the resolution capabilities and investigation depths of different electrode arrays. For the case of a homogeneous half-space, some examples of sensitivity matrices for commonly applied electrode arrays are given in Figure 5.4. Each of these examples shows that there are areas of positive as well as of negative measured apparent resistivity when the structure in that area has a higher resistivity than the surrounding material. Negative sensitivities always occur in the space between a current and a potential electrode, whereas the sensitivity is always positive between two current electrodes and between two potential electrodes. The spatial sensitivity generally decreases with increasing distance from the electrodes (Knödel et alii, 2008). The plots in the left side of Fig. 5.4 show sensitivities for small electrode spacing, whereas those on the right side show sensitivities for larger electrode spacing. It can be seen, for example, in plots (*c*) and (*d*) that the sharp, almost vertical boundary between positive and negative sensitivities is the reason why pole-dipole arrays have a very good lateral resolution. The fairly high resolution of dipole-dipole measurements in the case of small targets results from a structured sensitivity distribution (*e* and *f*). Nevertheless, it can also be seen that inhomogeneity near the electrodes significantly influences the measured apparent resistivity. Experience shows that the results of Schlumberger arrays are mainly determined by the ground conditions below the potential electrodes (*g* and *h*). Finally, the fairly smooth sensitivity distributions shown in plots (*i*) and (*j*) explain the comparatively low lateral resolution of a Wenner array. However, this array is advantageous if the investigation area is subject to electromagnetic noise. In general, the geology of interest has a 3-D resistivity distribution. Normally, this would require a 3-D resistivity survey. Nevertheless, this is, as already mentioned, very time consuming and expensive at present. In many practical cases the problem can be reduced to a 2-D or even a 1-D case, but it must always be kept in mind that the measurements can be influenced by objects outside the arrays. In the 2-D case it is assumed that the resistivity of the ground varies only in the vertical and one horizontal direction. There is no resistivity variation in the second horizontal direction (strike direction).
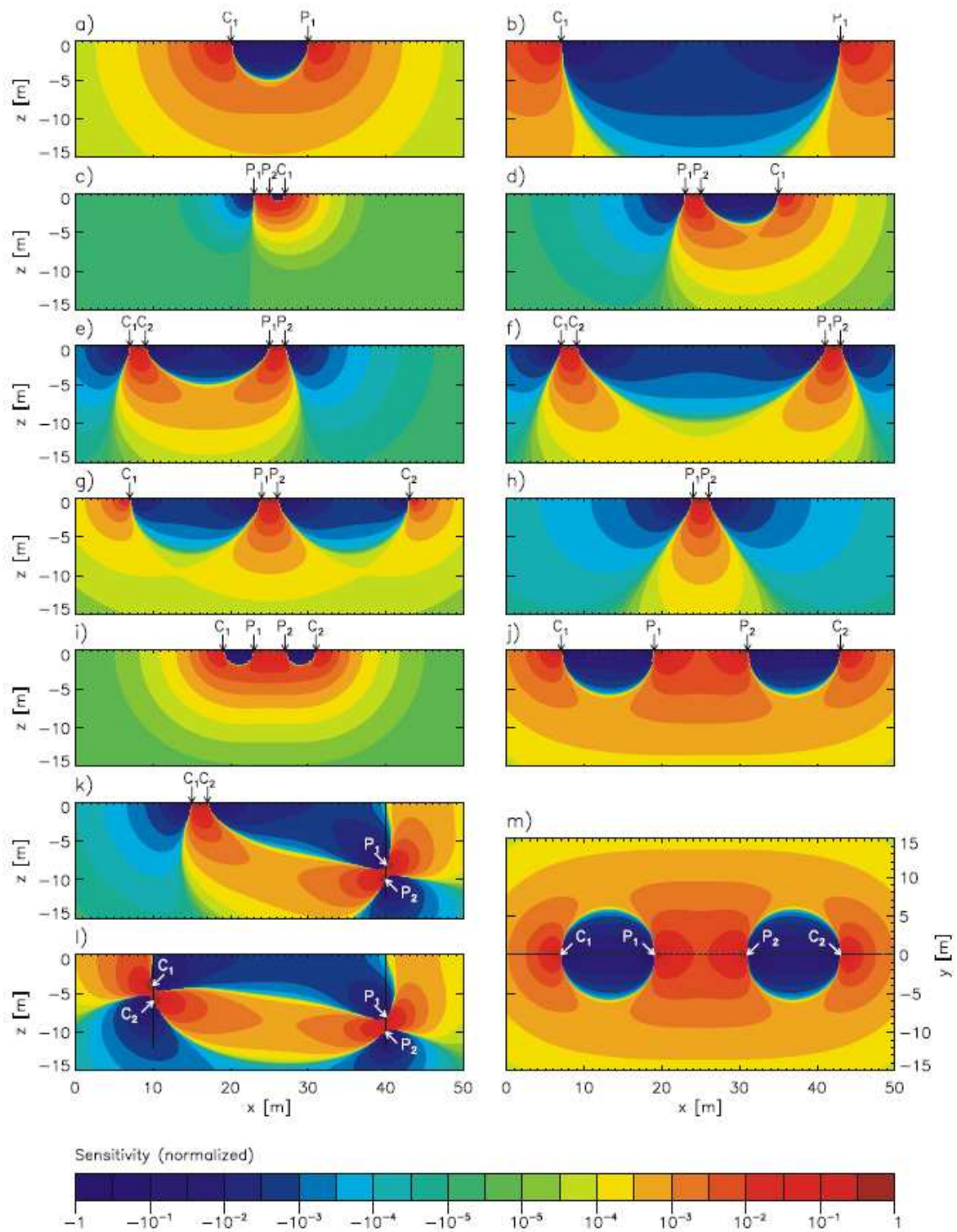
Figure 5.4 - Sensitivity of several electrode arrays, examples for the 2-D-sensitivity distribution in a homogeneous half-space: (a,b) pole-pole, (c,d) pole-dipole, (e,f) dipole-dipole, (g,h) Schlumberger array, (i,j) Wenner array, (k,l) dipole-dipole with electrodes in boreholes, (m) Wenner array but x-y-plane of the sensitivity. All plots are normalized with respect to the maximum of each matrix (Knödel et alii, 2008).

As a consequence, survey profiles should run perpendicular to the strike of such structures. There are still problems with the determination of the confidence intervals and parameter limits of models for the 2-D and 3-D cases, which generate amlargeuity. Amlargeuity is influenced by several factors: the structure of the grid used to approximate the geological

89

structures, limited data density, and errors in the data. Although these issues can limit the confidence associated to the measurements, a correct calibration with other geophysics surveys or direct methods can assure the model effectiveness.

5.4 Inversion of the measured data

Concerning the data treatment, the first step to make as previously stated is the choice of the correct electrodes configuration, in order to achieve the best results for the target, which need to be described. Some commercial software have introduced the forward modelling program, where the subsurface resistivity distribution is specified and the purpose is to calculate the apparent resistivity that would be measured by a survey over such a structure, and it can be an useful tool, particularly during the planning stage of the survey. However, the most important part is the data inversion, because after the field survey, the resistance measurements are usually reduced to apparent resistivity values. The data is visualized as a graphic in which all the points of equal apparent resistivity are correlated by a curved called *isoresistive* and different colour are associated to different isoresistive values.

The data inversion corresponds to find a model that provides the correct interpretation of the apparent resistivity values in order to generate the most reasonable representation of the subsoil. The model has a set of model parameters that are the physical quantities that have to be estimated from the observed data. The model response is the synthetic data that can be calculated from the mathematical relationships defining the model for a given set of model parameters. Such model is an idealized mathematical representation of a section of the earth. Primary, the set of all observed data can be written as a column vector **y**, as well as both the model response **f** and the model parameters **q**:

$$y = col(y_1, y_2,......y_n), f = col(f_1, f_{2,}.......f_n), q = col(q_1, q_2,......q_n);$$ (5.12)

The difference between the observed data and the model response is given by the discrepancy vector **g**. All the errors produced by the discrepancy can be reduced by several equations, which have been developed to provide a correct data inversion. From these basis and form the measured data, a two-dimensional (2-D) resistivity models can be therefore calculated by using several inversion programmes and related equations, which are characterized by complexes mathematical techniques; a correct 2-D model discretisation methods must be chosen with the purpose of divide in certain cells or regions the measured

subsurface. To get a good model, the data must be of equally good quality. Bad data points are divided in two categories: *systematic,* usually caused by some sort of failure during the survey not referred to the true resistivity measurements, and *random*, which are linked with the resistivity anomalies due to telluric currents or low signal-to-noise ratio. The manual picking out the bad data points signify a difficult but important pre-inversion element. Commercials software disposes of a series of default settings to provide an inversion of the apparent resistivity vales. The problem of non-uniqueness is well known in the inversion of resistivity sounding and other geophysical data; however, the accuracy of the result is only as good as the accuracy of the assumptions made.

For the same measured data set, there is wide range of models that can give rise to the same calculated apparent resistivity values. To narrow down the range of possible models, normally some assumptions are made concerning the nature of the subsurface that can be incorporated into the inversion subroutine; indeed in almost all surveys, something is known about the geology of the subsurface. The name of the principal methodologies can be just introduced, the mathematical treatment avoid from the aims of these research:

- Gauss-Newton method.
- Marquandt-Levenberg method, (Lines and Treitel, 1984).
- Least-square method.
- Smoothness-constrained method, (Loke and Barker, 1996).
- Occam inversion (LaBreque et alii, 1996).
- Robust inversion.

For this project, the program RES2DINV Version 3.54 (Loke, 2008), exploiting a method based on a powerful iterative computation, was utilized. In this inversion program, the subsurface is divided into small rectangular blocks (Figure 5.5). The program uses a heuristic algorithm partly based on the position of the data points to generate the size and position of the model blocks, using a sophisticated algorithm to subdivide the subsurface, so that the arrangement of the blocks is loosely tied to the distribution of the data points in the pseudo-section. Each block represents a data point of apparent resistivity. The depth of the bottom row of blocks is set to be approximately equal to the equivalent depth of investigation. The number of blocks normally does not exceed the number of data points.
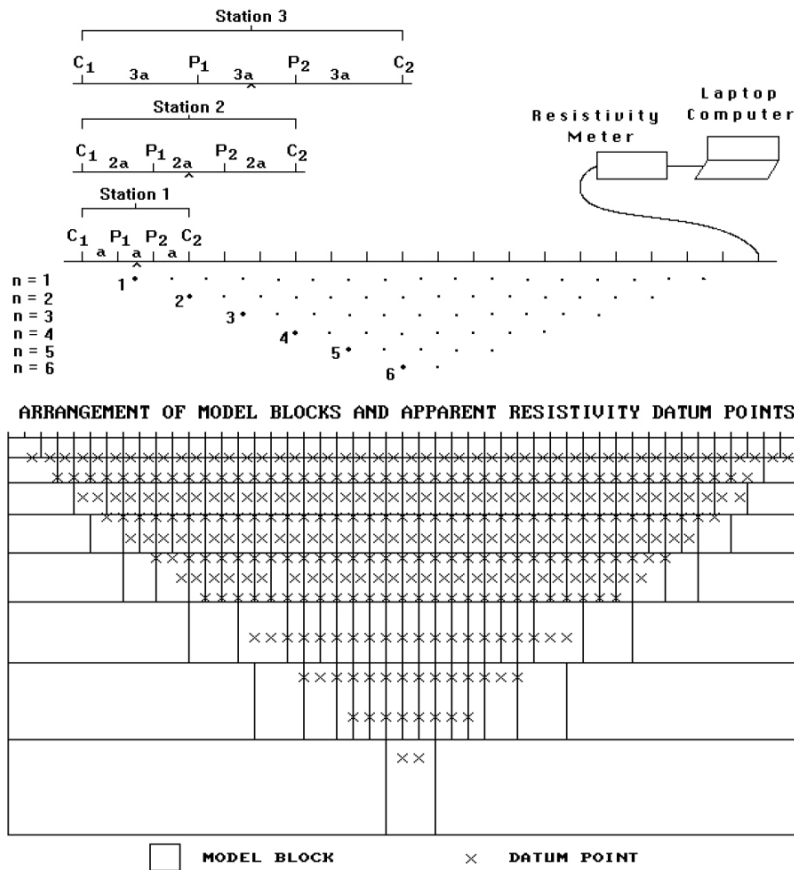
Figure 5.5 – Electrical tomography: sequence of measurements to build up a pseudo-section and arrangement of the blocks together with data points used in the inversion model (Loke, 2008), where C_1C_2=AB and P_1P_2=MN.

In surveys over areas with significant changes regarding the elevation of the ground surface, the effect of the topography must be taken into account when carrying out an inversion of the data set. While the traditional methods were using some correction factors for the topography, in the current programs the method incorporates the topographic effect into the inversion model. The arrangement of model blocks tries to reduce the difference between measured apparent resistivity values by adjusting the resistivity values of model blocks. Since there is a significant topographical relief along the survey lines, a correction for topographical effect is made. When the program reads a data file with topographic data, it will automatically select a finite-element method, which incorporates topography into the modelling mesh used. Then the topographic modelling is performed by inverting the data set. The final products of processing by the program are refined images of resistivity distribution in the subsurface.

5.5 River Embankment application

The resistivity method is a well established and widely used methodology in a variety of engineering and environmental investigations. The method is particularly attractive when monitoring on existing dams as well as river embankments, as it is non-intrusive but still has the potential of detecting changes in the inner parts of the embankment itself. Recent development of the method has been astonishing, both in data acquisition and data processing; such development in computational power has allowed for more efficient processing of data, which is encouraging for investigations with large amounts of data, such as three-dimensional investigations and repeated measurements.

Trying to summarize all the electrodes configuration that is possible to set up in electric tomography surveys, regarding the research aims, which concern the description of the river embankments, the Wenner array is an attractive choice for a survey carried out in a noisy area (due to its high signal strength) and also if good vertical resolution is required. The dipole-dipole array might be a more suitable choice if good horizontal resolution and data coverage is important. The Wenner-Schlumberger array (with overlapping data levels) is a reasonable all round alternative if both good and vertical resolutions are needed, particularly if good signal strength is also required. In case of a system with a limited number of electrodes, the pole-dipole array with measurements in both the forward and reverse directions might be a viable choice. For surveys with small electrode spacing and require a good horizontal coverage, the pole-pole array might be a suitable choice.

Generally speaking, resistivity monitoring on embankment and dams offers the possibility to measure material parameters and might therefore detect changes in composition of the core material, which follows when internal erosion is developing. Neiderleithinger et alii, 2007 have shown the geophysical measurements potential to give non-destructive information into embankments and subsoil. They are able to provide information on structure, material types and (with limitations) water content. Resolution and effort has to be balanced, because of the needing of site specific calibration. The resistivity, as already stated, depends on material, porosity, moisture content, salinity of pore water and other parameters. The results are thus often difficult to interpret. Electric tomography method determines integral values over a certain volume, and the reconstruction calculations ("inversion") are used to determine the approximately true subsurface resistivity distributions.
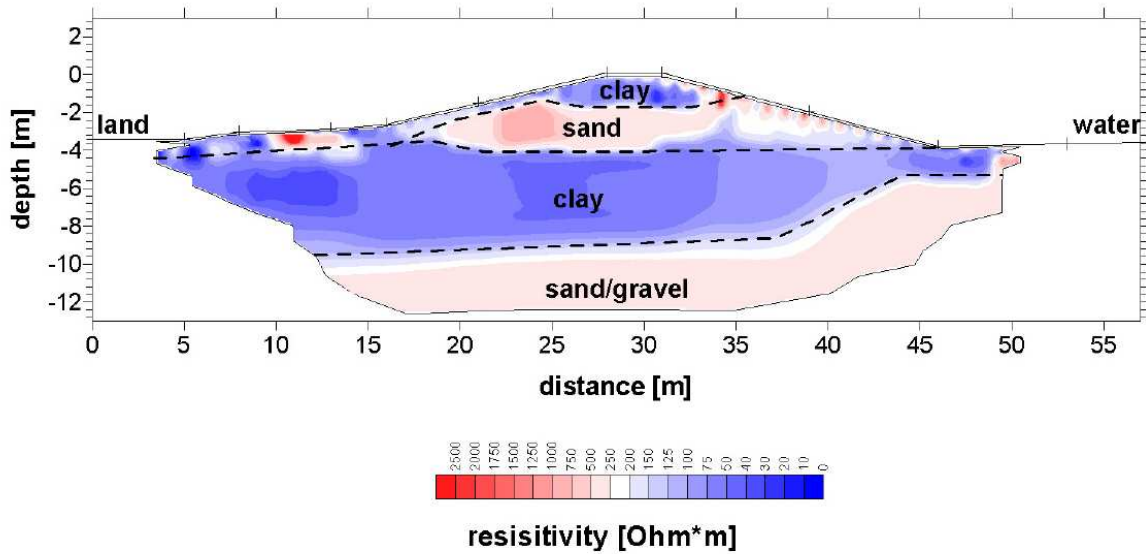
Figure 5.6 - 2D vertical electric tomography section through river embankments (Neiderleithinger et alii, 2007).

Figure 5.6 shows the result of a survey over an old river embankment (Neiderleithinger et alii, 2007); 44 electrode positions (distance in centre part 1 m, dipole-dipole configuration) were used. The resistivity distribution reveals not only the levee structure but also subsurface materials. Sans and gravel have much higher resistivities that clay, mud or peat. The water table is in the clay layer at about five meters depth, but it is no visible in the resistivity image.

With regard to this research project, some resistivity investigations were performed at various places on Reno River embankments and for the Samoggia Levees, which suffered a piping phenomenon, following hard and continuous precipitations. Resistivity pseudo-sections were measured along several profiles both longitudinal and transversal on the embankments. Data were first collected on Reno river embankments, in the summer 2007 using a dipole-dipole array and a multi-channel system. This system consists of a multi-channel board for connecting two current and eight potential electrodes to a SuperSting R8 IP8 channels by AGI, with multi-channel software. A common electrode spacing of two meters was used for all pseudo-sections. The application consisted in a comparison of various methodologies (GPR and MASW were also tested), in order to verify the advantages and the drawbacks of each method. Concerning the electric tomography measurements, these resulted in an investigation depth of around 20 meters, which was largely deeper than the river embankment thickness, so that a lack of precision and accuracy for the first meters from the surface affected the measurements. The inversion process needed some iteration, passing from the measured apparent resistivity pseudo-section, to the final inverted section (figure 5.7).

94
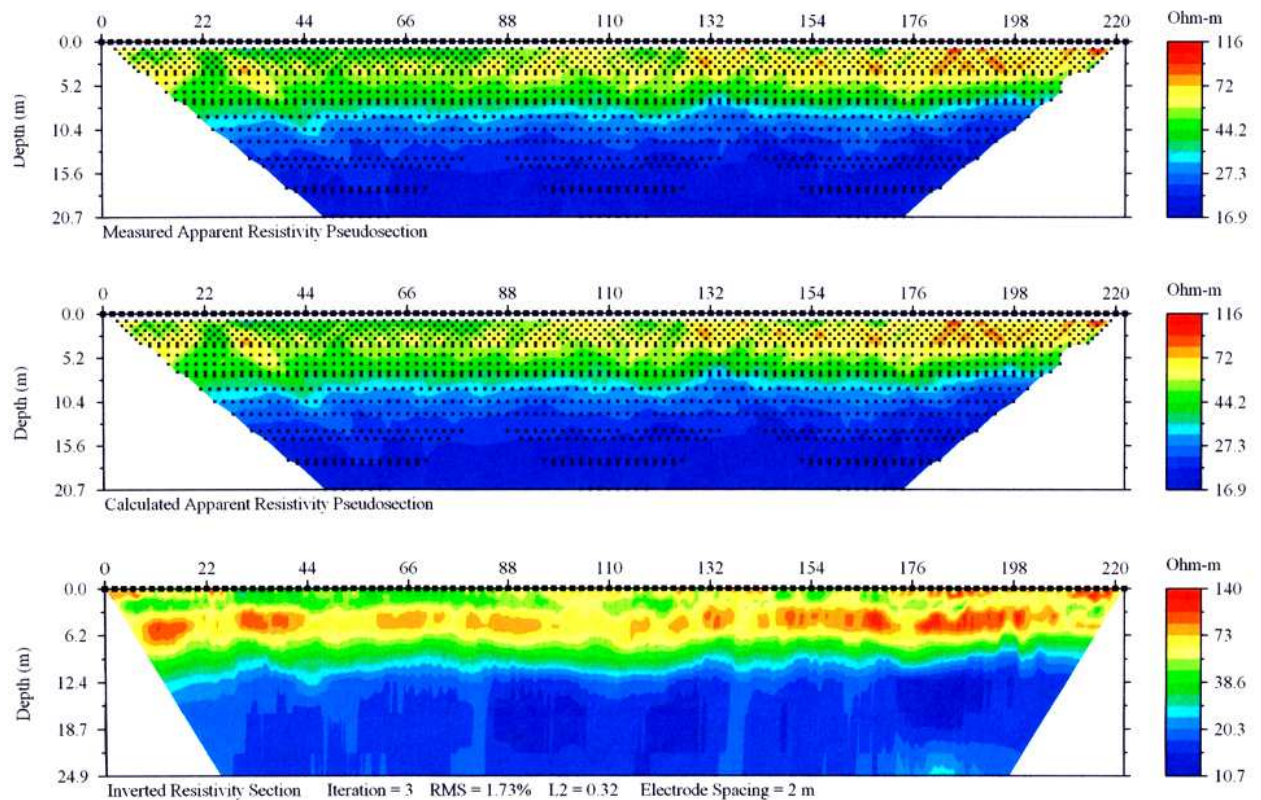
Figure 5.7 – Passage from apparent to real resistivity pseudo-section for the electric tomography measurement, through Reno river embankments.

After the piping event of 20th May 2008, the Regione Emilia-Romagna committed works of analyses, reparation and/or reconstruction of the Samoggia Stream embankment segments affected by the piping itself. Concerning the geophysical measurements, during the summer of 2008 the resistivity data were collected along both longitudinal and transversal profiles; Indeed, the initial plan was to provide geophysical measurements on the river levee before the reconstruction, in order to compare and calibrate the results given by geophysical methodologies with the real condition of the embankment internal structure itself. Unfortunately, the immediate necessity of mitigation works, provided under the supervision of STBR, has prevented such application and the tests had to be provided after the reconstruction and the reparation of sand boiling occurrences; however, many consideration can be made. The other geophysical methodologies involved in the campaign were EM induction (FDEM) and of course the GPR. The system used is the georesistivimeter ABEM mod. SAS4000 (maximum power 100 W), characterized by a sensitivity value of around one micro-volt, using a switch – box ABEM mod. ES464 and three set of multi-polar cables of 16 electrodes (hence 48 electrodes total). The measurements were performed using a dipole-dipole array (Figure 5.8) with 2 meters electrode separation. For example, if we use a

sequence of measurements for the dipole-dipole electrode array for a system with 40 electrodes, all the measurements will be performed with electrode spacing of "1x2 meters". For this case in the first measurement, electrodes number 1, 2, 3 and 4 are used. Electrode 1 was used as the first current electrode C1, electrode 2 as the second current electrode C2, electrode 3 as the first potential electrode P2 and electrode 4 as the second potential electrode P1. For the second measurement, electrodes number 2, 3, 4 and 5 are used for C1, C2, P2 and P1 respectively. This is repeated down the line of electrodes until electrodes 37, 38, 39 and 40 are used for the last measurement.
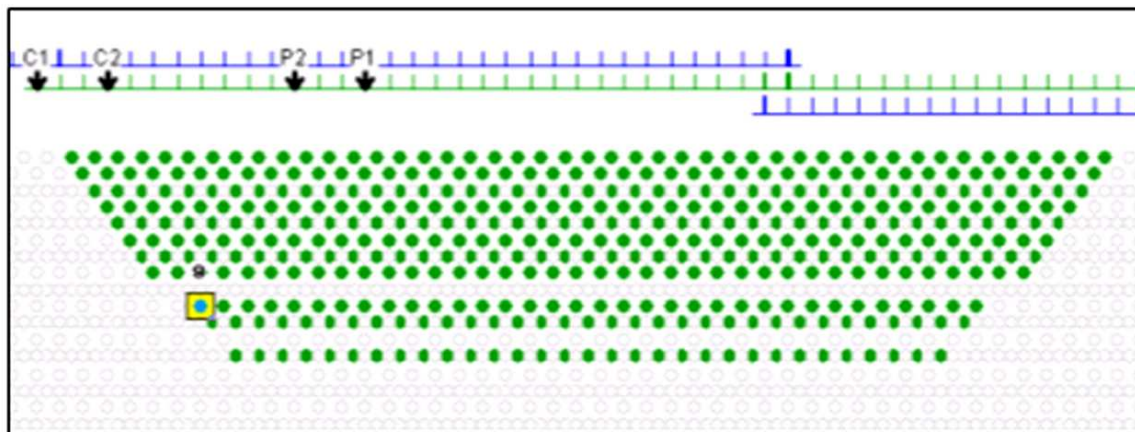
Figure 5.8 – Electrical tomography: acquisition settings for the dipole-dipole configuration, and collected data points used in the inversion model (Loke, 2008), where C_1C_2=AB and P_2P_1=MN.

6.   GPR APPLIED TO DIFFERENT TASKS

This chapter includes a detailed description of the most important profiles carried out using GPR methodology. It is divided into five parts representing the most important issues affecting the embankment of the Reno river basin. The following description has been chosen because of the constant emergence of new issues affecting this part of the Po Plain. At the beginning, this research was carried out with the aim to monitor levees throughout the year using GPR methodology. Unfortunately, many difficulties arose with regard to the realisation of seasonal measurement campaigns, essentially because of the massive amount of vegetation present on the embankments themselves (a number of programmed cuts and cleaning works are required) and because of the static hydrologic conditions (principally dry) throughout the entire duration of this research. However, the GPR, even if some interesting consideration can be carried out, seems to be inadequate for a high-quality monitoring campaign, mainly due to its insufficient depth penetration and the inconsistency of its measurements.

At some test sites, GPR results have been compared to those found using other non-invasive techniques, such as MASW, electric tomography and EM induction methodologies. Hence, with regard to the most important problem affecting the embankment of the Reno river basin, the measurement campaigns that have been carried out treat:

- **Areas affected by seepage and piping occurrence.**

- **Embankment segments rebuilt in the past**

- **Detection of animal cavities**

- **Inspection of the embankment internal structure**

- **Localization of stratigraphic contacts beneath river embankments**

It is important to remember that this research is part of a survey funded by the Reno River Basin Regional Technical Service (STBR) of the Regione Emilia-Romagna and that it has been a useful instrument in the detection of the hydraulic and geotechnical conditions of river embankments. The hydraulic safety of the Reno River, one of the main rivers in North-Eastern Italy, is indeed of primary importance to the Emilia-Romagna regional administration. Therefore, all the profiles carried out on the embankments as well as the results of this

research (especially radargrams) are included as a JPEG file in the Geographical Information System (GIS), available to the Regional Administration, and they represent the first major database related to geophysical measurements used for the embankment safety evaluation.

6.1   GPR campaigns settings

Before introducing all the results of this thesis, it is important to provide a brief summary of the characteristics of GPR. Recorded GPR signal represents the wave field of electromagnetic waves reflected from interfaces and objects in the surveyed environment. The results of the measurement are shown using the radargram. In radargrams, the longitudinal axis corresponds to the length of the measured profile while the vertical axis corresponds to the travel-time the radar reflection reached the system. Before their interpretation, it is useful to adjust recorded radar data using several wave filtration processes (to remove electronic noise and amplify the received signal). Finally, it is necessary to transform the vertical time axis into the depth scale. The easiest process to use is to utilise the reflection equation of the normal line electromagnetic signal. It is obvious that the recalculation to the depth units depends on the knowledge of the relative permittivity. This is invariable dimensionless material (the relationship between the velocity of electromagnetic waves spread in vacuum and wave velocity in a given environment). For the embankments environment this value can be estimated. The depth setting error for anomalous objects in a radar cross-section when using the values, specified in chapter three, should not exceed more or less twenty percent. As previously stated, GPR investigation depth is defined as the depth beneath which the signal received is too weak to be detected in the presence of noise. The embankments of the Reno River and the Napoleonic Channel are about ten to twelve meters high and the embankments of Reno River tributaries are five to eight meters high. Even if a frequency of 30 MHz is suggested for such depth of investigation (Morris, 2005) its scarce resolution has led to the choice of antenna frequencies higher than 100 MHz, so that ground-coupled and shielded antennas have been used. For each site, many data from in situ direct measurements (boreholes stratigraphy and/or cone penetration test with pore-water pressure management (CPTU)) are available. These kinds of data are fundamental for geophysical data calibration: they have enabled researchers to estimate some physical properties of the soil and to derive their relative dielectric constant (ε_r). Most of the investigated soils are sandy clayey silts (50% silt, 30% sand, 20% clay on average) with slight to considerable variations in the percentages of the three components.

6.1.1 Ground Penetrating Radars employed

The main campaigns were carried out using various GPR devices, which are the property of universities or private companies, in order to test the different Georadar operability and choose the best configuration. For whom it may concern, GPR websites and other information are successively reported.

- **Zond 12-e (Radsys, Latvia)**: employing 300, 500 MHz antennas (http://www.radsys.lv), it was utilized during the July 2007 campaign on the Reno River embankments, providing around 10 km of profiles, which produced some interesting results; unfortunately, the results are affected by many problems related to the inappropriate antenna design as well as the scarce resolution of the radargrams. The data elaboration has been carried out using the Prism2 software, released by the same Company.

- **RIS-MF (IDS, Italy)**: The main GPR campaign survey was carried out in October 2007 using the RIS-MF (IDS) Radar (http://www.idscompany.it/). More than 15 km of profiles were carried out and therefore more than 5 km of embankments were investigated in approximately ten working days. Results from GPR test areas will be presented in this chapter. The set of antennas selected is composed of a 100 MHz bi-static (100 transmitting, 100 receiving) antenna, a multi-frequency unit with three channels made up of 200 MHz and 600 MHz mono-static antennas, and a third channel represented by a bi-static cross-polar configuration (transmission 200 MHz – reception 600 MHz). RIS Ground Penetrating Radar was again used in October 2008 with a 400 MHz antenna to investigate the site affected by piping phenomena on the Samoggia Stream embankments. The acquired data, in raw format, which are not influenced by the automatic calibration realised during the acquisition campaign, have been elaborated with the IDS software GRESWIN2.

- **Ramac (Mala instrument)**, (Department of Earth Sciences, Prof. Farabegoli) Reno River embankments, near Bosco (BO), were analyzed in an April 2007 survey campaign using this Ground Penetrating Radar via the employment of 250 MHz and 500 MHz (http://www.malags.com/Home.aspx) antennas. Many problems related to the wet conditions and the homogeneity of the fine materials composing the embankment structure heavily compromised the data elaboration as well as the profile usefulness.

- **SIR-3000 (GSSI)**: (Department of Geophysics, Prof. Tinti). During the February 2007 survey campaign, the Geophysical Survey Systems Inc. (GSSI) SIR-3000 Ground Penetrating Radar and a mod.5103 antenna, which incorporates a transmitter, receiver and

electronics and has a frequency of 400 MHz, have been employed (http://www.geophysical.com/SIR3000.htm). The antenna unit, which is top and side-shielded, is mounted inside a special cart that plays a role of protection and enables a constant antenna coupling with the ground. The elaboration has been realised in the Department of Geophysics using the RADAN 6.5 software released by the same Company. Another survey campaign, the first one carried out as part of this project, was provided in August 2006 on a Reno River embankment one-hundred meter segment, with the use of a 100 MHz antenna.

6.1.2 Velocity determination

Chapter 3 has already introduced the velocity propagation and the different ways to estimate it; for the purpose of this research, two methods have been chosen. Generally, where detailed geotechnical information was available, the velocity estimation has been conducted assuming representative soil values from the literature, derived from laboratory electromagnetic characterisation; this method has been adopted considering the typical Reno River embankment structure, which is made up of sand and silt in slightly different ratios. A more complex but more accurate estimation is represented by the calibration with reflectors observed both in the field and by using other geophysical techniques, that will be treated successively. This method has been applied for the Savena Abbandonato Stream, where a metallic object giving a reflected signal has been put into the ground at a known depth. However, this kind of velocity test is no longer valid under the reflector depth.

- Values derived from the literature. The velocity estimation is conduced assuming representative soil values from the literature, derived from laboratory electromagnetic characterisation together with empirical application in comparable environmental conditions; this method has been adopted considering the typical Reno River embankment structure, which is made up of sand and silt in slightly different ratios. The method used to assume electric properties values becomes really practical when known reflector or hyperbolas are not present in radargrams as the velocity estimation can be realized assuming a gradual velocity change. For embankments lithology, generally characterized by fine grains, if a passage between, for example, 0.11 m/ns to 0.09 m/ns in the deeper subsurface is expected, the possible error would be lower than 10%. Under very unfavourable conditions (coarse sand (0.14 m /ns), overlying silt (0.09 m /ns)), the error could amount to an over-estimation of interface depth by ca. 20% if the surface velocity is used for the time–depth conversion of the entire radargram. However, the change in radar

electrical conditions makes it possible to assign a realistic velocity to each layer and thus reduce the possible error (Sass, 2007). Where a gradual change of electrical properties of the subsoil is supposed, principally due to a change in moisture porosity and hence compaction conditions, slight changes in velocity can be hypothesised and, in order to simplify the elaboration process, a unique average value of velocity can be assumed. Alternatively, if the radargram reveals some hyperbolas, many computations can be carried out; the slope of the asymptotes of the hyperbola is controlled by the velocity of propagation and thus it is possible to calibrate the dielectric permittivity between the antenna and the target and give a calibration and conversion of the two-way travel time into depth. The radius of curvature at the peak of the hyperbola and the lengths of the asymptotes (by taking into account the antenna pattern) give the size of the object causing it. The ellipse drawn within the hyperbola indicates the size of the object, assuming that the object is a circular cylinder with axis perpendicular to the plane of the data image (Olhoeft, 2000). For the greater part of the GPR profiles, the velocity evaluation has been executed through the dielectric constant (K) estimation of the materials, which constitute the river embankments structure, and by means of the computation that can be done when hyperbolas at different depths in the radargrams occur. The average value of $K = 9$ ($v = 10$ cm/ns) was considered whereas no calibration with reflectors observed in the field were provided. Another example of velocity estimation is given by the Samoggia Stream campaign, carried out in July 2008. Some profiles, carried out for the detection of conduits and their correct positioning, have been carried out over a road track, which has brought the author to estimate a dielectric constant (K) of around 7, a minor value with respect to the average soil value. This estimation is in accordance with the obtained results; the detected targets are indeed situated at around 0.95 m depth from the surface (verified with penetration tests). By means of the velocity calibration and conversion test, according to Equation 3.3, the average values of $K = 7$-8 and therefore velocity (valid just for the material above the conduits) $v = 11$ cm/ns have been obtained. Moreover, the computation that has been carried out with the slopes of the asymptotes of the hyperbola pretty gives the same result.

▪ Calibration with reflectors observed in the field. For such velocity test, as well as for the detection of anomalies and heterogeneities, some theoretical assumption must be taken into account. The radar reflection from the pipe or a single object is the result of electromagnetic wave propagation described by the radar equation and geometry through, among other things, the Fresnel reflection coefficient in amplitude, Snell's law in angle,

and the Stokes scattering matrix in polarization. In general, roughly equidimensional objects, such as cubes or spheres, that are at least 1/3 of a wavelength in cross-sectional size in typical noisy environments (or about 1/10 of a wavelength in exceptionally quiet environments) are resolvable if they have sufficient contrast in properties compared to the background (Olhoeft, 2000). Under such conditions, the physical relationship between spatial sensitivity (*S*) and wavelength (*λ*) is:

$$S = \frac{1}{3}\lambda \; ; \tag{6.1}$$

In theoretical soil conditions (soil with *K* = 9) may be considered *S* = 0.33 m and *S* = 0.16 m for antenna frequency equal to 100 MHz and 200 MHz, respectively. Obviously, not only the target size is of importance; in addition to the dielectric contrast, the depth of the target and the signal to noise ratio connected are of primary importance. Moreover, to define two separate anomalies inside the ground, Annan (2001) suggests that, considering ΔZ as the spatial separation to be resolved in metres and *K* as the dielectric constant or relative permittivity, the constraint on the centre frequency, f_c, takes the form:

$$f_c^R > \frac{75}{\Delta Z \sqrt{K}} \; ; \tag{6.2}$$

which means that a 100 MHz antenna in theoretical soil conditions (soil with *K* = 9) could resolve two separate objects located at a distance not shorter than 25 cm. Real conditions, with environmental noise and wet condition as well as heterogeneities affecting the soil, demonstrate that this value can be much larger. Typically, for geologic context this type of soil has a ε_r value range of 5 to 30, depending on the saturation conditions (Daniels, 2004); however, the direct experience for Reno River and its tributaries' embankments has revealed that this value can generally vary within a range of 6 to 15. For each site, many data from in situ direct measurements (boreholes stratigraphy and/or cone penetration test with water pore-pressure management (CPTU)) are available. These kinds of data are fundamental for geophysical data calibration of the soil and are necessary to derive their relative dielectric constant (ε_r). All the radargrams that will be presented have already experienced the velocity calibration, which achieves a correlation between the EM wave two-way travel time of the received signal and the real depth of the related reflection.

GPR in situ tests, performed by burying a metal object at a known depth (Figure 6.1), reveal that *K* value may be considered reliable for the soils where the tests have been performed. The reflections given by the test at a known depth (*d*) correspond to an EM two-way travel time (*t*), so that the velocity through the medium (*v*) can be calculated by using the Equation 3.15. The velocity can be also calculated by using the Equation 3.16; by combining the previous relationships and calculating the values of *d* and *t*, the following equation is obtained:

$$K = \left(\frac{ct}{2d}\right)^2 ;$$

(6.3)

This method of velocity estimation has been applied for the Savena Abbandonato Stream, using a 400 MHz antenna. According to the Equation 6.1, taking into account that a metallic object of at least 8.3 cm in diameter could be detected, such target was put at around 95 cm of depth. By means of this test, carried out on the internal flank of the Savena Abbandonato Stream levee, close to Uberseto (BO), the values of *K* = 5.8 and therefore velocity *v* =12.5 cm/ns have been obtained.
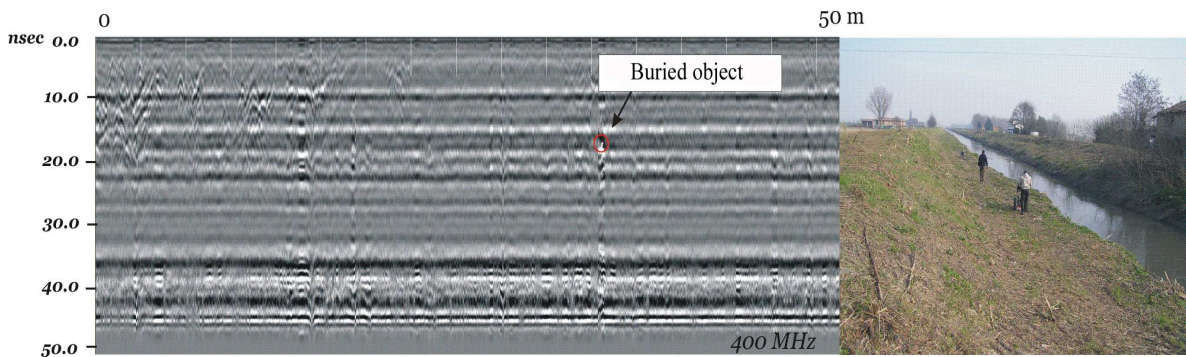
Figure 6.1 – Test carried out with buried object on the lateral flank of the Savena Abbandonato levee to obtain an EM wave velocity and dielectric constant quantification.

Such value of dielectric constant is therefore lower (and thus corresponds to higher velocity) with respect to the type of soil comprising the main part of the Reno River and its tributaries' embankment system; this result shows the higher presence of sandy materials. Such presence is confirmed by the amount of borehole and laboratory tests provided in the past for the embankment of this stream. Therefore, the obtained velocity has been used only for the Savena Abbandonato Stream embankments.

6.1.3 Surveys

The GPR methodology has been applied to the Reno River and its tributaries, together with the Napoleonic Channel. Throughout the duration of this research, a total amount of 40 km of GPR data profiles have been collected, employing four different GPR devices, to provide a detailed description of almost 15 km of river embankment segments. Some of these profiles refer to the same embankment segments, which have been investigated using different antenna frequencies (the Multi-frequency antenna produces a set of three profiles simultaneously). Some profiles have been carried out by measuring a definite segment but pertaining to the geometrical dimensions of the embankments (up to 12 meters, divided into three to four steps), the investigation of different embankment steps has been provided. Moreover, other parts of the levee have been investigated in separate campaigns using different GPR, in order to compare the quality of the results. Many tests have been carried out both in well-known areas in order to verify specific issues (stratigraphy, animal cavities and repaired zones) and in areas with no information available. The main GPR campaign survey was carried out in October 2007 with RIS-MF (IDS Ingegneria dei Sistemi, Pisa, Italy) radar, using a bi-static 100 MHz antenna and a multi-frequency 200-600 MHz antenna with two different antennas was used. The MF antenna set is mounted inside a special cart that plays a role of protection and enables a constant antenna coupling with the ground, while the 100 MHz antenna needs to be trailed by an operator. GPR scans have therefore been triggered by an odometer wheel with the resolution of one vertical scan per horizontal centimetre and a sampling rate of at least 512 samples per scan. A series of parallel profiles have been carried out to verify the lateral spreading of punctual anomalies present in the subsoil of the Samoggia Stream embankments; the IDS Georadar used, employing a 400 MHz antenna, has given excellent results. The acquisition software K2, released by the same Company, with the initial imposition of the dielectric properties relative to the material analysed, enables an approximate field calibration of the EM signal, which consists in an automatic *background removal* filter and automatic *gain* applications, to better visualize the radargrams and immediately detect anomalies and heterogeneities during the field measurements.

The GSSI profiles have been run in continuous mode as well and traces were triggered with odometer wheels. The GPR profiles were recorded at five traces per meter, and each trace was resolved using 2048, 16-bit samples. The GPR units have often been towed commercial carts, with antennas mounted in wooden/plastic mini-sleds, to prevent interference with nearby metal objects or surface roughness. The different antennas have been driven along the same tracks, with common start and stop points. Given that most of the

energy is limited to a finite bandwidth, an appropriate use of band limiting filtering may improve signal-to-noise without significantly altering the data. Taking into account the information obtained from the amplitude spectra of the raw data, for a 400 MHz antenna, a common band pass filter of 200 MHz to 800 MHz was applied to the whole set of profiles to improve the signal quality.

Another large campaign was provided using Zond 12-e GPR, which shows interesting results but has been affected by several problems related to the shallow penetration depth and scarce radargrams resolution. All the tests carried out with GPR devices have brought a good experience with the different GPR configurations and parameter settings. Most of the profiles were collected in with a distance interval between traces of a few centimetres. In this acquisition mode, each trace of the radargram is the result of a definite and variable stacking application, in order to improve the signal-to-noise ratio. Outcrop conditions, with relatively smooth surfaces and scarce vegetation presence, have made the acquisition of profiles in continuous mode possible, which provides greater horizontal resolution. Basically, the data have always been acquired in the same steps of the embankment, at the same altitude, so that no horizontal normalization has been necessary.

However, the data exhibit several problems. In many profiles, there is horizontal banding running across the image as a result of the less than optimal coupling of the antenna to the ground and unwanted oscillatory ringing of the antenna. Many difficulties have been encountered with regard to some of the profiles planned, especially concerning seasonal campaigns of measurement, essentially because of the massive amount of vegetation present on the embankments themselves (a number of programmed cuts and cleaning works are required) and because of the static hydrologic conditions (principally dry) throughout the entire duration of this research. Some embankments that were appositely cleaned for the geophysical measurements during the survey still maintained a surface roughness principally due to the presence of large roots or surface irregularities, as presence of constructions materials. All of these irregularities have triggered the "clutter" phenomena, described in Chapter three. Concerning the reliability of measurements, however, the GPR, even if some interesting consideration shall be done, seems to be inadequate for a high-quality monitoring campaign, mainly due to its insufficient depth penetration and the inconsistency of its measurements. Indeed, there is no simple parameter, such as water content or low frequency conductivity, that can be used as a convenient measure of dielectric loss in the employed frequency range 100 MHz to 1 GHz; therefore, any numerical consideration can be done.

Concerning the penetration depths, the materials making up the embankments have shown strong signal attenuation, which impedes to make any consideration about the entire embankment structure. Seasonal changes in EM wave penetration are present; during the summer, in dry conditions, the penetration depth increases with respect to the rest of the year where the moisture content is higher and therefore the attenuation arises. However, the changes in penetration capability between dry and relatively wet seasons are not as significant: indeed, where dry soils occur, the first meter of subsoil is often characterized by strong reflections, especially due to the irregular and fractured surface that the clay particles of the embankment soil produce when desiccated. Moreover, the embankment material at shallow depth, when it is mainly composed of silt with a slight amount of sandy or clayey elements, maintains a certain grade of humidity and its contents are not particularly affected by seasonal changes, apart from flooding. Indeed the oscillations of the water table inside the embankments are often not influenced by the surroundings variations and in any case the first four to five meters of the embankment from the surface are affected just in case of flooding; such characteristics contribute to producing similar material moisture conditions during the different hydrogeological seasons.

6.1.4 Signal Processing

The general objective of signal processing as applied to surface-penetrating radar is either to present an image that can be readily interpreted by the operator or to classify the target return with respect to a known test procedure or template. After the GPR data acquisition, this data must be processed in order to be more easily visualized and interpreted. Since data obtained from GPR surveys is similar to data obtained from seismic reflection surveys, many of the same techniques used to process seismic data can be used to process GPR data. Many commercial programs guarantee an adequate data processing; GRESWIN2 by IDS and RADAN 6.5 (GSSI) were mainly used for this research. In many cases, it is possible to use the results from a GPR survey with very modest processing. In these cases, the only processes that need to be carried out are to convert the data to a usable digital format, make gain adjustments to the data, and determine the depth to each eventual reflector in the subsurface (this involves converting time to depth).

For the purposes of this research, some standard procedures were followed; nevertheless, where it was necessary, some alternative actions or reiterations of the standard procedures were chosen. The first processing step is to remove the artefacts in the data. The **time zero** must be set at the first energy of arrival, and for these kinds of measurements, the

first arrival characterizes the interface air-ground. The time zero is also a function of the system timing, cable lengths, and antenna positioning. The horizontal black line is positioned at time zero and it shows the position of the line plotted across the top of the image (figure 6.2). The time zero is set up in order to mark the half-cycle of the reflected wavelet, which corresponds to the air-ground interface.
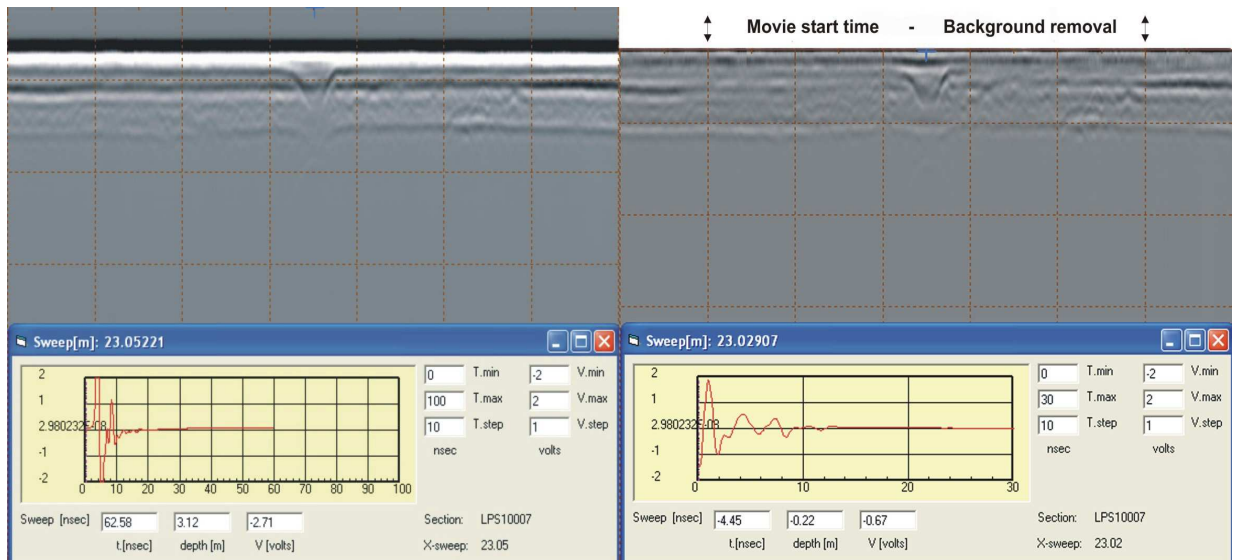
Figure 6.2 – Comparison between raw radar data acquired with a 200 MHz antenna and time zero determination with the average scan subtraction.

The average of all the scans, which have been accumulated, can be removed using the **background removal** filter in order to eliminate the antenna ringing and horizontal banding across the image; in figure 6.2 such elimination is shown. This part of the processing enables an efficient radar image enhancement and it can be applied in different phases of the processing itself; for 100 MHz antenna measurements, it has been used as the last filter of the processing, providing a final data cleaning. For higher antenna frequencies (200, 400, 600 MHz) its usage during the firsts steps of the processing has proven suitable. The background removal, besides the banding and ringing effects, can also remove other horizontal features such as flat lying geology and other planar reflection (as well as water table in flat profiles); indeed particular care was paid when using this filter. A **Vertical filter** has been applied to remove the radio frequency interferences from nearby wireless phone and portable radio transmissions and clean the frequencies irradiated by the wideband GPR antennas, which are significantly higher or lower with respect to the antenna central frequency; this can decrease the quality of the received data. In fact, in certain cases, these frequencies amplify the noise effects and they must be filtered through the band-filter. Concerning the data acquired with

the IDS GPR system and therefore processed with GRESWIN2 software and the RADAN 6.5 released by GSSI, the signal processing has been carried out with the familiar application of such vertical filters. As it is understandable, the purpose of filtering is to remove unwanted background noise. To remove this unwanted noise, the time-domain trace data is converted to the frequency domain using the Fourier transform. Desired frequencies are zeroed out, and then the trace is converted back to the time domain using the inverse Fourier transform. Figure 6.3 shows the typical wave spectrum panel (software GRESWIN2), with the presence of all the parameters relative to the emitted EM wave for a 200 MHz antenna. However, for each profile carried out, the environmental conditions as well as the eventual presence of electromagnetic disturbance fonts have been evaluated in order to provide the best vertical filter application. In some cases, a slight **horizontal filter** has been applied to give a strong cut to the horizontal banding across the image; its usage has been limited to those profiles where only punctual anomalies needed to be analyzed. The power spectrum (MHz) of the wave, presents a peak, associated to the central frequency of the antenna that was employed. The frequency peak differs slightly with respect to the nominal central frequency of the antenna. Moving away from the antenna central frequency it becomes apparent that the power of the emitted wave decreases, reaching the zero values (in dB) in proximity of the frequency 800 MHz. The low-pass filter (removing low-frequency signals) and high-pass filter (removing high-frequency signals) guarantee an adequate cleaning of the EM wave.
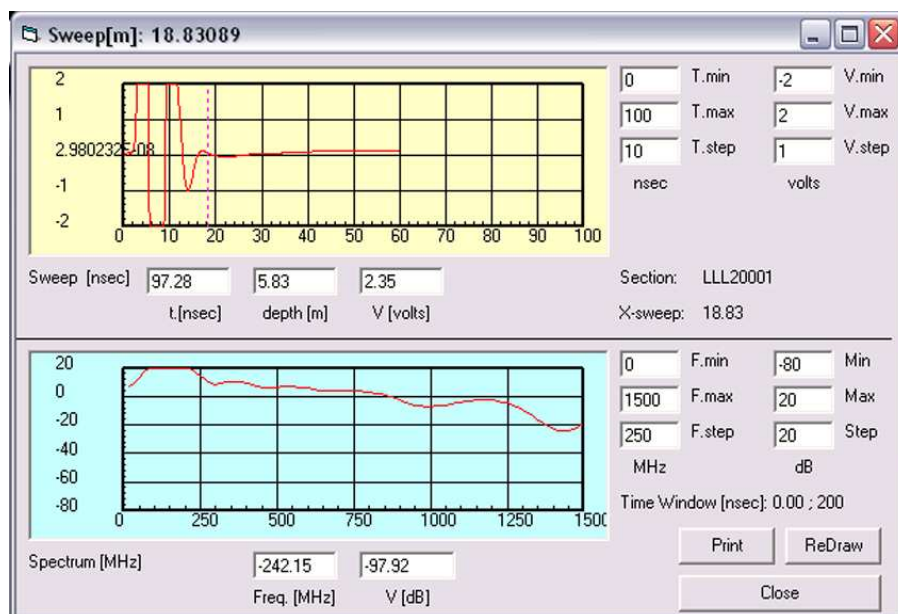
Figure 6.3 – GPR wave and frequency spectrum for a single trace about a 200 MHz antenna, which have leaded the vertical high-pass filter choice.

As the transmitted signal from a GPR unit penetrates into the ground, attenuation of the GPR trace occurs; for embankment soils, which are fine grain in size, the attenuation is strong. This attenuation can be corrected by applying **gain adjustments** to each trace. Several models exist for computing gain adjustments, applying mathematical models for the exponential or linear amplification of the trace, without losing all the absolute amplitude information.
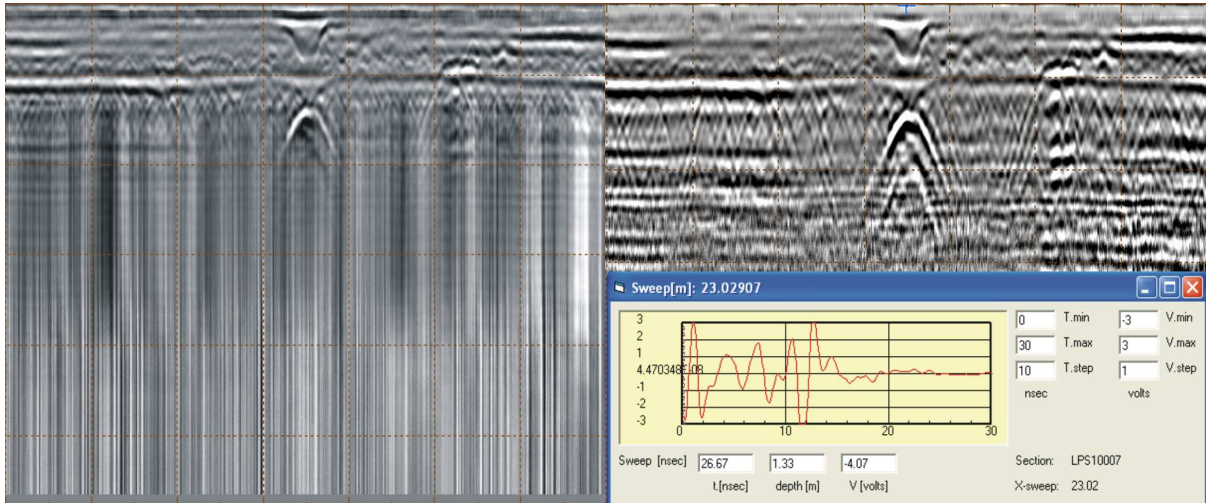
Figure 6.4 – Processing phases, characterized by the gain adjustment, followed by vertical high-pass and low-pass filtering and enhancement stretch.

In one model, each data value in the entire trace is multiplied by a factor related to the depth of the signal. GRESWIN2 software enables the application by default of two kinds of gain: one that provides a linear amplification of the trace (linear gain) and the second (smoothed gain) that adjusts the data with sharp amplification along the trace itself. RADAN 6.5 software offers by default a 5-point range gain curve, which occasionally has been re-adjusted to the variable soil conditions, with typical gain values varying between 30 and 50 dB. An image processing contrast **enhancement stretch** was applied in some cases to improve details in the image. This last step loses all the absolute amplitude information (that will be recovered later) and enhances not only geological details but also noise. These steps were carried out to improve the ability to see the tails of the conduits hyperbola, which are to be used in determining the velocity and size of the conduits, as well as to evidence the boundaries between soil horizons characterized by different electric properties and by slight reflections that need to be evidenced. The processing phases applied to GPR data are shown in figures 6.2 and 6.4. Figure 6.3 represents the continuation of data processing, with the gain adjustment application, which enables the identification of the hyperbola. It shows also the

following processes to clean the reflected signal, aimed at visualising as best as possible the hyperbola tails. The **migration** process relocates reflections to their true spatial position based on the velocity spectrum, thereby producing a real structure map of subsurface features. An image processing hyperbola mask was applied to the data with regard to Samoggia Stream embankments so as to collapse and focus the hyperbola. The image after such processing shows only the scattering cross-section of the visible radius of curvature of the target.
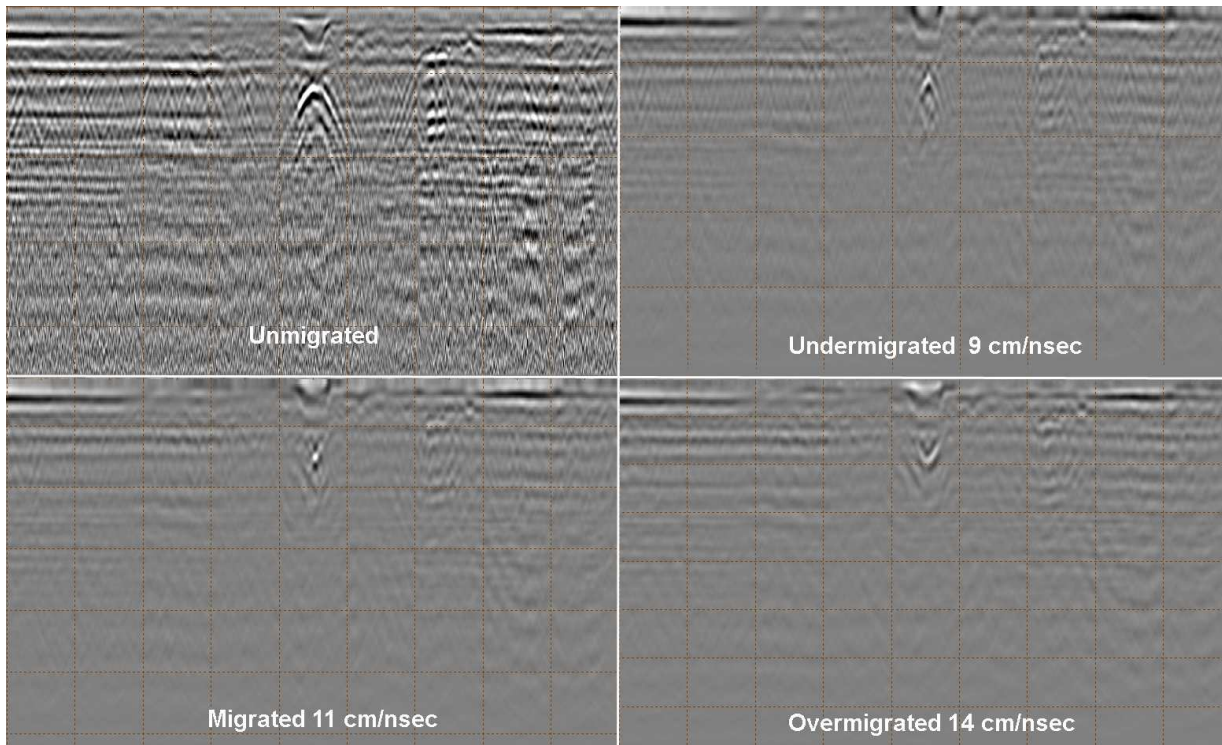
Figure 6.5 – Migration process applied to subsurface anomaly with an average velocity of 11 m /ns; the consequences of inaccurate velocity estimation, where the target is not focused, are clearly noticeable.

By looking at other hyperbolas in the images (especially if they are situated at various depths), their over or under migration focusing (residual hyperbolic shapes pointed upwards or downwards) indicates the variability of the velocity and hence dielectric permittivity throughout the section. Figure 6.5 shows the application of the migration process subsurface conduit, with an average velocity of 11 m/ns estimated by the tails of the hyperbola; the consequences of inaccurate velocity estimation, where the target is not focused, are clearly noticeable.

6.2 Areas affected by seepage and piping occurrence

The Reno River basin is frequently affected by hydraulic crises. In recent years, two episodes of piping phenomena and consequently hydraulic emergencies occurred. The first one, dated October 2005, affected the Quaderna Stream embankments, while in May 2008 the Samoggia Stream levees suffered the same crisis. This case will be treated in the Chapter describing the multidisciplinary approach with various geophysical methodologies. Concerning the Quaderna Stream emergency, following heavy rainfall, near San Salvatore in the Municipality of Medicina (BO), the raised level of the river flood led to a so-called "siphonage" into the embankment structure, with outcropping water from the base of the embankment itself, which seriously compromised the safety of all the surrounding areas. Some emergency works prevented the embankment breakage, and subsequently some reconstructing works were carried out to ensure the stability of the entire structure. In order to verify whether some heterogeneities still affected the river bank and to implement the geotechnical database, a GPR campaign was provided, and the STBR (Reno river Basin Technical Service) carried out three penetrometric (CPT) tests and one borehole test in October 2007.

6.2.1 Quaderna Stream

The GPR profiles were carried out along the Quaderna Stream embankments in October 2007, in dry soil conditions, with the aim of identifying heterogeneous zones as well as possible instability areas near the levee segment reconstructed after the 2005 piping phenomenon. The RIS (Ingegneria dei Sistemi) GPR was utilised in this campaign, employing two antennas, a 100 MHz one, which can penetrate to an adequate depth, and a 200 MHz antenna, employed to analyse some fractures that were slightly visible on the ground from the top of the embankment.

The vegetation that was covering the entire embankment work has disrupted the campaign, creating uncoupling phenomena effects and slowing down the velocity acquisition. Over the zone where the 2005 piping phenomenon occurred and where succeeding embankment renovation works were carried out, some profiles, employing 100 MHz and 200 MHz antennas, were carried out, in order to verify the new structural conditions; the other profile, with 100 MHz antenna, was carried out in another repaired zone (figure 6.6).

Concerning the profiles carried out over the area affected by the piping phenomena, it is important to note that such piping phenomenon occurred at the embankment base and that

the GPR depth penetration capability was not adequate; nevertheless, some consideration must be done.
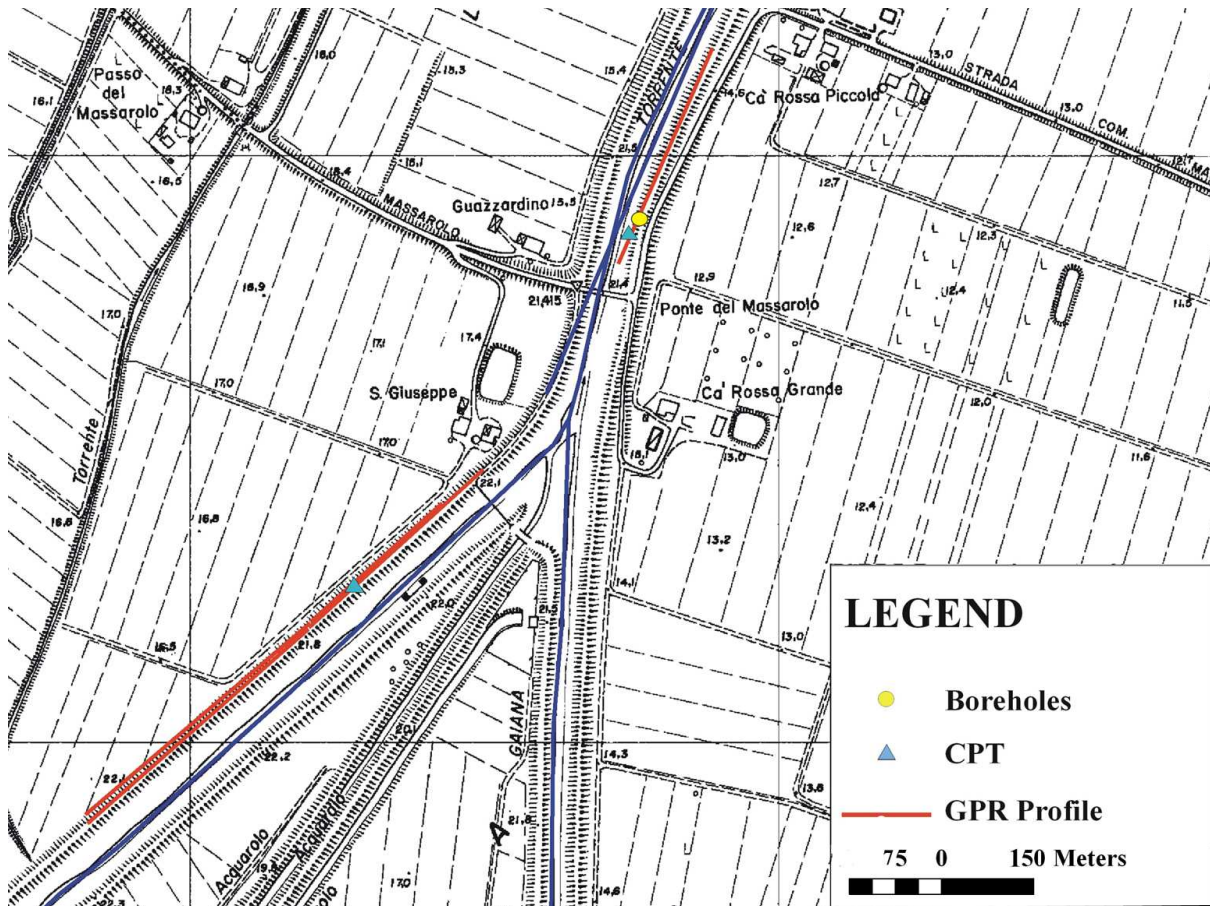
Figure 6.6 – Planimetry of the study area near San Salvatore (BO), with GPR surveys carried out in October 2007 campaign and location of the direct measurement tests.

The colour visualization, which highlights all the positive and negative strong amplitude of the received signal, was chosen to better estimate and roughly locate the resistive layers. The reflections are usually associated with boundaries that separate zones with different electric properties; using the radargrams with colour visualization, it is apparent that the first layer encountered by the EM wave produces strong reflections. This means that the wave, passing from the air to the ground (which can be hypothesised as $\varepsilon_r = 9$) give as a response a strong amplitude reflection that is proportional to the ratio between the electric properties of the two different horizons (Equation 3.10). The 100 MHz profile, 450 m long, carried out with direction SW – NE over the piping phenomenon occurrence, has revealed some strong reflections. The limit between the presence of reflections and their disappearance however is noticeable at around 4 meters from the surface throughout the first meters of the profile (SW side), becoming shallower going toward NE. Many large reflections characterize the first meter and a half up to two meters of the subsoil: they can be referred to many

fractures presents on the embankments surface, which increase the surface roughness and resistivity contrast between the host fine grain-size material and the heterogeneities. In some cases, a kind of horizontal boundary can be traced at around two and half meters in the middle of the profile; its presence can be related to changes in soil moisture, because the comparison with the Cone Penetration Test does not reveal any noticeable correlation.
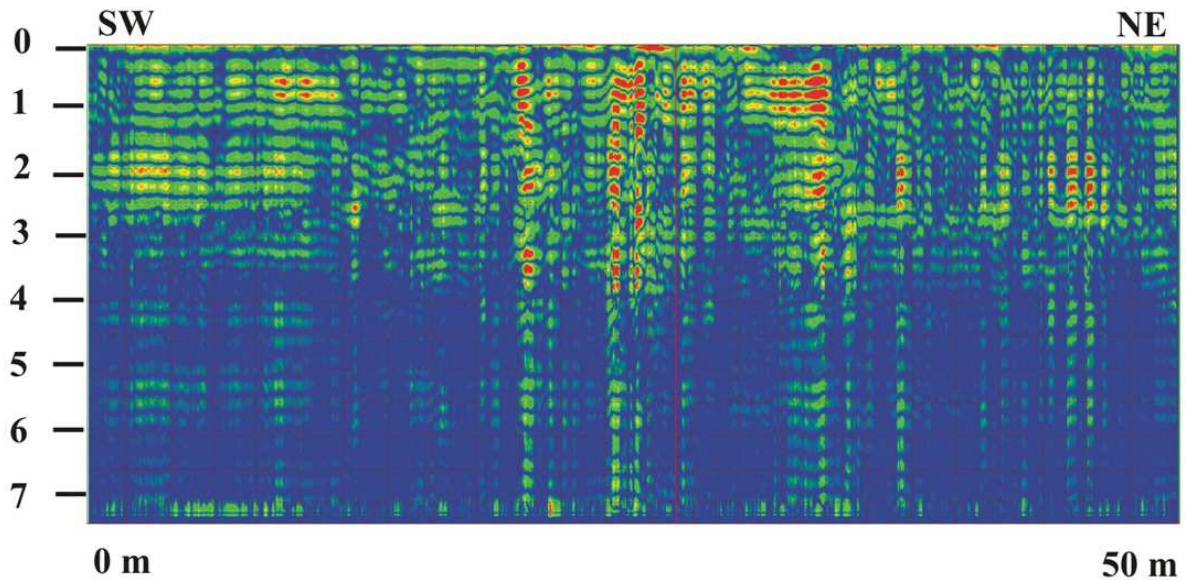
Figure 6.7 –GPR anomalies on Quaderna Stream embankments, relative to fractures and heterogeneities zone, encountered with a 100 MHz antenna.

With regard to the profile carried out over a segment of the embankment that was repaired recently, it was carried out employing a 100 MHz antenna shows a rather regular radargram. The reparation works have included a re-profiling of the embankment, insertion of carryover (in theory fine grain-size) material and its compaction. The surface of this part of the embankment includes several small reflections associated with minor heterogeneities, verified by the presence in the immediate subsoil of pieces of roots and brick fragments. Proceeding in depth, there is a constant zone with an absence of reflections that spreads around one to two meters in depth, while below two meters from the ground other slight amplitude reflections occur for a variable thickness of two to three meters (figure 6.8).

In the complex, the radargrams are characterized by slight anomalies, related probably only to slight heterogeneities with the materials employed for the embankment reconstruction and renovation. The direct tests reveal the presence of fine size materials: prevalently silt with weak sandy fraction and with slight percentage of clay, until the depth of around nine to ten meters, with rare fragments of brick and plant roots into the first five meters.
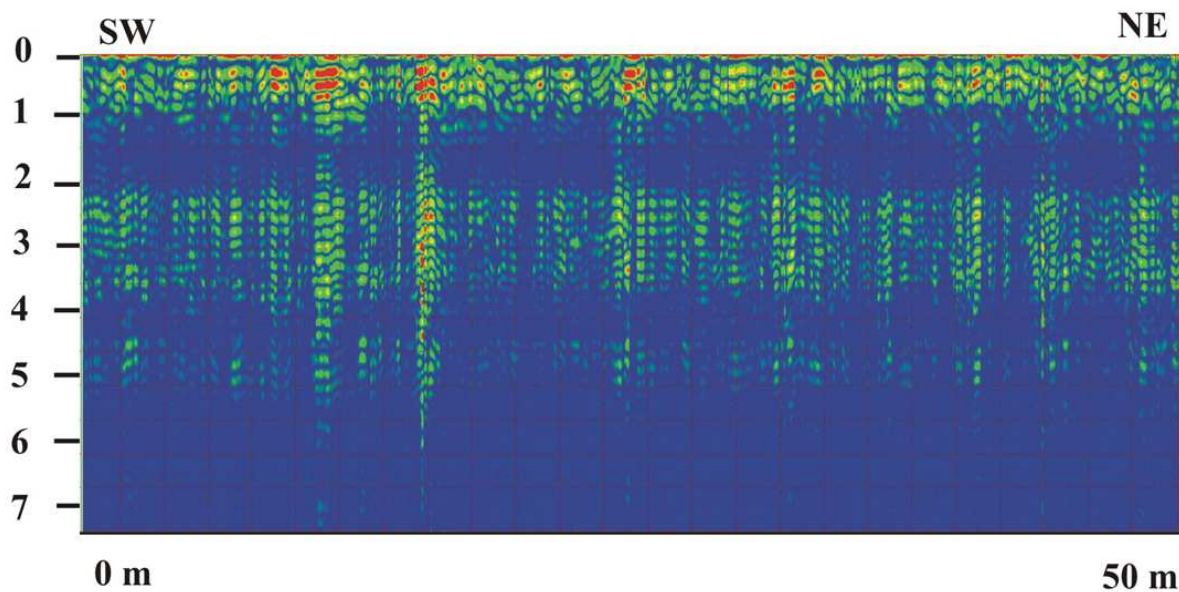
Figure 6.8 – GPR anomalies on Quaderna Stream embankments, related to heterogeneities zone. 100 MHz antenna was employed.

Looking at the figure 6.9, while the stratigraphic column does not reveal any important passage (excluding some small heterogeneities like small isolated fragments), the CPT test shows an initial peak of resistance in the first meter of depth.
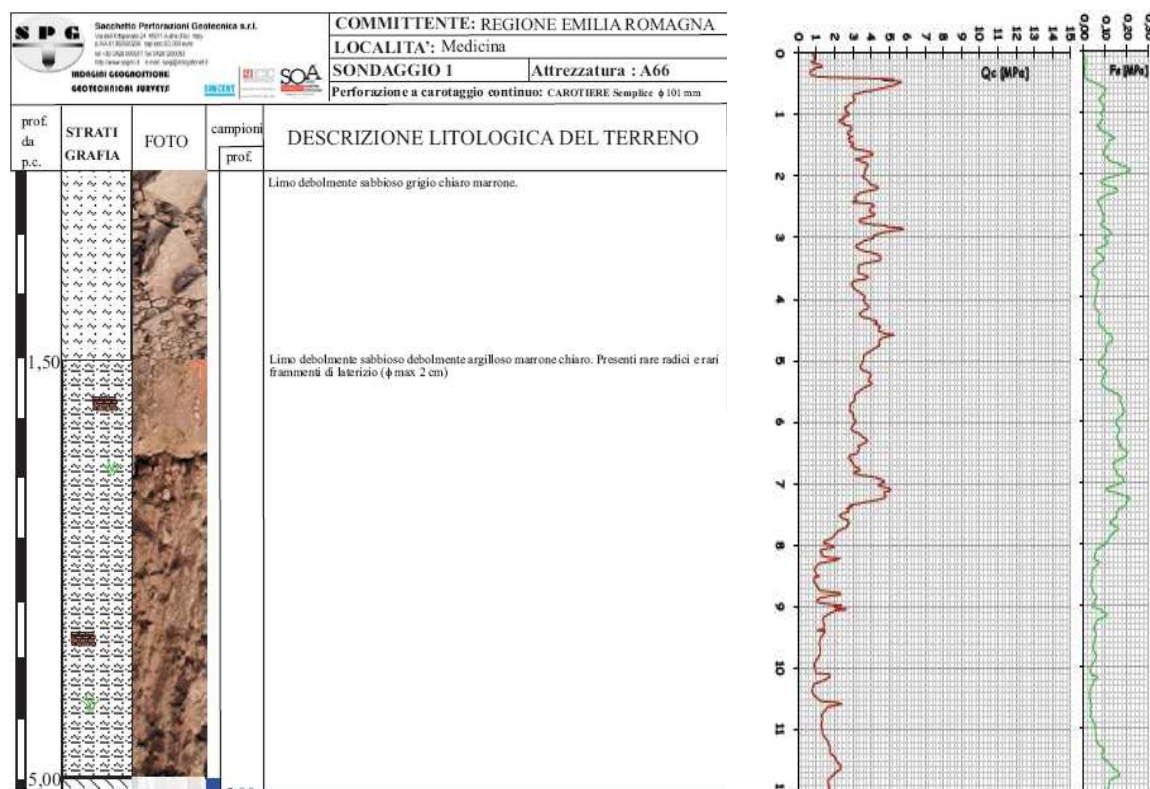
Figure 6.9 – The Borehole and CPTU tests, carried out on the renewed embankment, show uniform geotechnical properties.

A slight rising of resistance occurs at around two and half meters to three meters, which could be linked to the reflections present in the radargram. However, according to the direct tests, this embankment presents similar resistance values and approximate stratigraphic uniformity and it could be taken as an example of homogeneous embankment.

6.3 Embankment segments rebuilt in the past

The reconstruction of embankment segments that were previously affected by breakage and other structural damages, must be carried out with the important preventative measure of introducing the new structure into the old one as best as possible. In many cases in the past, during a flooding occurrence, the embankment contact zones between new and old structure, which were not correctly linked and therefore creating a weaken line, suffered major stresses and many stability issues, resulting totally unsafe. Such hydrogeological crisis happened in the past highlight once again how most of the problems that can interest embankments occur along discontinuities that could be hardly detectable with traditional techniques. Generally the reconstruction works, where is not necessary the realization of engineering works (e.g. structures in concrete) schedule the reutilization of the soils that compose the original embankment structure with the eventual addition of fine grain-size materials, possibly available in the surroundings.

The correct reconstruction and connection of the new segment into the old embankment was analysed through the GPR usage, carrying out many profiles in correspondence of such zones, rebuilt in the past for breakage, piping phenomena or animal cavities occurrence. The profiles aim to distinguish the renewed parts from the original structures, in order to localize areas previously repaired in the recent past as well as remote past and with no historical information available and therefore individualize potential weakness zones. With the purpose of understand if GPR can be capable to recognize new and old segments, some known embankment parts, where reconstruction works were provided in the past, were chosen as test area.

6.3.1 Reno River

The first segment analysed behave to the Reno River embankments, and is located near Bosco, Municipality of Malalbergo (BO). This segment, in hydrographical right side, was affected by an important breakage in 1990, following a large piping phenomenon occurred in coincidence of a methane pipeline, property of National Society Methane

pipelines (SNAM), which was crossing the Reno River embankments in correspondence of the embankment base. Renovation works were carried out in short time, through the reintroduction of the new embankment segment into the old structure as well as a new methane conduit in a safe position. During the October 2007 measurements campaign, some profiles were carried out measuring the segment, which was rebuilt by the renovating works (figure 6.10). With regard to the geometrical dimensions of the embankments (up to twelve meters, divided in three to four steps), the investigations of different embankment steps, in order to acquire as much quantity of data as possible of the entire embankment, were provided.
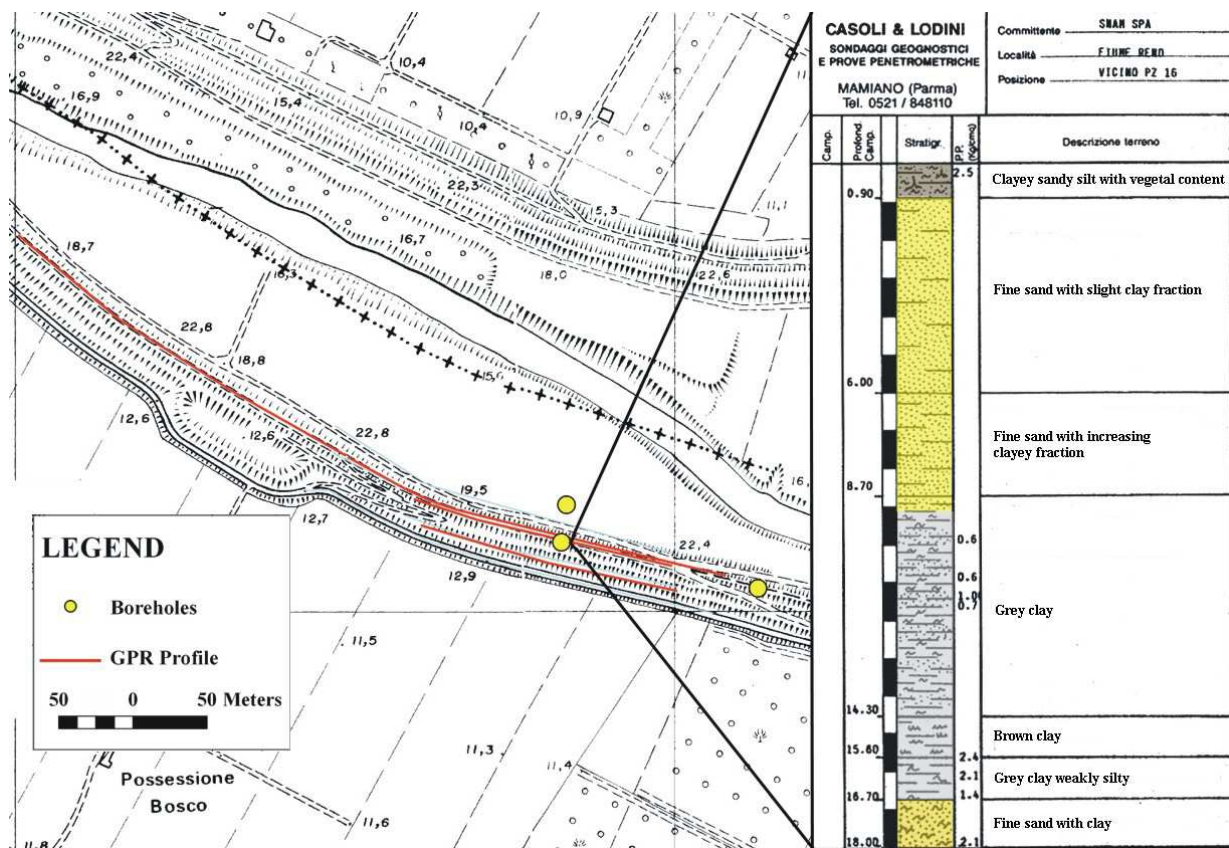
Figure 6.10 – Planimetry of the study area near Bosco (BO), with location of the borehole measurement tests and of GPR profiles (on the left); particular of the borehole carried out over the reconstructed embankment segment.

The environmental state has proved optimal, characterized by dry conditions and with the green coverage of the embankments perfectly smooth, which has guaranteed the good coupling between the antenna and the ground. The GPR produced by MALA Geosciences, employing 250 MHz and 500 MHz antennas (April 2007) and GPR released by IDS with the employment of a 100 MHz antenna, were used. The April 2007 campaign was very unproductive because of the scarce penetration of both the antennas utilised; thus, the October

116

2007 campaign was provided with the objective to reach as deeper penetration as possible. Along the profiles, carried out on the top of the embankment, the presence of reflections at the beginning of the profile is noticeable. Such reflection are characterized by a deepen tendency going towards SE (figure 6.11). For almost the entire profile, the penetration capability of the EM wave is reduced to less than four meters, due to the signal-to-noise ratio consistent decreasing going deep, despite the lithology encountered with the direct tests (figure 6.10) is constituted by fine sand with presence of clay. The motivation is given by the fact that the first meter from the surface is characterized by large clay content, producing many reflections that attenuate the signal. Such reflections disappear in correspondence of the passage between the soil layers, to fine sand horizon, as confirmed by the borehole visible in figure 6.10. Under this passage, the larger part of the investigations is devoid of reflection, showing homogeneity.
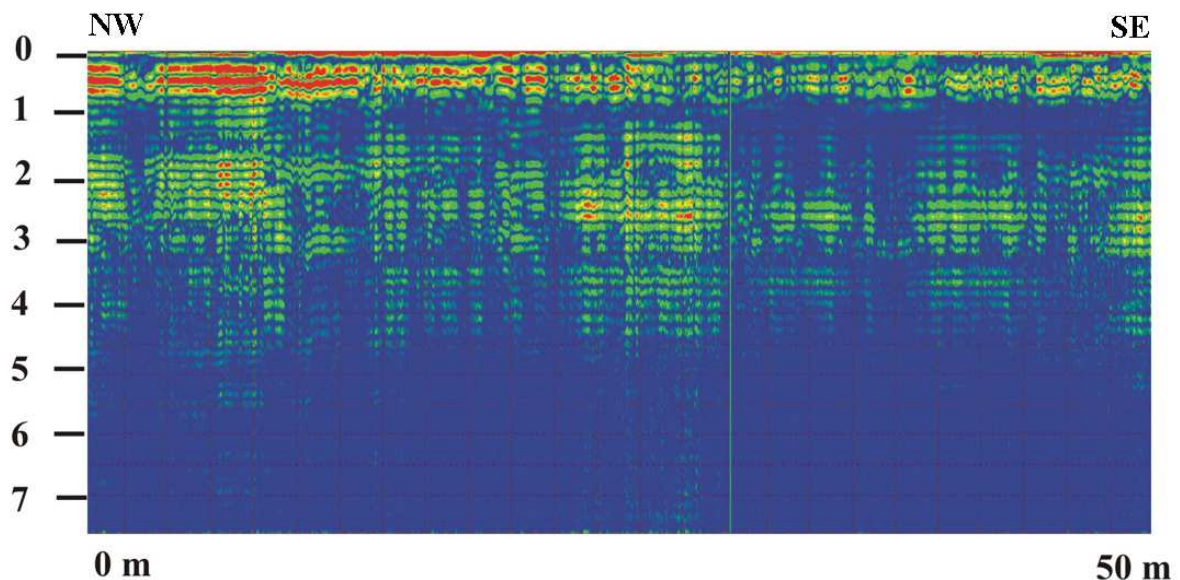
Figure 6.11 – GPR reflections on Reno River embankments, with a deepen tendency going towards SE. A 100 MHz antenna was employed.

Around the zones where the new segment was reconstructed and attached to the old structure, the reflections decrease in amplitude and the embankment results homogeneous for the entire area analysed, which result slightly less respect to the beginning of the measurements and in general, one of the smaller depth reached during the entire GPR measurement campaigns. Moreover, any changes in electrical properties, passing over the reconstructed area, were notified.

The external steps were analysed with the employment of 100 MHz and 200 MHz antennas; the 100 MHz has failed the attempt to detect the new position of the SNAM

methane pipeline, which was probably posed under the embankment base. The 200 MHz antenna has reached the depth of around one meter, giving a detailed description of the first meter concerning stratigraphic changes and rock boulders to metallic objects detection, but resulting useless for an adequate evaluation of the research purposes. The new part, which was reconstructed utilizing the same materials of the old embankment, was not individuated, demonstrating its optimal reinsertion into the original structure and the impossibility of GPR to resolve eventual slight changes in electrical properties.

6.3.2 Gaiana Stream

The second levee that was analysed with the purpose of new embankment segments recognition, behave to the right hydrographical side of Gaiana Stream embankment system, located in the municipality of Medicina (BO), where, during the flooding event of 2005, the initial formation of a siphonage leaded to the structural collapse (figure 6.12).
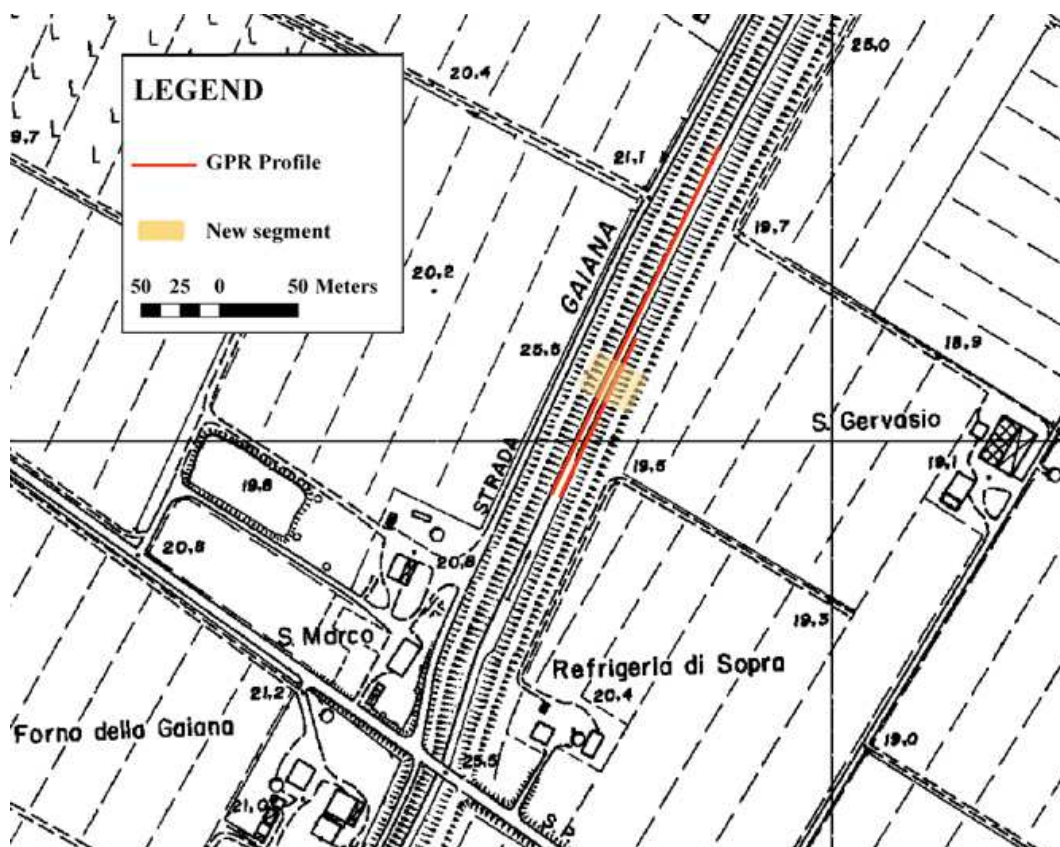
Figure 6.12 – Planimetry of the study area near San Salvatore (BO), with GPR surveys carried out in October 2007 campaign employing 100 MHz and 200 MHz antennas.

The embankment is composed by a unique large bank without intermediate external steps and it reaches the high of four to five meters. A profile of one hundred meters was

carried out using a 100 MHz antenna, to achieve the structural evaluation for the complete embankment elevation, but the results were seriously compromised by the irregular surface of the embankment top. Must be mentioned, that before to carry out the GPR profiles, an apposite campaign of embankment maintenance was provided. The necessity was given by the massive presence of vegetation could obstacle the passage of the GPR device and antennas. Despite the cleaning works, the roots left by the cuts and the very irregular surface (often composed by heterogeneous materials) have influenced the radargrams, that are affected by many reflections and traces "jumps", which are associated to the uncoupling phenomenon between the antenna and the ground.

The 200 MHz antenna was mounted on a special cart provided by IDS, therefore the profiles were carried out without the contact with the rough surface, improving the signal to noise ratio and guaranteeing a constant data acquisition. In proximity of the embankment-reconstructed segment, still recognizable during the field survey for the presence in surface of construction material fragments, strong reflections occur from one to one and half meter of depth, validating the hypothesis of a layered structure, with a horizon mainly composed of coarse construction and carryover material. Unfortunately, any direct test is available for this segment, therefore any comparison was done and all the suppositions need to be confirmed. A large hyperbola is clearly visible in the left part of the profile of figure 6.13. In this case, although the 200 MHz antenna is shielded, high-frequency interference creates a false target inside the ground. In the complex, this survey has reported negative results, because of the scarce penetration depth reached by 200 MHz antenna, the practical difficulties encountered by 100 MHz dragging, and the lack of a direct test methodology, important to calibrate and therefore validate the hypothesis formulated.
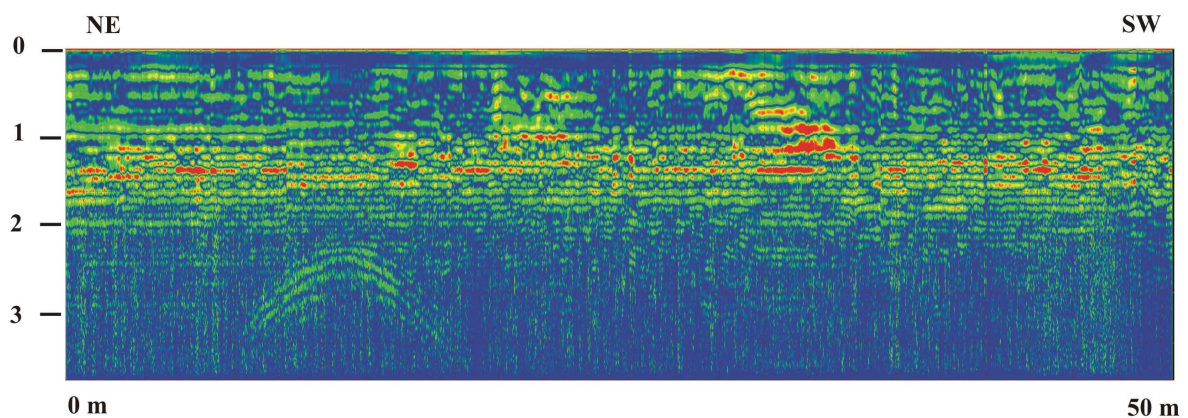
Figure 6.13 – GPR reflections on Gaiana Stream embankments, associated to inhomogeneities in the first two meters. Presence of high-frequency interference on the left part of the radargram; 200 MHz antenna was employed.

6.3.3 Ghironda Stream

The third study area chosen for the structural evaluation of embankment segments rebuilt in the past is localized along the Ghironda Stream, which is a tributary of Samoggia Stream; the embankments that bound this small tributary are five to six meters high and the usage of a relatively low-frequency antenna can guarantee an adequate description of their structure. Some months before the measurements, the presence of several cavities excavated by animals has seriously compromised the stability of the embankment structure; thus, many segments of the embankments were rebuilt (figure 6.14). Unfortunately, no geotechnical information is available and therefore no correlation with direct tests was done.
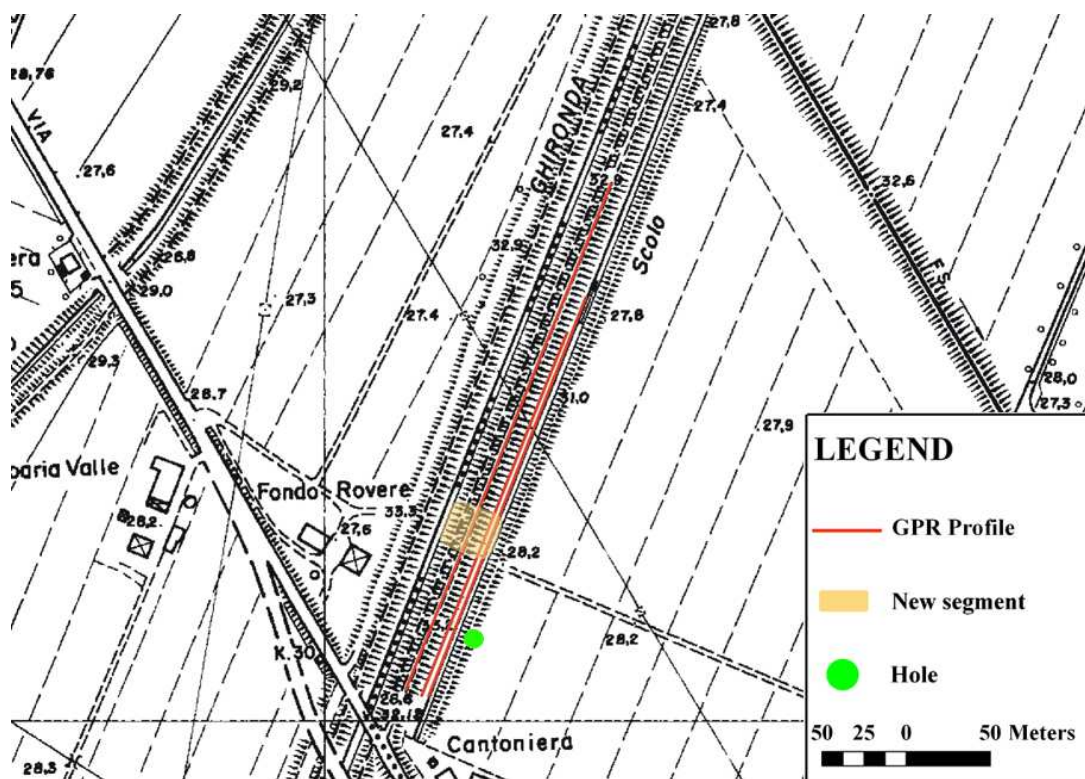
Figure 6.14 – Study area on the Ghironda Stream embankment, for structural evaluation and cavities detection.

The GPR capability for the repaired zones detection was tested, employing a 100 MHz antenna, which is able to reach the depth of four-five meters. Also for this study area no geotechnical information are available. Through a GPR profile, carried out at the top of the embankment, it was possible to identify zones with strong reflections until the depth of four meters. The figure 6.15 shows this profile and two segments of respectively 12 and 10 meters, characterized by an increment of reflections, are visible; these areas corresponds to known

recently repaired areas. In this case, higher GPR reflections define more porous and thus less compacted soil.
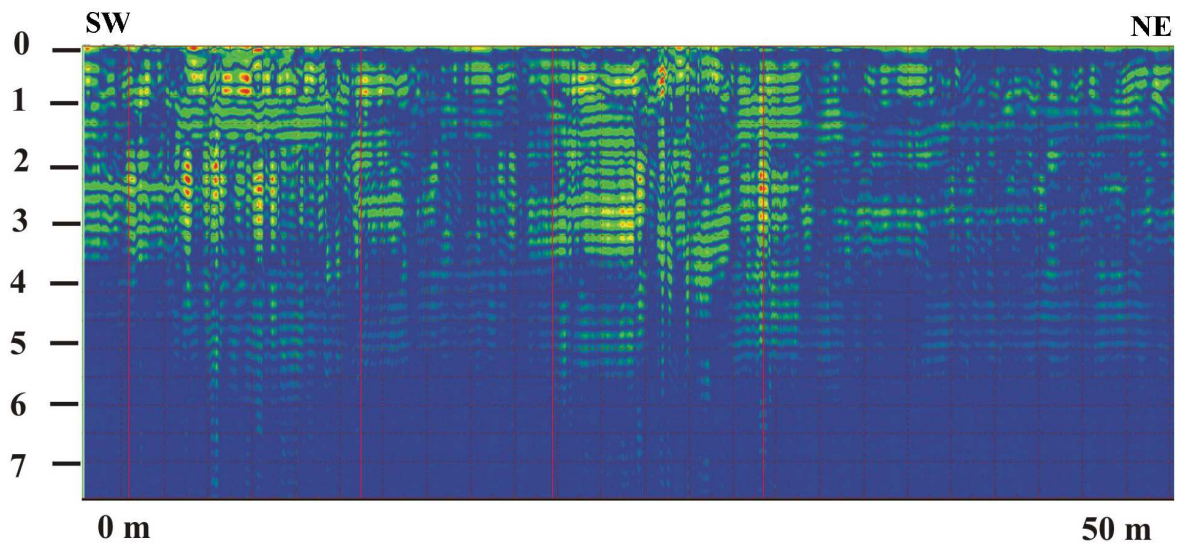
Figure 6.15 –GPR anomalies, produced by areas with different porosity and thus different compaction status (100 MHz antenna).

Making a brief summary, the GPR has suffered many problems and just seldom it was useful to identify changes of structural conditions inside the embankments which were rebuilt in the past. Repaired areas are well recognizable if they were executed recently, because new material is more porous and therefore less compacted, with respect to the old one. Reparations executed several years ago are difficult to detect with GPR because the soil compaction and the electric properties of the materials, influenced also by the moisture content, with time become similar to the surroundings.

6.4 Detection of animal cavities

Digging activities of animals and roots of plants have negative effects on the dike stability. As a result, voids may occur in levee bodies. Dikes are part of the landscapes and are influenced by biological processes. Recently, some authors have employed GPR to verify known cavity detection in river levees with a covering in concrete (Sheng-Huoo et alii, 2002). Concerning the Italian situation, despite of the strong Po Plain anthropization, several mammals have found a comfortable habitat both in the internal and external part of river embankments, where they are proliferating. As previously stated, the species, which can be found on the river embankment habitat, are some various mammal types; the European badger (*Meles Meles*)**,** the fox (*Vulpes Vulpes*)**,** the wild rabbit (*Oryctolagus cuniculus)* and the nutria (*Myocastor coypus)*. While the fox and the European badger are animals historically involved

121

in soils and dikes erosion, recently the occurrence of others species has significantly increased the embankment safety issues. The observation of the cavities occurrence enables to establish that wide embankment structures (Reno River and Napoleonic Channel) are affected prevalently by fox and European badger cavities; the nutria, which needs an habitat close to the river water level, mostly built their cavities inside the river bed and only minor embankment structures or irrigation channels are affected by this phenomena. The 1996 Samoggia River breakage and the flooding on the countryside nearby the Savena Abbandonato Stream were ascribed to the presence of cavities inside the embankment, which created a strong reduction of resistance.

The tests provided for the cavity detection were carried out wherever there was a hole or cavity evidence, in order to verify the advantages and drawbacks of GPR methodology. The GPR profiles were carried out using various antenna frequencies, from 100 MHz to 600 MHz, trying to find a compromise between depth penetration and spatial resolution.

6.4.1 Napoleonic Channel

The first embankment segment, which was studied, belongs to the Napoleonic Channel, and in October 2007 showed the presence of a large cavity on the external flank of the embankment itself.

Figure 6.16 – GPR investigation to detect a cavity over the Napoleonic Channel embankments, employing a MF (200- 600 MHz) antenna.

This cavity resulted excavated by a fox (*Vulpes Vulpes*) and was located just at one meter depth below the top of the embankment, with a diameter in entrance of around 40 cm (probably decreasing going inside). The multi-frequency antenna 200 – 600 MHz can be used employing three channels to receive the signals; therefore, it can scan the ground with the mono-static 200 MHz and 600 MHz antennas and with the cross-polar 200 MHz transmission to 600 MHz reception antenna. These configurations in theory enable to achieve an adequate penetration, an optimal spatial resolution and therefore a compromise between them at the same time, thanks to the simultaneous usage of such multi-frequency GPR unit. Unfortunately, no profiles carried out over the cavity, even changing antenna polarization during data acquisition as well as applying deconvolution or implementing amplitude enhancement during the processing, have given any cavity evidence.

Probably the fine granulometry of the material that constitutes the embankment has compromised the outcomes, significantly attenuating the EM wave. Moreover, the cavity was spreading inside the embankment flank not in horizontal direction, but following a down-inclined path and after around half meter two tunnels having a divergent direction resulted excavate. Therefore, the results are negative: EM wave attenuation, clutter and scattering phenomena occurrence, have demonstrated that the employment of high frequency antennas, although suitable for the good spatial resolution, is inappropriate for such grain size and porosity soil condition.

6.4.2 Ghironda Stream

Chapter two have already introduced how holes excavated by animals (foxes and nutrias) can seriously compromise the hydraulic safety of river embankment as they may trigger seepage or piping phenomena. Several tests were implemented for the determination of holes development inside the embankment. Along this Reno river tributary, many entries of animal holes were discovered by the local Reno River basin service workers at the base of the embankment itself, at a depth of one meter from the embankment external step. A set of 100 MHz and 200-600 MHz antennas, released by IDS was used in GPR survey, but only the 100 MHz has showed some results, because of the penetration issues encountered by the higher frequency antennas. During the measurements campaign 350 m of profiles on the top of the embankment and 250 m on the first external step were carried out. The main aim was to see if, as well as the entrance, the main developing of the hole inside the embankment is recognizable. Comparing to many trials on holes, only the largegest one, with a size of about 40 cm, was detected (Figure 6.17). Together with the entrance, another non-homogeneity

close to the main, is evident: this may be a portion of the hole inside the embankment. The difficulty for detecting other cavities is due to the size of the holes in diameter, which are probably slightly lower than the antenna resolution.
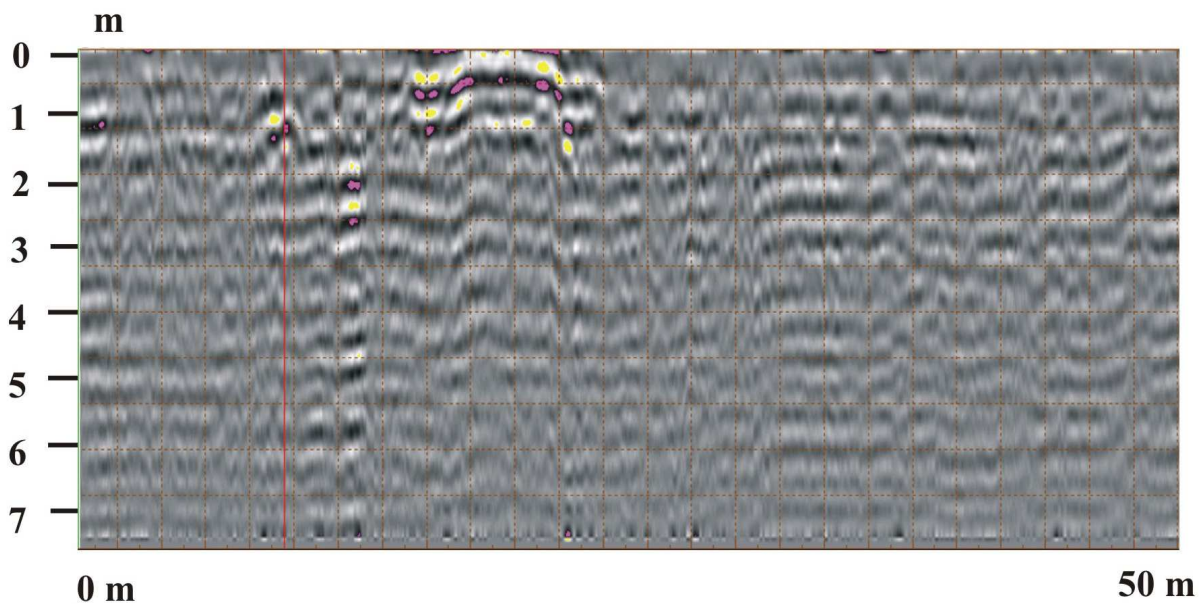
Fig. 6.17 –GPR anomalies, referred to cavity excavated by a *myocaster coypus*, detected employing a 100 MHz antenna.

In the complex, the results are partially negative: the employment of high frequency antennas, although suitable for the good spatial resolution, was seriously compromised by the EM wave attenuation in the first meter of subsoil, due to clutter and scattering phenomena occurrence. The 100 MHz antenna, which has reached the target depth, is unable to detect punctual targets smaller than 40 cm of diameter and however, as deeper the target as higher must be the contrast in dielectric properties to produce any noticeable reflection. Moreover, the moisture conditions and the embankment geometric factors significantly influence the GPR measurements, which have achieved just one interesting result, for the small Reno tributary levee.

6.5 Localization of stratigraphic contacts beneath river embankments

Many studies in the past has revealed how the GPR can be an useful tool when some shallow geologic information are needed; Dominic et alii (1994) demonstrate that Ground Penetrating Radar is an important tool for studying shallow stratigraphy, where the ground conductivity is low enough to enable radar reflections from depths of interest. GPR capability was tested in the determination of buried geological structures makes this technique a powerful tool in sedimentology (Smith and Jol, 2003); even if the extraction of meaningful

information on the deposition style and on the sedimentary structures needs systematic and accurate data processing (Neal, 2004). Making the treads of such well-developed studies, the localization of stratigraphic horizons beneath the Napoleonic Channel river embankments was tested employing the relatively low frequency 100 MHz antenna, obtaining good results.

6.5.1 The Napoleonic Channel case

Within the survey programme, managed by the Region Emilia-Romagna, the study of the "Cavo Napoleonico" Channel takes a primary part due to its strategic role in the lower hydraulic network of the Reno River. The Napoleonic Channel was originally designed with the purpose of diverting part of the floods of the Reno River into the River Po. Another function is to keep a considerable volume of water inside its own bed, in order to reduce the flooding (overbank spillage) risk along the artificial course of Reno River, that starts from the village of Sant'Agostino (FE) and extending eastward to the Adriatic Sea. The project, left unfinished at the beginning of the XIX Century, had been modified substantially in its hydraulic and geotechnical characteristics. This has led to an increase of the flooding hazard in areas that have already experienced catastrophic events caused by the local streams in the past. The historical studies and reconstructions carried out and described in Mazzini et alii, 2006, demonstrate that the excessive attention of the designers to the hydraulic efficiency of the canal has generated important geotechnical drawbacks, such as the intersection of the waterway with abandoned channels. That lack of necessary awareness of geotechnical problems could also be related to an immaturity of geological sciences applied to engineering works, especially in Italy during the '50s. Finally, two different ways could be indicated to face the geotechnical problems. The first is to complete the coating of the channel segments that show excessive filtration phenomena; the second consists of reinforcing the remote control of the hydraulic levels so that the managers could be able to use the Napoleonic Channel respecting the thresholds established with the simulations obtained from numerical procedures. Although the first solution is at the moment impracticable, not having sufficient financial resources, the second one shows some weaknesses due to the uncertainty of measurements and to the eventual unpredictable events during the hydraulic management procedures.

Geometrical settings

The Napoleonic Channel, 18 km long and of and 180m wide, has the double function. Firstly it diverts away Reno flood waters (shifting its discharges to the Po, or keeping them

inside its own course, as an emergency reservoir, for a maximum capacity of 1.8 million m^3), with a southward flow direction, and secondly, it acts as an alimentation waterway for the CER (Emiliano-Romagnolo Channel), with opposite flow direction. To succeed in this double function, the channel bed slope is equal to zero. The connection to the other streams is regulated by two hydraulic concrete structures. A third structure governs the water flow to the CER and, if needed, it could be used in the opposite direction for hydraulic safety. Because of the very high permeability of the channel bed, the "Cavo Napoleonico" cannot be used at its maximum capacity. Indeed, the fill-in volume cannot exceed one third of the maximum filling size, and it can be utilized for the irrigation procedure only for a limited period of time during the year (from April to September).

The problems related to the Napoleonic Channel positioning concern firstly the fact that the Napoleonic project was supposed to connect the Reno to the Po through the lower Panaro River, but the project was changed and it passes directly to the River Po, forcing the canal onto a very highly permeable zone. Secondly, the technical request for greater hydraulic efficiency made it necessary to raise the levees in order to reach higher heads, necessary for the correct hydraulic performance of the Emiliano-Romagnolo Channel, was at the same time the cause of the stress increase on the terrains under the earth embankments. In Figure 6.18a, the courses of the hydraulic network of the Napoleonic Channel are illustrated in relation to the two rivers and the Emiliano-Romagnolo Channel. In Figure 6.18b, on a larger scale, the present course of the canal is shown and compared to the one built in the first years of the XIX century (dashed lines); the two paths are coincident from the village of Sant'Agostino to Bondeno (FE). So, even if the modification of the Napoleonic original project has brought a potential hydraulic improvement to the channel, it has determined geotechnical conditions of the new artificial levees that cannot guarantee the flood safety of the restricted areas, even after the partial impermeable coating works carried out on the channel bed during the '60s and '70s.

The Napoleonic Channel embankments as well as the surrounding areas are fully defined by direct tests carried out during last decades. The GPR was tested in this context just to verify its capability to detect shallow stratigraphic horizons.

Results

Along the Napoleonic Channel, data relative to three sections were studied in detail. The internal structure of the embankments can be referred to a general model, such those represented in Fig. 6.19A, B and C.
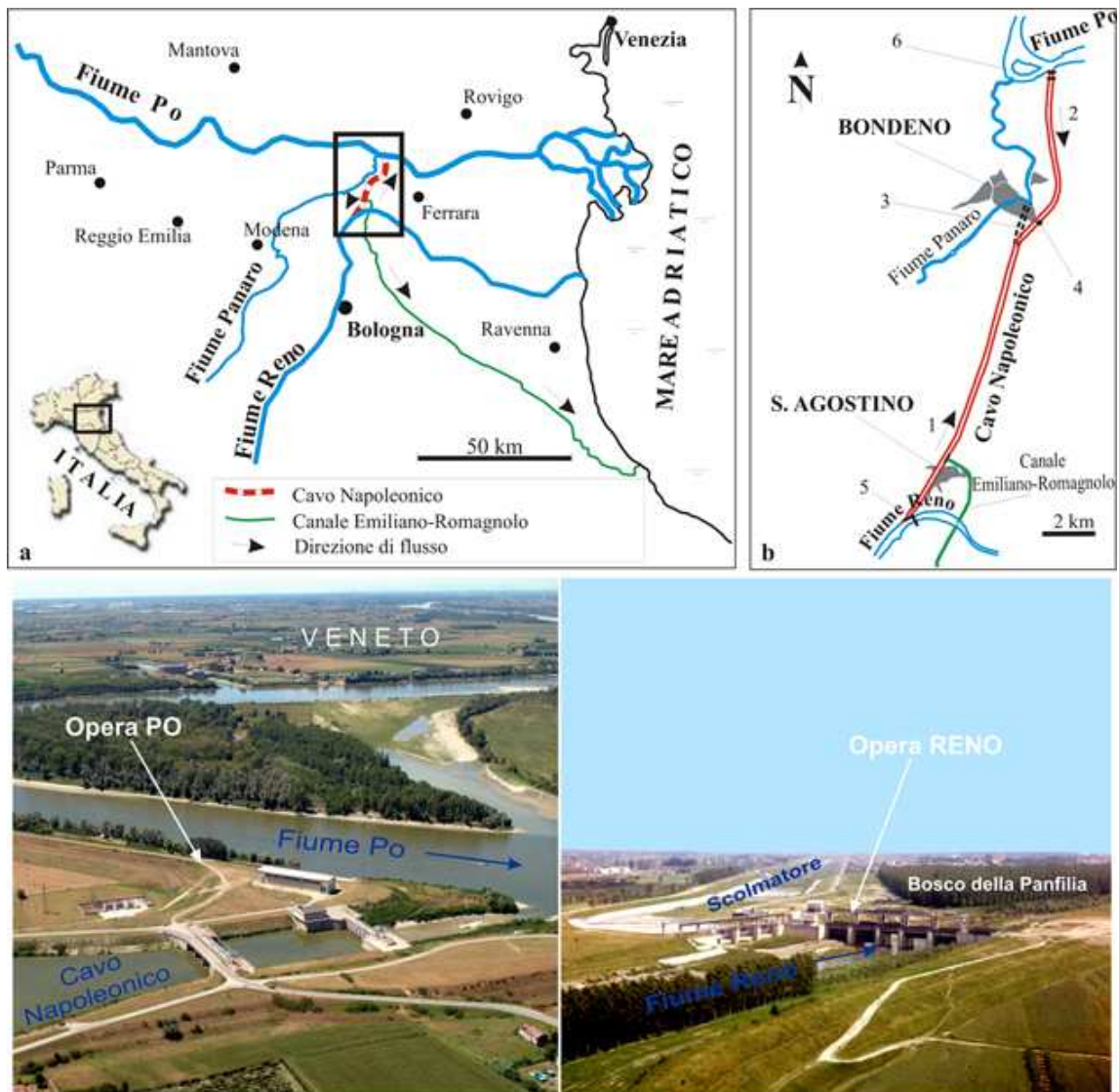
Figure 6.18 - Localisation of the study area, on a small scale (a) and in detail (b). Numbers indicate respectively: 1, flow direction of Reno floods; 2, flow direction of water drifted from River Po to Emiliano-Romagnolo Channel; 3, morphological trace of the old course of the Channel (Napoleonic project); 4, 5, 6, important concrete hydraulic structures (Opera Po and Opera Reno) visible also form aerial photos, from Mazzini & Simoni, 2006, redrawn.

The stratigraphic sequence consists of:

i)   the artificial river embankment, 8 m height (silt prevalent);

ii)   in situ alluvial deposit, 2-10 m thick (silt prevalent);

iii)   paleochannel, variable thickness (medium sand).

For the section of Figure 6.19A, GPR was used to check the embankment structure. Because of the silty soil, both 100 MHz and 200 MHz antennas suffered a strong diffraction process in the signal. Along its course, the Napoleonic Channel crosses repeatedly a Po paleochannel (Mazzini *et al.*, 2006). GPR capability for the detection of the top of the sandy body was tested, in order to verify its lateral continuity (Section B and C in Figure 6.20). With

127

respect to the base of the embankment, cone penetration tests identify the top of the sand respectively at 2 m (CPT 1) and 10 m below (CPT 2) going northward.
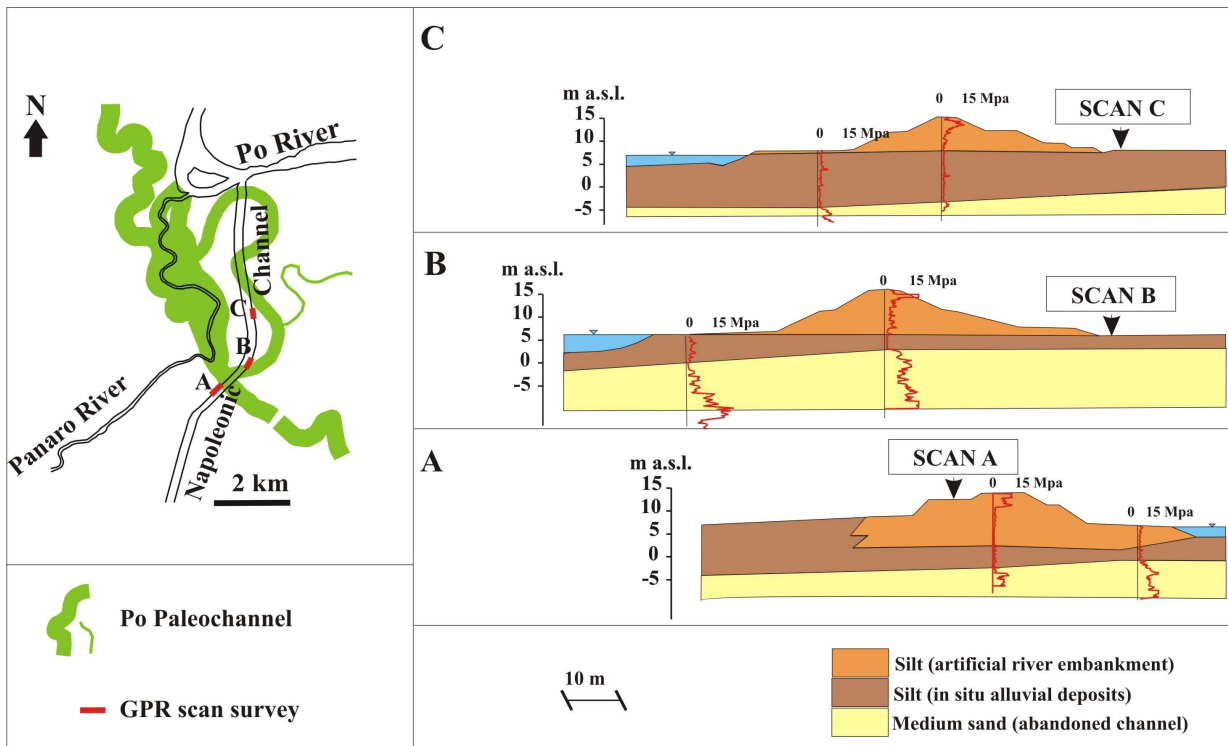
Figure 6.19 - GPR surveys location along the Napoleonic Channel (site 1 in Fig. 1) and stratigraphic sections of the embankments obtained by in situ direct measurements. SCAN A, B, C: location of the GPR survey.

The GPR survey (100 MHz antenna) was carried out for about two kilometres between sections B and C (Figure 6.18). For the entire length of the GPR profile, the road asphalt covering the silty soil level is recognizable. In the first hundred meters of the survey (SCAN B in Figure 6.20), it is possible to clearly recognize, at a depth of two m, a sandy layer. The signal becomes too weak at four meters deep because of the presence of the water table, confirmed by piezometers in the vicinity. This strong contrast becomes more and more discontinuous going northward and, at the end of the survey line, it disappears (SCAN C in Figure 6.20).

Some important aspects in the use of GPR comes out during the survey: the topography surface perfectly smooth by the asphalt coverage of the road and its dielectric properties, which imply a weak signal attenuation has enhanced the acquired data; furthermore, it is always recommended a calibration with other direct and/or indirect measurements. The detection of shallow stratigraphic horizons between soils with a noticeable difference in lithology or moisture content, like medium sand and silt was verified.

128

It was also possible to check the lateral continuity of a paleochannel at the base of the embankment.
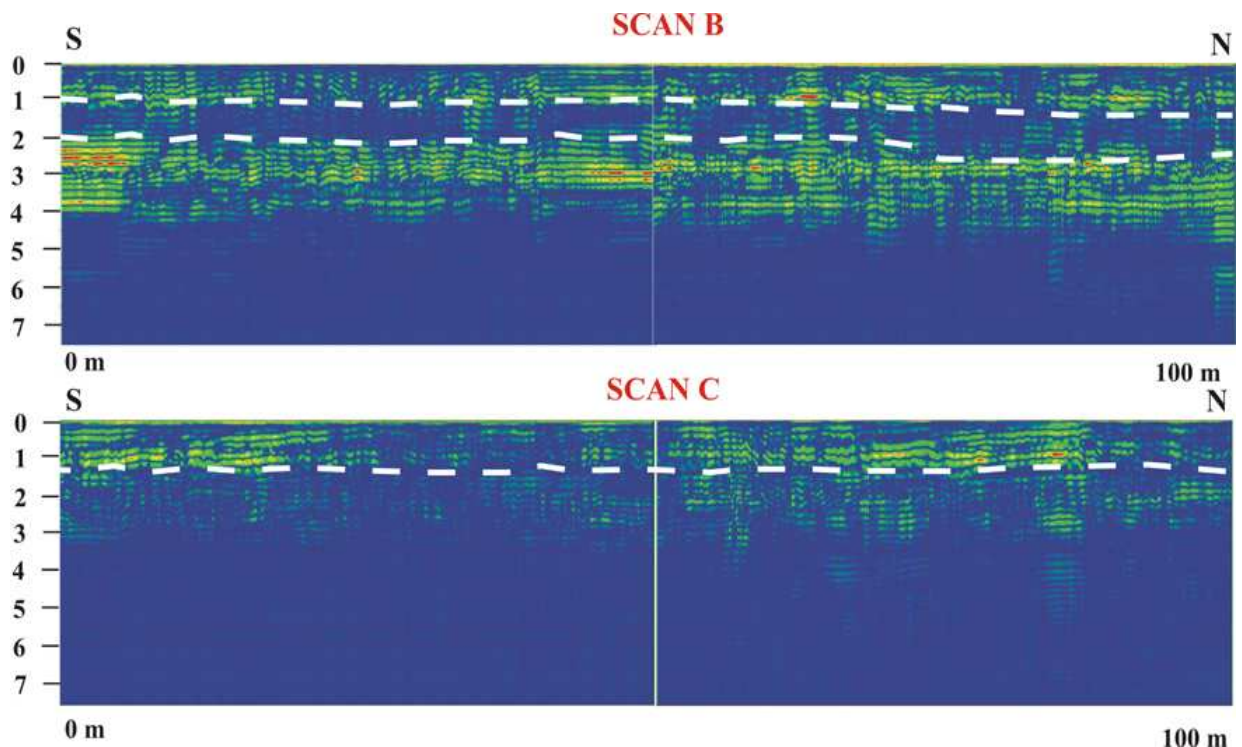
Figure 6.20 - Non-homogeneity horizons (white dashed lines) detected with GPR along the Napoleonic Channel (see Fig. 6.19 for location). SCAN B and C (100 MHz antenna): it is possible to notice how the contact between silt and sand at 2 m depth disappear passing from SCAN B to C (Biavati et alii, 2008).

6.6 Inspection of the embankment internal structure

The fluvial embankments of the Reno River and its tributaries system has shown in the Lower Po Plain territory a series of geotechnical and hydraulic problems that in many cases, during exceptional flood events, have resulted in serious inundations. The events that were particularly severe, in these Region are the embankment breakages of Reno River in 1990, Samoggia Stream in 1996, and piping phenomena of Quaderna Stream in 2005 and Samoggia Stream and again the levee breakage of Reno River (this one particularly serious, which has occurred at the end of this thesis compilation) in 2008.

Trying to make a summary of all the possible issues that afflict this part of the Emilia-Romagna territory, the main causes of the structural embankments weakening, can be related to:

- Land subsidence
- Variations in water discharge.
- Variations of river bed profiles.

129

- Anthropogenic interventions (expansions of urban areas, quarry exploitation of the river beds, underground excavations, etc.);

- Consolidation of underground terrains (below the dykes);

- Consolidation of the earth embankments (dykes).

- Piping or seepage problems;

- Animal excavations and biological alterations.

The STBR (Regional Technical Service of the Reno River Basin) of the Regione Emilia-Romagna has recently begun a survey programme, financed by the Authority of the Reno River Basin (Autorità di Bacino del Reno 2002), and focused on the study of the hydraulic and geotechnical conditions of the river dikes inside the territory under its jurisdictional authority (Mazzini & Simoni 2004). The geotechnical investigations, brought to formulate many considerations; the levees, inspected with standardised field or laboratory tests results affected by many different problems like subsidence, erosion, landslides, piping, animal excavation, human impacts, but over all by the inappropriate building techniques that were used throughout history. As a result, the flood defence system of the complex Reno River network does not operate as it should in many important nodes. Therefore, in spite of the well developed system of embankments of the Reno River and its tributaries, dating in some cases over one hundred years, there is a lack of knowledge on their structural status because the geotechnical surveys (such as SPT-CPT tests, boreholes) achieve just punctual data. Hence, the large longitudinal extent of the embankments (several hundreds of kilometres) has placed great interest in non-destructive geophysical methods, which, compared to other methods such as drillings, allow a faster and often less expensive acquisition of high-resolution data. The knowledge of the existence and the position of eventually non-homogeneity zones into the embankment are relevant problems in term of hazard and hydraulic risk, especially if river embankments themselves are old (more than one century), inserted in a densely populated area, subjected to periodic important floods and at last, detailed information on history and structure are missing.

The need to carry out a survey of hundreds of kilometres of river embankments for identifying, primarily, these weakness zones, is also a requirement of the regional government authorities. Just in this context, GPR suitability was tested in the study of river embankments; the main purposes were the detection of stratigraphy, animal cavities and burrows, buried pipelines, non-homogeneities in general and also related to different phases of construction and repaired areas of the embankment itself.

6.6.1 Savena Abbandonato Stream

The Navile-Savena Abbandonato channelization is a complex system of artificial drainage of the area that surround Bologna, which includes as a whole: the main hydrographical grid formed by the watercourses Navile, Battiferro, Diversivo and Savena Abbandonato, its basin and the areas connected either from the hydrographic or functional point of view with the catchment basin itself. The catchment basin, which is part of the basin of the Reno River, is about 111 Km² and its hydrographic grid has a length of 75 Km, 48 of which are embanked. The Savena Abbandonato is the old riverbed of the Savena River, which was deviated during the second half of the eighteen centuries and is a Reno River right tributary. The old riverbed was still used for drainage and irrigation, until the last century, when it was utilized as sewerage system, increasing the damages associated to the pollution. During heavy rainfalls, the Savena Abbandonato catches the meteoric waters of a widespread basin and its reduced riverbed area results in a scarce drainage capability. Moreover, in some parts along its course, seepage phenomena occurred in the recent past, associated to the presence of cavities excavated by animals as well as waterproofing inadequacy of the embankments.

Many destructive tests were provided in the last years, to acquire as much knowledge as possible of the materials of which the embankments are made up. These punctual data, demonstrate the high heterogeneity and three-dimensional anisotropy of both embankments and their fundament ground, which has different grain size associated to the alluvial deposits. According to boreholes and cone penetration tests, a simplified but effective embankments structure model was carried out: three main lithotechnic units were recognised:

- **A Unit (artificial)**

     Savena Abbandonato embankment materials, artificial, with the presence of heterogeneous materials, mainly fine sand, silty sand and sandy silt with subordinate presence of clay levels or medium to fine sand. The large differences between the deduced stratigraphic sections demonstrate that these embankments are insufficient to provide a safe waterproofing of the structure; indeed these materials were roughly taken near the river bed, in order to build as faster as possible the structure. The thickness of this first unit is variable from four to five-six meters.

- **B Unit (silty-sandy unit)**

     This is a typical alluvial unit, typical of a heterotrophic environment, with several series of depositional events, with their own energy amplitude and duration, due to the very unstable hydrographical regime, which affected this Po Plain part. This unit, even

131

with lateral and vertical variations, can be considered a unique body, until extensive geophysical tests will try to clarify its real composition. The granulometric composition is larger than the first unit and this unit results constituted by medium to coarse sand (mostly in the left hydrographical side), fine sand and alternation of clayey, silty lenses. Hence, an extremely high permeability could be found randomly in some parts of this unit. The surrounding fields, wherein sowing seeds and fruit trees cultivation is prevalent shows silty granulometric characteristics associable to this unit; its base coincides with the C unit.

- **C Unit (silty-clayey unit)**

The C unit underlies the previous at three to five m. depth from the surface, and it is mainly composed by dark-grey clays with subordinate levels of medium to fine sand, sometimes silty sand. These levels represent some river paleochannel, characterized by the elevate instability of the environmental conditions; however, the dominating part is composed by swamp conditions, leading to a very fine size material deposition. The average contains of gravel, sand, silt and clay for the three units are shown in the table.

	% Gravel	% Sand	% Silt	% Clay
Unit A	1	29	53	17
Unit B	2	59	29	10
Unit C	1	11	57	31

Table 6.2 - average contains of gravel, sand, silt and clay for the three units recognised by the geotechnical tests (Gelati, 2003).

During the heavy rainfalls of December 2002, the Savena Abbandonato Stream embankments suffered of seepage phenomena in the segment comprised between the confluences of Diversivo Channel (which partially deviate the Navile Channel water) and the Reno River. Following such events, that created several flooding in the surrounding fields, the STBR commissioned geotechnical investigations to define the geological model of the embankments because, despite of the reconstruction and refurbishing works that were actuated in the past for such embankments, no documentation about the soil characteristics of the surrounding as well as basement area was available. The results of the geotechnical campaign demonstrated that the high embankment permeability in correspondence of the seepage phenomena could be possible only due to the presence of cavities excavated by animals (Gelati, 2003).

The GPR campaigns were carried out in three different embankment segments; the first study area was defined in 2006, in Uberseto locality, near Altedo (BO), in correspondence of the seepage phenomena of 2002 (Figure 6.21). The measurements were done just in February 2007, after the well-time cleaning works, but no information were obtained in other seasons, because of the rapid formation of a huge vegetation nap that constantly covers this embankments segment.
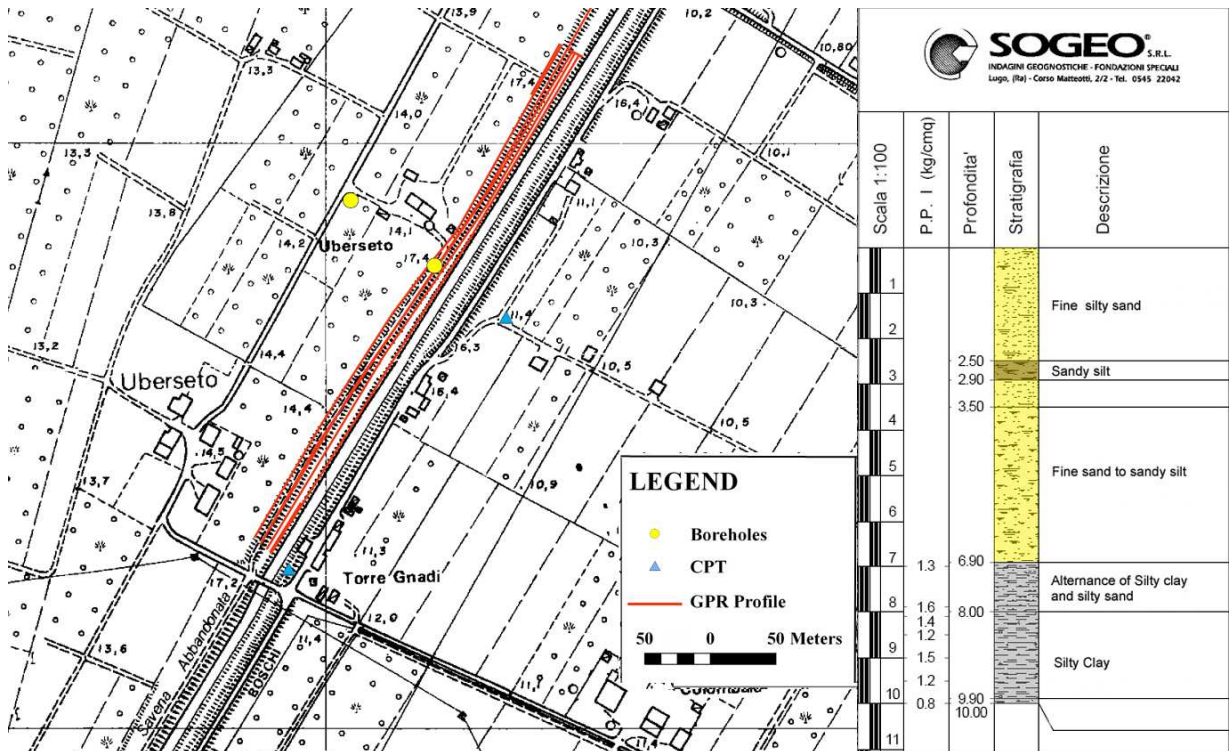
Figure 6.21 – Study area on the Savena Abbandonato embankment, near Altedo (BO), with the employment of 400 MHz antenna; a stratigraphic column of the subsoil is associated on the right.

The February 2007 campaign was carried out using SIR-3000 Ground Penetrating Radar, released by GSSI, transmitting and receiving EM signals with a 400 MHz antenna. The data were elaborated with the commercial software RADAN 6.5, released by the same company. The 400 MHz antenna has detected interesting zones with higher permeability inside an internal step of the embankment, characterized by strong porosity, revealing the presence of several punctual anomalies, caused by vegetation roots as well as voids occurrence (figure 6.22). The wave velocity inside the ground was estimated in 12 cm/nsec through the positioning of a metallic object at known depth, as explained in the paragraph 6.1.2. These small anomalies, detected until the depth of one meter and half were verified with manual trenches provided on the flank of the embankment step, confirming the hypothesis formulated with the GPR data analysis.
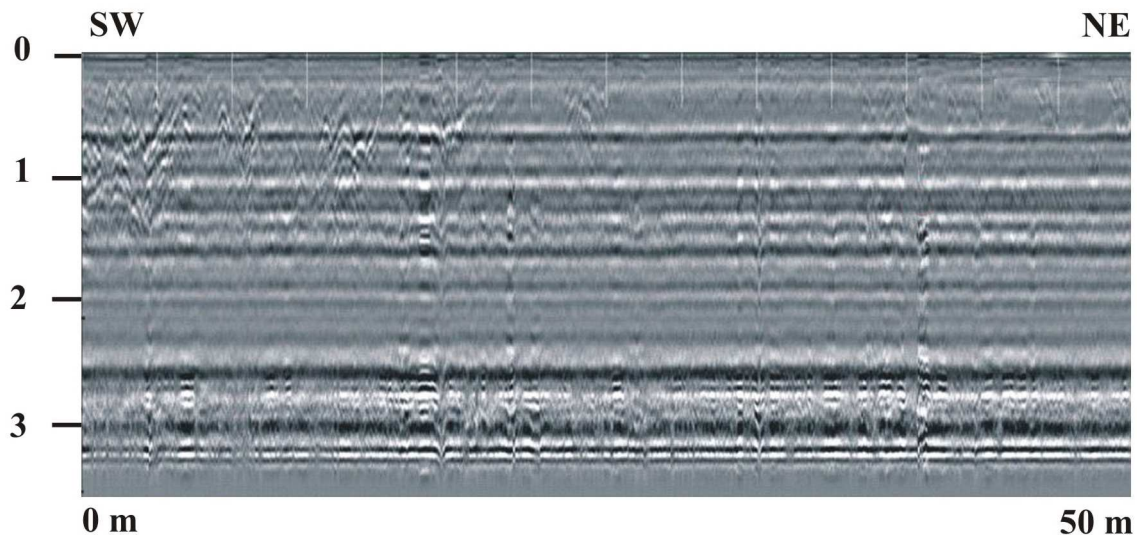
Figure 6.22 – GPR profile, carried out using a 400 MHz antenna, which reveals the anomalies presence on the left part of the radargram.

The 400 MHz antenna results useful for the determination of small anomalies at shallow depth, but there is no evidence of stratigraphic passages inside the investigated subsoil; however, there are no geotechnical information about the embankment stratigraphy in this segment. The radargrams are characterized by some "antenna ringing" effect that is produced by the horizontal banding phenomenon. The ringing is associated to the fictitious repetition (with regular intervals) in the radargram time axes of strong superficial reflections, that risk to cover the eventual horizontal boundaries, which is related to changes of electric properties (and therefore lithologic passages). The 400 MHz antenna results also insufficient to provide a description of the embankment structure; its penetration capacity is not more than two-two and half meters so that the profiles acquired on the embankment top do not furnish any information about the structure of the embankment itself.

Along the external basis of the embankments, other profiles were carried out, in order to localize the water table as well as the boundaries between the superficial soil horizon and the deeper layer, calibrating the results with the stratigraphic column of figure 6.21. Must be remembered that in sediments, dielectric properties are primarily a function of mineralogy, porosity, water saturation, and they depend on the lithology, component geometries, and electrochemical interactions. In addition, the dielectric constant of soil is a function of the percent of water in the soil, increasing with increasing water percentage in the soil. The horizontal surface where the GPR profile was carried out can compromise the results of the processing, because the "*background removal*" function, which removes the average of all the scans accumulated, besides the banding and ringing effects can remove other horizontal

features such as water table. Nevertheless, the 400 MHz antenna guarantees a good resolution and the fine lithology of the subsoil, which contains lateral variations in terms of granulometric composition, can produce oscillations in depth of the water table. Hence, if a not planar water table occurs in consequences of the capillarity phenomenon, the associated reflection thus can be detected through the horizontal banding filters application. The figure 6.23 illustrates a clear banding at around two meters and half, that is characterized by a *Ricker wavelet* that gives a 180° phase change and the three major half-cycles have a − + − (black/white/black) phase, indicating the expected reflection at interfaces from higher to lower permittivity. Such banding shows a very regular profile and in addition, it is situated whereas the signal-to-noise ratio is too low to produce such reflection. However, the water table presence can be estimated at the variable depths of one meter and half to two meters, whereas an undulate continuous reflection marks the entire radargram, described by a positive–negative–positive pulse + − + (in grey scale white/black/white).
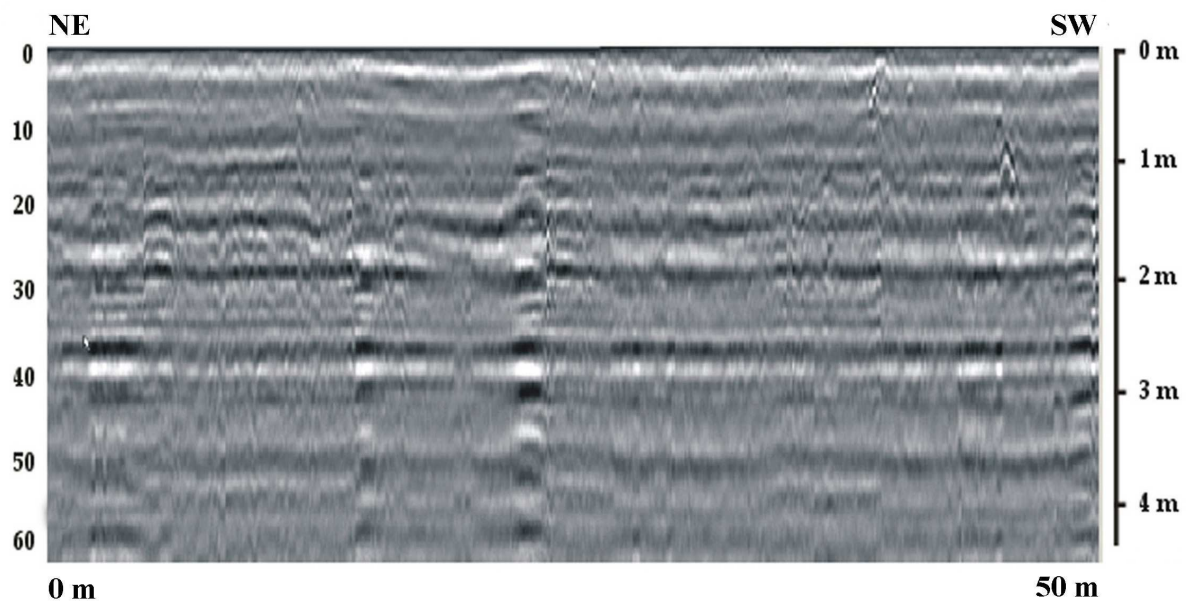
Figure 6.23 – GPR profile with 400 MHz antenna, carried out on the external basis of the embankment, which evidences the possible presence of reflections caused by the water table top.

These oscillations can be confirmed by the fact that the lithology is composed by prevalent sandy horizons, which result in a slight capillarity phenomenon. This phase polarity corresponds to the expected reflection with this antenna at interfaces from lower to higher permittivity, which actually is given by the passage from unsaturated to saturated soil. Unfortunately, the water table detection for the embankments soil type and stratigraphic column is a contradictory task and for all the profiles carried out, the margin of uncertainty is too high to make an adequate estimation. Anyway, this profile evidences also in its right part

a hyperbola at one meter depth that can be associated to a buried object belonging to carryover materials.

The other segments, respectively in the fractions of Capo d'Argine and Cà dei Fabbri, located at twenty kilometres northward Bologna, were chosen whereas cleaned levee and smooth surface at the top of the levee itself were found. These segments are also interesting because many constructions as private houses as well as warehouses were built just below the embankment structure and no geotechnical data are available. Generally, the granulometry of the materials that compose the Savena Abbandonato Stream embankments presents larger amount of sand and consequently more heterogeneity with respect to the other Reno River catchment embankments; therefore, EM wave deeper penetration capability was reached.

The Capo d'Argine GPR profiles were carried out using the 100 MHz antenna and the MF (200-600 MHz) antenna (Figure 6.24). With regard to the MF antenna, interesting results were produced both with the employment of 200 MHz monostatic antenna and with the cross-polar configuration, which transmits the impulse at the nominal frequency of 200 MHz and receives using the 600 MHz antenna.
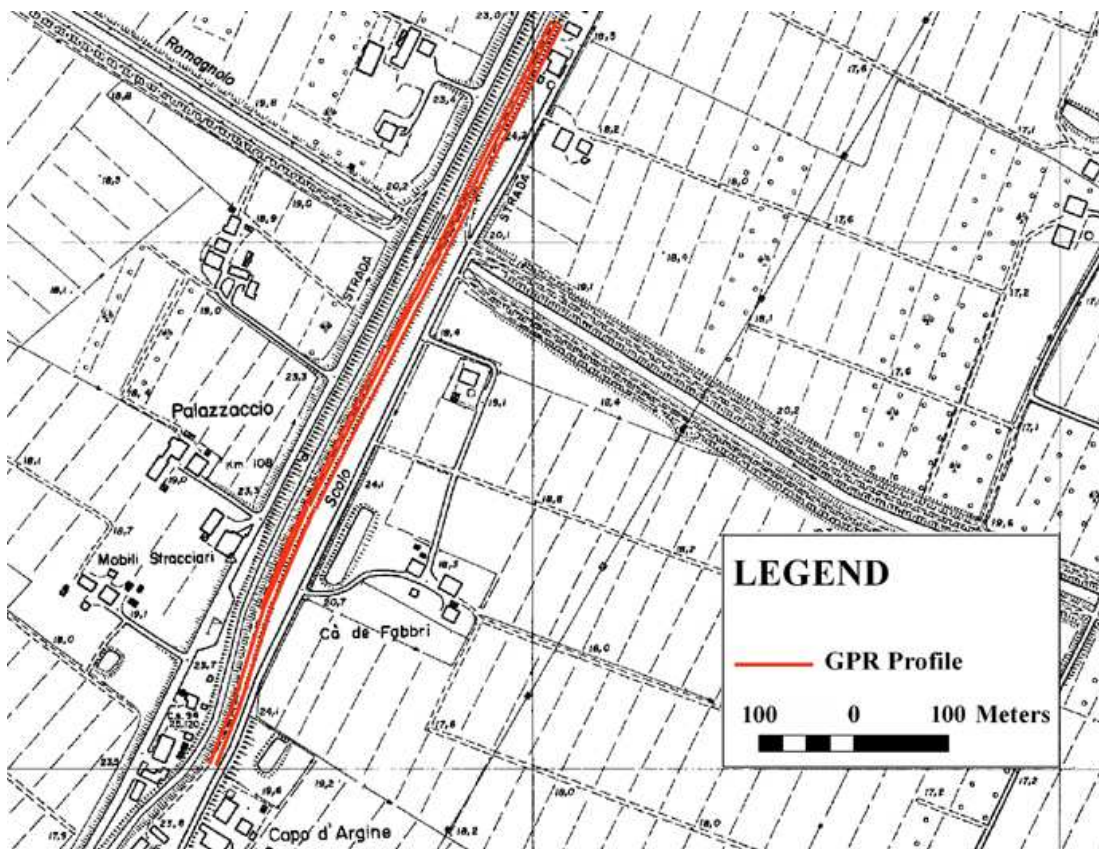
Figure 6.24 – Study area on the Savena Abbandonato embankments, for structural evaluation and cavities detection: 100 MHz and MF (200-600 MHz) antennas were employed.

The filtering values were chosen considering the frequency spectrum in order to capitalize to energy emitted by the GPR and to provide an efficient signal cleaning. The application of 200 MHz to 800 MHz high-pass and low-pass filters respectively has brought to a better radargram definition. In some profiles, the prevalence of sand inside the embankment material has improved the penetration capability of the EM wave. Therefore, for 200 MHz antenna applications, the signal-to-noise ratio was adequate until a depth of two to two and half meters and therefore the obtained results have maintained the expectations. Such operating frequencies were functional to the detection of many punctual heterogeneities and anomalous zones inside the first two meters of the embankment, which are prevalently linked to the occurrence of heterogeneous carryover materials (figure 6.25). The massive amount of carryover materials (especially rock boulders and bricks) significantly increases the permeability of the upper embankment structure, assessing a high grade of instability to this segment of Savena Abbandonato Stream embankments. The risk associated to breakage and seepage phenomena is restrained by the geometric factors that characterize this alluvial plan part of the Savena Abbandonato course. Indeed, this riverbed, which was used for drainage and irrigation until the last century, was recently channellized and utilized as sewerage system; the straight direction of the artificial riverbed and its reliable slope increase the discharges into the Reno River but mitigate the possibility of persistence of high water-levels into the riverbed during flooding.

Concerning the results obtained with the employment of the 200-600 MHz cross-polar configuration, the depth achieved is less with respect to the depth gained with the 200 MHz antenna, but the spatial resolution and the details about the buried objects were improved. Furthermore, the cross-polar configuration, with respect to the 200 MHz antenna, has a different dipole orientation and thus a different footprint; such displacement guarantees the coverage of a wider area and therefore permits to roughly understand the spreading of the detected targets. All the profiles analysed shows some frequent punctual anomalies and heterogeneous zones, and the lithologic passages of the first one meter are well-evidenced with respect to the 200 MHz antenna results. The penetration depth has seldom reached two meters, and in most of the cases under the meter and half the signal-to-noise level has resulted too low. The Figure 6.25 shows some evident hyperbolas and other reflections associated to heterogeneous zones. The presences of metallic objects on the profiles generate some multiple vertical reflections, which mean total reflections of the EM wave (Figure 6.25b). Some objects are detected with both the configurations; therefore, they result fairly spreads and the presence of houses as well as warehouses in the immediate surrounding could lead to

hypothesise the occurrence of conduits (Figure 6.25a) and zones excavated, filled and thus compacted, where anomalous materials seem to be placed (Figure 6.25b).
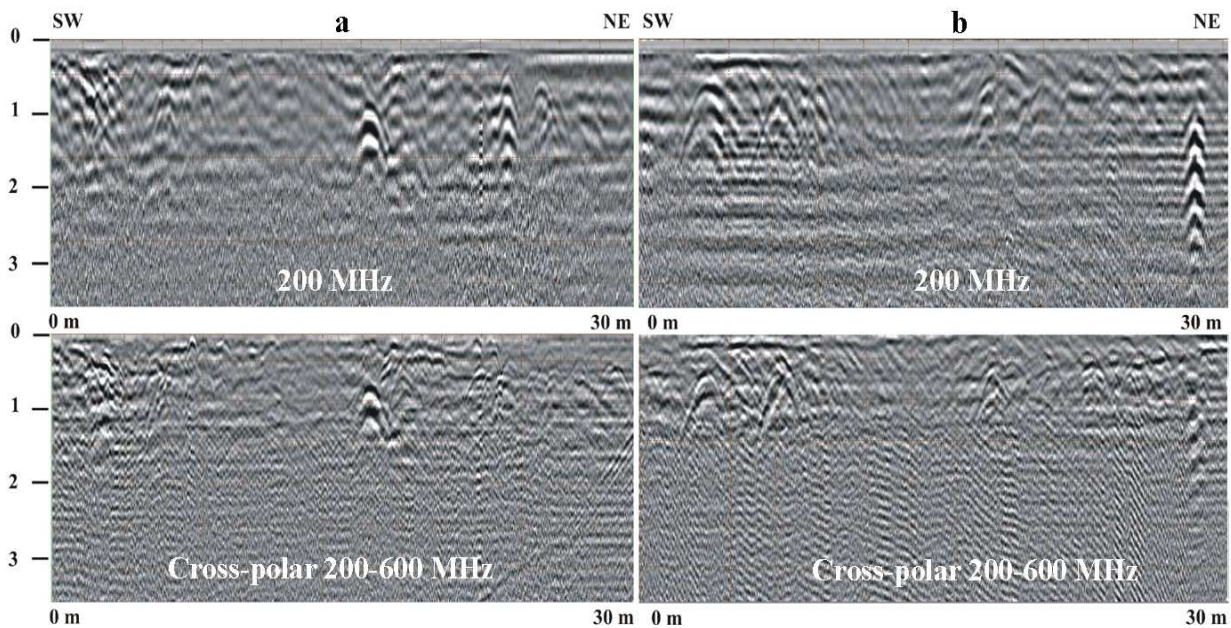
Figure 6.25 - GPR profiles carried out using MF antenna (monostatic and bistatic configurations), carried out on the top of the embankment, which evidences: a) presence of many reflections caused carryover materials, b) metallic objects.

The antenna 100 MHz usage can provide the description of a consistent part of the embankment; this is the unique case whereas the dimensions of the embankment as well as the granulometric conditions have enabled to reach the base level of the embankment itself (5-6 meters from the surface). The profiles carried out using the 100 MHz follow the same path of the previous profiles and shows the major reflections that were detected with the employment of the 200-600 MHz antenna; however, some parts of the radargrams, elaborated with the GRESWIN2 software, show zones without reflections. The 100 MHz antenna has often acquired noisy data, which create some banding effects of difficult interpretation. The spatial resolution respect to the higher frequency antennas is obviously reduced but the EM wave is able to identify an important boundary (Figure 6.26) at around four meters depth. The lack of geotechnical information, as well as other geophysical measurements, does not permit the recognition of such evident change in dielectric characteristics. Some hypothesis can be done: the almost horizontal shape of the boundary should be associated to the water table level or should be due to various phases of construction, which can be justified by the high heterogeneity of the entire embankment segment. However, the noisy level of the data and the presence of some artificial banding on the left part of the profile do not assure the hypothesis formulated; once again, this case demonstrates how a multidisciplinary approach is necessary to understand the causes of potential instability of the embankments.
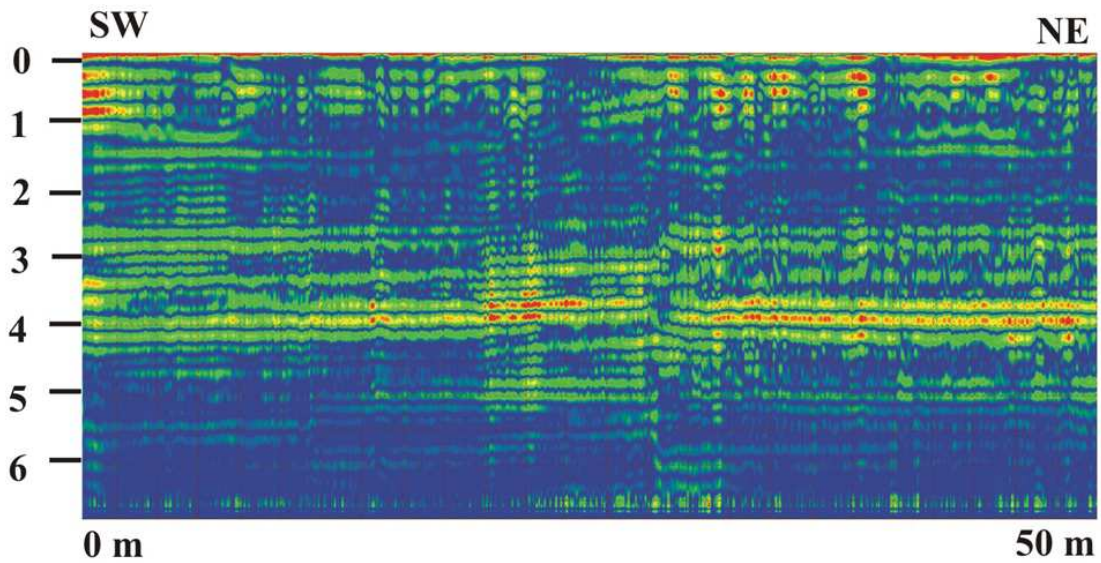
Figure 6.26 - GPR profiles carried out using 100 MHz antenna, carried out on the top of the embankment, which evidences presence of an evident boundary at four meters depth.

The Cà dei Fabbri segment, located at two kilometres northward the Capo d'Argine area test, was also chosen because of its vegetations-free and smooth surface at the top of the levee.
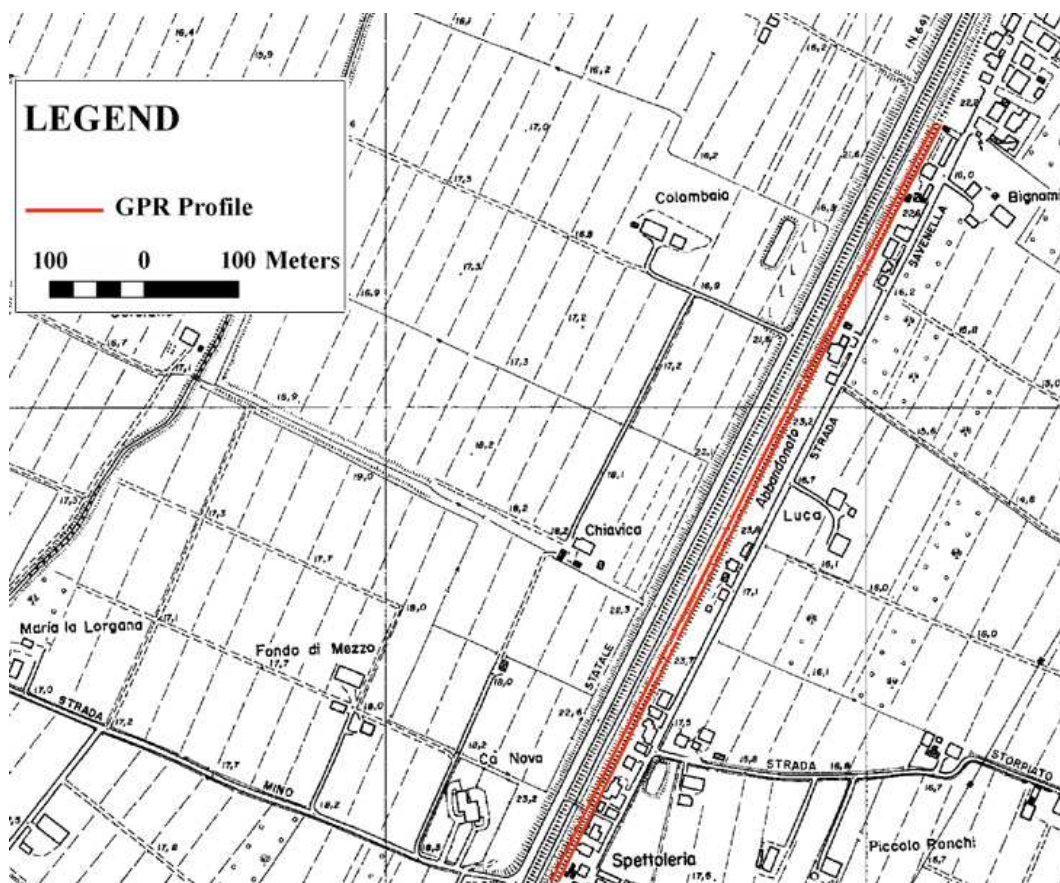
Figure 6.27 – Study area on the Savena Abbandonato embankments near Cà Dei Fabbri, for structural evaluation and cavities detection, with the usage of MF (200-600 MHz) antenna.

The antenna employed was just the MF, realizing a profile on the top of the embankment of around 775 meters (Figure 6.27) The granulometry seems to present the same lithologic characteristics (larger amount of sand with respect to the other Reno River catchment embankments) and consequently the same conditions for the GPR measurements was encountered.

The figure 6.28 evidences the results obtained by the three configurations employed with the antenna MF. The 600 MHz monostatic channel, even if is able to detect many tiny anomalies, results too sensitive and suffers strong signal attenuation; therefore, antennas that produce EM waves at higher frequencies than 200 MHz are insufficient to make measurements in river embankments.
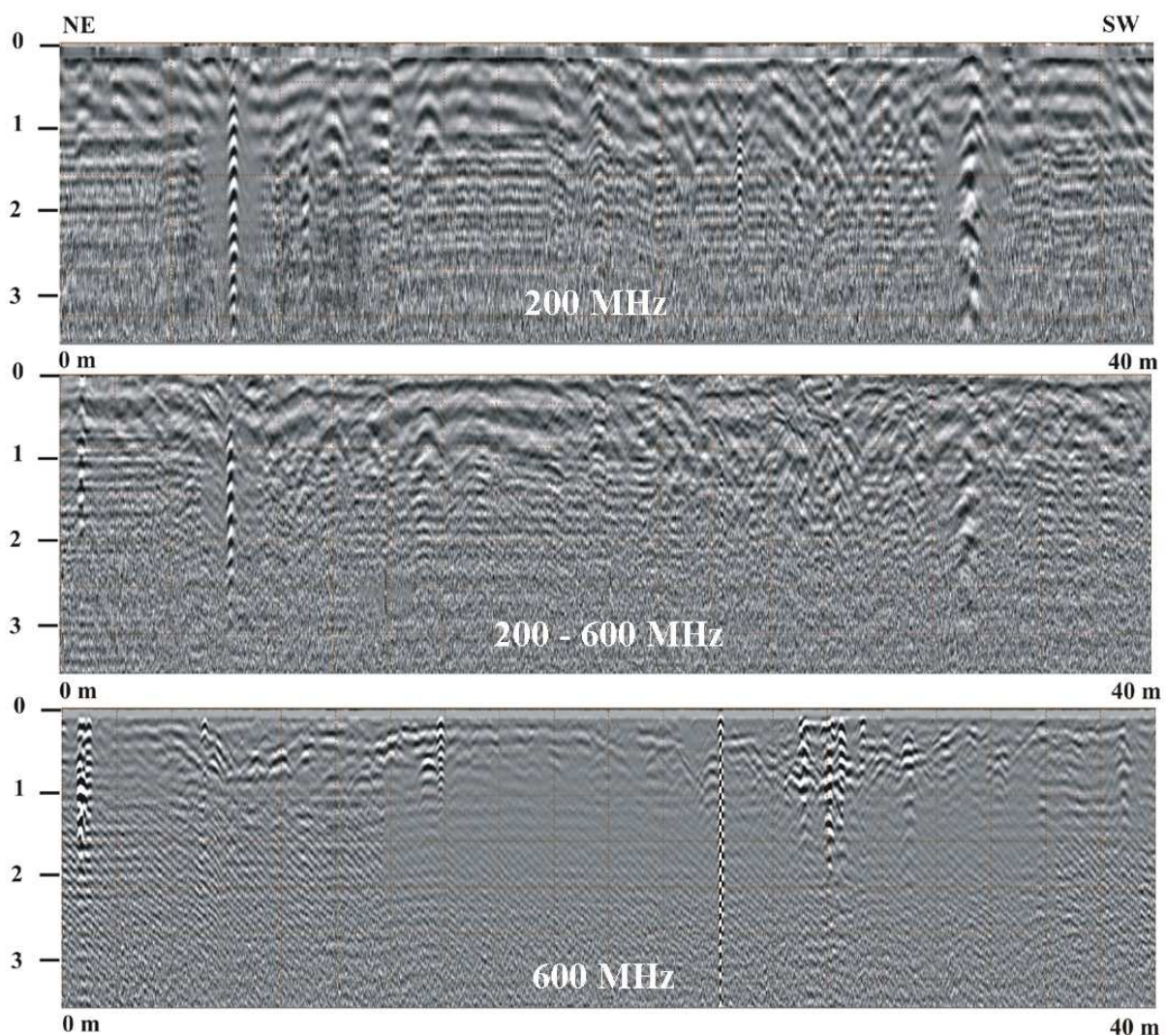
Figure 6.28 – GPR profiles carried out using all the configurations available for the MF antenna, carried out on the top of the embankment, which evidences presence of many reflections caused by carryover and metallic materials.

The 200 MHz antenna and the cross-polar configurations give comparable results, individuating metallic objects and several hyperbolas in the first meter and half until two meters from the surface.

To make a summary, in homogeneous soil, the GPR is able to identify shallow isolated objects with a size higher than the maximum resolution of the antenna employed. For the Savena Abbandonato Stream embankments, it was possible to identify pipelines and objects having a high permittivity contrast. In case of several anomalies without repeated reflection at depth, they were interpreted as isolated blocks inside filling soil; isolated small anomalies with strong reflection at depth are probably related to metal objects. Even if the employment of a 100 MHz antenna has guaranteed a good penetration depth, the scarceness of the information related to the reflection individuated, demonstrates once again how a multidisciplinary approach is necessary to understand the causes of potential instability of the embankments.

6.6.2 Reno River

Along the Reno River the embankment segment situated in locality Case Reno Sabbioni, near Malalbergo (BO), was chosen as first area test of the entire campaign of measurements (Figure 6.29). This area, situated on the hydrographical left side of the Reno River is adjacent to the segment affected by the breakages of 1949-1951 and of 1990 (in the right hydrographical side) that was caused by the presence of a methane conduit; this conduit was built inside the embankment body and created a line of weakness, which triggered the breaking event. This area was chosen because it is comprised between breaking events that took place in the past. The campaign aims to implement some GPR profiles together with another geophysical method, commonly used (electric tomography). The area was chosen also in concomitance with direct measurement tests (boreholes and CPT tests) and a series of vegetation cuts. Three GPR campaigns were carried out over this embankment. The first one was carried out in August 2006, with employment of SIR-3000 GPR, commercialized by GSSI, employing 100 MHz antenna; the second one was carried out in November 2006, with a relatively high frequency antenna (200-600 MHz, from IDS, 4 channels RIS MF and master MF antenna). The third and last campaign, in October 2007, was provided with RIS Ground Penetrating Radar (IDS) also employing again the 100 MHz antenna frequency. The campaigns have realize with the same hydrological dry conditions, even if the atmospheric humidity (and consequently of the first half meter of subsoil) of November can be considered higher.
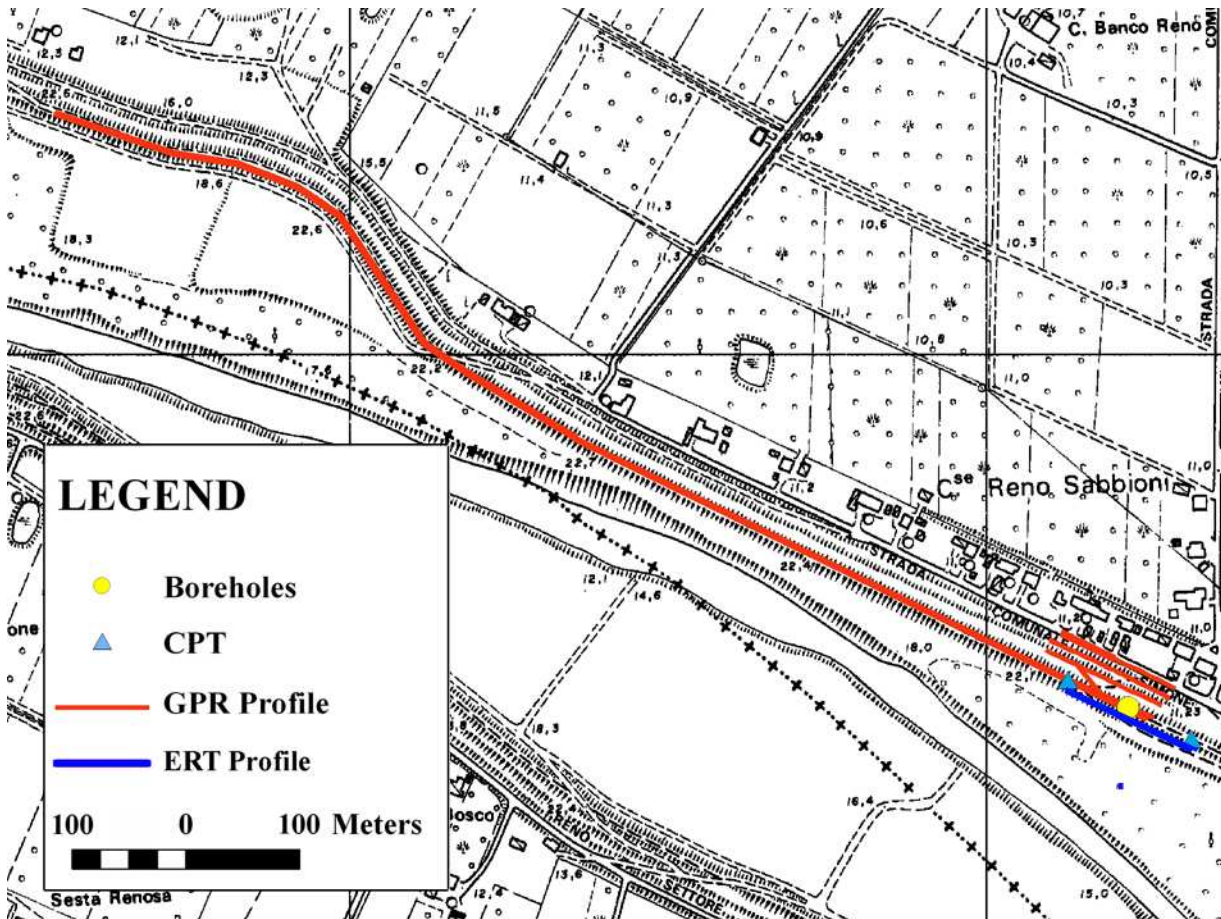
Figure 6.29 – Study area on the Reno River embankments near Malalbergo (BO), for structural evaluation, with the employment of a 100 MHz antenna.

The stratigraphy reconstructed from CPT and Boreholes information (Figure 6.30) is characterized by a complex structure, revealing a typical sequence for the Reno River and its tributaries embankments. Inside the study area the river bank, which is about ten meters high, is mainly made up of silty sand. At a depth of three and half meters it is possible to notice a slight difference in lithology (from silty sand to silt) and compaction. For manmade embankments, it is typical to detect both in boreholes and in CPT layers of the same material, recognizable for different grade of compaction, which represent different phases of construction. Usually three main units are recognizable as:

- A: River embankment (artificial), typically represented by sandy silt.
- A': Artificial river embankment, with horizon (where present) characterized by silty clay.
- B: Fluvial sediments, typically represented by silty sand.
- C: In site material, typically represented by clay.

142
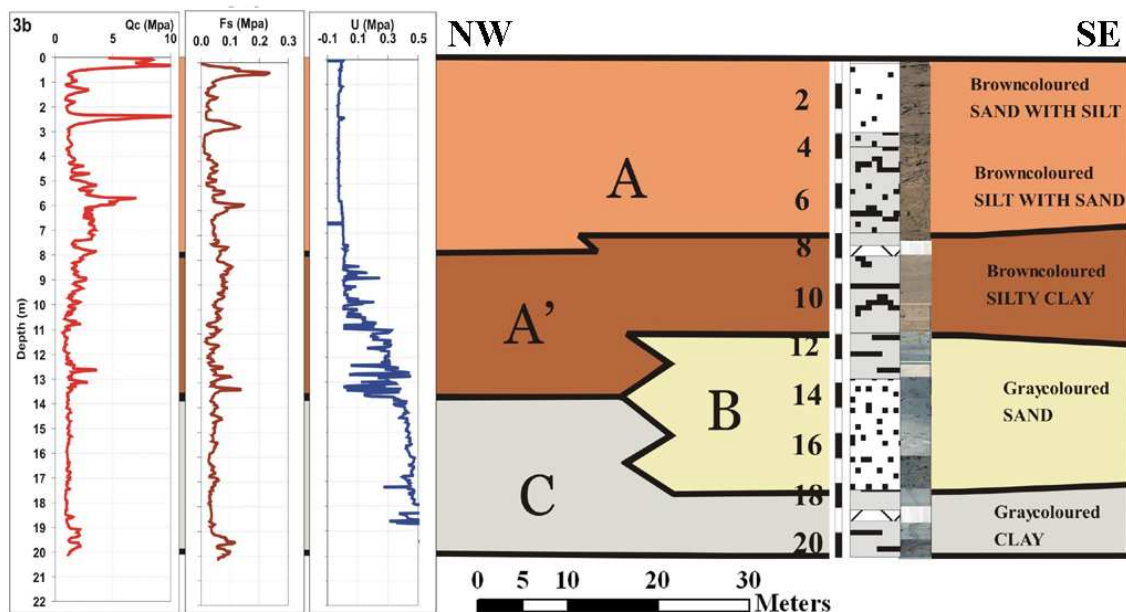
Figure 6.30 - Longitudinal cross section of the embankment, deduced by the borehole and CPT tests.

The GPR survey was organized by implementing mainly longitudinal profiles with various frequency antennas. Some results have obtained with a relatively low frequency antenna (100 MHz, from GSSI sir 3000) and with a relatively high frequency antenna (200-600 MHz, from IDS, 4 channels RIS MF and master MF antenna). The lowest frequency antenna is expected to have a deeper penetration and a minor resolution at shallower depth with respect to the higher frequency antenna (Davis & Annan, 1989). In both the analysis a dielectric constant $K = 9$ ($v = 10$ cm/nsec) was supposed. This has suggested by the interpolation make automatically in slightly wetter conditions (November 2006) by the IDS master MF antenna, and seems to be reasonable for sandy silt material (Daniels, 2004). For dry conditions one expects a lower K (higher v), but velocity values higher than 10 cm/nsec are not reasonable for such kind of material. Figure 6.31a shows a profile that was made with the 100 MHz antennas in the at the top of the embankment during dry conditions in August 2006; this profile evidences two continuous boundaries, which, according to the imposed dielectric constant, lie at two and five meters depth, respectively. They do not match with any lithologic horizons seen in the borehole stratigraphy; nevertheless, they match with CPT information, which in these points show same material with higher compaction. The Figure 6.31b shows the profile that was carried out in October 2007, where many reflections were detected, which could be associated with some boundaries but not continuous and that are not clearly comparable with the August 2006 profile. GPR demonstrates to suffer a lack in repeatability and further geophysical surveys need to be implemented in order to check if they are apparent reflective horizons (due to the cable effect or antenna ringing).

143

a)

b)
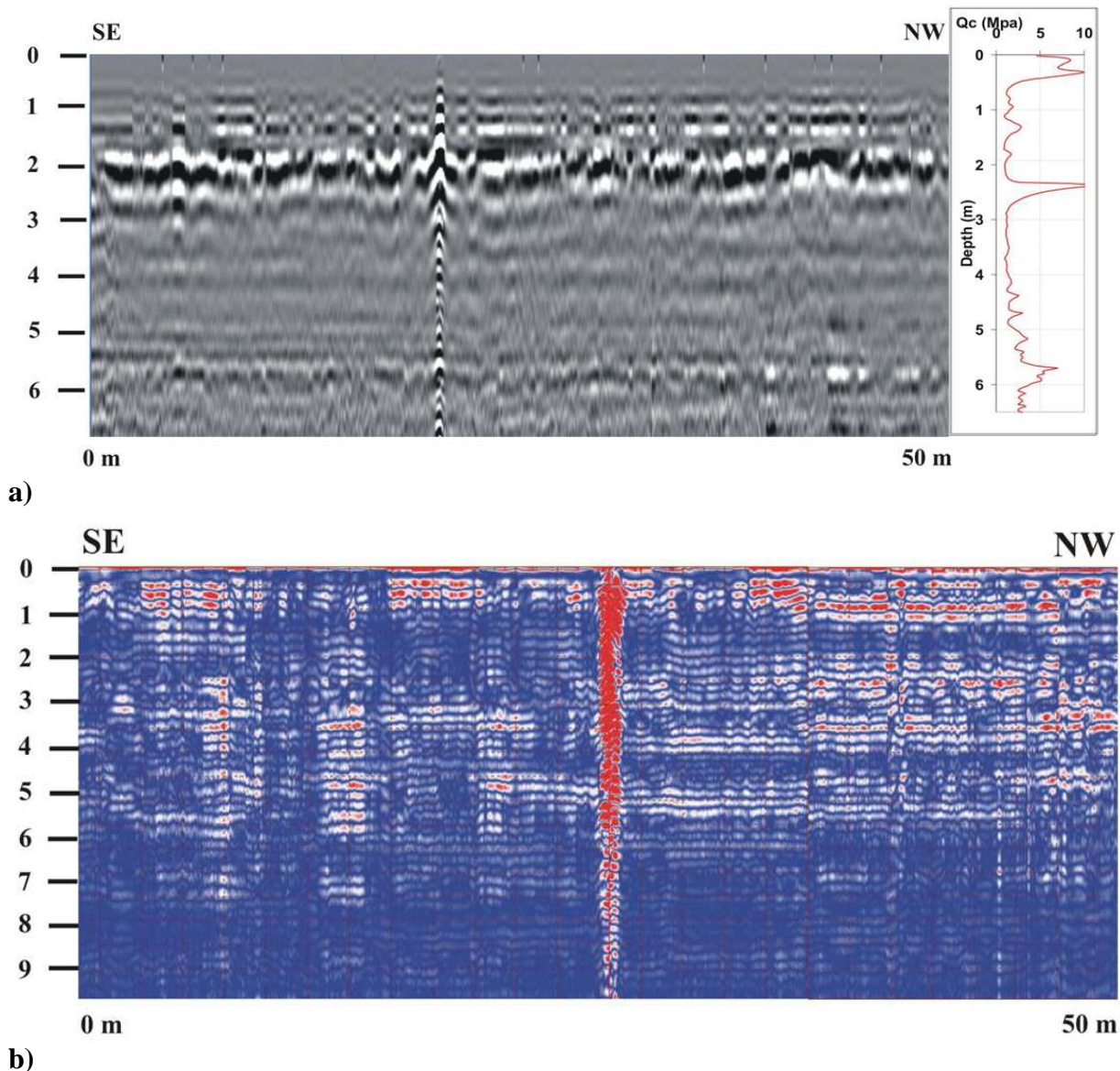
Figure 6.31 - GPR profiles carried out using 100 MHz antenna, carried out on the top of the embankment: a) two continuous boundaries at two and five meters, b) many reflections but no evident boundaries. Borehole test produce strong reflections at the centre of the radargrams.

Therefore, the electric tomography (see location in Figure 6.30) was implemented with a data acquisition system for multi-electrode resistivity surveying by ABEM (Terrameter SAS 1000) with electrode spacing of two meters. Wenner configuration was chosen, because of its strongest signal intensity and the consequent reduction of noise that are important factors when a survey close to zones characterized by antrophic activities is needed. Results (Fig. 6.32) show that the upper layer with relatively high resistivity has a progressive increasing thickness in the Northeast direction. This layer corresponds to Unit A', as correlations with boreholes and CPT confirm. Anyway, this measurements give not detailed information about the internal structure of the embankment and has suffered many problems during the acquisition phase, both for the presence of a strong noise and for the atmospheric conditions,

144

very hot and dry, that have critically reduced the capability of transmitting and receiving currents for the georesistivimeter. Furthermore, the Wenner array, that for the noisy environmental conditions is capable to produce a good signal intensity, has proved insufficient to provide a description of the lateral variations inside the entire embankment structure.
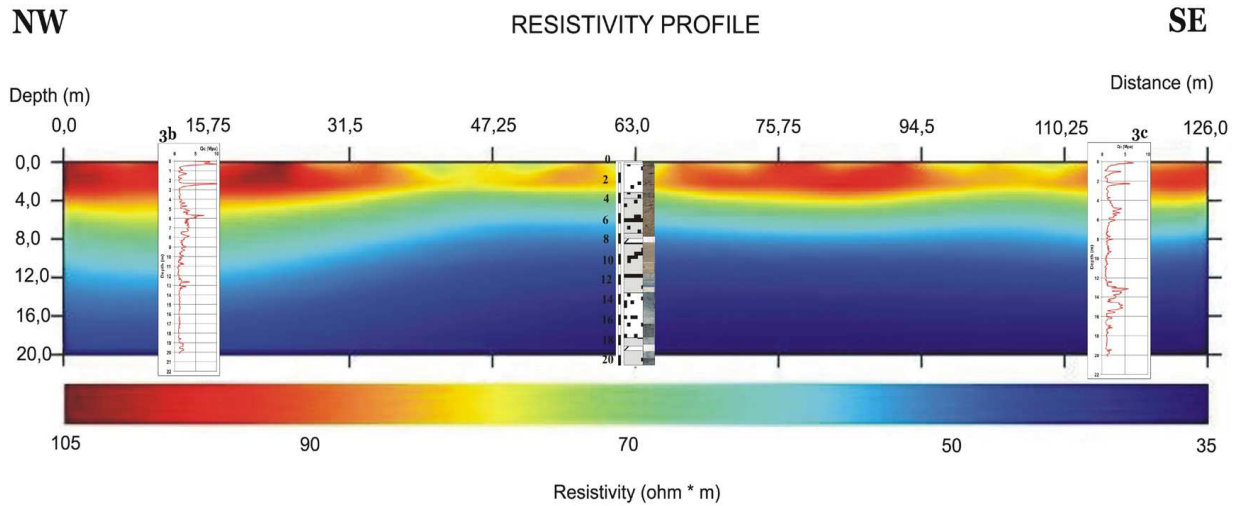
Figure 6.32 - Electric tomography section obtained with Wenner configuration (2 m electrode spacing).

The 200-600 MHz antenna was used in November 2006 in the same embankment segment, but at different levels with respect to the 100 MHz antenna survey, given that on the top of the embankment any consideration can be done with shallower penetration depth. For both the embankment steps and the road level profiles, any sharp boundary can be identified: some small anomalies are probably related to local inhomogeneities. Profiles implemented with 200-600 MHz antenna on the external side of the riverbank (first step level and base level) show several anomalies related to different kind of discontinuity. In the profile of Figure 6.33a, it is possible to notice one discontinuity at one meter depth with a quite good lateral continuity, interpreted as a level of compaction. At the same time, narrow parabolas indicate discrete small targets that could be brick fragments or roots at shallow depth. Profile obtained along the road at the base of the riverbank (Figure 6.33b) shows very clearly discontinuities with a spacing of about 30 cm that are probably related to the reinforced bars of the asphalt and some pipelines and conduits.

Pertaining to the profiles (for a total length of approximately one kilometre), carried out using the 100 MHz antenna in October 2007, some other reflections and anomalies were detected. The best vertical filter application has resulted the 80 MHz (high-pass) and 500 MHz (low-pass), that were chosen after many empirical attempts for their capability to enhance anomalies definition from three to five meters of depth.

145
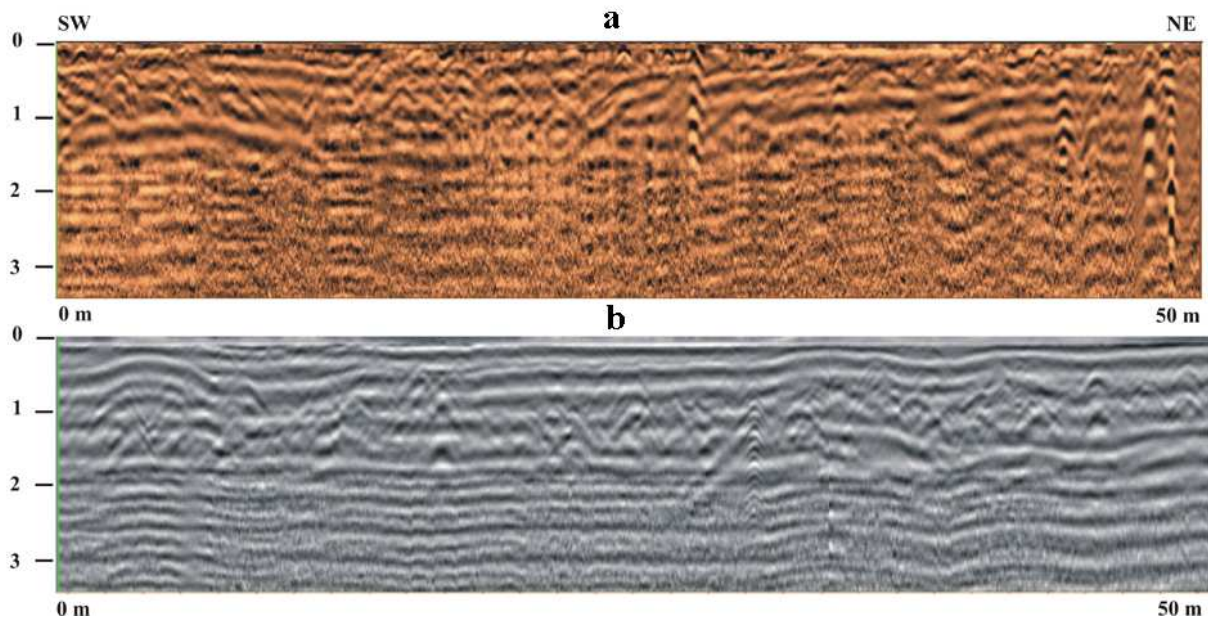
Figure 6.33 - GPR sections carried out using the 200 MHz antenna: a) along the external flank of the river bank, b) the road level.

Anyway, the penetration depth has never exceeded the six meters that is insufficient to provide a complete and satisfactory description of the embankment, which has an average high of twelve to thirteen meters. The passage over the borehole test triggers many multiple reflections; however, some levels with different electric properties are noticeable. The borehole evidence some slight changes in material composition, passing from the first layer in fine sand with silt to a horizon characterized by mostly sandy silt with small presence of clay. Over this horizon, a peak of CPT cone resistance occurs, perhaps referred to the same geological conditions of the surrounding material, but with higher compaction. The sandy silt lens, of half-meter thickness, overtops another layer with the same characteristic of the first. Some profiles show sub-horizontal boundaries with good reflection coefficient, which could identify some stratigraphic levels at different depths between two and half meters to five. A deeper boundary at around five to six meters, which corresponds to another relative peak on the CPT test, could be associated to other variations in porosity, but it is located near to the noise threshold and does no represent a certain datum. At a certain distance from the borehole test, the GRP profiles show some strong banding again around three meters depth and some slight not continuous reflections derive from six meters (Figure 6.34). Despite of the scarce depth calibration with the changes evidenced with the direct tests, nevertheless many lateral variation and some boundaries inside the material that compose the embankments can be roughly detected.
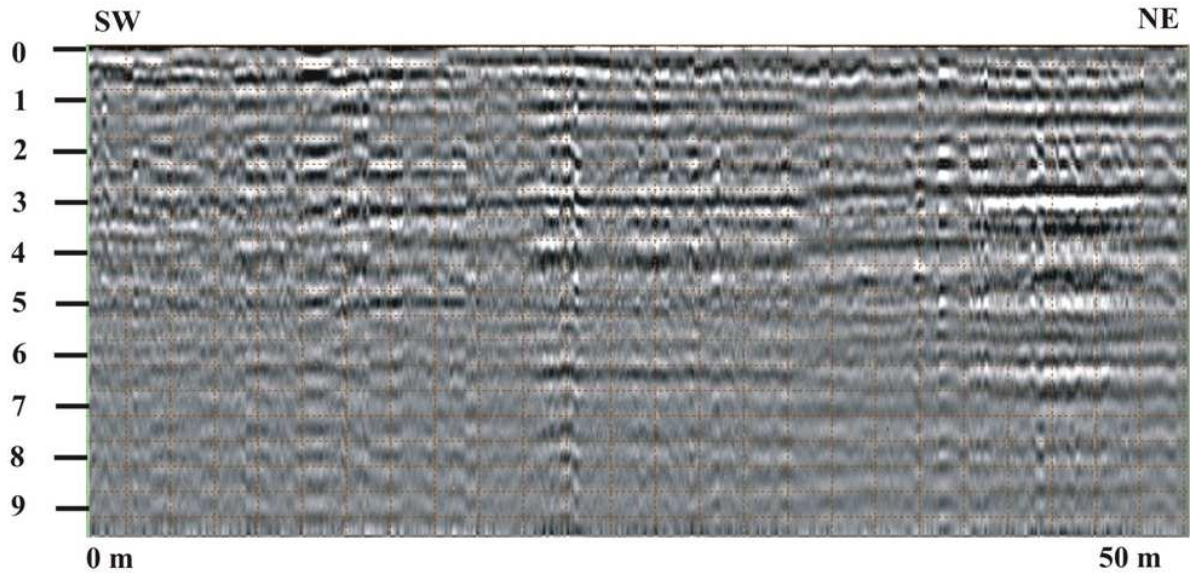
Figure 6.34 – GPR profile with 100 MHz antenna, carried out on the top of the embankment, which evidences a possible boundary caused by porosity or lithologic changes.

The 100 MHz antenna was useful also to detect targets at shallow depth: some profiles have detected punctual strong anomalies inside the first meter from the ground (Figure 6.35).
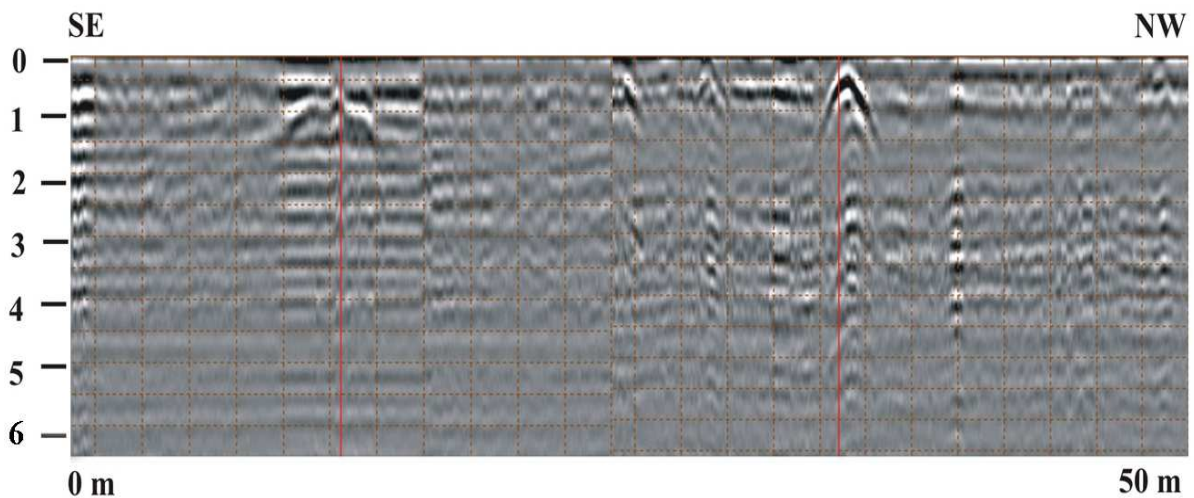
Figure 6.35 – GPR measurement, carried out on the top of the embankment, which has detected many conduits at shallow depth, employing 100 MHz antenna.

To remark is the fact that the polarity of the reflections clearly shows a passage from a material characterized by lower permittivity to another that has it higher. Such anomalies represent conduits that are used for the irrigation of the field both inside the flood bed and in the surroundings of the embankment; however part of them are clearly visible from the embankment and the positioning on the top of the embankment itself does not preclude the structural safety in case of flooding. Therefore, the GPR applicability for the detection of

heterogeneous zones and materials inside the embankment and dikes is partially verified for the Reno River and its tributaries, principally because the high of the structures has always resulted larger than the penetration capability of the GPR. Furthermore, the profiles carried out along the longitudinal flanks of the embankments have proved ineffective to describe the structural core, because of the large dimensional spreading of the embankments themselves.

6.6.3 Napoleonic Channel

The Napoleonic Channel is an artificial channel that connects Reno and Po rivers with a double function as a flood control reservoir and an irrigation canal. As recent geological and geotechnical investigations reveal (Mazzini et al., 2006) its pathway intersects abandoned channels and fluvial ridges related to ancient course of the Po River. The channel riverbed is not always coated in correspondence of these intersections, thus seepage phenomena can occur.
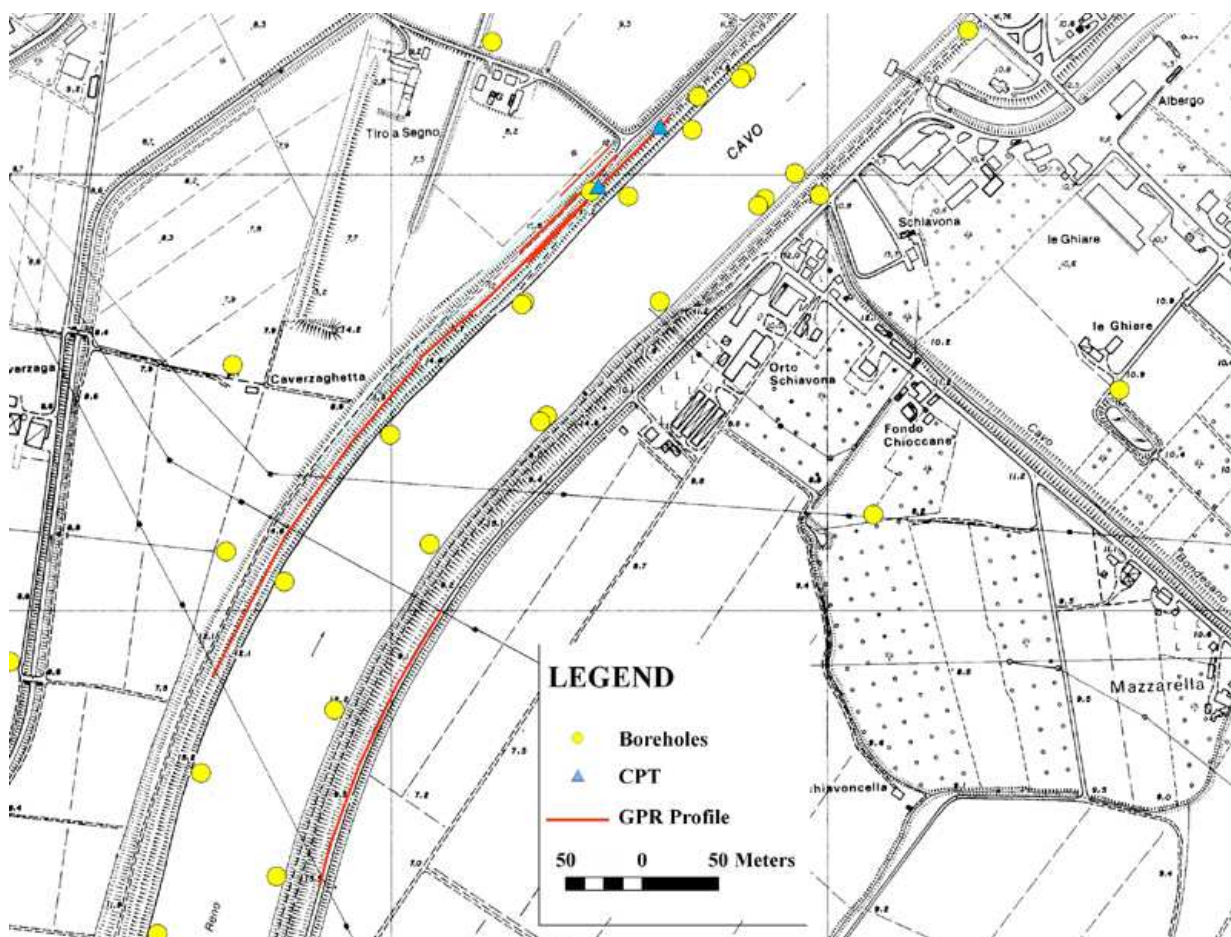
Figure 6.36 – Study area on the Napoleonic Channel embankments near Bondeno (FE), for structural evaluation, with the employment of a 100 MHz as well as MF (200-600 MHz) antennas.

The study area, shown in Figure 6.36, is situated above one of these points of intersection; the main aim was to check riverbank conditions in order to prevent possible piping or seepage events. Along the 18 km of Napoleonic Channel longitudinal spreading, the massive geotechnical campaigns through boreholes and CPT tests have revealed the stratigraphy of the levee foundation, without giving any information about hat the embankments. From preliminary direct tests and drillings it was notified that the embankments are prevalently constituted by silt and clay. The GPR profiles were carried out using several configurations and antennas MF (200-600 MHz) and 100 MHz with the IDS GPR, 150 MHz and 300 MHz with the GPR by Radsys, but the very fine lithologic conditions has always impeded the EM wave to reach a deeper penetration than two meters. The profiles were carried out both at the top and on the external flank of the embankment, for a total length of more than one kilometre; the profiles carried out on the top in particular have suffered a strong attenuation, with a powerful level of noise.

The only result achieved by the 100 MHz is just relative to the detection of a large anomaly relative to the methane conduit of SNAM society at around 50 - 60 cm depth, according to the velocity estimation considering a higher dielectric constant ($K = 12$, $v = 8,6$ cm/nsec). Is noticeable also the reflection caused by the material excavated to pose the conduit and then re-compacted, which produce a change in porosity and therefore electric properties (Figure 6.37)
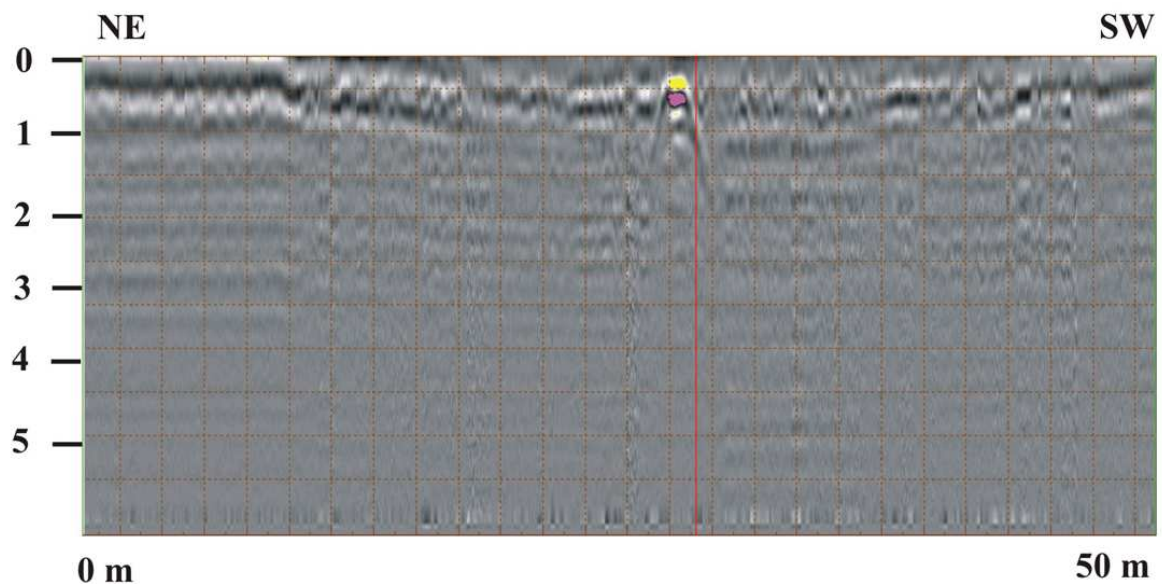
Figure 6.37 – GPR measurement, carried out on the top of the embankment, which has detected a methane conduit at shallow depth, employing 100 MHz antenna.

As already stated, for the external flank of the embankment, even if geotechnical investigation are not available, from preliminary stratigraphic analysis is unmistakable that

the riverbank is mainly made up of silty and clay material. The monitoring tests were implemented with 300, 150 MHz antennas (Zond Georadar, by Radsys) and 200-600 MHz antennas (IDS RIS MF Georadar). Because of the high percentage of clay fraction, the radar signal was highly attenuated with all the used antennas. Nevertheless, surveys carried out in the external side of the embankment, as shown in Figure 6.19A (SCAN A), in November 2006 with the IDS Ground Penetrating Radar employing 200-600 MHz antenna (Figure 6.38) clearly show a channel-shape boundary twenty meters wide and one and half meter deep. This horizon is probably related to an old weakness point of the embankment that was perhaps filled with heterogeneous carryover material and thus compacted. Below one and half m depth, the high attenuation is probably due to also to high moisture conditions that do not allow recognizing any target and the signal-to-noise ratio results to low to give any information.
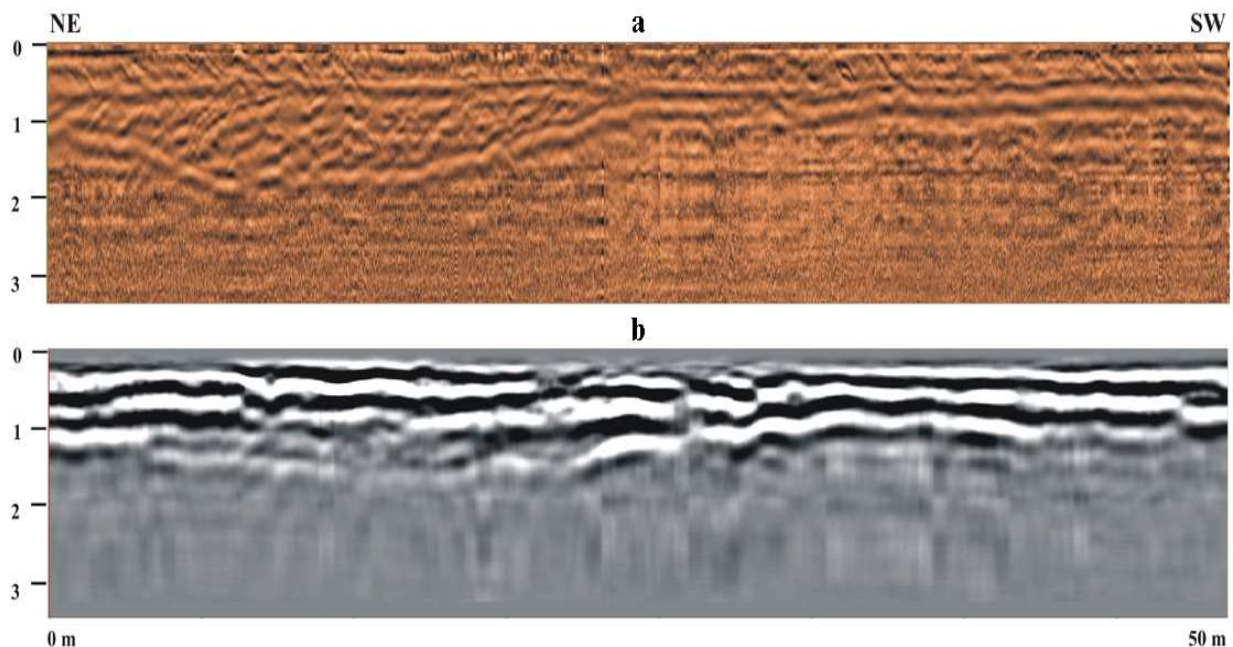
Figure 6.38 – GPR measurements along the Napoleonic Channel (Figure 6.19, SCAN A for positioning) and comparison of the results obtained with a) GPR IDS MF (200-600) MHz antenna and b) Zond 12-e with the use of 300 MHz antenna.

With regard to the necessity to verify the accuracy of the data obtained by the various GPR campaigns, as well as to assess the effective capability of the employed acquisition systems and antenna sets, during July 2007 a test was provided. A profile, employing Radsys GPR over the external flank of Napoleonic Channel embankment, was carried out over the segment where the lithologic horizon previously described was identified. The antenna employed was a 300 MHz nominal frequency. The software Prism2 released by Radsys company was utilised for the data elaboration; a comparison of the results has permitted to verify the differences between the two system employed and the scarceness of the data quality

150

that the elaboration with Prism2 software has given. Figure 6.38a, obtained from the 200 MHz antenna channel, clearly identify the horizon lower boundary, enables a rough identification of the heterogeneous condition of the filling material, localize the upper margin, and evidences the levelling and compaction works provided. Figure 6.38b shows the scarce definition of the horizon clearly detected by 200 MHz antenna, even if in theory the 300 MHz antenna must have higher spatial resolution. The differences can be attributable, besides the quality of the elaboration software, also to fact that the frequency spectrum for the 300 MHz antenna has showed for all the profile carried out two peaks at around 30 - 50 MHz and 140 MHz; such frequency lowering compromise the spatial resolution but improve the depth penetration.

In the complex, considering always essential a calibration with direct in-situ measurements, it is possible to assert that GPR was a useful tool for some issues concerning the inspection of the embankment internal structure. It has achieved some good results for the detection of areas with a strong difference in compaction, such as refurbished levels and recently repaired areas: it is important to mention again that GPR cannot quantify the compaction state. Some advantages and drawbacks were encountered for the description of shallow stratigraphic boundaries between soils with a noticeable difference in lithology or moisture content, like medium sand and silt, but when small electrical properties changes occur, it present many detection difficulties. The employment of GPR results valuable for the recognition of shallow isolated objects like blocks, metal objects and pipelines. Therefore the GPR can be considered a valid technique when a detailed study of river embankment is needed or to detect local shallow anomalies. Unfortunately, with the chosen antenna frequency of 100 and 200 MHz, the survey results were always significantly influenced by the low investigation depth, due to the high silt fraction of the embankment materials. This aspect is a strong limitation of the method: a maximum investigation depth of four to six meters over an embankment height ranging from five to twelve meters is fairly restraining. Spatial resolution is similar to the size of the expected targets: actually, objects of known nature and shape were clearly detected. Nevertheless, to achieve a good detection of many, but not all types of defects leading to failure of the embankment, a site-specific calibration and the employment of complementary geophysical methods are necessary.

7.   CASES OF MULTI-DISCIPLINARY APPROACH

7.1 The Samoggia Stream piping phenomena

7.1.1 Introduction

The Samoggia River is the longest left bank tributary to the Reno River. The total area of the basin, closed at the river cross-section of Calcara, is 178 km^2. The drainage basin is constituted mainly by mountain areas; the maximum altitude is 850 m above sea level (m.a.s.l.), while the main stream length is 60 km. Soils and rocks of sedimentary origin, which are mainly covered by broad-leaved woods, mainly compose the mountain areas. The bottom valleys are mainly floodplains for the most part covered by farmlands and urbanised. Because of their low permeability and their extension with respect to the total drainage basin surface, mountain areas give a remarkable contribution to the formation of flood flows, which are principally generated by infiltration excess runoff (Brath et al, 2006). During last centuries, many floods occurred in the low basin, the absence of levees or any protection bank was permitting annual flooding events, with no dangerous effects in the social context. As the anthropization increased, protection works were carried out and flooding or breaking events were recorded. Here is present a brief review, by Poluzzi (1995), of the last century events, (Figure 7.1):

- 1937 - 30th of August, Large breakage event in the left bank in Lorenzatico.
- 1937 - 2nd of September. Breaking event on the Samoggia right side, in Bagno, close to Sala Bolognese.
- 1956 – Night from 30th of April to 1st of May, Samoggia stream breakage, close to Le Budrie village, in left hydrological side. In order to prevent the flooding in San Giovanni in Persiceto town, several cuts were provided in the railway tracks Bologna Verona, which banks were an obstacle for the water drainage. Other events in the surrounding streams occurred.
- 1966 – 4th of November, breakage closet to Forcelli, huge flooding of 5.000 Ha; it was the largegest breakage in that century.
- 1966 - 4/5th of December, over flooding event, with no piping or breakage event.
- 1966 - 4/5th of December, liquefaction breakage for the right bank in Bagno, near to Sala Bolognese, and second event that produced two large rips in Samoggia stream levees.

- 1996 – 9th of October, breakage triggered by three large piping phenomena occurrence on the left bank, closet to Forcelli and Sala Bolognese, with large flooding in the surroundings.

From figure 7.1 appear dramatically how this area is often affected by flooding phenomena and how resolve these issues will be of primary importance for the Emilia-Romagna regional administration. Such an embankment failure risk suddenly came out again in the spring of 2008, nearby the two last dramatic flooding events of last century. Is useful here remember that "*piping*" is a subsurface form of erosion, which involves the removal of subsurface soils in pipe-like erosional channels to a free or escape exit. Although it develops in different types of soils and under a wide range of physic-chemical conditions, piping materials are commonly highly erodible (Masannat, 1980).
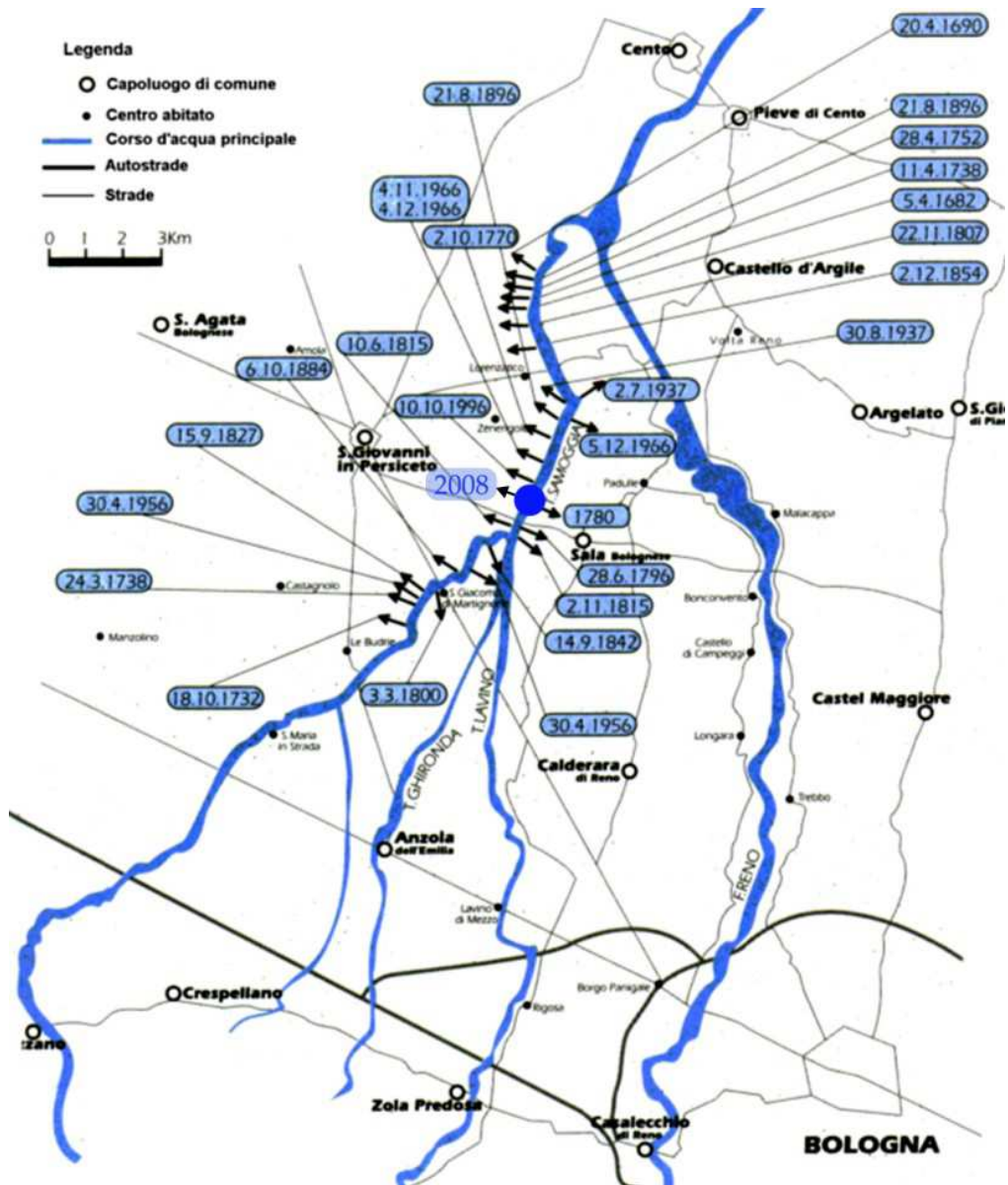
Figure 7.1 – Geographic sketch of Samoggia low basin with breaking, piping and overflooding events occurred in the last centuries (Luciani, 2002).

7.1.2 The piping phenomena of 20th may 2008

Following several arid seasons, the last spring Italy was besieged by a constant low-pressure atmospheric front, which have produced many rainfall episodes, triggering various issues, principally related to embankment safety for the Northern part of Italy. Around the half of May, after heavy precipitation events, a seepage and consequently piping phenomena have occurred in the left flank of Samoggia River banks, close to the Sala Bolognese village (many times in the past involved in similar issues), compromising the safety of a large anthropized area. The piping phenomenon was characterized by a kind of *sand boiling* triggering. Generally, a *sand boil* occurs when the upward pressure of water flowing through soil pores under the levee (under seepage) exceeds the downward pressure from the weight of the soil above it. The underseepage resurfaces on the landside, in the form of a cone of sand. Boils signal a condition of incipient instability, which may lead to erosion of the levee toe or foundation or result in sinking of the levee into the liquefied foundation below (Ozkan, 2003).

In the Samoggia Stream case, the seepage phenomenon has occurred not under but inside the levee and no real sand boiling effect was evidenced, but there was a strong outcropping of coarse sandy and sandy material. The figure 7.2a shows the area of piping phenomena occurrence and is clearly visible how much this segment of Samoggia Stream was affected in the past by embankment failure. The location of sand outcropping points, although approximate, shows that the breaking events of 1996 were hundred meters toward valley distant; hence, defects of embankment reparation after the 1996 breakage have to be excluded. The number of seepages was significant, nevertheless mostly of them were stopped up before any piping occurrence, thanks to the well-timed operation of waterproof blanket installation in the internal side of the banks. Therefore four apposite "*coronelle*" were built to constrain the water flooding just where the piping phenomena were much stronger. A "*coronella*" is a mitigation work, which consists in a ring of sandbags surrounding and containing the soil boiling or water outcropping, in order to contrast the pressure of the fluid that comes out for piping. Around the "*coronelle*" number one and two areas, during the embankment rebuilding works, a large tunnel (Figure 7.2b), formed by the piping phenomenon, and it was discovered inside the embankment itself. This demonstrates how serious the event was; the timely renovation works were provided a rapid safety mitigation risk, nevertheless they have impeded a correct calibration and detection of such hole with geophysical measurements for the purposes of this research.

Figure 7.2 – a) Sala Bolognese area, from a picture of 1996, where are shown the three last phenomena that occurred in Samoggia Steam left embankment. b) Hole excavated by the 2008 piping phenomenon.

If we regard the hydrometric measurements in a station near to the piping occurrence site (figure 7.3), it is visible how the hydrometric level has suddenly raised during the night between the 19th and 20th of May and the early morning of the 20th, triggering the piping phenomena. The first waterproof protections were put around 11 a.m. to build the *"coronelle"*. During the afternoon the water has reached the highest level (30,25 m.a.s.l), and the overtopping phenomenon was prevented for just 1.60 m. Must be taken in account that the STBR (Regione Emilia-Romagna Technical Service for the Reno River Basin) in 2004 managed some works for the rise of Samoggia levees; such refurbishment has proved providential. Moreover, the water level reached in 2008 event was just around 30 cm less than the level reached for the 1996 breakage.
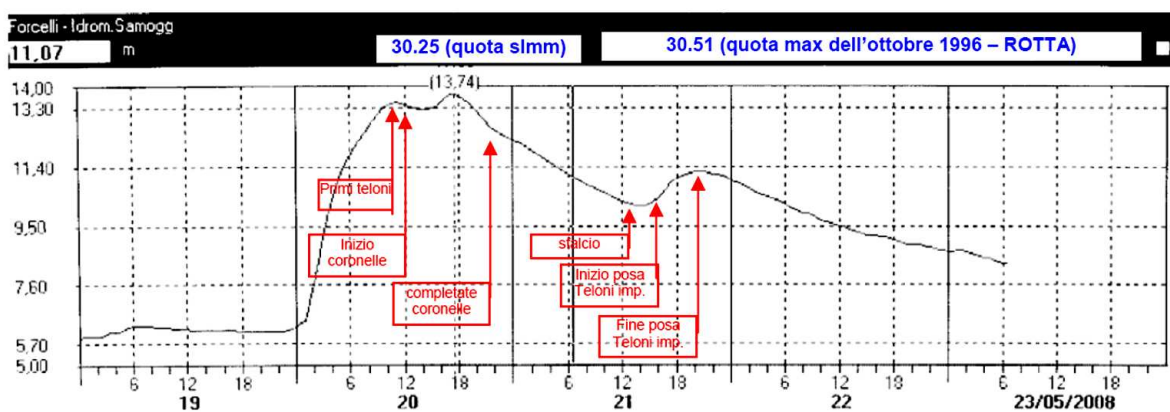
Figure 7.3 – Hydrometric levels reached by Samoggia Stream and provided works for safety mitigation.

Some interesting occurrences were the rapid emptying of one *"coronella"* (the n. 1, figure 7.2a), which was built to constrain the water flooding and the abruptly increasing water flux coming out from the lower level *"coronella"* (the n. 2 in figure 7.2a). Such phenomenon

156

indicates that the two ways that the water has excavated inside the embankment were suddenly linked by a structural collapse or material liquefaction.

7.1.3 The lithostratigraphic model

In addition to the Reno River and Savena Abbandonato stream geotechnical campaigns, also for the Samoggia stream many destructive tests were carried out in the last years, to acquire as much knowledge as possible of the materials that constitute the embankments. These punctual data, that will be treated next paragraph, demonstrate the high inhomogeneity and three-dimensional anisotropy of both embankments and their fundament ground. For the embankments, the anisotropy is strictly linked with the human activities history, which consist of repeated restoring, rising, restoring works, while for the foundation ground the geomorphologic evolution was of fundamental importance. According to several boreholes and cone penetration test carried out near the piping area, a simplified but effective embankments structure model was provided (Luciani, 2002): three main litotechnic units were recognised:

- **A Unit** (*"Anthropogenic"*). This unit is constituted by Samoggia embankment materials, artificial, with main presence of silty-sand, insufficient to provide a safe waterproofing of the structure: these materials were roughly taken near the riverbed, in order to build the structure as faster as possible. The materials compaction status results variable, with a peak value associated to the point resistance and rather difficult estimation of physic-mechanical characteristics. (c_U = 72 - 304 KPa, c' = 0 - 27 KPa and φ' = 20° - 29°). Permeability tests evidence values from 10^{-6} e 10^{-8} m/sec (with rare values around 10^{-5} m/sec).

- **S Unit** (*"Superficial"*). This unit represents the natural embankment (0–3 m from the ground level.) composed by mainly brown coloured clay and silt, with some sand lenses, deposited by all the previous Samoggia Stream flooding, affecting the bank structure with an extreme anisotropy. Hence, an extremely high permeability could be found randomly in some parts of the embankments. The lenticular geometrical shape of these deposits and their longitudinal extension can create (as we will see for the piping phenomena of May 2008) dangerous situations of transversal permeability peaks occurrences. In situ permeability values are comprised between 10^{-6} and 10^{-8} m/sec, while laboratory tests give rather different wrongly results, probably associated to the "scale effect". Compressive (Triaxial cell) tests provide values of c_U = 136 KPa (UU test), of c' and φ' respectively 5

KPa and 25° (CU tests); c'= 7 KPa φ' = 20° are the values obtained by Direct Shear Testing.

- **I Unit** (*"Impermeable"*). This unit underlies the superficial unit at three-four m. depth from the surface, and is mainly composed by dark-grey clays and it can be dissevered into two different subunits (I_1, I_2), because of the different values provided by Cone Penetration Testing. The superficial unit (I_1), which has 1-2 meters of thickness, shows a weak point resistance, slightly less, comparing to the underlying layers, due to the consistent amount of organic materials. Direct Shear Testing were provided only for two samples, obtaining similar results (c_U = 182 - 209 KPa, c' = 3 - 5 KPa and φ' = 20° - 25°), contrasting with both CPT profiles and pocket penetrometer, which indicate a larger compaction of I_2 Unit. By Hydraulic point of view, however, both Units I_1 and I_2 have the same very low permeability, edometric tests reveal values for the permeability coefficient comprise between 10^{-11} and 10^{-12} m/sec. Breakage effects never affected these layers.

Taking in accounts all the information provided by the borehole and cone penetrating tests, a stratigraphic section of the left side of the Samoggia stream embankment (visible in the map of figure 7.9) is shown in figure 7.4, with the hypothetic water table, deduced from the borehole tests information, which is referred to data acquired at the end of January.
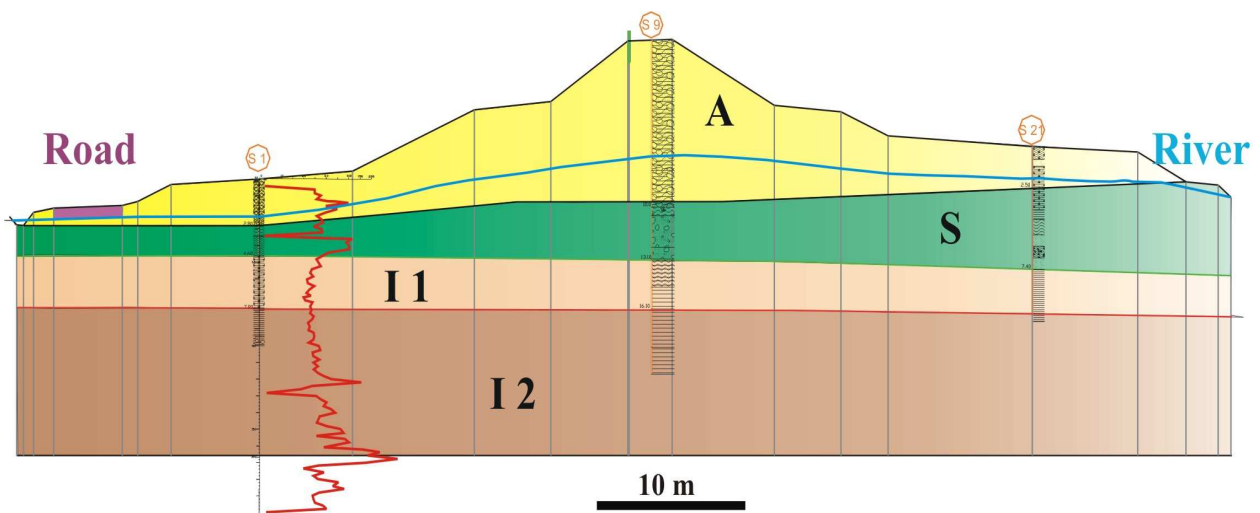
Figure 7.4 – Cross section of the Samoggia left riverbank, comparison between stratigraphy and CPT values, with litho-technical Unit identification (detail of borehole on figure 7.9).

After the 20th of May 2008 event, the Regione Emilia-Romagna has committed works of reparation and reconstruction of the Samoggia Stream embankment segment that suffered piping phenomena. The initial plan was to provide geophysical measurements on the river levee before the reconstruction, in order to compare and calibrate the results given by

158

geophysical methodologies with the actual conditions of the embankment internal structure. Unfortunately, the immediate necessity of mitigation works, carried out under the supervision of STBR, has prevented such application and the tests had to be provided after the reconstruction and the reparation of sand boiling occurrences; however, many considerations can be made. The geophysical methodologies involved in the campaign were the EM induction (FDEM), electric tomography resistivity (ERT) and GPR, which will be following treated.

7.1.4 Ground Penetrating Radar

The GPR campaign was conducted with IDS Georadar, which was kindly lent by Prof. Santarato and Prof. Peretto of Ferrara University, using a 400 MHz antenna, mounted on a special survey cart with encoder wheel. The elaboration was carried out using the software also released by IDS, GRESWIN2. GPR profiles were carried out along the river embankment, both at the top and external first step, as well as along one road, which represents the levee base (figure 7.5); no transversal sections were produced, due to the scarce GPR manoeuvrability over the steeply and roughly embankments flanks surfaces. The GPR capability of detection profile, carried out at the top of the riverbank was significantly reduced because the high antenna frequency was not able to reach an adequate depth and the survey was considerably affected by strong EM wave attenuation phenomenon, due to the large amount of clay contents in the first half meter of depth. Moreover, several traces on the surface, left by the caterpillars used to repair the structures, have created rough conditions that have affected the coupling antenna-ground and by consequence, the relative radargrams quality. Another profile was carried out along the first step of the embankment, between the road level and the levee top; this time as well, the presence during the previous days of the levee-reconstructing site has substantially deteriorated the surface conditions and GPR has suffered this problem, yielding scarce results concerning depth penetration and data quality. All of these issues confirm how this methodology (employing ground-coupled antennas) for riverbanks can be negatively influenced by not homogeneous surface conditions, which are unfortunately common for the entire area of Reno River basin, excluding some areas where local administrations have provided special systematic maintenance and cleaning plans of the river embankments itself.
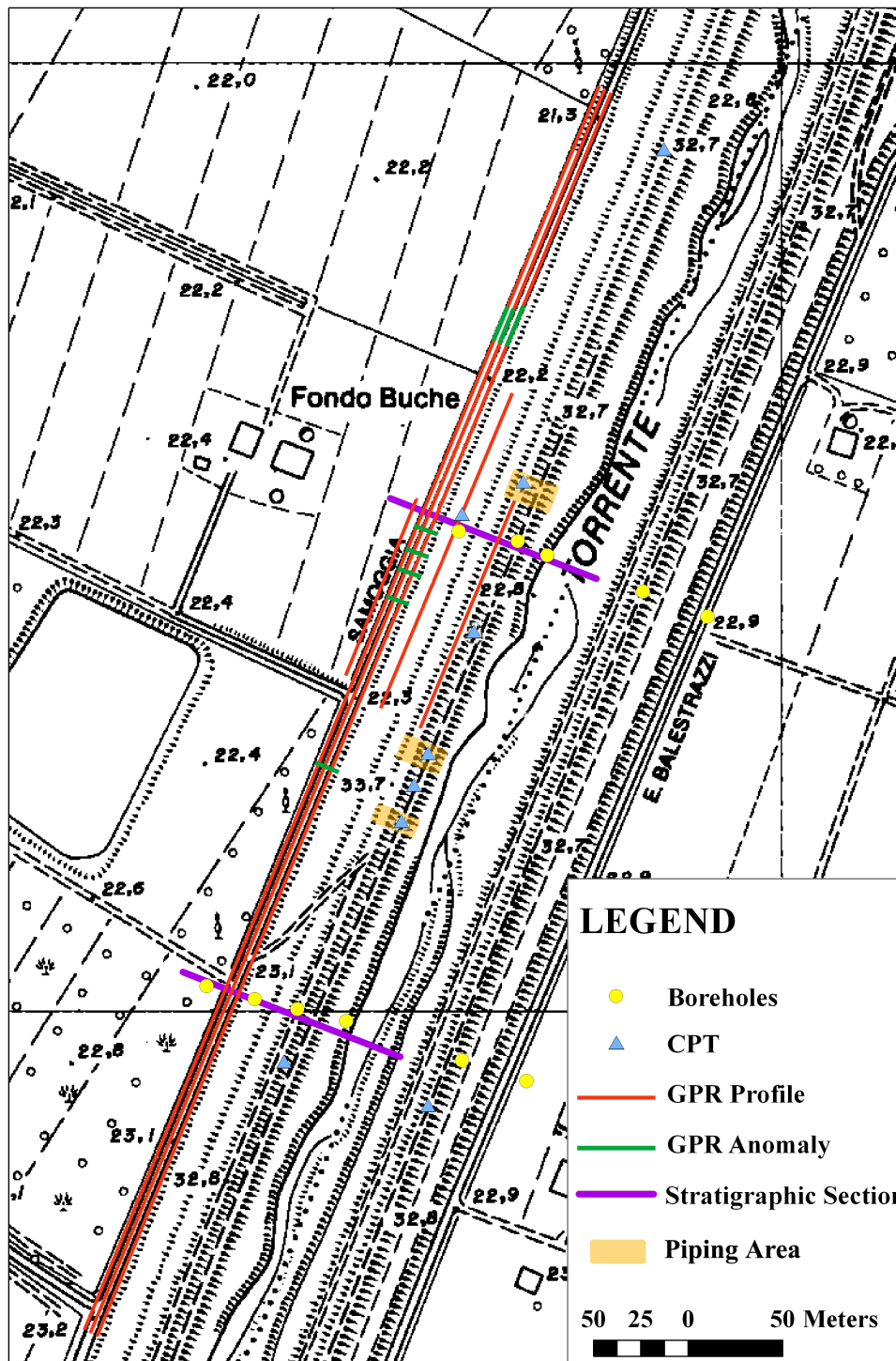
Figure 7.5 - Planimetry of the study area, with GPR surveys carried out in the July 2008 campaign; the orange coloured rectangles represent the piping occurrence zones.

Finally, important results were produced using the GPR over the road, which constitutes the embankment base. Primary, the signal processing was carried out using the familiar application of vertical filters; the radargrams after the application of high-pass filter present a high noise effect if the frequency spectrum is cut at 100 MHz as well as 200 MHz. A second filtering with same parameters enables the noise elimination (especially applying

200 MHz filter). The nominal frequency of the antenna (400 MHz) differs slightly with the central frequency, which results around 263 MHz. According to the frequency spectrum (figure 7.6), a 750 MHz low-pass filter was chosen. The filters choice, based on the necessity to reach as much deep as possible, avoiding the noise effect, strictly linked with the low frequencies, has brought the double vertical filter application, before and after the gain (signal power amplification).
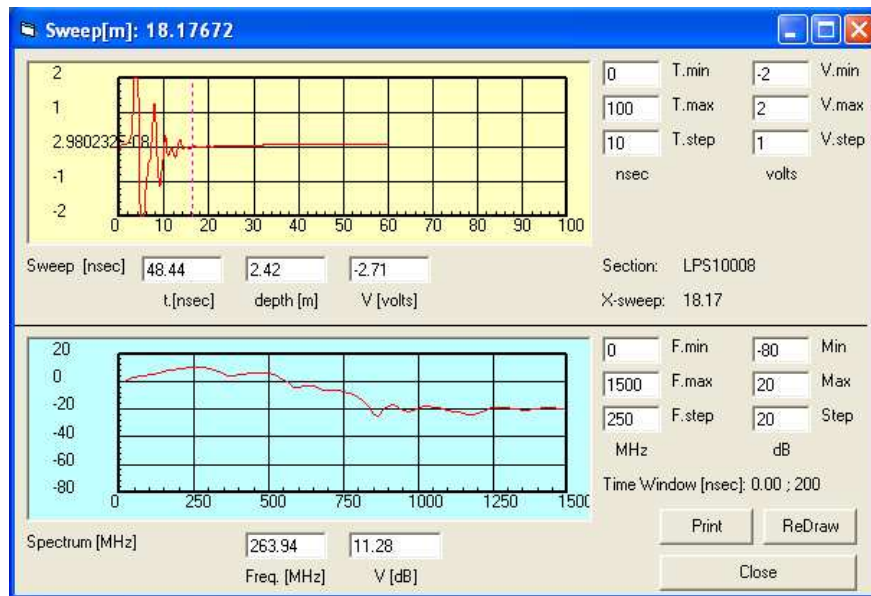
Figure 7.6 – GPR wave and frequency spectrum for a single trace, which have leaded the vertical high-pass filter choice.

Three parallel profiles of approximately 700 m length were carried out, both at the sides and in the centre of the road, along the longitudinal axis of the riverbank, with an interval of around two and half meters. Several markers were put in order to guarantee a good radargrams calibration, producing a semi-three-dimensional section of the road track itself. Suddenly is clearly visible how the EM wave penetration increases comparing to the previous profiles, due to the road surface (mainly composed by rounded gravel clasts) conditions, and some results are evident. First of all an anomalous zone, detected in all the profiles and characterized by many reflections, of 20 – 25 m length, is recognisable in the northern part of the profiles. The heterogeneous area seems to be characterized by a large clast dimensions increment and the EM wave penetrates in the ground until the depth of two to two and half meters. This anomalous zone, acknowledged by means of a bibliographic research in the STBR archives, is the reconstructed part of the road, filled with drainage material, which was built after the breakage event of 1996: the figure 7.7 proposes the comparison between such areas with the reconstruction work images.

Besides its capability to locate changes in dielectric properties and therefore lithologic passages at shallow depth, the GPR results the most precise and efficient tool for punctual anomalies detection. Indeed, the most important result of GPR campaign has achieved over the road, along the riverbank base, by the detection of five conduits in concrete, transversal to the road longitudinal axis; they represent a drainage work, which was unknown to the Regional Administration and the Reno Basin authorities. The GPR scans was triggered by an odometer wheel with the resolution of one vertical scan per horizontal centimetre and a sampling rate of at least 512 samples per scan, the time window was set in order to obtain a good compromise between penetration depth and resolution.
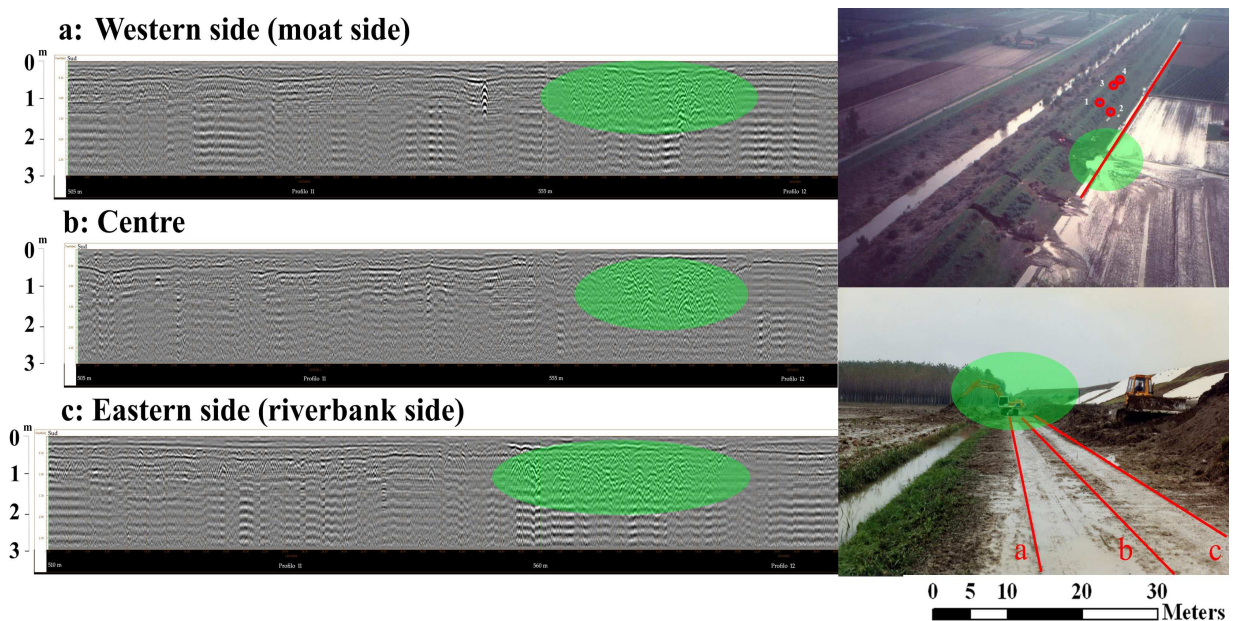
Figure 7.7 – GPR profiles carried out over the road at the riverbank base, anomalous area and comparison with 1996 reconstruction works pictures.

The data acquisition has achieved the localization and orientation of eventually conduits or pipes; hence, the horizontal electric polarization is parallel to the long axis of the road and traverses perpendicular across the pipe, maximizing the coupling respect to polarization. Four conduits were posed with an interval of 15 - 20 meters, while the fifth is quite far from the others; however, all of them result coincident with the seepage-affected area. Moreover, two of these conduits are situated in coincidence with an area, situated in proximity of the scarp relative to the first step of the embankment, which was previously excavated and shows occurrence of large boulders, probably constituting a kind of drainage structure. The author, in order to verify the conduits occurrence and their characteristics, was provided a manual test: a small borehole was burrowed close to the moat that bound the road and the depths of such conduits, as well as physical characteristics of both material and

162

conduit itself, were estimate. The conduits are situated at around 0, 95 m depth from the road surface: by means of this test, according to Equation 3.3, the average values of $K = 7\text{-}8$ and therefore velocity (valid just for the material above the conduits) $v = 11$ cm/ns were obtained. This value is in accordance with the previsions, because of the road conditions, which have brought the author to estimate a dielectric constant $K = 7$. Furthermore, also the computation that were carried out using the asymptotes slopes of the hyperbola pretty gives the same result. According to the GPR profiles, the estimate diameter of such conduit is around 25 – 30 cm; they drain the water into the moat that bound the road. The Figure 7.8 presents a particular of the three profiles carried out, some hyperbolas are detected, and they can represent punctual heterogeneities inside the road layer or just below it. The green highlighted areas represent the detected hyperbolas, which can be related to the concrete conduits; these hyperbolas are visible in all the three radargrams carried out and such occurrence shows a continuity of these anomalies in the direction transversal to the road longitudinal axis.
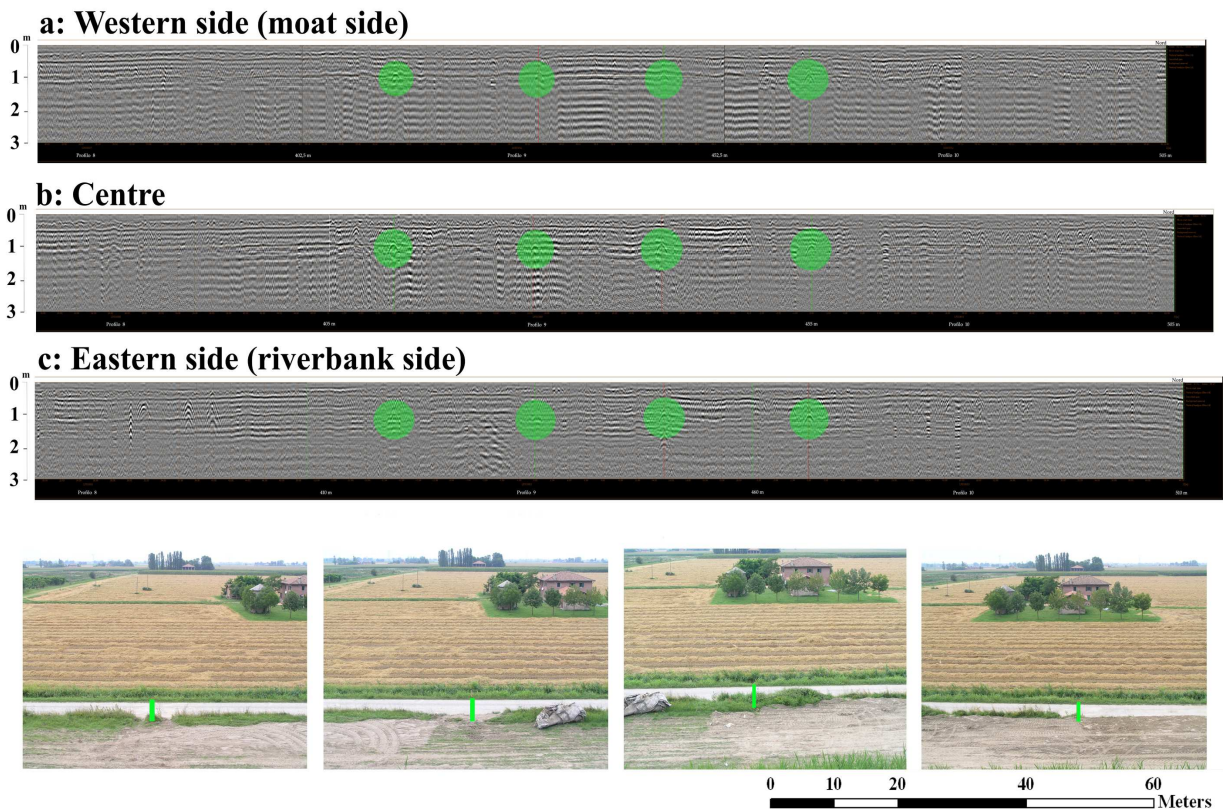
Figure 7.8 – GPR profiles carried out over the road at the riverbank base, green areas represent the detected drainage conduits, with their relative localisation on the pictures.

Figure 7.8 shows also the location on pictures of the four conduits, which is relative to the four anomalies in green, visible in the map of figure 7.5. When many anomalies have

occurred in just one profile, and were not visible in the other radargrams, therefore they were recognised as just punctual heterogeneities (e.g. clasts in brick or gravel).

7.1.5 Electrical Resistivity Tomography

As previously stated, this method is based on rocks specific resistance measurements, using large amount of the electrodes, which are located along the profile or round the surface. The electrodes are connected by special cable, which enables consecutive connections of the electrodes in current or potential function. This creates many four-electrode arrangements to be measured with different geometry and different reached depth. The measurement is executed automatically, therefore all the operations are computer controlled. According to IMPACT project (Morris, 2005) electric resistivity methodology is the most recommended way to describe dike structure and homogeneity, seepage phenomenon and to recognise lithologic contacts until a reasonable depth.

	N° Electrodes	Length (m)	Orientation
Profile 1L	112	222	SSW – NNE
Profile 2T$_1$	38	74	W – E
Profile 3T$_2$	39	76	W – E
	189	**372**	

Table 7.1 – Detailed Scheme of the electric tomography profiles, which were carried out over the embankment.

For this application, the acquisition part was carried out using the ABEM mod. SAS4000 (maximum power100 W) georesistivimeter, characterized by a sensitivity value of around 1 micro-volt, using a switch – box ABEM mod. ES464 and three set of multi-polar cables of 16 electrodes (hence 48 electrodes total). The measurements were performed using a dipole-dipole array (Figure 5.5) with two meters electrode separation. Three profiles were carried out (table 7.1): one parallel to the levee longitudinal axis, which cover all the piping occurrence area and the two others transversal to the embankment carried out over strategic zones. The longitudinal profile was provided with the roll-along technique, which schedule the detachment of one cable section and is connection on the other end, continuing in the measuring process. The two transversal profiles of approximately 75 meters were carried out in order to give more details of the embankment-spreading; one is placed just over the piping zone that were affected by the sort of sand boils effect, another in the zone involved in

filtration issues and where concrete conduits were detected. The dipole-dipole electrodes configuration was chosen, because of its high sensitivity to detect vertical variations; even if such configuration has not the strongest signal to noise ratio, the overall depth reached during the measurement, which depends on the maximum distance of the electrodes, can be estimate around 15 meters and is comprehensive of the embankment base.
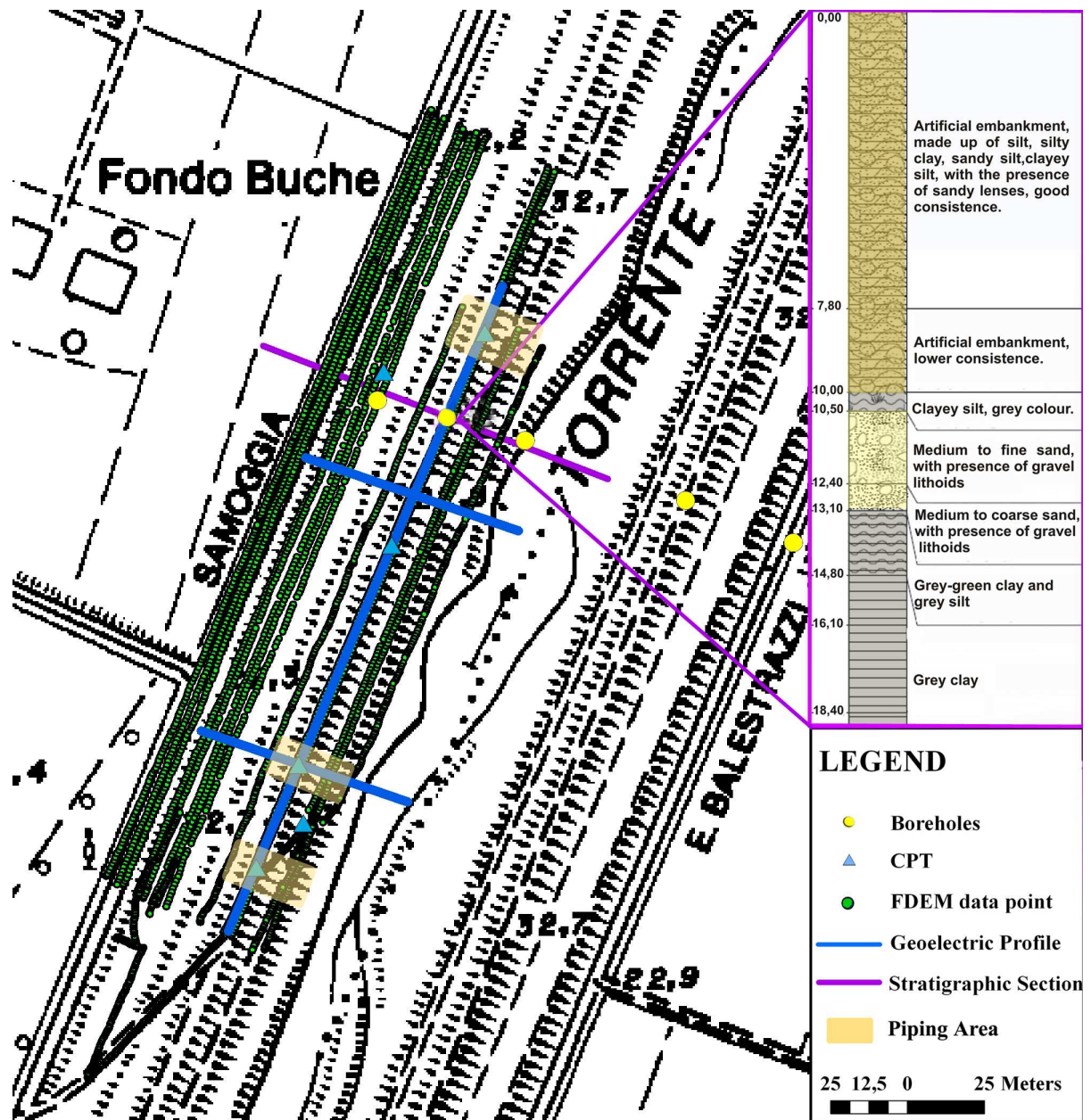
Figure 7.9 – Scheme of the EM induction and electric tomography profiles, which were carried out over the embankment, with borehole test carried out on the top of the embankment.

The cone penetration tests as well as borehole results enable the calibration of the resistivity data collected, producing an association of some resistivity intervals with different lithologies, which characterize the embankment structure (table 7.2).

TYPE	RESISTIVITY	TYPE	RESISTIVITY
Clay	< 15 Ωm	Sandy Silt, Silty Sand	> 25 – < 45 Ωm
Silty Clay	> 15 – 30 Ωm	Sand	> 50 Ωm

Table 7.2 – Range of resistivity values, which can be associated with the lithologies that compose the embankment.

Moreover, four additional CPT (Cone Penetrating Tests) were carried out some days after the piping phenomena on the top of the embankment; they permit to associate and calibrate their resistance values with the electrical information and properties achieved with the geophysical measurements. The results showed in figure 7.10 demonstrate a good superimposition. Therefore, for the profile carried out on the top of the embankments, some resistivity distribution models can be described: primary, the subsoil appear to be subdivided in three electro-strata:

- First electro-stratum, generally conductive ($\rho <$ 40 Ωm – blue colour), which is placed for around one meter of thickness from the surface. Although it is not always present (is not well visible in the transversal sections), an association can be however done with the material that covers the embankment structure. Indeed, 2004 maintenance works provided a silty-clayey superficial cover for the embankment segment analysed, that can correspond to this superficial layer.

- Second electro-stratum, generally resistive ($\rho >$ 45 Ωm – green/red colour), which can be identified as horizon containing sand, silty sandy and sandy silt, with a relevant amount of sand lithology until the progressive 100 m. The electro-stratum thickness is approximately constant (around 4 m) and its base is estimable at 26 and 27 m (m.a.s.l.). This electro-stratum was involved in the 20th of May piping event, as a matter of facts the sand boiling effects, resulted by the excavation of the large hole (figure 7.2b) have occurred inside this resistive horizon.

- Third electro-stratum conductive ($\rho <$ 15 Ωm – lilac/blue/cyan colours), which is identifiable as clay horizon having a variable thickness from 5,5 m (until 100 meters of progressive) and around 2,5 m (form the progressive 100m until the end of the profile).

166
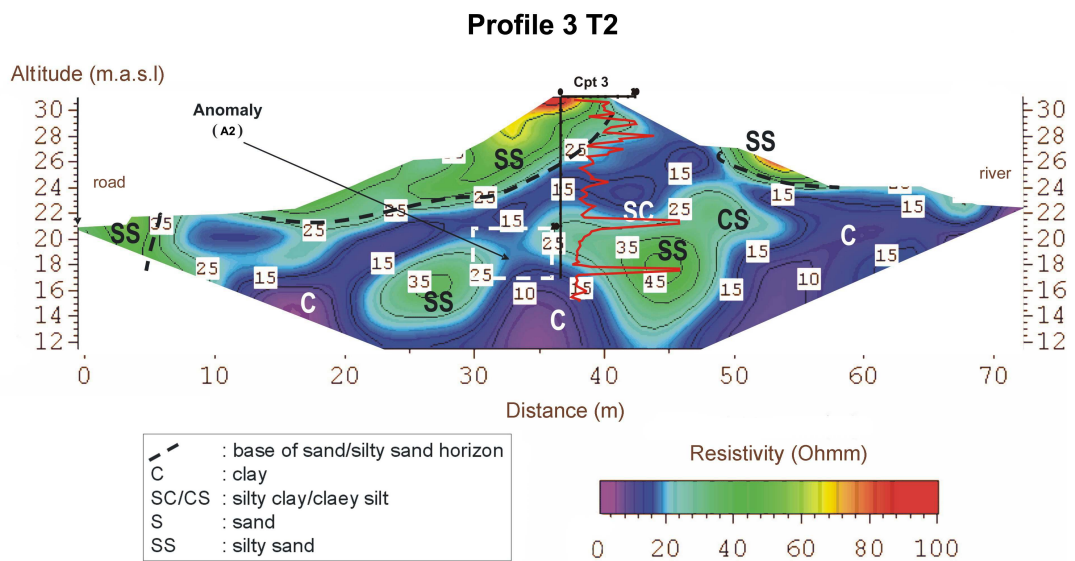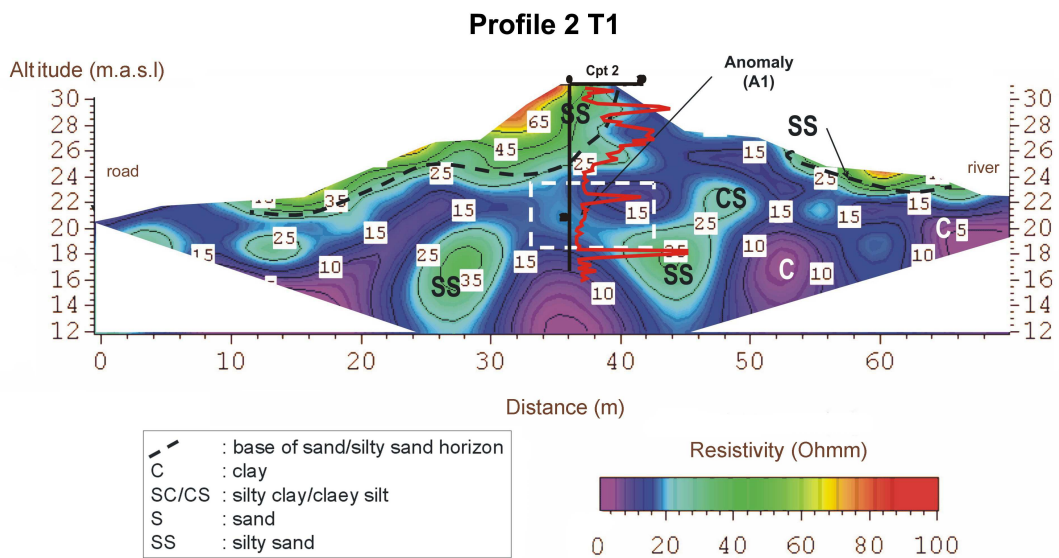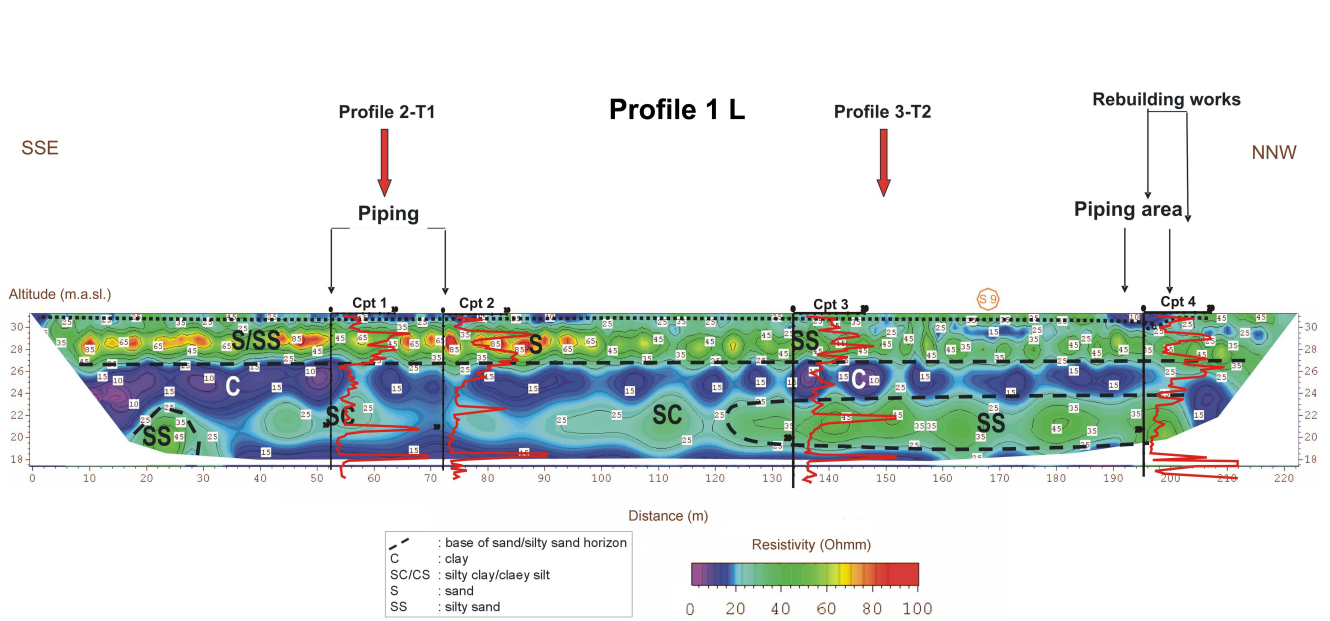
Figure 7.10 – Electric tomography pseudo-sections, with CPT (cone penetration tests) associated, for a calibration and a verification of the material proprieties.

167

The upper contact is roughly horizontal and (excluding some reliable fluctuations) is attestable between 26 and 27 m (m.a.s.l.). The lateral spreading and continuity of this horizon sometimes appears interrupted by the presence of zones with higher resistivity values ($\rho > 15$ Ωm), which are not associable with the clay soil matrix.

▪ Fourth electro-stratum averagely resistive ($25 < \rho < 45$ Ωm – cyan/green colour), which has strong characteristics of inhomogeneity, being composed by clayey silt, sandy silt and silty sand, with a larger amount of sand contains from the beginning to 30 m of progressive and form the progressive 120 m to the end. Between the 30 m and 120 m progressives, the average thickness (around 5 m) is slightly reduced and clay components are prevailing ($\rho < 25$ Ωm).

Concerning the transversal sections, (figure 7.10) although characterized by some slightly difference, they can be described by the following electro-strata:

▪ Superficial resistive body ($30 < \rho \lesssim 80$ Ωm – green/red colour), it interests the embankment portion for the first 3-4 meters in the Section 2, until the depth of 26 m.a.s.l. (Section 3), and is associated to the second electro-stratum recognised in the longitudinal section. For both profiles, this horizon characterizes the top of the embankment and it disappears at around 10 m of progressive. This body is also present in the first internal step of the embankment, with a thin thickness (from one to two meters) between the progressives 52 m and 68 m.

▪ Two resistive bodies ($25 < \rho \lesssim 35$-45 Ωm – green/blue colour) which are characterized in section by a lenticular shape and are localized approximately between the progressives 20 – 30 m (altitude comprise between 13 and 20 m.a.s.l.) and 35 – 50 m (altitude comprise between 13 and 24 m.a.s.l.). The resistivity values are associated with the presence of medium-fine size sediments as well as sandy silt, sometimes with larger amount of sandy fraction. The section 3 presents larger bodies, which seem to be connected because of the anomaly A2 around the progressives 33 m and 50 m, respectively at 24.5 and 19 m.a.s.l. Such anomaly may be a possible continuity zone (even with smaller values of resistivity) and the separate lenses could represent a unique body. Moreover, others areas of possible continuity are noticeable in both the transversal sections: section 2 indeed, although the bodies appear distinct and confined, shows an anomaly between the progressives 34 – 40 m (A1 anomaly), which could represent a slight continuity zone among the superficial resistivity body and the lower sandy and silty lenses.

▪ Conductive soil matrix ($\rho \lesssim 15$ Ωm – blue/violet colour) in both sections, which is characterized by typical values of fine material as clayey sediments.

7.1.6 Frequency Domain Electromagnetism

The innovative electromagnetic method (FDEM induction), was tested and verified in European Projects (Boukalová and Beneš, 2007); it carries out basic assessment of the dikes condition and their material composition in large areas with quick and not highly money-consuming measurement. During the geophysical measurements campaign a dipole electromagnetic profiling device (Profiler EMP – 400) was applied to test conductivity (as well as resistance) of the different materials inside the entire embankment structure and part of the surrounding area. EMP-400 device is a frequency domain system, recently released by GSSI, in which, acquiring multiple frequencies, the user can select the frequencies that provide the best results for a specific application. The Profiler was configured to measure simultaneously three frequencies, 1000 Hz, 5000 Hz and 10000 Hz. The nomogram usage (as previously explained in Chapter 4.1, and showed in Figure 4.2) enables the rough estimation of the skin depth. The *skin depth* is defined in classical EM theory as the distance in a homogeneous medium over which the amplitude of a plane wave is attenuated by a factor of $1/e$, or to about 37% of the original amplitude. The practical depth of investigation, defined as a maximum depth at which a given target in a given host can be detected by a given sensor, according to the experience of some authors (Smith et alii, 2004, Boukalová and Beneš, 2007) can be many times lower and it is significantly reduced by layering and homogeneity too. The depth of investigation for a given skin depth increases with target conductivity and conductivity contrast, and it decreases with the detection threshold. Therefore, after a comparison with electrical and stratigraphic properties of the ground, for the three frequencies, 1000 Hz, 5000 Hz and 10000 Hz, the depth of penetration can be estimate respectively as 12-14 m, 9-10 m, 5-6 m.

The system can be deployed in either the vertical or horizontal dipole mode, but this time the vertical configuration, which guarantees a deeper penetration (twice respect to the horizontal configuration) was selected. The output is the mutual coupling ratio (Q) in parts per million (p.p.m.) for both the in-phase and quadrature, and the apparent conductivity in mS/m. All survey acquisition parameters and EM data are stored on internal memory. Coupled with the EMP-Profiler, a GPS is provided and some special reference data was acquired. Several parallel profiles on the road and the embankment steps were carried out, excluding area with high vegetation coverage and the steeply embankment scarps, with a frequency of sampling of 1 Hz, hence one measure each second was registered, which permits the operator to maintain a normal walking velocity during the acquisition. A total amount of 3634 data points were collected, as it can visible in Figure 7.9. Each profile can be visualised as 1D resistivity

graphic. Figure 7.11 shows some important anomalies detected by the FDEM methodology, which has the velocity acquisition as a winning factor, even if its results are decidedly qualitative.
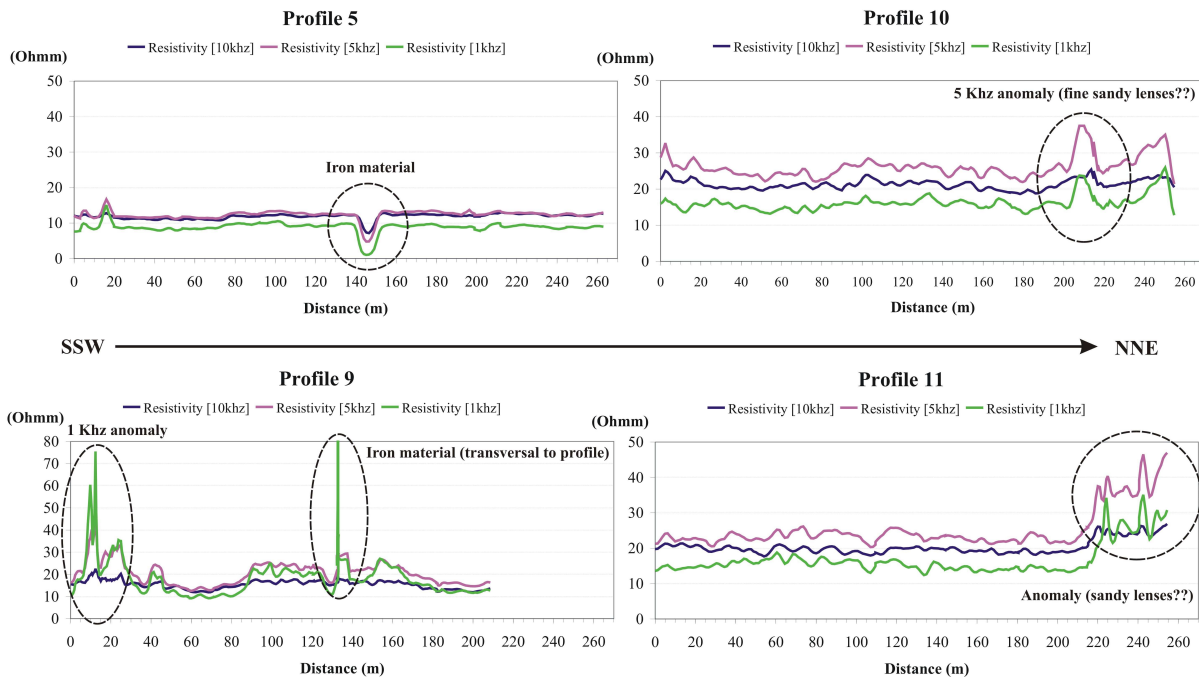
Figure 7.11 – EM profiles carried out over the entire embankment segment and major anomalies detected.

The Profile 5 of figure 7.11 is referred to the first step of the embankment, just over the road level. It shows homogeneous low resistivity properties with a strong anomaly related to iron material presence at very shallow depth, associable to the rest of iron structure employed to contain the piping, as well as maybe a kind of drainage system just above. A series of renovating were provided for the Samoggia Stream embankments in October 2008 with the positioning (from the surface at the top of the embankment itself) of 200 meters long by 15 meters deep benthonitic diaphragms, which provide a waterproofing of this segment of Samoggia Stream levees. An artificial basin (to mix the water and the benthonite) was excavated in this first bank for some meters, revealing very compacted clayey material, confirming the EM profile estimation. The Profile 9 in figure 7.11, carried out over the second step, just under the top of the embankment, has revealed again the presence of almost superficial iron material (especially detected by the lower frequency,) associated to high values over 600 Ohmm, which can be explainable with the polarization of the iron conductive material with respect to the inductive field. A strong resistivity (values around 70-80 Ohmm) anomaly was localised in the first 30 meters, probably associated with the 8 m depth sandy lenses, which can be visible in the transversal sections. Profile 10 and 11 of figure 7.11 are

referred to the top of the embankment; we can notice a general higher resistivity value with respect to the profile 5, especially for the frequency 5 KHz and some anomalies are present. It can be understandable if we look on the longitudinal and transversal sections, which show an evident presence of sand and silty sand at the depth of 2-4 meters and from 8 to 10 meters. Indeed, the 5 KHz and 1 KHz show a similar pattern, influenced by the presence of the fourth electro-stratum averagely resistive (noticeable are the resistive anomalies on the right part of the profiles), while the 10 KHz has lower values because is significantly influenced by the third conductive electro-stratum, just above. All the apparent resistivity values measured with the EMP-Profiler can be plotted to form a resistivity qualitative map (using Surfer8 program, interpolation settings) for each frequency employed. Indeed the results of the measurement are produced in the form of curves (graphs) of apparent resistivity along the tested profile for the individual measured frequencies (Figure 7.12).
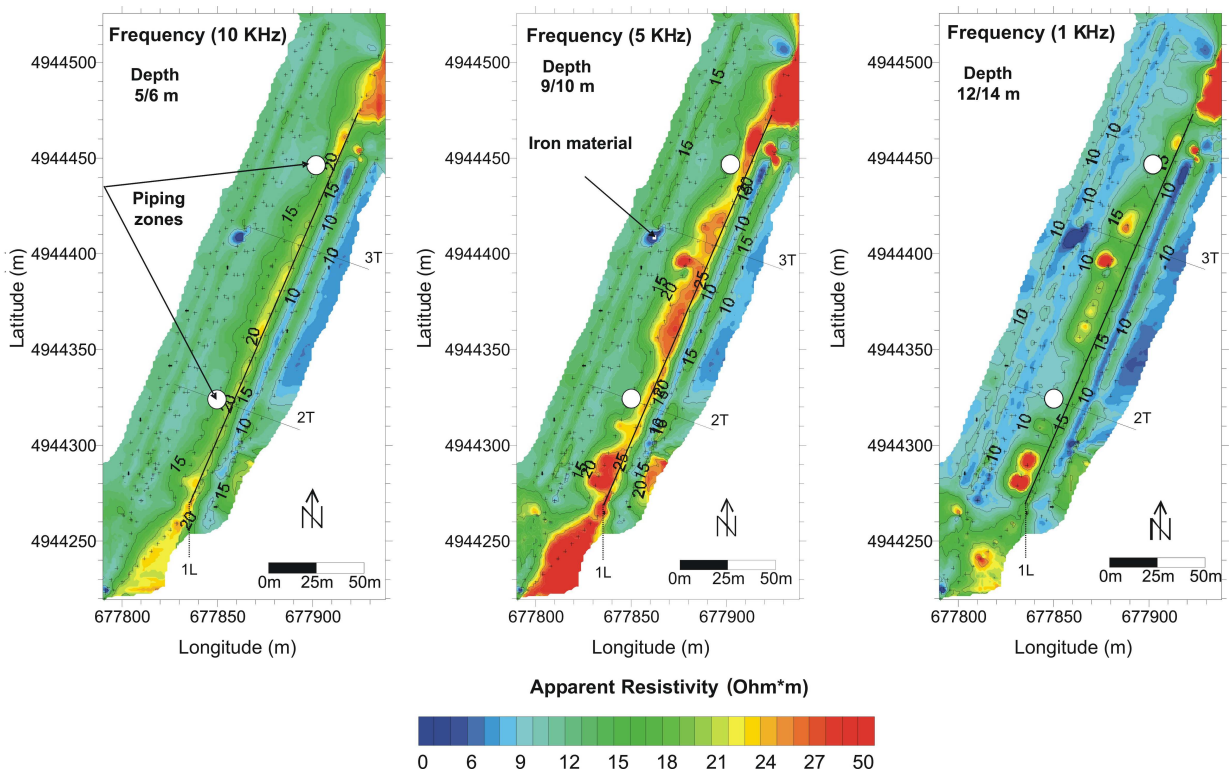
Figure 7.12 – EM maps of apparent resistivity distribution over the entire embankment segment.

The curves allow the qualitative analyse of embankment material homogeneity, locate zone with relatively higher resistivity and with the suspicion or larger grain size horizons. A calibration and a verification of the FDEM method with the electrical resistivity method was provided for the longitudinal profile carried out on the top of the embankment: the three frequencies data acquired with the GSSI EMP-400 were compared with the electrical pseudo-section. Some consideration can be done:

- The frequencies 5 KHz and 10 KHz are characterized by a similar electrical behaviour but an anomaly occurs. Indeed the 10 KHz profile results slightly more conductive (average value: 62 mS/m) with respect to he 5 KHz frequency profile, (average value: 38 mS/m). Generally this differences are not expectable if we consider that in normal lithologic conditions, as lowest the frequency as higher the conductivity, because at shallow depth the surface effect increase normally the resistivity response. 5 KHz data are deeper than the 10 KHz data but their resistivity values result higher. Is important now to remember that the FDEM device provides a measure of the apparent resistivity, ρ_a and it should be considered as some sort of average resistivity encountered in the heterogeneous underground. The relatively low frequency employable with the EMP-Profiler (at most 10000 KHz) does not enable to evaluate the first shallow meters. We can notice that the first 5-7 meters of the embankments are more conductive and therefore contain more fine material than the first 10, which confirm the fact that at 8-10 meters of depth from the embankment top a sandy and hence resistive horizon is located.

- The frequency 1 KHz, which can reach in these soil conditions roughly up to 12-14 meters depth, shows the presence of significantly conductive material that can be related with the low resistivity horizon comprises between 22 and 26 m.a.s.l. depth of the longitudinal electric tomography profile 1. Indeed, the lower, more conductive one attenuates the resistivity contribution of the upper resistive layers. The resistivity values and their relative oscillations are associable to presence of lateral lithologic variation inside the conductive layer, for example the occurrence of the fourth electro-stratum composed by silty and sandy materials, which produces some local conductivity minimum. It measures lower resistivity values with respect to the 5 KHz profile, which can be related with the conductive electro-stratum (mostly clayey as it can be visible in the borehole test) after the 10-12 meters depth, as well as with the presence of the water table.

The results of the previous campaigns, especially the European Project GEMSTONE (Boukalová and Beneš, 2007), carried out employing FDEM methodology, where the writer was involved, has revealed that this method has a very good repeatability in the time. On condition that the device will be calibrated and the stability of measured data will be certified, this method can be also used for quick repeated measurements. It allows prompt location of sections with abnormal changes of conductivity in the course of time (e.g. in time of high water level) which are often correlates with some leakage or in-homogeneities section.

7.1.7 Discussion of the results

Before to analyze the results of the geophysical campaign, some considerations must be done; concerning the moat that bound the road parallel to the embankment longitudinal axis, some public associations for the environmental safety have recently notified that sometimes during the wet as well as the dry seasons, the water inside the moat itself is characterized by a strong contains of iron particles, which confer it a red colour (figure 7.15). One stratigraphic section of the embankment, obtained through boreholes tests reveals the presence of possible drainage level that probably is developed transversal to the levee longitudinal axes, at around 10 m depth from the embankment top and around 3 meters depth from the first external step. This drainage could be constituted also by iron structures that are currently going rusty.

A series of renovating works were provided for the Samoggia Stream embankments in October 2008, regarding the positioning (from the surface at the top of the embankment itself) of benthonitic diaphragms (supposed 300 meter of length by 10 m of depth), which have to provide a waterproofing of this segment of Samoggia Stream levees. In this occasion, several hundreds of meters of Samoggia Stream both side embankments was properly cleaned by the vegetation as well as the moat that bound the road, which was also excavated, in order to operate a better drainage of the surrounding fields. This operation has finally evidenced the presence of the conduits previously detected by the GPR surveys (figure 7.8). Such underground conduits cross the road and link a kind of drainage system under the first step of the embankment made up of boulders and iron gabionade. The gabionade is located approximately under the scarp that separates the road and the first step level and drains the water directly to such conduits. During the renovating works, an artificial basin (to mix the water and the benthonite) was excavated in this first bank for two meters, revealing very compacted silty clayey material and no evidence of larger grain size material for the drainage, therefore it leads to locate the boulders and drainage occurrence just under the scarp close to the road. After such renovation works, the external fronts of the conduits (previously occluded by the vegetation and by the material deposed during last decades), were appearing inside the moat and prevalent dry conditions were noticeable, except the conduit in figure 7.13a, which was having a consistent flux of red water.

Some field tests were carried out to check the conductibility of the red water contained in the moat, the results present sweet water with no alteration of such physical parameter. The entire area, affected by the last fifty years seepage and breakage events (nowadays are still

visible several alluvial fans from aerial photos) is actually located over a Plio-Pleistocenic intense trusts zone, now reactivated (general view on Figure 2.2).

Figure 7.13 – a) October 2008, the moat that bound the road at the embankment base is receiving red coloured water drained by one of the detected conduits in concrete. b) July 2008, the GPR utilised (400 MHz antenna) and the trace of such conduit, detected and marked.

A constant water table control, using piezometers and conductivimeters could reveal some important aspect of the tectonic evolution of this part of the lower Po Plain basin; however, this argument is beyond the scope of this research. Nevertheless, the needing of a drainage system under the left embankment of Samoggia Stream can be preliminary explained checking the cartography of the Region Emilia-Romagna; a comparison between the historical topographic surveys was carried out for this research, and it brings to the location of some characteristic ponds around the study area. The ponds that characterize this part of the Po Plain are called "*maceri*": artificial basins of sweet water with dimensions of generally one tenth of hectare that were excavated in the past for the textile industry of hemp (*Cannabis sativa*). This kind of production was abandoned in the second half of the XX century and since that a large amount of "*maceri*" were filled by soil material in order to recover space for agriculture and new constructions. The "*macero*", which is visible in the left part of the Figure 7.14, was filled with soil material probably during the fifties or after the large flooding event of 1966, since then no historical data are available. Its position is interesting, because coincides with the area where the largegest piping phenomenon occurred. Moreover, with respect to the first map of 1933, is noticeable the presence of the wide "*coronella*" on the northern part of the 1979 map, highlighted by the green colour, which was carried out in 1966.

174

The geophysical multidisciplinary approach brings some others information. The electric tomography pseudo-sections show that the superficial layers have relatively high values in resistivity generally for the first two meters of depth at the top of embankment and in both the first internal and external step. Such anomalous areas can be explained following the historical events and renovation works. After the 1966 flooding the Samoggia River left embankment was moved of about 20 m toward west, in order to guarantee a wider space and storage capability of the pensile riverbed. The material was moved from the old position to the new one; therefore, the materials that constitute the first internal flank now represent the rest of old embankment. Hence, a large part of the old embankment itself was placed into the new position and it could show the same electric properties.
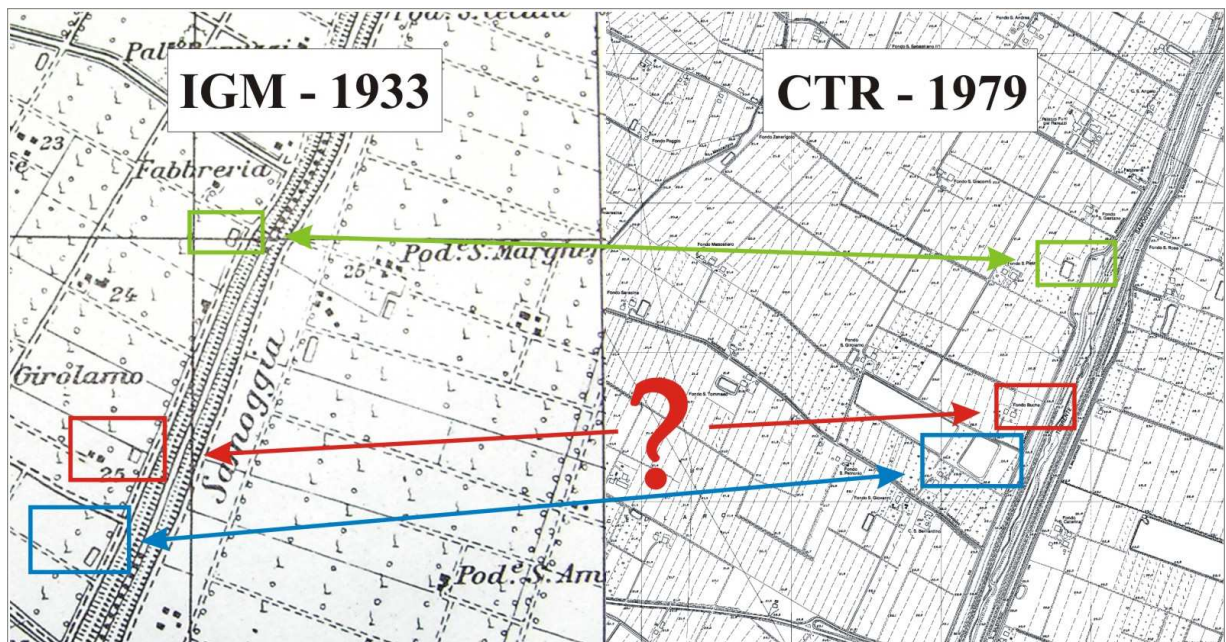
Figure 7.14 – Topographic surveys carried out in 1933 (left) and 1979 (right), blue and green lines evidence the analogies, while the red line evidences the anomaly between the two maps.

Analyzing the electric tomography pseudo-sections, two other important things are noticeable: for example, the predominantly sand horizon occurrence between one to four-five meters depth from the top of the embankment, which was affected by the piping phenomena. Such horizon can results dangerous, because there is an evident lack of waterproofing behaviour and the relatively high permeability, given by the large sand percentage inside the embankment probably triggered the piping phenomena of the 20th of May. The hole that was excavated by the larger piping phenomenon, visible in figure 7.2b, has taken place in this horizon; unfortunately, the geophysical measurements were carried out just after the rebuilding works and the electric characteristics of the excavated cavity were not verified.

Another issue evidenced by the electric tomography both in longitudinal and transversal sections is the presence of a fine sandy zone or lenses, placed just below the embankment structure, approximately at nine meters depth. The longitudinal pseudo-section evidences this consistent layer, which is around three meters thick, and its presence is really well definite just above the area affected by both piping phenomena and drainage structure (gabionade, conduits) occurrence.
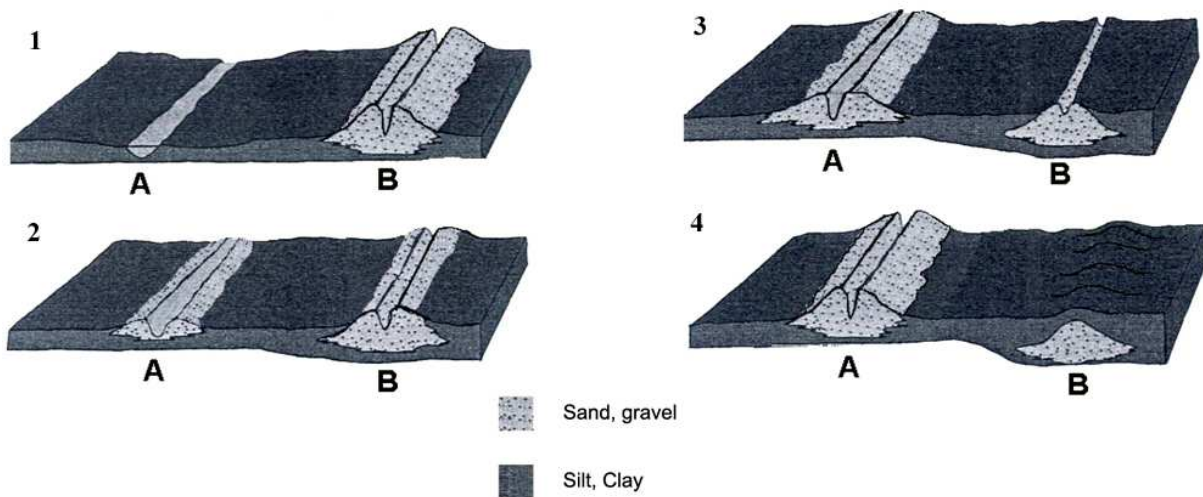
1. **The river leaves the old position B to migrate in A.**
2. **Formation of the prominence in A and lowering of B.**
3. **The alluvial fans of A begin to cover B.**
4. **B is finally covered inside the ground.**

Figure 7.15 - Formation and evolution of a typical "dosso" structure (Fuoco et al., 1999; modified).

The layer could represent an alluvial fan that is not visible from aerial photos or, with more probability, a paleochannel that constitutes a typical fluvial "*dosso*". Indeed, the dominating morphologic characteristic on this Po Plain part is the so-called "*dosso*": it is a fluvial prominence, which can be associated to a paleochannel and its top represents the position of the ancient stream. The figure 7.15 shows an example of a "*dosso*" evolution. Each paleochannel that was active for several centuries has created a prominence of the surface that nowadays is still visible in the Reno River basin. In most of the cases, such prominences result hidden by the alluvial events of the present rivers, subsidence and differential compaction, operated by the fine sediments (Luciani, 2002). A geomorphologic sketch of this segment of Samoggia stream has retrieved and it shows how a fluvial "*dosso*" interacts with the present course of Samoggia Stream (figure 7.16). Probably under the zone where the piping phenomena occurred, its position is moderately shallow (around eight-ten meters) and represent the permeable fourth electro-stratum. However, as well as many Po Plain rivers that have hanging riverbed, Samoggia stream, instead to capture the water that

percolates from the subsoil, operates the drainage of the surroundings area. Hence, this layer represents the way that the river adopts to drain the aquifer and is probably very well permeable.
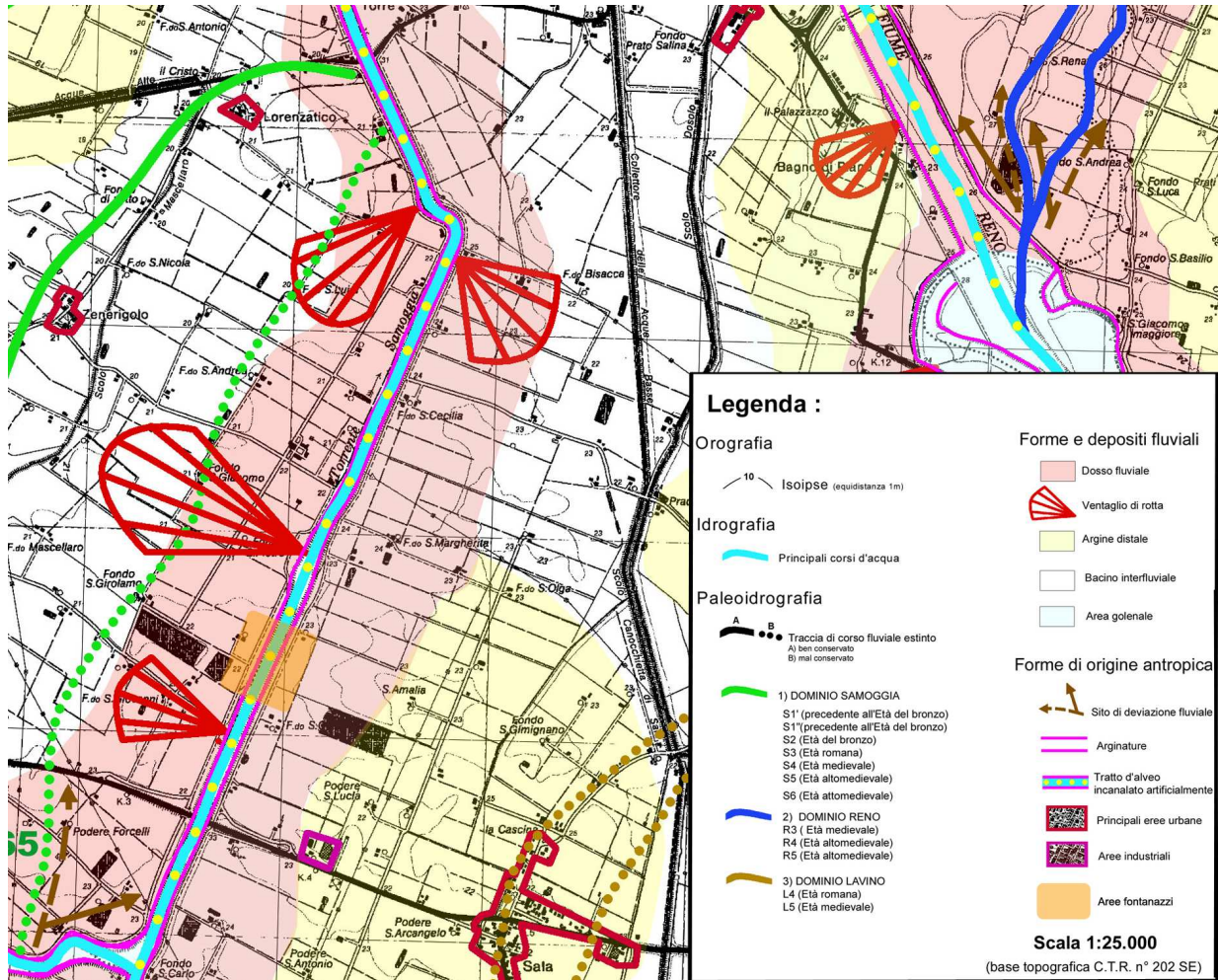
Figure 7.16 – Geomorphologic sketch around the Samoggia stream. The alluvial fans are evidenced in red; the highlighted areas in pink and orange represent respectively the "*dosso*" presence and the study area.

The amount of water drained by this layer from the river to the surrounding fields was already noticed in the past. Some verbal testimonies given by the citizens of the surrounding area demonstrate that this constant water outcropping, which was supposed to be a kind of source, probably influenced the decision to excavate the "*macero*" for the hemp production (showed on the left part of figure 7.14) just in this area. In the meantime, after the 1966 flooding the Samoggia River left embankment was moved as already stated of about 20 m toward west, in order to guarantee a wider space and storage capability of the pensile riverbed. The new embankment positioning covered the water outcropping, bringing to the source closure. The necessity of a drainage system can be therefore explained with the large

amount water infiltration due to the source coverage as well as the pond filling probably during the '70 (decline of hemp production), which constituted a large evaporation zone of the aquifer. Indeed, such events triggered the water table raising level, which had to be restrained with the construction of gabionade and an artificial drainage system. Nowadays, the drainage probably does not resolve the water infiltration and therefore, the embankment base results always completely wet; moreover, some plumes of higher resistivity can be detected in the longitudinal pseudo-section and in the transversal section 3 T2. They seem to link the lower sandy horizon to the upper, and a possible flux of water between them, in case of large pore pressure (case of flooding or rising level of the water table) can be hypothesized.

The complete geophysical campaign and the following considerations have brought the Technical Service of the Reno river Basin to adapt the dimensioning of the benthonitic diaphragms, choosing a deeper penetration inside the entire embankment body until the base of the deeper well permeable sandy horizon (fourth electro-stratum).

In conclusion, the study area close to Sala Bolognese (BO) has given very satisfactory results, concerning the simultaneous employment of various geophysical methodologies, each one able to describe different parameters related to the embankment structure. ERT methodology was a useful tool for the complete description of the embankment as well as its shallower foundation ground, being able to discriminate conductive and resistive bodies (i.e. passages between silty clayey to sandy materials). The calibration with CPT and borehole tests has validated the hypothesis formulated. This technique allows also recognising the areas affected by the piping phenomena as well as the potential weakness zones, characterized by larger amount of sand. FDEM technique has revealed the possibility to estimate the electrical properties of the subsoil with very fast acquisition and it can be considered as a fundamental tool for preliminary investigations. Modelling techniques that aim to carry out some resistivity pseudo-sections from EM data were not used because time-consuming and insufficient to provide quantitative as well as reliable results. Finally, GPR has investigated just the shallower part of the embankment, indeed the employment of a relatively high frequency antenna (400 MHz) results insufficient to give any information deeper than half to one meter depth, especially when high clay contains occur. However, even if a 100 MHz antenna would be utilized, the strong EM wave attenuation in the first meter of subsoil could have significantly reduced the signal amplitude. Nevertheless, the 400 MHz antenna was able to localize some strong anomalies along the road that bound the embankment, permitting to discover a conduits system to drain the water that infiltrate inside and under the embankment structure. Such detection, together with other information deduced by simultaneous

application of both geotechnical and geophysical measurements, has permitted to analyse and describe the complex history of this Samoggia Stream embankments segment.

7.2 The Reno River case

The fluvial embankments of the Reno River system has shown in this territory a series of geotechnical and hydraulic problems that in many cases, during exceptional flood events, have resulted in catastrophic inundations. As previously introduced in Chapter 2, the main causes of these problems can be related to hydrologic and morphologic changes as land subsidence, variations in water discharge and variations of river bed profiles. Others issues can be triggered by anthropogenic interventions (expansions of urban areas, quarry exploitation of the river beds, underground excavations, etc.), animal excavations and biological alterations. Problems concerning the scarce consolidation of underground terrains (below the dykes) and consolidation of the earth embankments (dykes) can therefore evolve in piping or seepage problems.

The levees, inspected with standardised field or laboratory tests result affected also by the inappropriate building techniques that were used throughout history. As a result the flood defence system of the complex Reno River network does not operate as it should in many important nodes. The STBR (Regional Technical Service of the Reno River Basin) of the Regione Emilia-Romagna has recently begun a survey programme, financed by the Authority of the Reno River Basin (Autorità di Bacino del Reno 2002), focused on the study of the hydraulic and geotechnical conditions of the river dikes inside the territory under its jurisdictional authority (Mazzini & Simoni 2004). The need to carry out a survey of hundreds of kilometres of river embankments for identifying, primarily, weakness zones, is also a requirement of the regional government authorities. Just in this context, GPR suitability was tested in the study of river embankments together with other geophysical techniques as MASW (Multi Channel Analysis of Surface Waves) and electric resistivity tomography (ERT). The detection of stratigraphy, animal cavities and burrows, buried pipelines, non-homogeneities represent the main purposes of this research.

The multi-disciplinary approach aims to provide most detailed information as possible of the structural characteristics of the embankments. Even if there is the needing of further investigations, it is possible to outline geophysical methods capability in the study of river dikes.

7.2.1 Introduction

Along the Reno River (Figure 7.17), near Dosso (BO) a comparison of GPR methodology with other geophysical techniques was carried out. A segment on left hydrographical side of the Reno River embankments was chosen as study area. Some direct measurements as borehole and CPT tests assure an adequate calibration of the geophysical data. The embankment is one of the highest structures encountered during the entire research, with its high of 12 meters; such embankment is composed by three external steps and one internal.
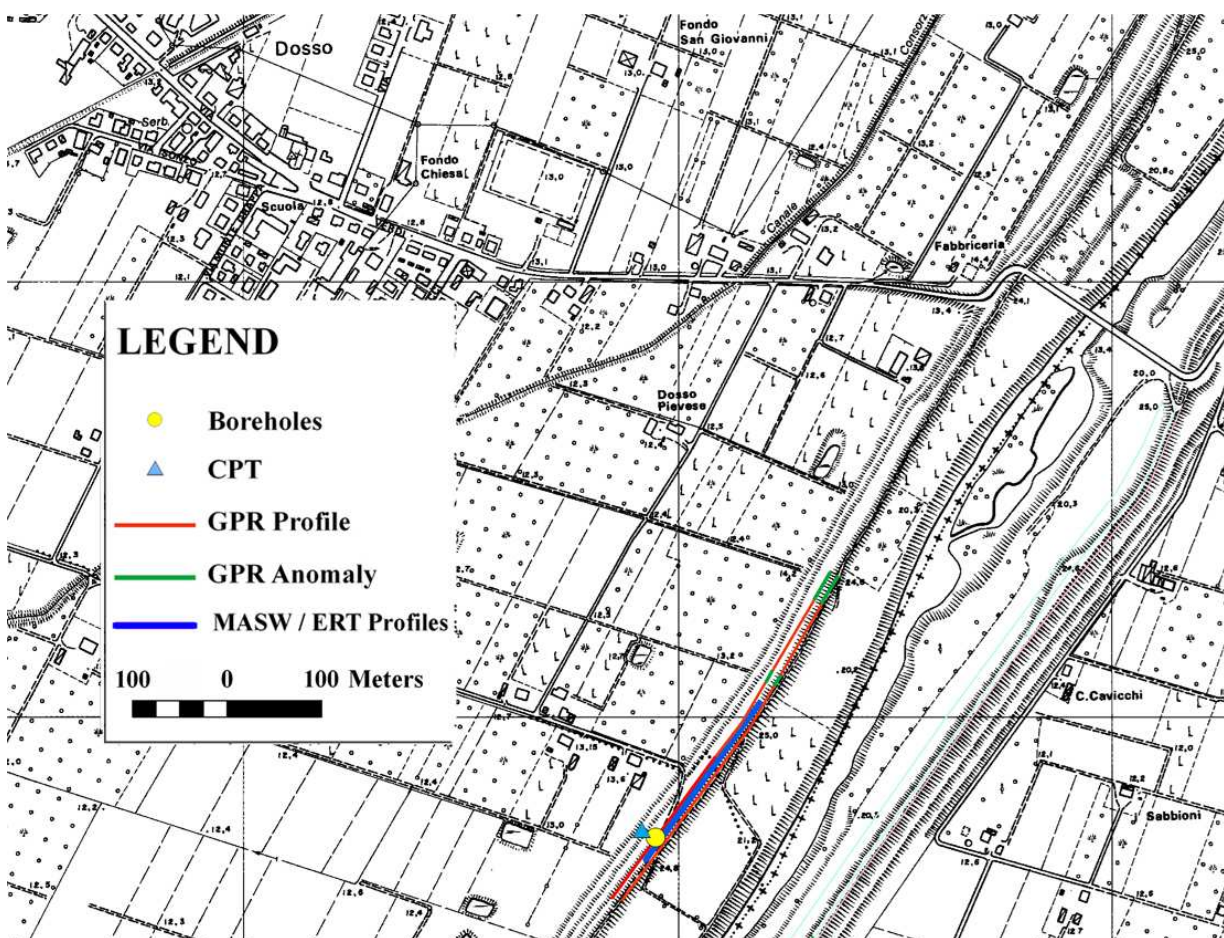
Figure 7.17 - Planimetry of the study area, with MASW, GPR and ERT surveys carried out in the June 2007 campaign near Dosso (BO); location of GPR anomalous zones.

The GPR was utilized in two different campaigns; the first, in July 2007, employing Zond 12-e by Radsys, with antenna 300 MHz and analyzing data with software Prism2. The second campaign was carried out in October 2007 in the same dry conditions of the previous test, through the employment of RIS-MF acquisition unit by IDS, using 100 MHz and 200 MHz antennas. Approximately 500 meters of profiles were carried out on the top of the embankment, showing some interesting results, beside the universal problem linked to the EM

wave attenuation in fine grain-size soils and even if there is a scarce correlation and repeatability between the two separate campaigns. Pertaining to the electric resistivity tomography (ERT) measurements, a SuperSting R8 IP8 channel AGI, kindly supplied by IdroGeoStudi, and software RES2DINV were employed to perform a complete investigation of the embankment and its foundation. Concerning the MASW methodology, Seismograph OYO - McSEIS-SX 24 Bit and software Sursfseis were employed. In the geophysical field the use of surface waves is not new, Indeed seismic reflection and refraction methods are well established, but in the geotechnical scale the SASW (Spectral Analysis of Surface Waves) method was used only recently worldwide. This technique consists of generating a perturbation at a point on the free surface of the site and then the travelling disturbance is measured at several stations on the same free surface. The speed of the surface waves depends on the geometry of the site as well as the stiffness of the soil. In addition, the attenuation of the registered signal with distance from the source is due to both the geometrical spreading and the material damping. MASW methodology is focused on the dispersion and the attenuation of Rayleigh waves, which represent the predominant components of motion of the surface waves in the far field. Complete descriptions of such methodology and new theoretical procedures were provided by Roma (2001) and Lai et alii (2002).
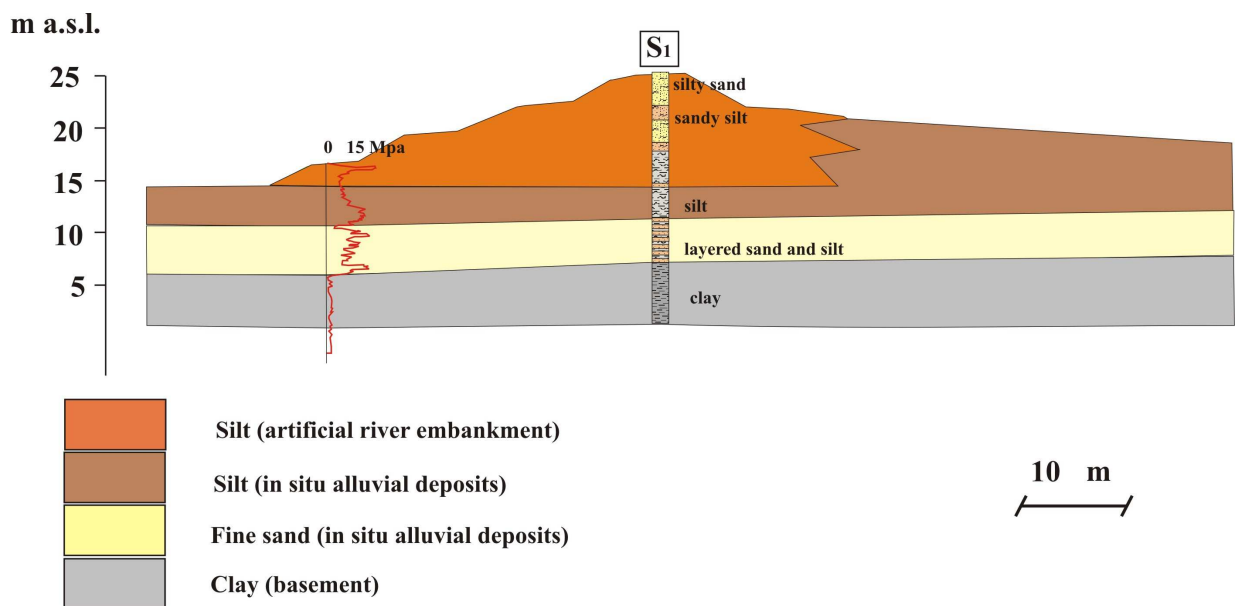
Figure 7.18 - Schematic section along the left side of Reno River with the location of GPR survey, deduced by both borehole and cone penetrometric test.

The geotechnical section of the embankment (Figure 7.18) is characterized by a major complexity structure with respect to the Napoleonic Channel as well as Samoggia Stream embankments. Borehole stratigraphy evidences the presence, besides the artificial

181

embankment (silt prevalent), of in situ alluvial deposits (silt and sand) covering the basement (clay). The artificial embankment is constitutes of an alternation of horizons with prevalent silty component, but with differences in sandy contains, which give to the embankment itself portions characterized by different porosity and therefore permeability. Such lithologic differences entail just slight changes in dielectric properties that are hardly detectable with the geophysical methods; however, some interesting information were notified.

7.2.2 Results

The MASW survey has covered a length of 23 m, with one meter spacing geophones (Figure 7.17a). Such application aims to obtain a geotechnical parameter and precise information at shallow depth. The elaboration has evidenced a strong Vs attenuation at a depth of about three meters. This confirms the presence, supported by the borehole data, of the latest level of construction; beside such latest level is made up of silty sand with respect to the former underlained sandy silt level, the mostly significant factor is that there is a difference in shear-resistance characteristics. Hence, such evidence was not given by the small lithologic change but probably the MASW survey has allowed the highlighting of this slight difference in geotechnical properties, being able to detect the higher compaction of the upper level and to confirm its lateral continuity (Figure 7.19). The depth penetration in not adequate to furnish a description of the entire embankment: to achieve it another measurement was planned with the geophones separation of two meters. Unfortunately, many problems due to cultural noise occurrence and some issues coming out for the data interpolation during the elaboration have invalidated this test.
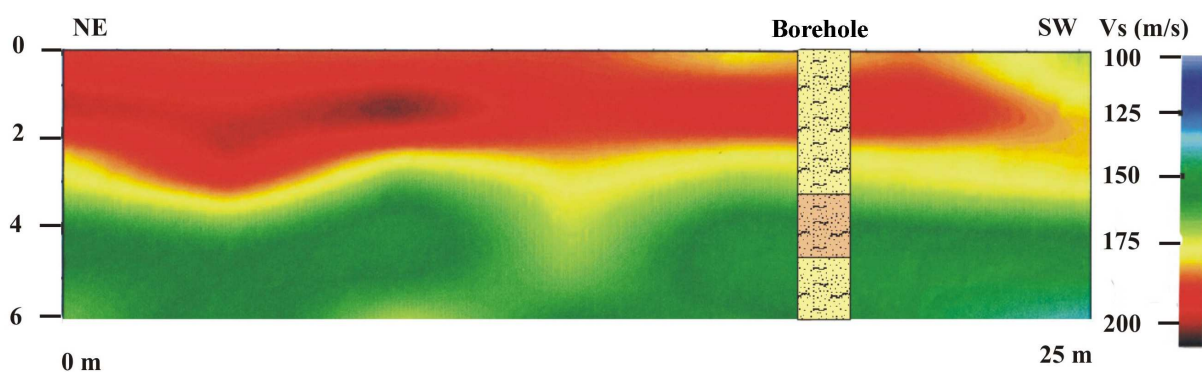
Figure 7.19 - Multi-channel Analysis of Surface Waves (MASW) investigation, carried out in Dosso (BO), is able to detect the higher compaction of the embankment upper level.

The electric tomography was made with an electrode distance of two meters, attaining a total length of the scan of 220 m. Results are coherent with the borehole data and definitely

more accurate than MASW information. The depth of investigation reached about 20 meters, allowing the detection of the embankment base, located at about 12 m depth. The difference in electric resistivity (strong reduction) at this depth is due to the sandy-silt to clay passage and probably to the presence of the water-table. Furthermore, the electric resistivity tomography individuates three major electro-strata that constitute the embankment structure (Figure 7.20).
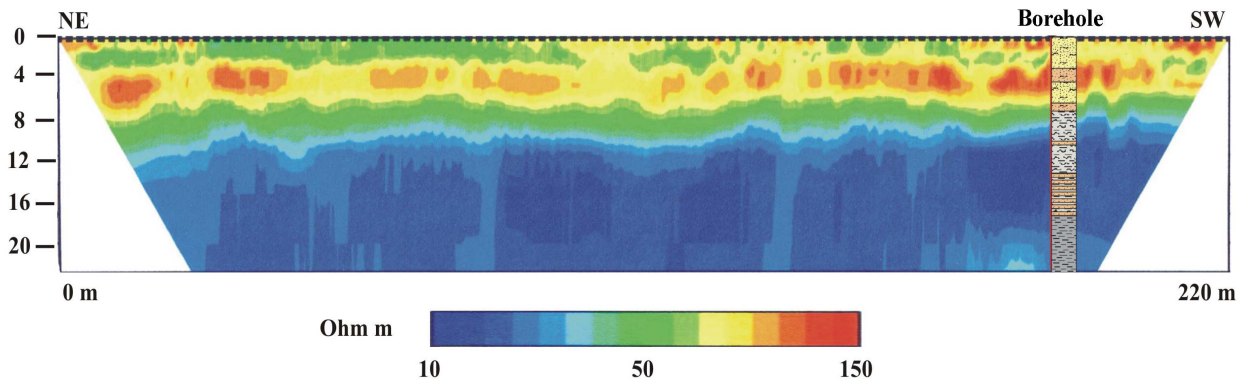
Figure 7.20 - Geophysical investigations carried out along the Reno River near Dosso (BO). Electric resistivity tomography easily reached the base of the river bank.

- First electro-stratum, generally resistive (30 Ωm < ρ < 100 Ωm green/yellow colours), which spreads for around three meters of thickness from the surface. Although it shows some heterogeneities (passing from slightly conductive to resistive), an association can be however done with the other geophysical measurements and the geotechnical tests; this electro-stratum, that covers the old embankment structure, represents the new level of construction.

- Second electro-stratum, generally resistive ($\rho > 50$ Ωm, with peaks of 140 Ωm, yellow/red colours), which can be identified as horizon containing sand, silty sandy and sandy silt, with a relevant amount of sand lithology in some parts of the pseudo-section. The electro-stratum thickness is approximately constant (around five m) and its base is estimable at from nine to ten meters depth. This electro-stratum has a lack of waterproofing and can result unsafe during flooding events because water can easily infiltrate, creating seepage and piping phenomena that can lead to the structural failure.

- Third electro-stratum scarcely resistive ($\rho < 40$ Ωm – green colour), which is identifiable as silty horizon having a variable thickness from three meters. The upper and lower contacts are roughly horizontal; the electro-stratum base corresponds to the artificial embankment base and (excluding some reliable fluctuations) is located at around twelve meters depth. Under the third electro-stratum there is a zone characterized by good

183

conductivity (ρ < 20 Ωm – blue colour), which is associated to the clayey natural soil matrix, with the presence of the water-table.

With regard to the GPR survey, the Zond 12-e, antenna 300 MHz device was employed for the first campaign, the antenna was pulled in contact with the ground, while the acquisition system was mounted on a mini-car that guarantees an extreme velocity of acquisition. Two kilometres of profiles were acquired with 512 scan/sec and just a minimum stacking applied, to prevent a reduced velocity of acquisition. Besides the scarce quality of the elaboration software, such acquisition mode has probably decreased the data quality; however, almost all the profiles show the presence of a boundary that is fluctuating at around two to three meters (Figure 7.21). When it is missing, some punctual anomalies (as carryover material presence) were detected.
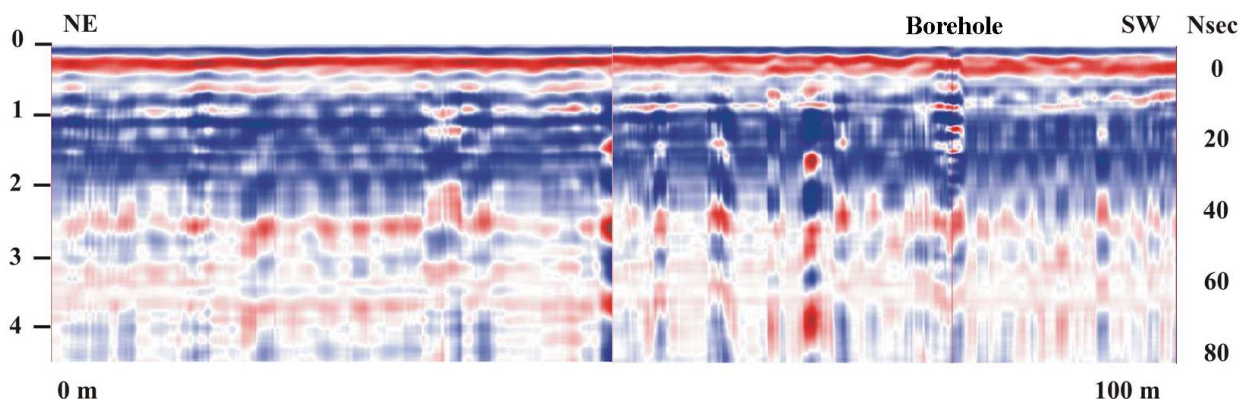
Figure 7.21 –GPR profile: 300 MHz antenna employed, a sharp boundary is present at around 2,5 m depth.

Concerning the second campaign, carried out in October 2007 with both the 100 MHz and 200 MHz antennas, it was carried out for 450 m on the top of the embankment. With the 100 MHz antenna employment, despite the investigation depth is limited to four-five meters, it is possible to mark the contact already noticed by MASW, ERT and by the first GPR campaign at about three meters depth between two differently levels. This contact is visible for the entire length of the scan: a stronger or a weaker signal may be related to soil differences, to moisture changes or/and higher or lower material porosity and therefore compaction state (Figure 7.22).

Such boundary does not result well definite; anyway, it is associated to series of strong reflections through the analysed section, that determinate a not linear threshold, which is developed longitudinally with lateral discontinuities. A large anomaly was detected at around 140 meters of progressive and it is characterized by strong amplitude reflection especially at two meters and half – three meters.
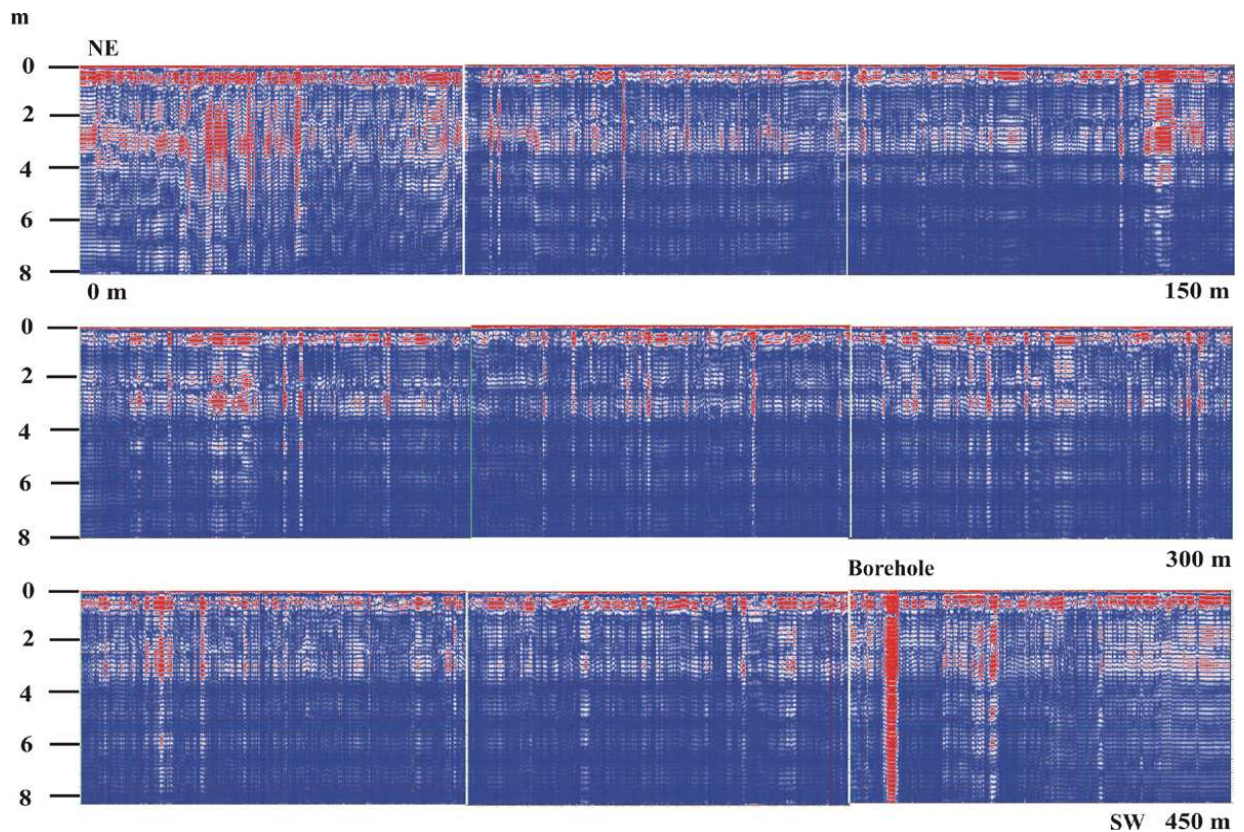
Figure 7.22 – GPR profiles acquired near Dosso (BO), 100 MHz antenna was employed: a sharp boundary is present at around three to four meters depth for the entire profile length.

In this case, GPR technique allows catching the electrical properties difference, but it is only thanks to the multidisciplinary approach adopted, that this feature can be well determined. A comparison between the two campaigns shows how this method does not assure an adequate repeatability; probably the GPR model changing, frequency and moisture conditions variability have compromised the results. Regarding to the results obtained with the employment of 200 MHz antenna, the penetration depth is significantly limited by the fine grain-size materials that constitute the embankment; hence the signal-to-noise ratio becomes too weakly just above the expected boundaries individuated by the geophysical measurements. The application of the *smoothed gain* function, with respect to the *linear gain* function is motivated by the necessity to enhance the deeper reflections instead of the superficial ones, determinate by the strong superficial boundary. The profiles carried out show a constant reflective horizon inside the first meter, which is only partially present into the 100 MHz radargrams. Two *ringing* noisy effects that produce some artificial horizontal banding occur respectively at two and three meters. The figure 7.23 shows a very strong anomaly already individuated by the 100 MHz antenna, due to an abrupt change in dielectric properties; therefore, large lateral heterogeneity is expected.

185

In conclusion, the study area of Dosso (BO) has provided some satisfactory results, concerning the simultaneous employment of various geophysical methodologies, each one able to describe different parameters related to the embankment structure. ERT methodology was a useful tool for the complete description of the embankment as well as its foundation ground, being able to distinguish conductive and resistive bodies (i.e. passages between silty clayey to sandy materials).
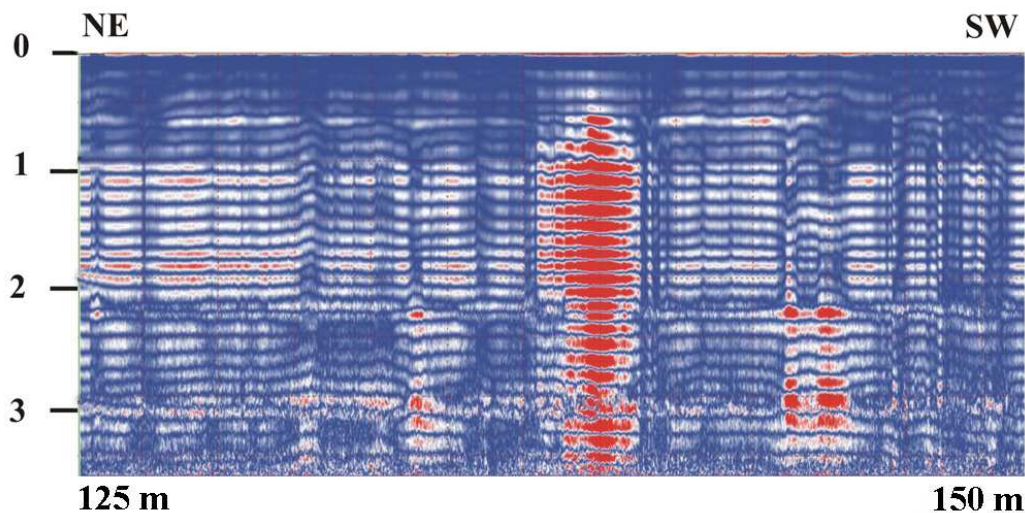
Figure 7.23 – GPR profiles acquired near Dosso (BO), particular of 200 MHz antenna profile: a sharp boundary is present at around three to four meters depth for the entire profile length. The large anomaly coincides with the one evidenced in figure 7.20.

Furthermore, this methodology, with the employment of eight-channel acquisition system that massively reduces the acquisition time, and a certain number of operators, it can guarantee the analysis of around one kilometres of profile length per day. MASW technique has revealed the possibility to estimate the geotechnical parameters through the analysis of the shear-wave velocity but it was influenced by the cultural noise of the surrounding anthropized area as well as some interpolation uncertainties during the elaboration. Finally, GPR has investigated just the shallower part of the embankment, without a sufficient repeatability (i.e. the comparison between the Zond-12e and the RIS Ground Penetrating Radars); however, it was able to localizes some strong heterogeneities that nevertheless need direct drills or other analysis to be adequately described.

186

8. CONCLUSIONS

This research was developed in merit of the agreement stipulated between the University of Bologna and the STBR of Emilia-Romagna Region, with the aim to provide a review pertaining the advantages and drawbacks of Ground Penetrating Radar usage, to assess the structural safety of Reno River and its tributaries embankments. GPR technique was chosen because the total length of river network in the Reno plain basin is too spread (about 500 km long) for the use of common geophysics techniques (seismic, gravimetry, electric resistivity tomography) in a preliminary phase of study, searching hazardous areas. The Reno River and its tributaries embankments were studied though the realization of around 40 kilometres of GPR profiles, employing various acquisition units and a wide range of antenna frequencies (from 100 MHz to 600 MHz). GPR as electromagnetic method lacks the resolution and depth penetration of resistivity surveys, but has the advantage of being rapid and less expensive. Therefore, the use of GPR was scheduled because of its high velocity of acquisition as well as the possibility to check the results directly during the data acquisition (fundamental in case of hydrological emergencies).

The GPR investigations are based on the emission of EM waves, which spread inside the ground and come back to the GPR timing unit as reflected waves, once they encounter changes in electrical properties of the materials constituting the subsoil. Generally, in geologic applications, GPR methodology performs excellent results when clean, coarse-grained materials such as quartz, sand as well as gravel occur. In fine-grained soils such as silt and clays, the presence of water is one of the most important factors determining GPR results; ions dissolved in the water give rise to an electrical conduction mechanism. Hence, the more ions dissolved in the solution, the higher the conductivity; as a result, clayey soils impose a strong reduction of EM wave penetration inside the medium. The Reno River and its tributaries embankments were built up utilizing carryover materials available in the riverbed surroundings, and they are mainly constitutes of silt, with variable contains of sand and clays, with random presence of objects in brick and metal. This high contains of fine grain-size materials have significantly influenced the depth penetration of EM wave and thus limited the applicability of GPR for the Reno River embankments structural safety assessment.

Concerning the GPR surveys, some practical aspects need to be considered: the topography surface must be clean from vegetation and it is not possible to work with rainy weather or with the wet condition of the soil. Considering always essential a calibration with

direct in-situ measurements, it is possible to assert that GPR technique applied to river embankment investigations has supplied some useful observations concerning the following cases.

Areas affected by seepage and piping

Beside the scarce results obtained when seepage and piping phenomena have occurred lower than the penetration depth reached by the GPR, such methodology has still the possibility to detect areas with different porosity and lithology. When a piping phenomenon occurs, it is often associated to strong erosion effects, which produce massive changes in material distribution inside the embankment part involved in that event. For Quaderna and Samoggia Streams many attempts were carried out in order to verify the lateral continuity of the internal structure of the embankments. For this task many other tests are needed, due to the GPR impossibility in both cases to reach an adequate penetration and therefore to detect such changes.

Embankment segments rebuilt in the past

The GPR has suffered many problems related to the environmental conditions and just seldom it was useful to identify changes of structural conditions inside the embankments, which were rebuilt in the past. The results were obtained only with the employment of a 100 MHz antenna, because higher frequencies are characterized by a strong increment of EM wave attenuation after the first meter of subsoil. Nevertheless, repaired areas are well recognizable if they were executed recently, because the new materials are more porous and therefore less compacted with respect to the old ones. Reparations completed several years ago are difficult to detect with GPR because with time, the soil compaction and the electric properties of the materials, influenced also by the moisture content, become similar to the surroundings.

Detection of animal cavities

In the complex, the results are partially negative: the employment of high frequency antennas, although suitable for the good spatial resolution, was seriously compromised by the EM wave attenuation in the first meters of subsoil, due to clutter and scattering phenomena occurrence. The 100 MHz antenna, which has reached the target depth, is unable to detect small punctual targets and however, as deeper the target as higher must be the contrast in dielectric properties to produce any noticeable reflection. Moreover, the moisture conditions

and the embankment geometric factors significantly influence the GPR measurements, which have achieved just one interesting result, for the small Reno tributary levee. The detection of animal cavities with the employment of geophysical methodologies remains an open issue: nowadays the best way to assure the hydraulic safety related to the presence of cavities is a constant surveillance of the river embankments as well as a constant cleaning and maintenance of the surface.

Inspection of the embankment internal structure

As already stated, the Reno River and its tributaries embankments were built up utilizing carryover materials available in the riverbed surroundings, and they are mainly constitutes of silt, with variable contains of sand, clays and with the random presence of objects in brick and metal. These settings confer a strong heterogeneity and many lateral variations inside the embankments, which can results in a lack of waterproofing as well as a structural weakness of the embankments themselves. With the chosen antenna frequency of 100 and 200 MHz, the survey results have significantly influenced by the low investigation depth, due to the high silt fraction and the embankment foundation level was never reached; therefore, no complete structural description of the embankment is available. This aspect is a strong limitation of the method: a maximum investigation depth of four to six meters over an embankment height ranging from five to twelve meters is fairly restraining. However, the spatial resolution is similar to the size of the expected targets: actually, objects of known nature and shape were clearly detected. This is the most valuable characteristic of GPR, because strong reflections referred to isolated objects are generally hardly detectable with other methods. Therefore the GPR can be considered a valid technique when a detailed study of river embankment is needed, or to detect local shallow anomalies. It has achieved some good results for the detection of areas with a strong difference in compaction, such as refurbished levels and recently repaired areas: it is important to mention again that GPR cannot quantify the compaction state. Some advantages and drawbacks were encountered for the description of shallow stratigraphic boundaries between soils with a noticeable difference in lithology or moisture content, like medium sand and silt, but when small electrical properties changes occur, it present many detection difficulties. The employment of GPR results valuable for the recognition of shallow isolated objects like blocks, metal objects and pipelines.

Localization of stratigraphic contacts beneath river embankments

Some important aspects in the use of GPR came out during the surveys carried out along the Napoleonic Channel: the topography surface perfectly smooth due to the asphalt coverage of the road that represents the embankment base and its dielectric properties, which imply a weak signal attenuation, has definitely enhanced the acquired data. Once again, encouraging results were obtained for the description of stratigraphic boundaries between soils with a noticeable difference in lithology or moisture content, like medium sand and fine silt. However, it is always recommended a calibration with other direct and/or indirect measurements. It was also been possible to check the lateral continuity of a paleochannel at the base of the Napoleonic Channel embankment.

Multidisciplinary approach

GPR has revealed its importance in case of shallow anomalies and boundaries detection, but cannot be considered as a methodology capable to furnish a sufficient description of the embankments structure. Nevertheless, with the usage of a unique geophysical methodology is impossible to achieve a good detection of the defects leading to failure of the embankment; therefore, in order to guarantee an adequate investigation and safety evaluation, a site-specific calibration and the employment of complementary geophysical methods are necessary. The Reno River case has evidenced the necessity to accurate analysis to acquire sufficient knowledge of the embankment structures. Beside the GPR efficacy for the detection of areas with a strong difference in porosity, which can be associated to compaction changes, electric resistivity tomography provides the better results when a lithologic section of the embankment is needed, while MASW technique can estimate the geotechnical parameters through the seismic waves analysis. The multi-disciplinary approach can guarantee the detection of lots of defects that can bring to the embankment failure. As a matter of facts, the Samoggia Stream case demonstrates how the simultaneous employment of various geophysical methodologies, which achieve different geotechnical as well as physical parameters related to the materials that constitute the embankments, have brought to an accurate reconstruction of the piping phenomena occurred last May 2008. Noticeable, is the advantage of the FDEM methodology (GEM-2 or EMP-400 devices) over both the OhmMapper and ERT techniques; indeed, its ski design, provides greater flexibility for investigating anomalies in dense vegetation and often allows more rapid data acquisition. A disadvantage is its lower resolution compared to the other systems.

This technique allow also to recognise the areas affected by the piping phenomena as well as the potential weakness zones, characterized by larger amount of sand. FDEM technique has revealed the possibility to estimate the electrical properties of the subsoil with very fast acquisition and it can be considered as a fundamental tool for preliminary investigations.

In conclusion, with the aware of the above-mentioned limits, GPR can be considered a valid technique for detailed studies of the river embankments shallower part and demonstrate impressive qualities to detect local sharp anomalies. To achieve a good detection of many, but not all types of defects leading to failure of the embankment, a site-specific calibration and the employment of complementary geophysical methods are therefore necessaries.

9. RECOMMENDATIONS

Geophysical techniques are able to detect many, but not all types of defects leading to failure. A detailed evaluation including resolution and effort studies is to follow. Additional techniques as CPT including seismic and electric cones are necessary for superior calibrations of surface measurements. As we have seen, GPR has revealed its applicability for detailed surveys, assuring a good compromise between acquisition velocity and data quality; however, it requires optimal surface conditions and only shallow depth is covered by this kind of investigation. For the future applications, the researcher must schedule the improvement in terms of usefulness and efficiency of the Geophysical Monitoring System, concerning the degrees of repeatability, quality assessment and velocity acquisition, of the geophysical data.

The Applied Geophysics is a branch in constant motion and development, with remarkable achievements by means of time-consuming, costs and data quality improvement. Besides the traditional techniques, for future researches, the OhmMapper and FDEM methodologies, even with all the possible limitations, can massively improve the knowledge of wide parts of the Emilia-Romagna as well as Europe river embankments.

ACKNOWLEDGMENTS

REFERENCES

AL-QADI, I.L., LAHOUAR, S. (2005) - *Measuring layer thicknesses with GPR* – Theory to Practice. Construction and Building Materials, Vol. 19, pp. 763 – 772.

AMOROSI, A., COLALONGO, M.L. (2005) - *The linkage between alluvial and coeval nearshore marine succession: evidence from the Late Quaternary record of the Po River Plain, Italy*. In: Blum, M.D., Marriott, S.B., Leclair, S.F. (Eds.), Fluvial Sedimentology VII. International Association of Sedimentologists, Special Publ., vol. 35, pp. 257–275

ANNAN, A. P., (1996) - *Ground-penetrating Radar: Workshop Notes*, Sensors and Software, Inc., Misissauga, Ontario, 106 pp.

ANNAN, A.P. (2001) - *Ground-penetrating Radar: Workshop Notes*, Sensors and Software, Inc., Misissauga, Ontario, 192 pp.

ANNAN, A.P. AND COSWAY, S.W., (1994) - *GPR Frequency Selection*: Proceedings of the Fifth International Conference on Ground-Penetrating Radar, Kitchener, Ontario, Canada, June 12-16, 1994, pp. 747-760.

ANNAN, A.P. AND DAVIS, J.L. (1976) - *Impulse Radar Soundings in Permafrost*: Radio Science, Vol. 11, pp. 383-394.

ASCH, T.H., DESZCZ-PAN, M., BURTON, B.L., BALL, L.B. (2008) - *Geophysical Characterization of the American River Levees, Sacramento, California, using Electromagnetics, Capacitively Coupled Resistivity, and DC Resistivity*. Open-File Report 2008-1109, U.S. Geological Survey, Reston, Virginia.

BAKER, G.S., JOL, H.M. (2007) - *Stratigraphic Analyses Using GPR*. Geological Society of America, Special Paper 432, pp. 181.

BELINA, F.A. DAFFLON, B., TRONICKE, J., HOLLIGER K. (2008) - *Enhancing the Vertical Resolution of Surface Georadar Data*, Journal of Applied Geophysics. Accepted manuscript, doi: 10.1016/j.jappgeo.2008.08.011.

BENNETT, H.H JR., SIMMS, J.E., SMITHHART, L.B., HARGRAVE M.L., BRITT, T., BALBACH, H.AND PITTS, D. (2005) - *Gopher Tortoise Nest Detection at Camp Shelby, Mississippi*, Engineer Research and Development Center, ERDC TR-05-6.

BIAVATI, G., GHIROTTI M., MAZZINI E., MORI G., TODINI E., (2008). *The use of GPR for the detection of non-homogeneities in the Reno River embankments (Northeastern Italy).* Proceedings of the 4th Canadian Conference on Geohazards: From Causes to Management. Presse de l'Université Laval, Québec, pp. 133-140.

BONDESAN, M. (2001) - *Hydrographical and environmental evolution of Ferrara Plain during the last 3000 years*. In: History of Ferrara. Vol. I "Cassa di Risparmio" of Ferrara, pp. 228-263. (in Italian).

BOCCALETTI ET ALII, (2004). Carta Sismotettonica *dell'Emilia-Romagna, scala 1:250000*, Note Illustrative, Servizio Geologico Sismico e dei Suoli, Ed. Selca, Firenze (In Italian).

BOUKALOVÁ, Z., BENEŠ, V. (2007) - *Dike break prevention as the process of flooding protection*. In Proceedings of 32nd Congress of the International Association of Hydraulic Engineering and Research, Vol. 1, Venice, 1-6 July 2007.

BRANDT, O., LANGLEY K., KOHLER, J., HAMRAN, S.E. (2007). *Detection of buried ice and sediment layers in permafrost using multi-frequency Ground Penetrating Radar: A case examination on Svalbard*. Remote Sensing of Environment), doi:10.1016/j.rse.2007.03.025, In press.

BRATH, A., MONTANARI, A., MORETTI, G. (2006) - *Assessing the effect on flood frequency of land use change via hydrological simulation (with uncertainty)*, Journal of Hydrology 324, pp. 141–153.

BROUWER, J.J.M. (2002) - *Guide to Cone Penetration Testing – On shore and near shore*. www.conepenetration.com/cpt3.html#test

CARDARELLI, E., MARRONE, C., ORLANDO, L. (2003) - *Evaluation of tunnel stability using integrated geophysical methods*, Journal of Applied Geophysics 52, pp. 93– 102.

CARMINATI, E., DOGLIONI, C., & SCROCCA, D. (2003). *Appennines subductionrelated subsidence of Venice (Italy)*. Geophysical Research Letters, 30. doi:10.1029/2003GL017001

CARMINATI, E., & MARTINELLI, G. (2002). *Subsidence rates in the Po Plain, northern Italy: the relative impact of natural and anthropogenic causation*. Engineering Geology, 66, 241–255.

CLAY, R.B. (2001) - *Why Two Ways Are Always Better Than One*. Southeastern Archaeology 20:1 pp.31-34.

COOK, J.C. (1960) - *Proposed monocycle-pulse, VHF radar for airborne ice and snow measurements*. AIEE Trans. Commun. and Electron, 79 (2), pp. 588-594.

COOK, J.C. (1974) - *Status of ground-probing radar and some recent experience*, Proc. Conf. Subsurface Exploration for Underground Excavation and Heavy Construction. Am.. Soc. Civ. Eng., pp. 175-194.

COOK, J.C. (1975) - *Radar transparencies of mine and tunnel rocks* Geophys., 40, pp 865-885.

COVELLI, C. (2006) - *Sulla formazione di brecce nei rilevati arginali: implicazioni relative alla protezione idraulica del territorio*. Tesi di Dottorato, Università degli Studi di Napoli Federico II. (In Italian),

CREMONINI, S. (2003) - *Alcune considerazioni sul profile longitudinale del Fiume Reno (Italia)*, Annuali di ricerche e studi di geografia, Anno LIX-Fasc 1-4, Pàtron Editore, Bologna (In Italian).

DANIELS, D.J. (2004) - *Ground Penetrating Radar*. Institute Electric. Engineers, London.2nd edition, 694 pp

DAVIS, J.L., ANNAN, A.P., (1989) – *Ground Penetrating Radar for High Resolution Mapping of Soil and Rock Stratigraphy*, Geophysical Prospecting 37, pp. 531 – 551.

DOMINIC, D.F., EGAN, K., CARNEY, C., WOLFE, P.J., BOARDMAN, M.R. (1995) - *Delineation of shallow stratigraphy using ground penetrating radar*. Journal of Applied Geophysics 33, pp. 167-175.

DOOLITTLE, J.A, JENKINSON, B., HOPKINS, D., ULMER, M., TUTTLE, W., (2005) – *Hydropedological Investigation With GPR: Estimating Water-table Depths and Local Ground-water Flow Pattern in Areas of Coarse-Textured Soils*, Geoderma, pp 13

EPA SUPERFUND (2005) – *Direct Push Technologies, Expedited Site Assessment Tools For Underground Storage Tank Sites: A Guide for Regulator*, EPA 510-B-97-001. www.epa.gov/superfund/programs/dfa/dirtech.htm

FELL, R., MACGREGOR, P., STAPLEDON, D. (1992) - *Geotechnical engineering of embankment dams*. ISBN 90 5410 128 8, Balkema, Rotterdam, pp 675.

FUOCO, M., ZIZZOLI, P., SOLA, S. (1999) – *Evoluzione paleoidrografica della pianura compresa tra Samoggia e Reno*. In: "Tra Reno e Samoggia: soluzioni per due fiumi", Edizioni Aspasia, San Giovanni in Persiceto (BO), pp. 11-24. (In Italian).

GELATI, L. (2003) – *Analisi Geologico-Tecnica dei Fenomeni di Filtrazione all'interno degli Argini del Torrente Savena Abbandonato in Prossimità di Altedo (Provincia di Bologna)*, Tesi di Laurea, Università di Bologna (In Italian).

GOODMAN D. (1994) - *Ground-penetrating radar simulation in engineering and archaeology*. Geophysics, vol. 59, n. 2, pp. 224-232.

HEILIG, A., SCHNEEBELI, M., FELLIN, W. (2008) - *Feasibility study of a system for airborne detection of avalanche victims with ground penetrating radar and a possible automatic location algorithm.* Cold Regions Science and Technology 51, pp. 178–190.

HENDRICKX, J.M.H., HONG, S-H., MILLER, T., BORCHERS, B., & REBERGHEN, J.B. (2003) – *Soil effects on GPR detection of buried non-metallic mines*, inside "Ground Penetrating Radar in sediments. Geological Society Special Pubblication". Geological Society, London Special Publications, 211, pp. 191-198.

HUANG, H. (2005) - *Depth of investigation for small broadband electromagnetic sensors*, Geophysics, Vol. 70, No. 6 November-December; pp.135–142.

HUANG, H. AND WON, I. J. (2003) - *Real-time resistivity sounding using a hand-held broadband electromagnetic sensor*, Geophysics, Vol. 68, No. 4 July-August; pp. 1224–1231.

KNÖDEL, K., LANGE, G., GERHARD, H.J. (2008) - *Environmental Geology: Handbook of Field Methods and Case Studies.* Bundesanstalt für Geowissenschaften, Berlin: Springer, 2008. ISBN 978-3-540-74669-0

JOHANSSON, S., FRIBORG, J. (2003) – *Long Term Resistivity and Self Potential Monitoring of Embankment Dams, Experiences from Hällby and Sädva Dams, Sweden.* CEATI Project No.T992700-0205 ,Investigation of Geophysical Methods for Assessing Seepage and Internal Erosion in Embankment Dams

JOL, H.M., BRISTOW, C.S (2003) – *Ground Penetrating Radar in sediments.* Geological Society Special Pubblication No. 211, London.

ISSMGE (2001) - International *Reference Test Procedure (IRTP) for the Cone Penetration Test (CPT) and the Cone Penetration Test with pore pressure (CPTU).* Report of the International Society for Soil Mechanics and Geotechnical Engineering.

LABREQUE, D.J., MILETTO, M., DAILY, W., RAMIREZ, A., OWEN, E. (1996) - *The effects of noise on Occam's inversion of resistivity tomography dat*a. Geophysics, 61, pp. 538-548.

LAI, C.G., RIX, G.J., FOTI, S., ROMA V. (2002) - *Simultaneous measurement and inversion of surface wave dispersion and attenuation curves*. Soil Dynamics and Earthquake Engineering 22 (2002), pp. 923–930.

LESTER.J, BERNOLD L.E. (2007) - *Innovative process to characterize buried utilities using GPR*. Automation in Construction 16, pp 546–555.

LEUCCI, G., (2006) - *Contribution of Ground Penetrating Radar and Electrical Resistivity Tomography to identify the cavity and fractures under the main Church in Botrugno (Lecce, Italy)*, Journal of Archaeological Science 33, pp.1194-1204

LINES, L.R. AND TREITEL, S. (1984) - *Tutorial: a review of least-squares inversion and its application to geophysical problems*. Geophysical Prospecting, 32, pp.159-186.

LOKE, M.H. (2008) - *RES2DINV version 3.57 Rapid 2-D Resistivity & IP inversion using the leasts-quares method*, ABEM Instrument AB, user manual. Internet site :http://www.geoelectrical.com.

LOKE, M.H., BARKER, R.D. (1996) – *Practical techniques for 3D resistivity surveys and data inversion*. Geophysical Prospection, Vol. 44.

LOIZOS, A. AND PLATI C. (2007) - *Ground penetrating radar as an engineering diagnostic tool for foamed asphalt treated pavement layers*. International Journal of Pavement Engineering, Vol. 8, Issue 2, pp. 147 – 155.

LUCIANI, P. (2002) – *Evoluzione Paleoidrografica e Studio della Stabilità degli Argini del Torrente Samoggia nel Tratto Compreso trai Comuni di San Giovanni in Persicelo e Sala Bolognese (BO)*, Tesi di Laurea, Università di Bologna. (In Italian).

MAINALI, G. (2006) – *Monitoring of Tailing Dams with Geophysical Methods*, Licentiate Thesis, Luleå University of Technology Department of Chemical Engineering and Geosciences Division of Ore Geology and Applied Geophysics, 2006-09-21.

MASANNAT, Y. M. (1980) - *Development of piping erosion conditions in the Benson area, Arizona, U.S.A*. Quarterly Journal of Engineering Geology & Hydrogeology; February 1980; v. 13; no. 1; pp. 53-61.

MAZZINI, E., SIMONI, G. (2004) - *Geotechnical and hydraulic aspects of the fluvial embankments in the Reno River plain.* In: Proceeding of the XXII National Congress of Geotechnique, 22-24 Set. 2004, Palermo. Patron Ed., Bologna, 555-562. (In Italian).

NAGY, L., TÓTH, S. (2001) - *Detailed Technical Report on the collation and analysis of dike breach data with regards to formation process and location factors. Investigation of Extreme Flood Processes & Uncertainty* – Additional Partners IMPACT-ADD Contract No.: EVG1-CT-2001-00037

MCNEILL, J.D. (1990) - Use *of electromagnetic methods for groundwater studies*. S.H. Ward (ed.), Geotechnical and Environmental Geophysics, 1, Society of Exploration Geophysicists, 191–218.

MORRIS, M. (2005) - *Investigation of Extreme Flood Processes and Uncertainly*, Project IMPACT, Final Technical Report, 72 pp. Project website: www.impact-project.net.

NEAL, A. (2004) - *Ground-penetrating radar and its use in sedimentology: principles, problems and progress*. Earth Science Reviews, Vol. 66, pp. 261-330.

NIEDERLEITHINGER, E., WELLER, A., LEWIS, R., STÖTZNER, U., FECHNER, TH., LORENZ, B., AND NIEßEN, J. (2007) - *Evaluation of Geophysical methods for River Embankment Investigation*. Proc. of EFRM Dresden, Germany.

NILSSON, B (1978) - *Two topics in electromagnetic radiation field prospecting*, Doctoral Thesis, University of Lulea, Sweden.

OLHOEFT, G.R. (2000) - *Maximizing the information return from ground penetrating radar*, Journal of Applied Geophysics 43, pp.175–187.

OTTO, J.C., AND SASS, O. (2005) - *Comparing Geophysical Methods for Talus Slope Investigation in the Turtmann Valley (Swiss Alps)*. Geomorphology, Vol. 76, Issues 3-4, pp. 257-272.

OZKAN, S. (2003) - *Analytical Study on Flood Induced Seepage under River Levees*. A Dissertation Submitted to Graduate Faculty of the Louisiana State University and Agricultural and Mechanical College in partial fulfillment of the requirements for the degree of Doctor of Philosophy in The Department of Civil and Environmental Engineering.

PICOTTI, V., AND PAZZAGLIA, F. J. (2008) - *A new active tectonic model for the construction of the Northern Apennines mountain front near Bologna (Italy)*, J. Geophys. Res., 113, B08412, doi:10.1029/2007JB005307.

PIERI, M. AND GROPPI, G. (1981) - *Subsurface geological structure of the PO Plain, Italy*. Pubbl. 414 P.F. Geodinamica, C.N.R., 23 pp.

POLUZZI, L. (1995) – *Il torrente Samoggia dai tempi più remoti ad oggi. Strada Maestra*, Quaderni della biblioteca comunale "G.C. Croce" di San Giovanni in Persiceto,Vol. 38-39, pp-160-199.(In Italian).

REZACOVA, D., PESICE, P., SOKOL, Z. (2005) - *An estimation of the probable maximum precipitation for river basins in the Czech Republic*, Atmospheric Research 77, pp. 407–421.

RICCI LUCCHI, F. (1984) - *Flysch, molassa, cunei clastici: tradizione e nuovi approcci nell'analisi dei bacini orogenici dell'Appennino settentrionale*. In: Cento Anni di Geologia Italiana. Volume Giubilare 1" Centenario Sot. Geol. Ital., pp. 279-295 (In Italian).

RICHARDS, K.S., REDDY, K.R. (2007) – *Critical appraisal of piping phenomena in earth dams*, Bull Eng Geol Environ No. 66, pp. 381–402.

ROE, K.C, ELLERBRUCH, D.A. (1979) – *Development and testing of a microwave system to measure coal layers thickness up to 25 cm*. Nat. Bur. Stds., Report No.SR-723-8-79 (Boulder, CO).

ROMA, V. (2001) - *Soil Properties and Site Characterization by means Rayleigh Waves*. PhD Thesis, Department of Structural and Geotechnical Engineering, Technical University of Turin (Politecnico).

SASS, O. (2007) - *Bedrock detection and talus thickness assessment in the European Alps using geophysical methods*, Journal of Applied Geophysics 62, pp. 254–269.

SHERIFF, R.E., GELDART, L.P (1982) – *Exploration seismology Volume 1: History, Theory and Data Acquisition*. Cambridge University Press, New York, New York.

SCHROTT, L., AND SASS, O. (2008) - *Application of field geophysics in geomorphology: Advances and limitations exemplified by case studies*. Geomorphology, Vol. 93, Issues 1-2, pp. 55-73.

SHENG-HUOO, N., CHING-KUAN, C., HONG-MING, L. (2002) - *Application of Ground Penetrating Radar on the Void-Detection in Levee*, Proceedings of The Twelfth (2002) International Offshore and Polar Engineering Conference. Kitakyushu, Japan, May 26–31, 2002.

SJODAHL, P. (2006) - *Resistivity Investigation and Monitoring For Detection of Internal Erosion and Anomalous Seepage in Embankment Dams*. Doctoral Thesis, Engineering Geology, Lund University, Sweden.

SMITH, B. D., OTTON, J.K., ZIELINSKI, R.A., ABBOTT, M.M., HUANG, H., WITTEN, A.J. (2004) - *Conductivity depth imaging of areas of shallow brine plumes at the USGS OSPER Site, Osage Co., Oklahoma*: Presented at 11th International Petroleum Environmental Conference, Albuquerque, New Mexico, October 11-15, 2004.Integrated Petroleum Environmental Consortium.

SOLDOVIERI F., PERSICO R., UTSI E., UTSI V. (2006) - *The application of inverse scattering techniques with Ground Penetrating Radar to the problem of rebars location in concrete*. NDT&E International No. 39, pp. 602–607.

Spies, B.R. (1989) - *Depth of exploration in electromagnetic sounding methods*: Geophysics, 54, pp. 872–888.

Spies, B.R., Frischknecht, C.F. (1991) - *Electromagnetic sounding, in Nalargehian, M. N.*, Ed., Electromagnetic methods in applied geophysics 2: Soc. Expl. Geophys., pp. 285–425.

Stramondo, S., Saroli M., Tolomei C., Moro M., Doumaz F., Pesci A., Loddo F., Baldi P., Boschi E. (2007) - *Surface movements in Bologna (Po Plain — Italy) detected by multitemporal DInSAR*, Remote Sensing of Environment 110, 304–316 pp.

Surian, N., Rinaldi, M. (2003) - *Morphological response to river engineering and management in alluvial channels in Italy.* Geomorphology, 50(4), pp. 307-326.

Sussmann T.R.,Selig, E.T., Hyslip, J.P., (2003) – *Railway Track Condition Indicators from Ground Penetrating Radar*, NDT&E International 36, pp.157 – 167

Smith, D.G.& Jol, H.M. (1995) - *Ground Penetrating Radar: antenna frequencies and maximum probable depths of penetration in Quaternary Sediments*, Journal Of Applied Geophysics, Vol. 33, pp. 93 – 100.

Vettore, L. (2008) – *High resolution geophysical surveys: Archaeological applications and its utilization in environmental contexts*, PhD thesis in Geosciences, University of Padova (Italian).

Yilmaz, O., Doherty, S. M., (1987) - *Seismic Data Processing Series--Investigations in Geophysics*, no. 2: Society of Exploration Geophysicists, Tulsa, Oklahoma, pp. 536.

Washington State Department of Ecology (1992) – *Dam Safety Guidelines.* Technical note I, Dam break inundation analysis and downstream hazard classification. Water Resources Program, Dam Safety Office, Olympia, WA, pp 34.

Won, I.J., Keiswetter, D.A., Fields, G.R.A., Sutton, L.C. (1996) – *GEM-2 – A New Multifrequency Electromagnetic Sensor*, JEEG, Volume 1, Issue 2, pp. 129 – 137.